PDE4 gene inhibition

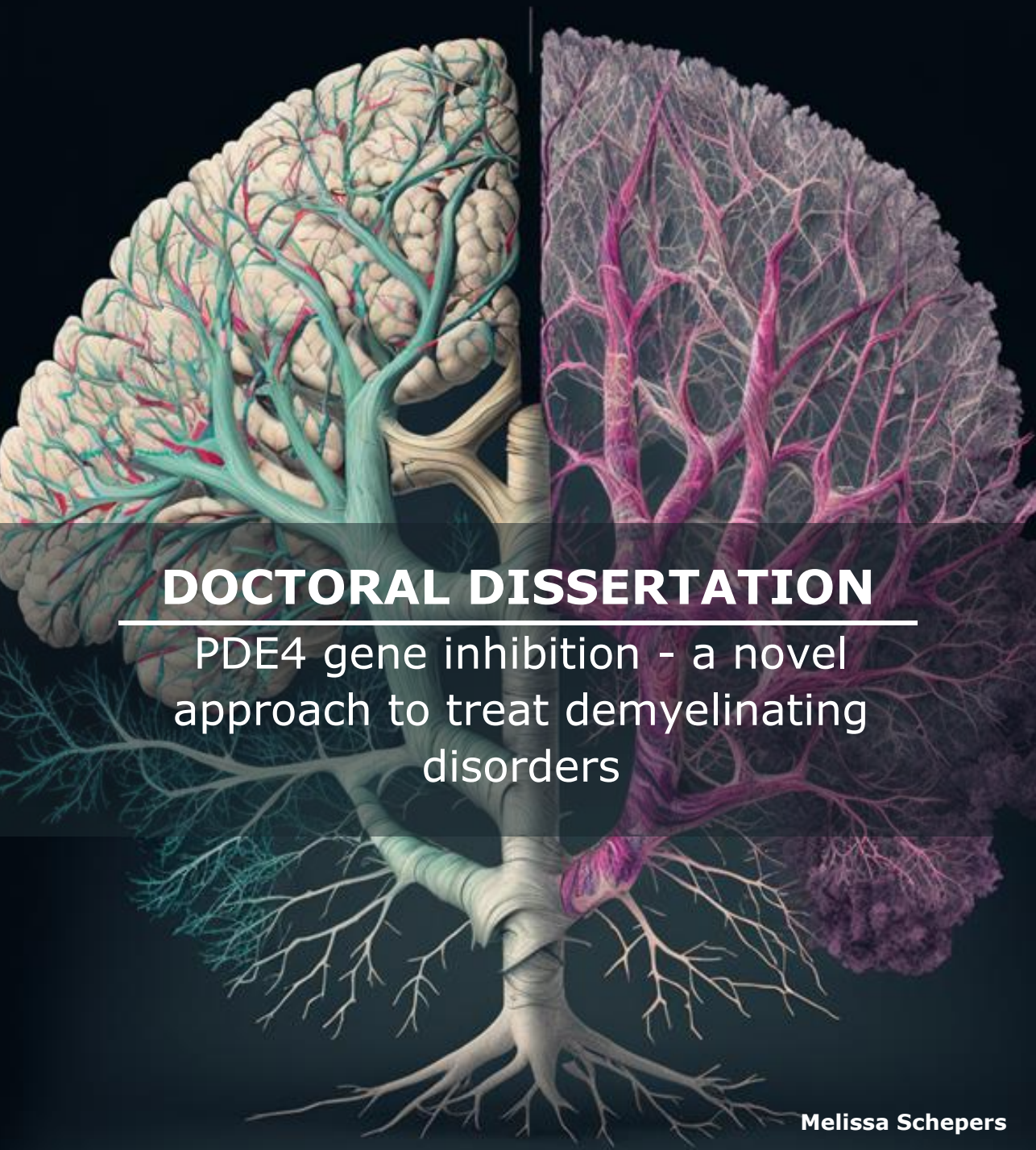

DOCTORAL DISSERTATION

PDE4 gene inhibition - a novel approach to treat demyelinating disorders

Melissa Schepers

Promotores: Prof. Dr Tim Vanmierlo | Hasselt University

Prof. Dr Jos Prickaerts | Maastricht University

Co-promotores: Prof. Dr Niels Hellings |Hasselt University

Prof. Dr Bart Rutten |Maastricht University

PDE4 GENE INHIBITION

A novel approach to treat demyelinating disorders

PROEFSCHRIFT

ter verkrijging van de graad van doctor aan de Universiteit Maastricht,
op gezag van de Rector Magnificus, Prof.dr. Pamela Habibovic

en

de graad van doctor in de Biomedische wetenschappen door de Universiteit Hasselt/tUL,
op gezag van de Rector, Prof. dr. Bernard Vanheusden
volgens het besluit van het College van Decanen,

in het openbaar te verdedigen op maandag 22 mei 2023 om 13.00 uur

door

Melissa Schepers

Promotores

Prof. Dr Tim Vanmierlo (Universiteit Hasselt, Belgium)

Prof. Dr Jos Prickaerts (Universiteit Maastricht, The Netherlands)

Co-promotores

Prof. Dr Niels Hellings (Universiteit Hasselt, Belgium)

Prof. Dr Bart Rutten (Universiteit Maastricht, The Netherlands)

Beoordelingscommissie (UM)

Prof. Dr Daniel van den Hove (Universiteit Maastricht, The Netherlands) (voorzitter)

Prof. Dr Andreas Bock (Leipzig University, Germany)

Prof. Dr Inge Huitinga (Universiteit van Amsterdam, The Netherlands)

Prof. Dr Veerle Somers (Universiteit Hasselt, Belgium)

Doctoraatscommissie (UH)

Prof. Dr Tim Vanmierlo (Universiteit Hasselt, Belgium)

Prof. Dr Jos Prickaerts (Universiteit Maastricht, The Netherlands)

Prof. Dr Niels Hellings (Universiteit Hasselt, Belgium)

Prof. Dr Bart Rutten (Universiteit Maastricht, The Netherlands)

Prof. Dr Bert Brone (Universiteit Hasselt, Belgium)

Prof. Dr Ir. Guy Nagels (Universitair Ziekenhuis Brussel, Belgium)

Doctoraatsjury

Prof. Dr Daniel van den Hove (Universiteit Maastricht, The Netherlands) (voorzitter)

Prof. Dr Inge Huitinga (Universiteit van Amsterdam, The Netherlands)

Prof. Dr Andreas Bock (Leipzig University, Germany)

Prof. Dr Ir. Guy Nagels (Universitair Ziekenhuis Brussel, Belgium)

Prof. Dr Veerle Somers (Universiteit Hasselt, Belgium)

Prof. Dr. Bert Brone (Universiteit Hasselt, Belgium)

Dr Sébastien Foulquier (Universiteit Maastricht, The Netherlands)

Financial support of Maastricht University and Hasselt University for the publication of this thesis is gratefully acknowledged

"Undertake something that is difficult; it will do you good. Unless you try to do something beyond what you have already mastered, you will never grow"

-Ronald E. Osborn.

Table of contents

List of abbreviations

AC	Adenylyl cyclase
ACTB	Beta Actin
AD	Alzheimer's Disease
ALS	Amyotrophic lateral sclerosis
cAMP	Cyclic adenosine monophosphate
AP	Area postrema
ASO	Antisense oligonucleotides
ATP	Adenosine 5'-triphosphate
AU	Arbitrary units
AUC	Area under the curve
BBB	Blood brain barrier
BCA	Bicinchoninic acid assay
BCL2	B cell lymphoma 2
BDNF	Brain-derived neurotrophic factor
BMDM	Bone-marrow derived macrophages
BMEC	Brain microvascular endothelial cells
BMS	Basso mouse scale
BMT	Bone marrow transplantation
BSA	Bovine serum albumin
cGMP	Cyclic guanosine monophosphate
CCR2	Chemokine (C-C motif) receptor 2
CD	Cluster of differentiation
CEL	Contrast enhanced lesions
CFA	Complete Freund's adjuvant
CRISPR	Clustered regularly interspaced short palindromic repeats
CKO	Conditional knock-out
CMAP	Compound muscle action potential
CMT	Charcot-Marie-Tooth
CNS	Central nervous system
COPD	Chronic obstructive pulmonary disease
CPT-cAMP	8-(4-Chlorophenylthio)adenosine 3’,5’-cyclic monophosphate
CRE	CREB response element
CREB	cAMP response element binding protein
CSF	Cerebrospinal fluid
CX3CR1	C-X3-C motif chemokine receptor 1
DAF	Diaminofluorescein-2 diacetate

DAPI	4,6’-diamidino-2-phenylindole
DCX	Doublecortin
DMEM	Dulbecco's modified eagle medium
DMSO	Dimethylsulfoxide
DMT	Disease modifying therapy
DNA	Deoxyribonucleic acid
EAE	Experimental autoimmune encephalomyelitis
ECL	Enhanced chemiluminescence
EDTA	Ethylenediaminetetraacetic acid
ELISA	Enzyme-linked immunosorbent assay
EPAC	Exchange protein directly activated by cAMP
ERK	Extracellular signal-regulated kinase
ESP	Electrospinning
FACS	Fluorescence-activated cell sorting
FBS	Fetal bovine serum
FDA	U.S. Food and Drug Administration
FITC	Fluorescein isothiocyanate
FM	Fluorescein maleimide
FRET	Förster resonance energy transfer
FVD	Fixable viability dye
GC	Guanylyl cyclase
GDNF	Glial derived neurotrophic factor
GFAP	Glial fibrillary acid protein
GFP	Green fluorescent protein
GPCR	G-protein coupled receptor
GSK3	Glycogen synthase kinase 3
GTP	Guanosine 5'-triphosphate
HBSS	Hanks’ balanced salt solution
HCN	Hyperpolarization-activated cyclic nucleotide
HEPES	4-(2-hydroxyethyl)-1-piperazineethanesulphonic acid
HGF	Hepatocyte growth factor
HPA axis	Hypothalamic–pituitary–adrenal axis
HRP	Horseradish peroxidase
HT	Hydroxytryptamine
IC50	Half maximal inhibitory concentration
ICAM	Intercellular adhesion molecule
ICC	Immunocytochemistry
IFN	Interferon
IGF	Insulin-like growth factor

IHC	Immunohistochemistry
IL	Interleukin
IM	Intramuscular
IV	Intravenous
KO	Knock-out
LCM	Laser capture microdissection
LPC	Lysophosphatidylcholine
LPS	Lipopolysaccharide
LTP	Long term potentiation
MAG	Myelin associated glycoprotein
MBP	Myelin basic protein
MCA	Middle cerebral artery
dMCAO	Distal middle cerebral artery occlusion
MDM	Monocyte derived macrophages
MEM	Minimal essential medium
MIF	Macrophage migration factor
MMP	Matrix metalloproteinase
MOG	Myelin oligodendrocyte glycoprotein
MRI	Magnetic resonance imaging
MS	Multiple Sclerosis
NAWM	Normal appearing white matter
NCV	Nerve conduction velocity
NEAA	Non-essential amino acids
NEM	Neural expansion medium
NET	Neutrophil extracellular trap
NG2	Neuron-glial antigen 2
NGC	Nerve guidance conduits
NGF	Nerve growth factor
NMDA	N-methyl-D-aspartate
NO	Nitric oxide
NOS	Nitric oxide synthase
NSC	Neural stem cells
OLG	Oligodendrocyte
OLT	Object location task
OPC	Oligodendrocyte progenitor cells
P (e.g. 3)	Postnatal day (e.g. 3)
PBMC	Peripheral blood mononuclear cell
PBS	Phosphate-buffered saline
PCR	Polymerase chain reaction

PDE	Phosphodiesterase
PDGF	Platelet-derived growth factor
PFA	Paraformaldehyde
PGK1	Phosphoglycerate Kinase 1
PI	Propidium Iodide
PI3K	Phosphoinositide 3-kinase
PKA	Protein kinase A
PKG	Protein kinase G
PLL	Poly-L-Lysine
PLLA	Poly-L-Lactic Acid
PLO	Poly-L-ornithine
PLP	Proteolipid protein 1
PMI	Post mortem interval
PMP	Peripheral myelin protein
PMS	Progressive multiple sclerosis
PN	Peripheral nerve
PNS	Peripheral nervous system
PPMS	Primary progressive multiple sclerosis
PRMS	Primary relapsing MS
iPSC	Induced pluripotent stem cells
PTX	Pertussis toxin
PZS	Perifeer zenuwstelsel
RA	Retinoic acid
RNA	Ribonucleic acid
ROS	Reactive oxygen species
RPL13	Ribosomal Protein L13
RRMS	Relapse remitting MS
RT	Room temperature
S1PR	Sphingosine 1 phosphate receptor
SC	Subcutaneous/Spinal cord
SCI	Spinal cord injury
SD	Standard deviation
SDS,	Sodium lauryl sulfate
SEM	Standard error of the mean
SOD	Super oxide dismutase
SOX10	SRY-Box Transcription Factor 10
SPMS	Secondary progressive multiple sclerosis
STAT3	Signal transducer and activator of transcription 3
TBI	Traumatic brain injury

TBS	Tris-buffered saline
TEM	Transmission electron microscopy
TGF-β	transforming growth factor β
TH17	T helper cell
TIA	Transient ischemic attack
TLR4	Toll-like-receptor-4
TNFα	Tumor necrosis factor α
TTC	2,3,5-Triphenyltetrazolium chloride
UCR	Upstream conserved region
VCAM	Vascular cell adhesion molecule
VEP	Visual evoked potentials
WAT	White adipose tissue
WB	Western blot
WT	Wild-type

CHAPTER 1

Introduction and scope of the thesis

In both the central nervous system (CNS) and peripheral nervous system (PNS), neurons are central to proper functioning of the human body. In the adult human brain, glia cells are as numerous present compared to neurons (1:1) (1, 2). Glia cells are acknowledged as crucial players in nervous system functioning and the most extensively described glia populations include microglia (CNS), and macroglia comprising among others astrocytes (CNS), oligodendrocytes (CNS) and Schwann cells (PNS) (1).

Neurons

Neurons are a specialized group of cells capable of transmitting both electrical and chemical signals throughout the body. The generated signals allow neurons to communicate with each other and other cell types within the body including muscle cells and gland cells. Structurally, neurons comprise of three main parts: a cell body or soma containing the cell's genetic material, branching dendrites extending from the soma which receives signals from other neurons, and a long thin axon carrying signals away from the soma to other neurons or effect cells. The arrangement and number of dendrites and axons can vary depending on the type of neuron (e.g. multipolar, bipolar, pseudounipolar and anaxonic). Through the release and reception of chemical signals, neurons can exchange information at specialized junctions or synapses. Overall, neurons are essential for transmitting information throughout the body and enabling us to sense, think, and act (3). Unfortunately, due to the inability of mature neurons to divide, neuronal destruction often leads to a neurological deficit leaving the nervous system vulnerable to damage from injury or disease (4). In the CNS, the regenerative capacity of neurons and axons is very limited leaving them unable to reconstruct a damaged neuronal circuit (5, 6). However, in contrast to the CNS, neurons with cell bodies located in the PNS are able to regenerate their axons upon damage to a certain degree depending on the severity of injury (7, 8).

Microglia

While neuroglia are typically derived from the neuroectoderm during embryonic development, microglia distinguish themselves from other neuroglia cell types as they are derived from the mesodermic layer which additionally gives rise to blood and immune cells (9). Broadly, in physiological conditions, two key features are attributed to microglia: continuously survey the CNS and respond to injury by mediating immune responses and maintaining CNS homeostasis (1). When external danger signals from invading pathogens or internal danger signals from damaged cells are encountered, microglia initiate a cascade of responses aiming to resolve the injury and thereby protect the CNS (10-12). Microglial activation is characterized by changes in cell surface receptor expression and the release of various inflammatory mediators. Depending on the stimuli, the molecular and phenotypic changes upon microglial activation can have either a protective and tissue-repair effect (anti-inflammatory phenotype), or a detrimental and neurotoxic effect (inflammatory phenotype) as characterized by the phenotypic markers and secreted inflammatory mediators (13, 14). Additionally, microglia have demonstrated to play a central role in maintaining CNS homeostasis through the control of neuronal stem cell proliferation and synaptic remodeling (15, 16). During an individual's lifetime, the number of microglial cells is carefully regulated and maintained through a dynamic balance between local proliferation and apoptosis (17).

Macroglia

The nervous tissue predominantly consists of neurons, microglia and macroglia, with this latter comprising, among others, astrocytes and oligodendroglia (CNS) or Schwann cells (PNS). Astrocytes are the most abundant and numerous type of glia cells in the CNS and play a number of important roles in maintaining the homeostasis of the CNS. In addition to regulating the extracellular ionic and chemical environment, astrocytes function as immune cells in the CNS since they are able to express class II major histocompatibility complex antigens and B7 and CD40 costimulatory molecules essential for antigen presentation and T lymphocyte activation (18). As immune effector cells, astrocytes can influence various aspects of inflammation and immune reactivity in the CNS by secreting a wide array of chemokines and cytokines (18). Upon astrocyte activation, reactive astrocytes populate the site of CNS trauma or disease which are characterized by high GFAP expression, an increased cellular proliferation rate and cellular hypertrophy (19).

Oligodendrocytes and Schwann cells are crucial for providing metabolic and functional support to electrical signal-conducting neurons through the production and maintenance of myelin in the CNS and PNS respectively (1, 20, 21). While oligodendrocytes only operate within the CNS, Schwann cells are capable of entering the CNS to help aiding in the repair of new myelin sheaths around demyelinating axons upon damage (e.g. spinal cord injury) (22). After injury, damaged oligodendrocytes can be replaced by newly formed oligodendrocytes derived from oligodendrocyte precursor cells (OPCs) which proliferate, differentiate and subsequently remyelinate the demyelinated axon (19). The subventricular zone, located around the tips of the lateral ventricles, is the major source of OPC in the adult brain from where OPCs start to migrate to the site of injury where they subsequently stop proliferating and start differentiating into mature myelinating oligodendrocytes (23, 24). However, the myelin regenerative capacity of OPCs is not infinite, as demonstrated by the progressive nature of the CNS disorder multiple sclerosis (MS) (25).

Unlike oligodendrocytes, the differentiation state of Schwann cells is not fixed as a process called dedifferentiation is ascribed to the phenotype of Schwann cells acquired upon injury (26). The ability of Schwann cells to adapt to an injury allows them to convert into premature Schwann cells that further support nerve regeneration through neurotrophic factor secretion (27). Following crushed nerves, Schwann cells are left without contact from axons in the distal stump and for a prolonged period of time until axons are regenerated (27, 28).

Neurodegenerative and demyelinating disorders

In neurodegenerative and demyelinating disorders such as multiple sclerosis (MS), spinal cord injury (SCI), stroke and Charcot-Marie-Tooth (CMT) disease, glial functioning is compromised and/or nervous tissue integrity is lost. Unfortunately, due to the destructive micro-environment created upon nervous tissue damage, the progressive cellular loss in these disorders, and the amitotic nature of neurons, spontaneous endogenous repair process are limited in nature, hence there is medical need for efficient therapeutic strategies capable of supporting glial cell functioning, thereby allowing neuroreparative processes to occur.

Multiple sclerosis

Multiple sclerosis (MS) is a chronic autoimmune disease affecting the CNS of which the exact etiology remains unknown (29). MS pathology is characterized by the infiltration of immune cells into the CNS, including myelin-reactive T lymphocytes, B lymphocytes and macrophages (30-32). Infiltrated B lymphocytes produce auto-antibodies targeting endogenous antigens such as the myelin basic proteins (MBP), proteolipid proteins (PLP) and myelin oligodendrocyte glycoproteins (MOG) (33). Furthermore, T lymphocytes and macrophages present in the CNS will start to produce cytokines and chemokines, thereby recruiting cytotoxic effector cells (34). The coinciding pathological processes lead to chronic inflammation, demyelination of axons, and the loss of myelin-producing oligodendrocytes (29, 35). In relapse-remitting MS (RRMS), remyelination occurs spontaneously through the differentiation of recruited OPCs into mature myelinating oligodendrocytes (36, 37). However, even though OPCs are often still present in CNS lesions, they

eventually fail to differentiate into myelin-producing oligodendrocytes, a process featuring progressive MS (PMS) (38, 39).

Worldwide, about 2.5 million people are currently diagnosed with MS with an incidence rate 2-3 times higher in women compared to men (40). The clinical manifestation of MS can be categorized in four disease patterns. The most frequent form of MS is RRMS (80-85% of the patients), which is characterized by episodes of increasing disability and neurological impairment (relapse) followed by periods of (partial) recovery (remission) (41). Approximately 60% of RRMS patients will evolve into secondary PMS, where symptoms progressively worsen without exacerbations or relapses (42). A small group of patients presents with a progressive form of the disease from onset onwards without exacerbations, which is categorized as primary PMS (10-15% of the patients) (43). Progressive relapsing MS is the least common (less than 5% of the patients) form and is characterized by incomplete recovery following relapses, leading to accumulating neurological impairments and therefore disease progression without true remission (44). Depending on the affected neuroanatomic area, symptoms can highly vary between patients. Overall, the most common symptoms include motoric (e.g. spasms and muscle weakness) and sensory (e.g. vision lost and neuropathic pain) dysfunctions (41). Additionally, 60-65% of the MS patients experience cognitive impairments which mainly affect the level of attention, the speed at which information is processed, and the overall memory performance (45, 46).

Current therapies available for MS patients are primarily directed to temper the overactive immune system in MS. However, the immunomodulatory and immunosuppressive drugs (e.g. IFNβ, dimethyl fumarate, ocrelizumab and natalizumab) currently prescribed are unable to halt or reverse disease progression and mainly result in symptomatic alleviation (47-53). During the early stages of PMS, treatments such as ocrelizumab and siponimod are still effective as they suppress the overactive immune system (54, 55). However, as the disease progresses, no approved therapy has been shown effective in restoring the damaged myelin or neurons in the CNS, emphasizing the need for alternative treatment development (56).

Spinal cord injury

Spinal cord injury (SCI) is a serious and often debilitating neurological disorder that can have lifelong consequences for patients (57). A SCI occurs when the spinal cord is damaged, often as a results of an external physical impact, such as a car accident or a fall, or a non-traumatic impact, such as tumors or infections (58, 59). The pathophysiology of SCI involves a range of cell types, including neurons, macroglia, microglia, neutrophils, lymphocytes and macrophages, and can be divided into two phases (60, 61). The primary injury, which is the initial mechanical damage occurring to the spinal cord, disrupts the blood vasculature and blood-spinal cord barrier at the injury site (62-65). The resulting edema and ischemia subsequently cause additional tissue damage and thereby initiates the secondary injury cascade, which involves a series of destructive events that further expand the injury site (66). The secondary injury cascade results in a disturbance of the ionic balance and an increase in glutamate excitotoxicity, which leads to the production of free radicals and eventually cell death (64). Activated microglia at the lesion site secrete inflammatory factors that further contribute to neuronal and glial cell death (67). In addition, the disruption of the blood-spinal cord barrier allows peripheral immune cells to infiltrate the injury site and participate in the inflammatory responses (67). Activated astrocytes will start to form a glial scar which, initially, helps to restrict the spread of the damage but later on hinders the regeneration of damaged neurons (68, 69). As a result, a persistent inhibitory environment for repair is created, consisting of the glial scar, inhibitor extracellular molecules and chronic inflammation.

Yearly, 250,000-500,000 people suffer from a SCI (58). The most common type of SCI in humans is a compression injury, which occurs when the spinal cord is compressed or squeezed (70). However, regardless of the cause, SCI is typically characterized by motor and sensory deficits that can be either temporary or permanent. Depending on the severity and location of the injury, this can result in partial or complete loss of sensory, motor, and/or autonomic functions below the site of the injury (59). If the injury occurs in the cervical region of the spinal cord, it can cause quadriplegia or tetraplegia (four-limb paralysis), while injuries to the thoracic or lumbar region can cause paraplegia (paralysis of the lower body) (71). In addition to paralysis and loss of sensation, people with SCI often

experience secondary complications such as urinary and bowel dysfunction, chronic pain, and spasticity, which can greatly impact their ability to perform daily activities (72).

To date, regeneration and recovery of function remain limited after SCI (73). Currently, no disease modifying therapies (DMTs) are available for managing SCI pathology. The main treatment strategies for SCI include surgical intervention to stabilize and decompress the spinal cord, physical rehabilitation, and the administration of corticosteroid drugs, such as methylprednisolone, to reduce the secondary injury response. While treatments can be effective in some cases, long-term recovery and perspective are often limited.

Ischemic stroke

Stroke is the second leading cause of death worldwide and a major contributor to permanent disability (74, 75). About 80% of all strokes are caused by a blockage of a major cerebral artery, which results in ischemia and is therefore classified as an ischemic stroke (76, 77). In the ischemic core, blood flow is severely reduced, leading to an imbalance between energy availability and demand, which subsequently leads to excessive cellular breakdown and irreversible tissue death (75, 78). The penumbra, on the other hand, is an area of brain tissue surrounding the ischemic core where blood flow is less severely impaired and the cellular tissue structure might therefore by salvageable (79, 80). During an ischemic stroke, the disturbed blood flow leads to a deprivation of oxygen and nutrient to both the ischemic core and penumbra, triggering an ischemic cascade comprising glutamate induced excitotoxicity, mitochondrial dysfunction and oxidative stress, that leads to acute neuroinflammation and neurological damage (81). The neuroinflammatory reaction following ischemic stroke includes the activation of resident microglia in the penumbra of the infarct, and leukocytes, such as monocytes, neutrophils and lymphocytes, are recruited to the lesion site. The influx and CNS migration of immune cells lead to an inflammatory response that can exacerbate tissue damage and impair recovery (80).

Approximately one in four adults is estimated to experience a stroke at some point in their lifetime and has an incidence rate of 1.5 times higher in men compared to women (82-84). While primary prevention efforts have contributed to a decrease

in the incidence of stroke in high-income countries, an increase in the incidence of stroke is observed in middle- and low-income countries (84). Worrying, however, is that the incidence of ischemic stroke in young adults is on the rise, indicating a need for targeted prevention strategies (84).

Currently, the only treatments available for ischemic stroke are recombinant tissue plasminogen activators (rtPAs) and mechanical thrombectomy surgery, which both can be effective in the acute phase of the ischemic stroke pathology (78). However, as these treatments have a narrow therapeutic window, they cannot be used for treating all ischemic stroke patients, highlighting the need for new therapeutic approaches (78, 85-87). Stroke survivors therefore often experience severe long term complications including motor impairments, dementia, depression and fatigue with minimal future perspectives.

Peripheral neuropathies

The PNS is responsible for transmitting motor, sensory, and autonomic information between the CNS and the limbs, organs, and tissues of the body. A variety of biological and environmental conditions, such as trauma, genetic mutations, chemical stress, infections and metabolic insults, can lead to axonal loss and demyelination, two pathological hallmarks of peripheral nerve degeneration.

Traumatic peripheral nerve injuries can be caused by a variety of different mechanisms including stretch, laceration, and compression. Stretch injuries, also known as nerve stretches occur when the nerve is stretched or torn as a result of trauma or overuse (88). Lacerations are injuries arising when the nerve is cut or severed (89). Finally, compression injuries, also known as nerve compression syndrome is caused when the nerve is compressed or squeezed by external forces (89). After a significant injury to a peripheral nerve, a process called Wallerian degeneration occurs. During Wallerian degeneration, the distal segment of the nerve and its surrounding myelin begins to break down, leading to the loss of connection with the target tissue. Following degeneration and as a first step to regeneration, Schwann cells begin to guide axonal outgrowth by forming aligned cellular tracks called bands of Büngner (90, 91). These bands of Büngner provide a favourable cellular and molecular environment that conduces regrowing axons

via hapotaxis back to their target during early PNS regeneration (90). By creating the bands of Büngner, Schwann cells demonstrate that their functional properties expand those from only providing the insulating myelin layer to actively support nerve repair (92). Overall, traumatic peripheral nerve injuries can have a wide range of symptoms, depending on the type and location of the affected nerve. Current treatment strategies include (pain) medication, physical therapy, and surgical intervention. However, still 50% of patients do not benefit from surgical reconstruction leaving them with a dysfunctional nerve function which highlights the need of new (93).

The most common inherited peripheral neuropathy is Charcot-Marie-Tooth (CMT) disease (94-97). Broadly, CMT can be classified into CMT1 and CMT2. Whereas CMT1 is a demyelinating peripheral neuropathy affecting primarily the myelinating Schwann cells, which will eventually results in axonal loss, CMT2 is characterized by direct axonal degeneration (98). Axon myelination in the PNS is essential to attain rapid saltatory impulse conduction. The multi-layered myelin sheath structure is achieved by wrapping the plasma membrane of Schwann cells around large-caliber axons. This precise arrangement and its integrity are disrupted in CMT type 1 causing malformation or deterioration of the myelin sheath or even demyelination (95). The most common form within CMT type 1 is CMT1A (prevalence ranging from 20-64%). CMT1A is caused by a tandem duplication of the peripheral myelin protein 22 (PMP22) gene (98, 99). Despite the wide range of genetic mutations that can cause CMT pathology in general, the symptoms of the disease are generally similar. People with CMT experience progressive weakness in their limbs, muscle malformations in their feet and hands, and loss of sensation in their extremities due to a length-dependent degeneration of peripheral nerves, which can subsequently lead to difficulties with walking, coordination, and other everyday tasks (100). Treatment for CMT is typically focused on managing the symptoms and may include physical therapy, orthopedic devices, and medications to control pain (101). However, as of to date, no effective treatments have been developed for CMT patients.

Therapies in the pipeline to stimulate neuroreparative processes

Even though great advances have been made regarding the development of new disease modifying treatments, it became clear that there remains a big unmet medical need for effective treatments capable of halting disease progression, stimulate neuro-repair and/or enhance remyelination. Currently, numerous new drugs and treatment options are being tested and clinically evaluated for their effectiveness for treating MS, SCI, ischemic stroke, peripheral nerve injury or CMT1A (Table 1.1).

Currently, 25 drugs are being tested in a phase III clinical trial for treating **multiple sclerosis**. Of those 25, eleven are being evaluated for their remyelination boosting potential. Among others, these include the sphingosine 1 phosphate (S1P) receptor modulators siponimod fumarate and ponesimod. S1PR modulators have previously been demonstrated to act immunomodulatory as they influence immune cell migration. However, growing evidence suggests that S1PR modulators possess mechanism beyond those of immunomodulation, including remyelination (102). In **SCI**, the majority of the therapies currently tested in a phase III clinical study include (stem) cell based treatment strategies focused on stimulating the regenerative process essential for functional recovery. Since the cause of an **ischemic stroke** includes the blockage of a major cerebral artery, it is of no surprise that the majority of phase III drugs for treating ischemic stroke (e.g. Glenzocimab, reteplase and urokinase) are focused on thrombolytic actions. However, alternatively, neuroprotective drugs targeting for example free radical toxicity or inhibiting the interaction between NMDA receptors and PSD95 (e.g. nerinetide and nelonemdaz) are currently evaluated in phase III clinical trials and provide a new therapeutic avenue for treating ischemic stroke. Compared to CNS disorders, peripheral neuropathies are clearly underrepresented regarding the number of treatments in the pipeline. While for **peripheral nerve injury** no treatment is currently being evaluated in a phase III clinical trial, only one drug reached the phase III clinical development stage for treating **CMT1A**. This latter includes a drug with fixed mini-doses of baclofen, naltrexone hydrochloride and sorbitol, thereby acts as a pleodrug targeting multiple biological networks (all data obtained by GlobalData).

Taken together, many new therapeutic strategies are currently in the pipeline for diminishing neuroinflammation, stimulating neuro-repair or enhancing remyelination. However, despite the efforts made over the past years, which resulted in a high amount of marketed drugs for treating for example MS or ischemic stroke, there remains a large unmet medical need effectively treating disease pathophysiology, emphasizing the urgent need for new therapeutic targets.

Table 1.1: Overview of the number of drugs in the pipeline for treating multiple sclerosis, spinal cord injury, ischemic stroke, peripheral nerve injury or Charcot-Marie Tooth disease type 1A (GlobalData extraction 13/12/2022).

Disease area	Development stage	Number of treatments evaluated
Multiple sclerosis	Discovery	52
	Preclinical	246
	Phase I	57
	Phase II	36
	Phase III	25
	Marketed DMT	19
Spinal cord injury	Discovery	10
	Preclinical	55
	Phase I	11
	Phase II	10
	Phase III	4
	Marketed DMT	0
Ischemic stroke	Discovery	15
	Preclinical	94
	Phase I	31
	Phase II	36
	Phase III	16
	Marketed DMT	1
Peripheral nerve injury	Discovery	0
	Preclinical	7
	Phase I	0
	Phase II	2
	Phase III	0
	Marketed DMT	0
Charcot-Marie Tooth disease type 1A	Discovery	4
	Preclinical	7
	Phase I	2
	Phase II	1
	Phase III	1
	Marketed DMT	0

Abbreviations: DMT = disease modifying therapy

Phosphodiesterases

The multifactorial pathogenesis of many neurodegenerative disorders including MS, SCI, and stroke comprise a bi-directional communication between the nervous system and immune system. In line, there is a growing body of evidence indicating that neurodegenerative and demyelinating disorders can be managed by either halting the destructive immunological interplay, stimulating repair processes, or both.

Key in a variety of intracellular processes involved in both neuroregeneration and neuroinflammation is the second messengers cyclic 3'-5' adenosinemonophosphate (cAMP) (103-105). Intracellularly, cAMP is produced from ATP by adenylyl cyclase (soluble or membrane-bound), while being rapidly degraded by a class of enzymes called phophodiesterases (PDEs) (106). The superfamily of PDEs can be classified into eleven families (PDE1-11) based on substrate specificity (cAMP or cGMP), mechanism of regulation, kinetic properties, and subcellular distribution (107, 108). Five PDE families (PDE1, 2, 3, 10 and 11) can hydrolyze and functionally inactivate both cAMP and cGMP, thereby comprise a dual substrate specificity (109). The remaining six PDE families specifically and exclusively hydrolyze cAMP (PDE4, 7 and 8) or cGMP (PDE 5, 6 and 9) (109). The PDE families jointly cover twenty-one PDE genes or subtypes (e.g PDE4A-4D), and, in turn, each subtype can have multiple isoforms (e.g. PDE4D1-9), yielding a total of at least 77 different protein-coding isoforms (**Fig 1.1**) (108). On a cellular level, the different contribution of PDE families, subtypes and subsequently isoforms yields a unique '**PDE fingerprint**' per cell type.

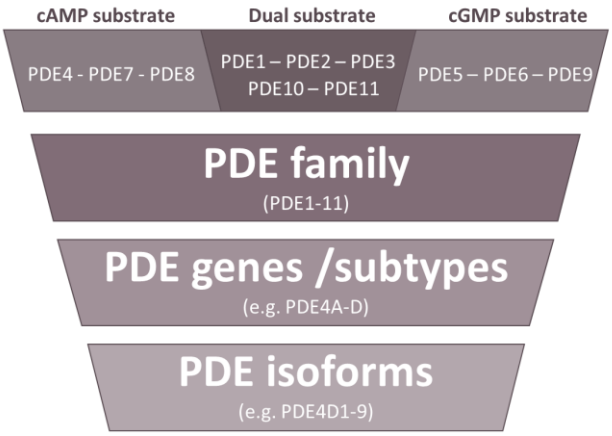

FIG 1.1: Phosphodiesterase (PDE) classification. The PDE superfamily hydrolyzes and thereby functionally inactivates second messengers such as cAMP and cGMP. The superfamily of PDEs can be classified into 11 families, based on among others their substrate specificity. Each family consists of several genes or subtypes and each subtype comprises multiple isoforms. The classification of PDEs up to the gene and isoform level yields a tight and orchestrated control of intracellular second messenger levels.

Of the different families, PDE4 is predominantly expressed in the CNS and immune cells (110-112). In mammals, the PDE4 family comprises four genes, thereby encoding PDE4A, PDE4B, PDE4C, and PDE4D (108, 109). Among these different genes or subtypes, there is high degree of sequence similarity within two regulatory domains (upstream conserved region (UCR) 1 and UCR2) and the enzyme's catalytic domain (**Fig 1.2**) (107-109, 113). Due to alternative promotors and alternative splicing, PDE4 subtypes generate collectively 25 different mRNA transcripts (Table 1.2) (108). The resulting isoforms can be categorized as long, short, and supershort depending on the presence of both UCR1 and UCR2, only UCR2 or a truncated UCR2.

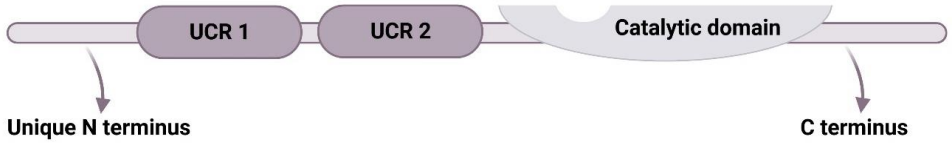

FIG 1.2: Structural overview of phosphodiesterase (PDE) 4. The PDE4 family can be subdivided into four different genes, which share a high degree of sequence similarity within the catalytic domain and regulatory domains UCR1 and UCR2. Due to alternative promotors and splicing events, multiple isoforms are generated comprising either both the UCR1 and UCR2 regulatory domain (long isoforms), only UCR2 (short isoforms) or a truncated version of UCR2 (supershort isoforms), each composing of a unique exon composition at their N terminus.

Table 1.2: Overview of the PDE4 classification

PDE family	PDE gene/subtype	PDE isoforms
PDE4	PDE4A	**Long isoforms:** PDE4A**4**, PDE4A**8**, PDE4A**10**, PDE4A**11**
		Supershort isoforms: PDE4A**1**
	PDE4B	**Long isoforms:** PDE4B**1**, PDE4B**3**
		Short isoforms: PDE4B**2**
		Supershort isoforms: PDE4B**5**
	PDE4C	**Long isoforms:** PDE4C**1**, PDE4C**2**, PDE4C**3**
	PDE4D	**Long isoforms:** PDE4D**3**, PDE4D**4**, PDE4D**5**, PDE4D**7**, PDE4D**8**, PDE4D**9**
		Short isoforms: PDE4D**1**
		Supershort isoforms: PDE4D**2**, PDE4D**6**

Phosphodiesterase 4 as a relevant target for treating neurodegenerative disorders

Orchestrating intracellular cyclic nucleotide signaling pathways has been investigated as a therapeutic strategy in a broad range of diseases, including different types of cancer, dermatological diseases, neurodegenerative disorders and inflammatory diseases (114-116). The second messenger cAMP is a key regulator of immune cell polarization and cellular differentiation-driven processes such as neuro- and myelin-regeneration. Increasing intracellular cAMP levels using cAMP analogues have been shown to increase neurite branching, stimulate neuronal survival, induce oligodendrocyte differentiation, and alter immune cell activation (117-119). The wide range of biological actions mediated by cAMP are mediated by its downstream effector proteins including among others: protein kinase A (PKA), exchange factor directly activated by cAMP (Epac), and hyperpolarization-activated cyclic nucleotide regulated channels (HCN) (**Fig 1.3**) (106, 119, 120). However, exogenous cAMP administration is accompanied by dose-limiting toxicities, including hypercalcemia and hepatotoxicity (121). Therefore, raising cAMP intracellularly needs to be achieved in a controlled and localized manner.

Despite the widespread therapeutic potential of PDE4 inhibition in preclinical research, the development of PDE4 inhibitors for clinical use has been hindered by severed adverse effects such as diarrhea, nausea, and vomiting (122). As a result, only three pan PDE4 inhibitors have been marketed because of their limited adverse effects and include roflumilast (Daliresp), crisaborole (Eucrisa) and apremilast (Otezla), which are used to treat chronic obstructive pulmonary disease, moderate atopic dermatitis, and psoriasis, respectively (109). PDE4 inhibitors have previously demonstrated to act immunomodulatory, stimulate neuroregeneration, and enhance remyelination, rendering them valuable candidates for the treatment of multiple neurodegenerative disorders (123-126). However, unfortunately, due to the high drug concentration required for sufficient CNS penetration, in combination with the widespread expression of PDE4, marketed full PDE4 inhibitors coincide with even more and severe dose-limiting toxicities at their therapeutic dose (127-129).

Therefore, new strategies should be implemented to rule out side effects while retaining the therapeutic potential of full PDE4 inhibitors. Interestingly, PDE4 subtypes and isoforms show distinct cellular distribution profiles (108, 130). Furthermore, PDE4 subtypes and isoforms can be translationally modified and engage specific protein-protein interactions, yielding a variety of confirmation states (an extensive state-of-the art summary of PDE4 biology is provided in our review (108). Inhibition of specific PDE4 subtypes, isoforms, or conformational states thereby renders a more targeted and precise approach to alter intracellular cAMP levels. Disentangling which PDE4 genes and isoforms underly distinct biological actions can therefore create a more targeted approach for modifying key processes in immunomodulation and neuroreparative processes, rendering a new powerful and clinically relevant target for treating multiple neurodegenerative and demyelinating disorders.

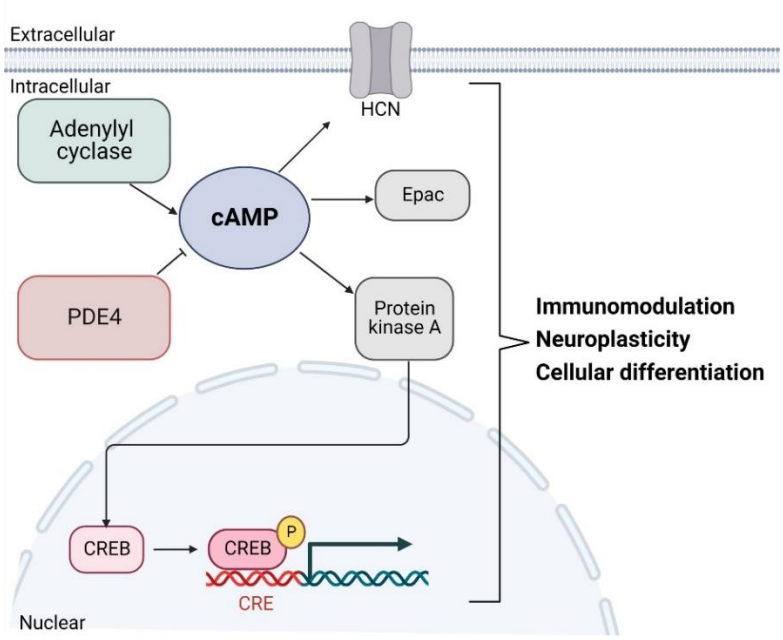

FIG 1.3: Simplified representation of downstream effector proteins of intracellular cAMP signaling. Abbreviations: PDE: phosphodiesterase; HCN: hyperpolarization-activated cyclic nucleotide regulated channel; Epac: exchange factor directly activated by cAMP; CREB: cAMP response element binding protein; CRE: CREB response element.

Scope of the thesis

As outlined above, PDE4 inhibition might be a relevant therapeutic strategy for attenuating neurodegenerative pathophysiology or stimulating neuroreparative processes. However, despite possessing the therapeutic potential, the use of a pan PDE4 inhibitor coincides with emetic side effects hampering its clinical translation. Therefore, the main aim of the current dissertation is to evaluate the therapeutic potential of PDE4 subtype and isoform inhibition as a novel and more targeted approach to treat demyelinating and neurodegenerative disorders, thereby circumventing unwanted side effects (**Fig 1.4**).

MS is the most common demyelinating disorder of the CNS. At best, current treatment strategies are able to slow down disease progression by targeting neuroinflammatory processes, thereby tempering early disease activity (131). However, available therapies have limited efficacy in preventing the transition towards the progressive stage of MS, where they are no longer effective. Hence, there is an urgent need for therapies that halt disease progression and boost repair processes. Second messengers such as cAMP and cGMP have previously been demonstrated to control inflammatory damage and induce CNS repair. Therefore, in **chapter 2**, an overview is provided of the role of PDE inhibition in limiting pathological inflammation and stimulating myelin and neuronal regenerative processes in MS.

The therapeutic potential of PDE4 subtype inhibition as a novel therapeutic agent for targeting distinct processes of MS is further evaluated in **chapter 3**. Using a range of techniques such as primary mouse cell cultures (OPCs and phagocytes), human cell cultures (iPSC-derived OPCs and monocyte derived macrophages), tissue cultures (cerebellar brain slices) and animal models for MS (EAE and cuprizone), the anti-inflammatory and myelination-promoting effect of PDE4B and PDE4D were investigated. Furthermore, the emetic potential of the subtype-specific inhibitors used was evaluated. Finally, using human post mortem tissue, *pde4d* isoform expression patterns were evaluated in neurons and oligodendroglia lineage cells. CRISPR-Cas9 was subsequently used to confirm biological relevance of *pde4d* isoform targeting in mouse derived cell cultures.

Neuroinflammation and neurodegeneration are central processes involved in a wide range of disorders. It is not surprising that PDE inhibitors have been extensively studied in the context of disorders other than MS. Therefore, we next explored the potential of PDE4 subtype specific inhibitors in the context of other CNS disorders. In **chapter 4**, both PDE4B and PDE4D inhibitors have been studied for their anti-inflammatory and regenerative processes in the context of SCI. Using the T-cut hemisection model, a well-defined corticospinal tract lesion was generated and an subsequent inflammatory reaction was elicited. Both functional and histopathological outcomes were evaluated following PDE4, PDE4B, PDE4D or a sequential PDE4 subtype inhibitor administration. Furthermore, PDE4 subtype inhibitors were evaluated for their neuroprotective and neuronal differentiation promoting effects using a luminescent human iPSC-derived neurosphere model. Next, **in chapter 5**, the therapeutic potential of the anti-inflammatory PDE4B inhibitor was evaluated in the pathogenesis of ischemic stroke. Using a proof-of-concept study, the PDE4B inhibitor was administered prophylactically and its effects on infarct lesion size and neuroinflammatory responses were evaluated. Finally, using human neutrophils, part of the neuroinflammatory response was evaluated *in vitro*.

In the PNS, Schwann cells are responsible for establishing myelination. However, besides their myelinating properties, Schwann cells play a crucial role in nerve regeneration following PNS neuropathies as they secrete neurotrophic factors supportive of nerve repair. Even though PDE4 inhibition demonstrated to stimulate *in vivo* axonal outgrowth across a PNS lesion, the direct effect on Schwann cells has not been demonstrated previously. Therefore, **in chapter 6**, the Schwann-cell differentiation promoting properties of PDE4 inhibition have been investigated *in vitro*. Using both 2D and 3D cultures and iPSC-derived neuronal co-cultures, the myelination and neuroreparative phenotype of Schwann cells was investigated. Next, the therapeutic potential of PDE4D subtype inhibition on the peripheral neuropathy CMT disease has been investigated *in vivo* in **chapter 7**. Motoric function evaluation, electrophysiological measurements, and post mortem myelination assessment were combined in a genetic mouse model for CMT1A to evaluate the potential of PDE4D inhibition to treat CMT1A pathogenesis.

To conclude, the main aim of the dissertation is to investigate the therapeutic potential of PDE4 subtype inhibition to treat demyelinating disorders. Different neurodegenerative animal models focusing on MS, SCI, stroke and peripheral neuropathies have been used to investigate the potential clinical relevance of PDE4B or PDE4D inhibitors. The main findings of the current dissertation are summarized and discussed in **chapter 8**.

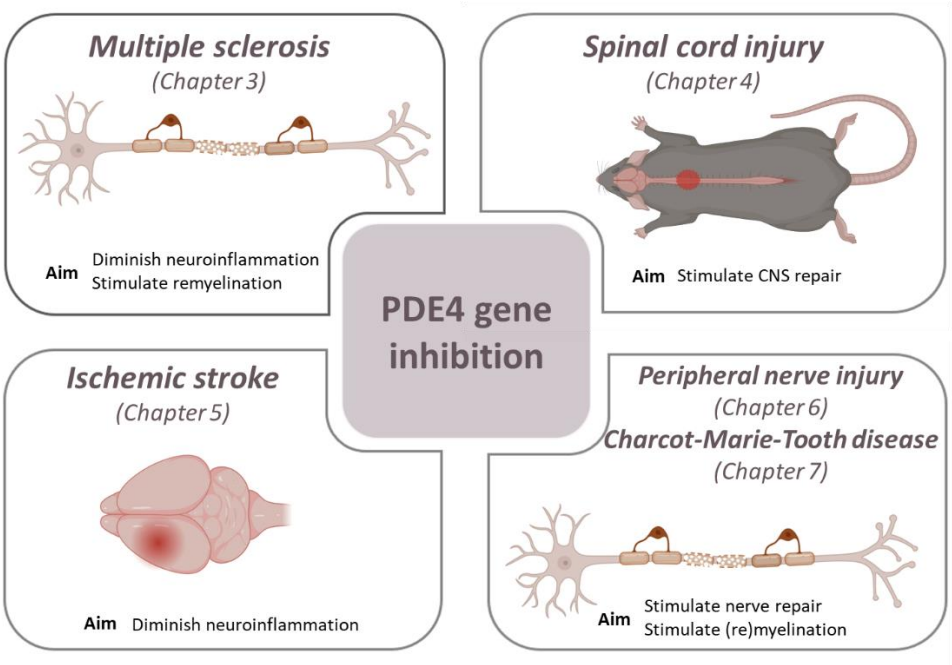

FIG 1.4: Overview of the thesis. The main aim of the dissertation is to evaluate the therapeutic potential of PDE4 subtype inhibition as a novel and more targeted approach to treat demyelinating and neurodegenerative disorders. Different neurodegenerative animal models were used to evaluate the anti-inflammatory and neuroreparative properties of pan PDE4 inhibition, PDE4B inhibition or PDE4D inhibition and included multiple sclerosis (**chapter 3**), spinal cord injury (**chapter 4**), stroke (**chapter 5**), and peripheral neuropathies such as peripheral nerve injury (**chapter 6**) and Charcot-Marie-Tooth disease (**chapter 7**).

CHAPTER 2

Targeting PDEs – towards a tailor-made approach in neurodegeneration and demyelination treatment

Based on:

Targeting phosphodiesterases – towards a tailor-made approach in multiple sclerosis treatment

Melissa Schepers, Assia Tiane, Dean Paes, Selien Sanchez, Ben Rombaut, Elisabeth Piccart, Bart P.F. Rutten, Bert Brône, Niels Hellings, Jos Prickaerts, Tim Vanmierlo

Published in Frontiers in Immunology

Declaration of own contribution:

M.S. performed a literature search and participated in manuscript writing

Abstract

Multiple sclerosis (MS) is a chronic demyelinating disease of the central nervous system (CNS) characterized by heterogeneous clinical symptoms including gradual muscle weakness, fatigue, and cognitive impairment. The disease course of MS can be classified into a relapsing-remitting (RR) phase defined by periods of neurological disabilities, and a progressive phase where neurological decline is persistent. Pathologically, MS is defined by a destructive immunological and neuro-degenerative interplay. Current treatments largely target the inflammatory processes and slow disease progression at best. Therefore, there is an urgent need to develop next-generation therapeutic strategies that target both neuroinflammatory and –degenerative processes. It has been shown that elevating second messengers (cAMP and cGMP) is important for controlling inflammatory damage and inducing CNS repair. Phosphodiesterases (PDEs) have been studied extensively in a wide range of preclinical disease models as they breakdown these second messengers, rendering them crucial regulators. In this review, we provide an overview of the role of PDE inhibition in limiting pathological inflammation and stimulating regenerative processes in MS.

Introduction

Multiple sclerosis (MS) is a chronic immune-mediated demyelinating disorder of the central nervous system (CNS) affecting more than 2.5 million people worldwide, making it the most common neurodegenerative disease in young adults (132). Although the exact etiology remains unknown, MS is thought to develop due to an interplay between susceptibility genes and environmental factors that are yet to be fully elucidated (133). The clinical course of MS is characterized by various clinical symptoms, including gradual muscle weakness, fatigue, and cognitive impairment, which arise in either episodic periods or progress during the disease course (134). Current FDA-approved treatments modulate the prominent immune responses of MS, but are unable to halt disease progression (135). Hence, there is an urgent need for the development of new therapeutic strategies. In recent decades, phosphodiesterase (PDE) inhibitors have shown to exhibit immunomodulatory and neuroprotective functions rendering them interesting candidates for the management of MS disease.

Clinically, MS can be divided in three distinct classifications: relapsing remitting MS (RRMS), primary progressive MS (PPMS) and secondary progressive MS (SPMS). RRMS is the most frequent subtype, affecting approximately 85% of MS patients and can be recognized by periods of remittance (136-138). This early stage of MS is characterized by the presence of active, inflammatory lesions characterized by perivenular infiltration of myelin-reactive lymphocytes and macrophages, resulting in demyelination of the axonal branches (136-138). These inflammatory relapses are followed by the activation of an endogenous repair mechanism called remyelination, resulting in a period of functional recovery (136-138). Fifty percent of RRMS patients undergo a transition to the progressive form of the disease within a period of fifteen years, labelled SPMS (43, 139). Additionally, approximately 15% of MS patients are classified as PPMS and endure gradual accumulation of disability from disease onset without experiencing an initial relapsing course (140). Despite a decrease in frequency of new lesion activity during these chronic stages, there is an accumulation of chronically demyelinated lesions accompanied by an increase in neurological deficits, and a gradual decline in motoric and cognitive function (43). These chronically demyelinated lesions are characterized by a reduced number of oligodendrocytes,

as well as the formation of astrogliotic scar tissue and prominently demyelinated axons, subsequently leaving axons vulnerable to axonal transection (141).

The pathogenesis of MS is thought to be driven by the massive extravasation of myelin-reactive T and B lymphocytes into the CNS across the blood-brain barrier (BBB) (142). Perivenular infiltration of these auto-reactive lymphocytes disturb the homeostatic immune balance in the brain, leading to a pro-inflammatory microenvironment and subsequent CNS damage (143). Despite this, phagocytes are the principle effector cells during the neuroinflammatory and neurodegenerative processes of MS and include infiltrated monocyte-derived macrophages and brain resident microglia and macrophages (144). In MS, the disturbed homeostatic balance in the CNS skews the activation status of macrophages and microglia, subsequently fueling the neuroinflammatory response or ceasing the inflammatory process through exerting neuroprotective functions (145). However, in the early course of MS, neuroinflammation not only induces demyelination but, it also activates remyelination. Early remyelination in active MS lesions is characterized by the expansion and mobilization of oligodendrocyte precursor cells (OPCs) (136-138, 146-149). Despite the presence of sufficient numbers of OPCs in the vicinity of pathological lesions, endogenous repair mechanisms gradually fail when disease progresses, resulting in chronically demyelinated axons embedded in gliotic scar tissue (150-154). When remyelination is not initiated, loss of myelin disrupts axonal function in addition to compromising the physical integrity of axons by increasing susceptibility to inflammatory mediators, glutamate mediated toxicity, and the disrupted trophic support provided by myelinating oligodendrocytes (155). It follows that, axonal ovoids, a hallmark of transected axons, are profoundly present in MS tissue (156).

Interestingly, cyclic nucleotide signaling pathways, such as cyclic 3’-5’ adenosinemonophosphate (cAMP) and cyclic 3’-5’ guanosine monophosphate (cGMP), have been shown to be responsible for a variety of intracellular processes involved in both neuroinflammation and CNS repair processes (103, 104, 157-159). Therefore, orchestrating cellular responses by altering the intracellular balance of cyclic nucleotides can be considered an important therapeutic strategy to modulate the pathogenesis of MS (103, 160). Upon an extracellular trigger, cyclic nucleotides are formed as second messengers to amplify the incoming

signal, subsequently activating protein kinases and ion channels. Cyclic nucleotides orchestrate divergent key cellular processes such as cellular differentiation and maturation (161). cAMP and cGMP are synthesized by adenylyl cyclase (AC) and guanylyl cyclase (GC) respectively. AC converts adenosine 5'-triphosphate (ATP) into cAMP while guanosine 5' triphosphate (GTP) is the substrate for GC to synthesize cGMP. In contrast, intracellular cyclic nucleotide levels are spatiotemporally regulated by the presence of PDEs (103). PDEs comprise a superfamily of enzymes that catalyze the hydrolysis of intracellular cyclic nucleotides. PDEs can be categorized into eleven PDE families (e.g. PDE1-11) that jointly cover twenty-one PDE genes (e.g. PDE4A-PDE4D) (130, 161, 162). Interestingly, each of these genes codes for different isoforms (e.g. PDE4B1-5), yielding a total of at least 77 different protein-coding isoforms. PDE gene families, genes, and isoforms can be distinguished based on their subcellular distribution, enzymatic activity, kinetic properties, and substrate specificity (107, 163). Five PDE families have a dual substrate specificity, meaning they can hydrolyze and inactivate both cAMP and cGMP (PDE 1, 2, 3, 10 and 11) (162). The remaining six PDE families specifically and exclusively hydrolyze cAMP (PDE4, 7 and 8) or cGMP (PDE 5, 6 and 9). The cell type-specific PDE expression of the isoforms yields a specific fingerprint that provides an incentive to develop custom-made PDE-targeting strategies (113, 130, 164). Different small molecules directed against specific PDE families, genes or isoforms have been tested in the context of neurodegeneration, neuroinflammation and CNS repair (104, 158, 159, 165, 166). In this review, we discuss experimental studies and clinical implications regarding PDE inhibition as a strategy for inflammatory damage control and stimulation of related repair processes in MS (**Fig 2.1**).

Inflammatory damage control in active MS lesions by inhibiting PDEs

Ceasing the inflammation that drives the neuroinflammatory and neurodegenerative responses in MS is considered a valuable therapeutic strategy. PDEs have been extensively studied for their anti-inflammatory properties. Several processes can be targeted to diminish the inflammatory response. PDE inhibitors are of interest due to their potential to 1) strengthen the BBB to prevent peripheral lymphocyte accumulation in the CNS, 2) restore the balance between pro-inflammatory and anti-inflammatory mediators including lymphocytes and phagocytes, and 3) prevent astrogliotic scar formation. Each of these potential aspects is further detailed below.

Blood-brain barrier

The BBB is comprised of smooth muscle cells, endothelial cells, pericytes and astrocytic endfeet, functioning as a barrier to restrict the entrance of peripheral immune cells and toxic molecules into the CNS (142). In early MS development, pro-inflammatory lymphocytes activate the endothelial cells of the BBB. Endothelial activation leads to an upregulation of cell adhesion molecules that promote the massive infiltration of myelin-reactive lymphocytes into the CNS (143, 167). Endothelial cells are linked by multiprotein complexes called tight junctions, which become dysfunctional in early MS development. Therefore, restoring the loosened tight junctions, and stabilizing the BBB can prevent further infiltration of immune cells into the CNS, subsequently halting or reducing disease progression.

The involvement of cAMP in endothelial barrier functions has been extensively studied. cAMP analogues, such as dibutyryl cAMP (dbcAMP), can decrease junctional permeability and therefore diminish trans-endothelial transport of both small and large molecules (168). Nevertheless, it is compartmentalized cAMP generation rather than the general accumulation of intracellular cAMP that coordinates barrier preservation or destabilization (169). Vascular permeability is enhanced when cytosolic cAMP is increased, while barrier integrity is maintained when cAMP accumulates in cellular vacuoles (169). In contrast to cAMP, the

outcome of directly increasing cGMP levels on endothelial barrier function is yet to be elucidated. However, indirectly raising intracellular cGMP levels, by increasing NO signaling has been shown to induce vascular smooth muscle relaxation, increase BBB permeability, and inhibit endothelial cell apoptosis (170, 171). Based on these results, increasing cGMP signaling does not seem to be a suitable therapeutic strategy for restoring BBB integrity during inflammatory relapses in MS. Therefore, solely cAMP or dual-substrate PDE inhibitors are discussed here as a therapeutic strategy for reducing BBB disruption.

In particular, the cAMP-specific PDE4 inhibitors have been evaluated for their potential to strengthen the BBB. In experimental autoimmune encephalomyelitis (EAE), a neuroinflammatory animal model for MS, the pan PDE4 inhibitor rolipram (2mg/kg, i.p injected twice a day) modified the cerebrovascular endothelial permeability and thereby restored BBB function (172). The same protective features of rolipram were observed in an animal model for stroke, where treatment preserved the expression of the tight junction proteins occludin and claudin-5 (173). Furthermore, the inhibition of PDE4D is of particular interest for altering BBB permeability since it colocalizes with the endothelial marker RECA-1 and the vascular smooth muscle cells α-SMA (174). However, the exact role of PDE4D in restoring BBB integrity remains to be elucidated. Both cAMP-specific PDE inhibitors and dual-substrate PDE inhibitors have been proposed as potential therapeutic targets. As such, administration of the PDE3 inhibitor cilostazol to a murine model for age-related cognitive impairement (1.5% w/w) over a 3 month period increased the amount of zona occludens protein 1 (ZO-1) and occluding, subsequently improving BBB integrity (175). Therefore, PDE inhibitors acting on the cAMP pathway are predicted to strengthen BBB functionality. Due to the opposing outcomes upon elevating cAMP in different subcellular compartments, elucidating which PDE enzymes are present in endothelial vacuoles and absent in the cytosol can hold the key for identifying which PDE needs to be targeted for restoring BBB integrity. Unraveling essential signaling peptides during translation will become indispensable for determining PDE compartmentalization.

Lymphocytes

Disrupted BBB integrity in MS patients facilitates peripheral immune cell infiltration. The two main subsets of infiltrating T lymphocytes in MS are CD4+ and CD8+ T cells (176). Various subsets of CD4+ T helper cells have been identified based on their cytokine secretion profiles. In particular, CNS Th1 and Th17 cell frequencies are increased in RRMS patients compared to healthy controls. Cytokines secreted by the different T cell subsets are critical mediators of the neuroinflammatory response. Upon activation, Th1 cells aggravate the neuroinflammatory response by secreting pro-inflammatory cytokines (e.g tumor necrosis factor α (TNFα), interleukin 1β (IL-1β) and interferon-γ (IFN-γ)), subsequently promoting cellular infiltration and activation of phagocytes and B cells (177). Th17 cells are mainly characterized by their production of interleukin 17 (IL-17), but exert a polyfunctional phenotype depending on their overall cytokine secretion profile. Pathogenic Th17 cells aggravate inflammatory processes by producing high levels of the pro-inflammatory cytokine IFN-γ, whereas non-pathogenic Th17 cells produce more protective cytokines such as IL-10 (178). IL-17 levels are elevated in the serum and cerebrospinal fluid (CSF) of MS patients and are correlated with MS disease severity, consequently suggesting a pathogenic role of Th17 cells in MS (179, 180). Moreover, regulatory CD4+ T cells (Tregs) from the peripheral blood of RRMS patients show a reduced suppressive capacity, suggesting Treg dysfunction in early MS stages (181). Treg formation is the result of activation of the dominant transcription factor forkhead box P3 (Foxp3) and by producing immunosuppressive cytokines (e.g. transforming growth factor β (TGF-β) and IL-10), Tregs inhibit auto-aggressive T cell responses (182). In addition to CD4+ T cells, autoreactive cytotoxic T cells (CD8+ T cells) are actively involved in MS pathogenesis. CD8+ T cells are found in large numbers in MS lesions in close proximity to damaged oligodendrocytes (183, 184). Therefore, halting MS disease progression can be accomplished by modulating lymphocyte responses through the restoration of second messenger levels using PDE inhibitors.

In the context of T lymphocyte proliferation, differentiation and activation, cAMP is the most extensively studied second messenger. Increasing cAMP levels attenuates the T lymphocyte-mediated immune response by reducing the

production of pro-inflammatory cytokines (e.g. IFN-γ, TNF-α and IL-1β), T cell proliferation and T cell activation (185-187). Increased levels of cAMP further drive the development of Tregs to maintain immunological homeostasis by suppressing the innate immune responses (187). Recently, it has been reported that anti-CD3/CD28 stimulation to activate naïve CD4+ T cells increased the enzymatic levels of PDE7, particularly the expression of the PDE7A1 isoform (188, 189). Accordingly, in EAE mice where T cells are highly activated, the PDE7 inhibitor TC3.6 was shown to increase mRNA levels of FoxP3 and augment the production of IL-10. Additionally, PDE7 inhibition was accompanied by decreased levels of IL-17 and reduced T cell proliferation (190). Conversely, PDE7A knockout mice did not show a difference in T cell activation and cytokine production, obfuscating the role of PDE7 in T cell-mediated immune responses and raising the possibility of an indirect effect of the PDE7 inhibitor TC3.6 (191). PDE4 is the most extensively studied cAMP-specific PDE in the context of modulating pro-inflammatory processes. As observed with TC3.6, inhibiting PDE4 decreased T cell proliferation and reduced the production of pro-inflammatory cytokines (TNF-α and IL-17) while increasing the production of anti-inflammatory cytokines (IL-10) in EAE mice (104, 190). Symptomatic treatment with 2.5mg/kg of the PDE4 inhibitor rolipram decreased the number of perivascular inflammatory infiltrates and was accompanied by a reduction of clinical symptoms in EAE mice (104, 190). Interestingly, upon anti CD3/CD28 costimulation of either human CD4+ naive or memory T cells, the enzymatic activities of PDE4A and PDE4D alone were upregulated, although mRNA levels of PDE4A, PDE4B and PDE4D were increased (112). Furthermore, knockdown of PDE4D in these activated human CD4+ T cells, using siRNA reduced their proliferation rate and inhibited the secretion of IFN-γ (112). In EAE mice, mRNA levels of the PDE4B2 isoform were increased in infiltrating T cells in the CNS (158). This increase in PDE4B2 was positively correlated with FoxP3 and TGF-β mRNA levels, suggesting a modulatory role for PDE4B2 in Treg regulation (158, 190, 192). Based on these findings, cAMP-specific PDE inhibition in T cells can lower the inflammatory cytokine production by acting directly on Th1 and Th17 cells or by regulating the immune response through Treg cells. Furthermore, the dual substrate PDE3 inhibitor cilostazol has been shown to ameliorate encephalitogenic specific T cell responses in EAE mice by reducing lymphocytic proliferation and IFN-γ production in the CNS (193). These findings

are consistent with the previous observations using cAMP-specific PDE inhibitors. Despite this, an involvement of cGMP in T cell regulation cannot be excluded as cGMP has been shown to be highly expressed in the cytoplasm of T cells (194-196). Upon NO treatment, T cell adhesion to ICAM-1 and PECAM-1 on endothelial cells of the human brain microvasculature is reduced in a cGMP-dependent manner (197). Accordingly, increasing both cAMP and cGMP by inhibiting specific PDEs can be considered as a potential therapeutic strategy to limit T cell activation by either lowering the pro-inflammatory cytokine production by Th1 and Th17 cells, or by enhancing the suppressive capacity of Tregs.

Although the perivenular infiltration of B cells is less prominent compared to T cells in MS, their contribution to the pathogenesis is highlighted by the anti-CD20 monoclonal antibody therapy that induces B cell depletion and subsequently limited the number of relapses in RRMS patients (198, 199). B cells exert a central role in the pathogenesis of MS by their antibody-independent functions that can either activate or suppress inflammatory responses (200). However, not much is known about second messenger signaling in B lymphocytes. Opposing results were reported depending on the nature of second messengers in B cell cycling (201). Treating murine B lymphocytes with the neurotransmitter acetylcholine indirectly increased the intracellular cGMP levels by stimulating the NO/cGMP pathway, consequently stimulating B cells to enter the cell cycling stages (201, 202). In contrast, adrenaline-induced intracellular cAMP inhibited the entry of B lymphocytes into the DNA replication stage of the cell cycle (201). The latter is consistent with the observations that forskolin, an activator of AC in the plasma membrane, arrested human B lymphocytes in the G1 phase of cell cycling and thereby inhibited B cell growth (203). Furthermore, forskolin promoted apoptosis in human resting B cells (203). However, there is little evidence that PDE inhibitors are able to modulate B cell responses. The PDE4 inhibitors apremilast, rolipram and Ro 20-1724 did not affected B cell differentiation, however they did inhibit IgE production in human PBMCs after IL-4 stimulation (204, 205). This decrease in IgE production was not observed upon PDE3 or PDE5 inhibition, which can be explained by the marginal PDE3 activity and lack of PDE5 activity in healthy B lymphocytes (204, 206, 207). While there is currently little evidence for a direct effect, indirect effects of PDE inhibitors on B cell responses in the pathogenesis of MS cannot be ruled out.

Phagocytes

Another strategy to control the inflammatory process in MS involves modulating the response of phagocytes in the CNS. In the CNS, phagocytes actively survey the CNS microenvironment in search of harmful pathogens and damage signals (208). In order to retain CNS homeostasis, phagocytes orchestrate different processes including synaptic pruning, shaping neurogenesis, and clearance of cellular debris and apoptotic neurons (209, 210). Depending on the environmental stimuli, phagocytes cover a divergent spectrum of activation states. Upon classical activation (e.g. IFN-γ as activation stimulus), macrophages and microglia polarize towards a more pro-inflammatory phenotype. These classically activated phagocytes contribute to the inflammatory response by producing pro-inflammatory cytokines and chemokines (e.g TNFα and IL-1β) and therefore mediate tissue damage (145). In contrast, upon alternative activation (e.g. IL-4 as activation stimulus), phagocytes polarize towards a more anti-inflammatory phenotype. These alternatively activated phagocytes are characterized by the production of anti-inflammatory cytokines (e.g. TGFβ and IL-10) and growth factors (e.g. IGF and BDNF). Additionally, anti-inflammatory phagocytes facilitate the clearance of cellular debris which enables the initiation of repair processes (145). It is postulated that persistent neuroinflammatory processes create an imbalance between pro-and anti-inflammatory phagocytes, resulting in neurotoxicity and subsequent neurodegeneration (211).

Interestingly, murine studies using EAE have demonstrated that a phenotypic switch of phagocytes from the pro- to the anti-inflammatory phenotype is associated with milder clinical scores (212). Moreover, after focal LPC-induced demyelination, pro-inflammatory phagocytes seem to drive OPC proliferation. However, it is the later switch to the pro-reparative phenotype that is necessary for OPC differentiation into mature myelinating oligodendrocytes that establish functional remyelination (212). Additionally, anti-inflammatory phagocytes are critical contributors in ceasing the inflammatory response and allowing CNS repair (212). Balancing the levels of cAMP and cGMP in phagocytes is considered critical for orchestrating phagocyte polarization and organizing phagocytosis (213). However, abnormally high levels of cAMP inhibit myelin phagocytosis *in vitro*, even though increasing cAMP skews the polarization towards an anti-inflammatory

phenotype characterized by high levels of arginase 1 (Arg1) (213, 214). Furthermore, cGMP has been reported to be associated with the actin cytoskeleton in phagocytes (215, 216) [63, 64]. Stimulating the cGMP-PKG pathway dramatically reorganized the actin cytoskeleton of microglia, giving them a phagocytosis-promoting morphology and subsequently enhanced clearance of apoptotic cells and cell debris (217, 218). In MS, internalization of myelin debris by phagocytes at the lesion site is crucial for allowing endogenous remyelination. Therefore, increasing intracellular cAMP or cGMP levels in phagocytes can either alter the inflammatory responses in the CNS or promote clearance of debris respectively, and can be considered a potential therapeutic strategy for MS.

In murine monocytes and macrophages, the PDE4B gene in particular has been related to inflammatory responses (219). Accordingly, PDE4B inhibition enhanced the secretion of the anti-inflammatory IL-1 receptor antagonist (IL-1Ra) in PDE4B-/- macrophages, at least partially through promoting the phosphorylation and subsequent activation of signal transducer and activator of transcription 3 (STAT3) (220). Furthermore, a positive correlation between PDE4B2 in APC cells (e.g. microglia and macrophages) and the clinical scores of EAE mice was observed (158). Transcriptional upregulation of PDE4B2 is predicted to mediate the activation of the toll receptor-4 pathway, characterized by the production of the pro-inflammatory cytokine TNF-α (221-224). Multiple studies suggest that peripheral inflammation is linked to the development of neuroinflammation (225, 226). In both humans and mice, spinal cord injury (SCI) triggered the expansion of the proteobacteria phylum, leading to an increased systemic endotoxemia that allows LPS from intestinal bacteria to enter the bloodstream, subsequently activating peripheral monocytes and macrophages (226-228). Subsequently, when inducing SCI in PDE4B knockout mice, inflammatory responses and endoplasmic reticulum (ER) stress were significantly decreased within the spinal cord (SC) of these mice, suggesting the critical involvement of PDE4B in (neuro)inflammatory responses potentially occurs by suppressing monocyte and macrophage activation (226). As with SCI, alcohol consumption induces endotoxemia and subsequent peripheral monocyte activation (229). In mice, alcohol-induced endotoxemia induced PDE4B expression in both peripheral monocytes and CNS resident microglia. This induced PDE4B expression was characterized by a decrease in cAMP levels and subsequent glial activation,

indicating a potential pathogenic role of Pde4b in alcohol-induced neuroinflammation (229). Besides PDE4, PDE5 inhibitors sildenafil and vardenfil have been studied for their effects on macrophage phenotype and CNS infiltration. Sildenafil treatment (10 mg/kg, daily s.c injected) improved clinical scores in EAE mice and increased the expression of Ym-1, a canonical anti-inflammatory macrophage marker in the SC of these mice. In addition, PDE5 inhibition promoted phagocytosis of myelin debris (212). Therefore, by inhibiting cAMP-specific PDEs, this pro-inflammatory response can be diminished and disease progression can be halted. In contrast, inhibition of cGMP-specific PDEs does not actively suppress the pro-inflammatory responses of infiltrating macrophages, but rather increases the phagocytosis rate, thereby promoting CNS repair processes.

Moreover, the role of PDEs in macrophage responses has been studied independently of pathological MS processes. For example, PDE3B has been implicated in regulating inflammasome activation of infiltrating macrophages in white adipose tissue (WAT). As such, PDE3B knockout mice displayed reduced serum levels of pro-inflammatory cytokines such as IL1β and TNFα in a peripheral lipopolysaccharide (LPS) challenge. PDE3B ablation significantly reduced macrophage infiltration in WAT of high fat diet-induced obesity mice (230). Additionally, PDE4 inhibition has been shown to reduce clinical symptoms of inflammatory diseases including arthritis and psoriasis by shifting the phenotypic balance of phagocytes (231-233). PDE4 inhibition with apremilast reduced dermal fibrosis by interfering with the release of IL-6 by anti-inflammatory macrophages. This resulted in a decreased fibroblast activation and collagen release in a skin fibrosis mouse model (234). The beneficial effects of PDE inhibition by macrophages that infiltrate the peripheral tissues give rise to multiple implications that are potentially exploitable in those that infiltrate the CNS. Understanding the role of PDE3B ablation as well as the inhibition of PDE4 and PDE5 in promoting macrophage phenotypic shifts in other pathological contexts can be implicated for controlling the phagocyte-related inflammatory responses in MS pathogenesis.

In microglia, PDE4 is the predominant negative regulator of cAMP (235). Roflumilast-mediated PDE4 inhibition increased the mRNA and protein levels of Arg1, skewing polarization of an anti-inflammatory phenotype in myelin-laden microglia, subsequently promoting repair processes in aged rats subjected to

chronic cerebral hypoperfusion (236). Inhibiting PDE4 suppresses LPS-mediated release of TNF-α and NO by activated microglia (222). However this reduction in NO production is abolished when co-culturing microglia with neurons, casting doubt upon this mechanism *in vivo* (222). Furthermore, the novel PDE4 inhibitor FCPR03 suppressed the release of pro-inflammatory cytokines (TNF-α, IL-1β and IL-6) *in vitro* in LPS stimulated BV2 microglia, and *in vivo* in the hippocampi and cortices of mice peripherally treated with an LPS bolus (237). Interestingly, inhibition of neuroinflammation was abolished when BV2 microglia were pretreated with a PKA inhibitor H89 (237), indicating that the cAMP-downstream PKA/CREB signaling pathway may be responsible for the suppressed production of pro-inflammatory cytokines upon FCPR03 treatment (237). Moreover, the cAMP/PKA signaling pathway inhibits NF-κB, thereby further suppressing neuroinflammation (237). The novel PDE4 inhibitor roflupram enhanced autophagy in both BV2 microglia and in microglia of mice peripherally injected with LPS (238). Autophagy is a process critically involved in maintaining homeostasis as it modulates inflammasome activation and IL-1β production by removing damaged mitochondria (239). Damaged mitochondria are an important source of ROS production that subsequently activates NLRP3-mediated inflammasome activation and IL-1β production (239). By inducing autophagy, roflupram suppressed inflammasome activation and IL-1β, consequently reducing neuroinflammatory responses in LPS challenged mice (238). Similar effects on autophagy and inflammasome activation were observed when PDE4B was specifically knocked down in primary microglia cells (238). The likely involvement of PDE4B in suppressing inflammatory responses is reinforced by the observation that ABI-4, a PDE4D-sparing PDE4 inhibitor, has been shown to reduce the release of TNF-α in LPS stimulated primary murine microglia (240). Likewise, presymptomatic treatment with the PDE7 inhibitor TC3.6 reduced microglial activation in an animal model for PPMS by decreasing a wide range of mediators of the neuroinflammatory processes including IL-1β, TNF-α, IFN-γ and IL-6 in the SC (241). Furthermore, increasing intracellular cGMP levels by inhibiting PDE5 after LPS stimulation decreased microglial NO, IL-1β and TNF-α production (242). In line with this, the PDE5 inhibitor sildenafil alleviates hippocampal neuroinflammation by normalizing microglial morphology and reducing microglial activation as shown by a diminished IL-1β production (243-245). Moreover, the

highly selective PDE10A inhibitor TP-10 reduced the number of CD11b+ reactive microglial cells in the striatum and thereby ameliorated brain pathology in an animal model for Huntington's disease, demonstrating its therapeutic potential in MS pathology (246). Furthermore, 10 μM Ibudilast, a non-selective PDE inhibitor targeting multiple PDE families (e.g. PDE4 and PDE10), suppressed TNF-α production in activated microglia but lacked efficacy in lowering other pro-inflammatory mediators such as IL-1β or IL-6 (247). Therefore, inhibiting PDEs independently of their substrate specificity in microglia diminishes pro-inflammatory responses and microglia reactivity.

Taken together, different PDE inhibitors can be considered a powerful therapeutic option for ceasing the inflammatory response in MS by altering the balance between cytotoxic and reparative phagocytes. Particularly PDE4B was shown to be critically involved in neuroinflammatory responses, making it an interesting target for developing MS therapies. Furthermore, PDE4B is upregulated in phagocytes following peripheral inflammation, and subsequently aggravates neuroinflammatory responses; a key process in the pathogenesis of MS. Therefore, interfering with this peripheral-central immunological cross-talk by inhibiting specifically PDE4B is an interesting strategy for treating RRMS patients that needs to be explored further.

Astrocytes

Astrocytes are the most abundant cells of the CNS and exert pleiotropic functions to protect and support other CNS cell types (248, 249). Due to their ideal position in the brain microvasculature, astrocytes can directly respond to infiltrating immune cells during the initial processes occurring in MS (250). Astrocytes produce growth factors and metabolites in order to maintain the homeostatic balance in the brain, but also ensure synaptic and BBB integrity (248, 249). However, during profound CNS injury, astrocytes become highly activated and undergo morphological and functional changes, yielding astrogliosis (251).

In an attempt to investigate whether PDEs are implicated in astrogliosis, it was shown that TLR signaling induced an upregulation of PDE4B, and more specifically increased the protein level of the PDE4B2 isoform (252). Accordingly, twice daily administration of ibudilast (20 mg/kg), a non-specific PDE inhibitor with

preferential affinity for PDE4, reduced astroglial activation in an animal model for Parkinson's disease (253). The same results were observed in a rat model for ocular hypertension, in which a decrease in gliosis was accompanied by decreased levels of pro-inflammatory mediators and enhanced neuroviability (254). Interestingly, ibudilast treatment was also demonstrated to prevent astrocyte apoptosis by increasing cGMP levels, suggesting a potential protective role for cGMP-specific PDE inhibitors (255). In line with this hypothesis, PDE5 inhibition by administering 10 µM sildenafil was shown to restore LPS-induced inflammation in astrocytes *in vitro*, as demonstrated by De Santana Nunes et al. (256). In relation to BBB disruption and immune cell infiltration, it is known that astrocytes express lymphocyte adhesion molecules such as ICAM-1 and VCAM-1 in inflammatory states (257). Elevation of intracellular cAMP levels counteracts the inflammatory activation of astrocytes, resulting in a downregulation of these adhesion molecules (258). As such, astrocytic cAMP signaling plays a prominent role in the prevention of peripheral lymphocyte infiltration. Aforementioned studies show that PDEs are greatly involved in the inflammatory aspect of astrocyte biology and that inhibition of selected PDE isoforms can result in the attenuation of astrogliosis.

Inhibiting PDEs to boost repair in chronically demyelinated MS lesions

Neuroinflammation and axonal demyelination associated with MS render neurons more vulnerable to degeneration. Stimulating repair in chronically demyelinated MS lesions is a promising strategy for treating progressive MS patients. The main processes to be addressed for boosting this repair include the stimulation of OPC differentiation into myelinating oligodendrocytes, remodeling of the existing neuronal circuits by enhancing neuro-plasticity/-protection to strengthen axonal conduction, and resolving inflammation that allows for phagocytic growth factor secretion (discussed above).

Oligodendrocytes

In the CNS, the myelinating cells responsible for remyelination are oligodendrocytes which function to maintain neuronal integrity, and facilitate signal conduction in the brain and spinal cord (259, 260). However, oligodendrocytes are known to be extremely vulnerable to damaging signals, such as neuro-inflammatory attacks or ischemic episodes (261, 262). Loss of oligodendrocytes can result in axonal damage and ultimately leads to demyelination and subsequent neurodegeneration. In an attempt to restore this loss of oligodendrocytes, newly myelinating cells can be formed by differentiation of OPCs into mature myelinating oligodendrocytes (260).

cAMP is a key driver of OPC differentiation (118). *In vitro* treatment of OPCs with cAMP analogues, such as dbcAMP or 8-bromo cAMP, support OPC differentiation based on the number of myelin basic protein (MBP) positive cells (263). A similar level of differentiation is observed when using forskolin (264). Accordingly, cAMP-specific PDE inhibitors are thought to stimulate oligodendrocyte development. Treatment of human OPCs with the PDE7 inhibitors TC3.6 or VP1.15 promotes their survival and accelerates their differentiation into mature myelinating oligodendrocytes by stimulating the ERK signaling pathway (265). In parallel, the potent PDE4-inhibitor rolipram (0.5 μM) was shown to boost rat OPC differentiation *in vitro* by increasing the percentage of MBP+ cells (118). Furthermore, based on G-ratio analysis, rolipram (0.5 mg/kg/day) enhanced remyelination in the caudal cerebellar peduncle following focal ethidium bromide-induced demyelination *in vivo* (118). In the presence of myelin-associated inhibitors, OPC differentiation is impaired *in vitro* due to an impairment in Erk1/2, p38MapK and Creb1 phosphorylation. However, 0.5 μM of rolipram treatment overcame the inhibitory effects of myelin protein extracts *in vitro* and relieved the induced differentiation block (118). Interestingly, daily administration of 0.5 mg/kg rolipram (by means of s.c. placed minipump) also appeared to protect oligodendrocytes from secondary cell death following experimental SCI, thereby highlighting its multifaceted mode of action during neurodegeneration (266). In relation to oligodendroglial cell death following ischemia, Nobukazu Miyamoto and colleagues administered 0.1% of a PDE3 inhibitor mixed in regular chow diet up to 28 days to rats suffering from chronic cerebral hypoperfusion. At a cellular

level, this resulted in a strong increase of newly generated oligodendrocytes and a subsequent enhanced rate of remyelination in hypoperfusion-induced white matter lesions after bilateral common carotid artery ligation. Even though PDE3 is classified as a dual cAMP/cGMP hydrolyzing enzyme, Miyamoto and colleagues solely investigated the PDE3 inhibition-mediated increase of cAMP and therefore attributed the positive effects on ischemic white matter injury mostly to a cAMP/PKA-mediated pathway (267). Nevertheless, a role for cGMP involvement cannot be excluded in oligodendrocyte differentiation processes. In particular, an increase in nitric oxide (NO)-induced cGMP signaling has been shown to be directly related to oligodendrocyte maturation as determined by an increased MBP and MOG protein expression level (268). The observed increase of maturation supports the rationale that cGMP-specific PDE inhibitors can also exert a positive effect on oligodendrocyte-mediated repair mechanisms. Accordingly, treatment of organotypic cerebellar brain slices with the widely known PDE5 inhibitor, sildenafil (1 µM) for 10 days enhanced the level of remyelination (212). Additionally, in the SC of EAE mice, treated with 10 mg/kg sildenafil once a day for 15 consecutive days (subcutaneous injection), oligodendrocyte maturation was induced in a cGMP-NO-protein kinase G (PKG)-dependent manner (212). Furthermore, sildenafil appeared to have a protective effect in a mouse model for demyelination, as demonstrated by a preserved myelin and axonal ultrastructure (269). Yet, these protective features of sildenafil are inconsistent with the findings of Muñoz-Esquivel and colleagues. Here, it was reported that sildenafil treatment diminished myelin expression and increased the expression of negative regulators of myelin (Id2 and Id4), which was consistent with the decreased myelination capacity of sildenafil treated oligodendrocytes (270).

Opposing results regarding the *in vitro* effects of sildenafil on OPC differentiation can be potentially attributed to the difference in inhibitor concentrations. In a later study conducted by Muñoz-Esquivel and colleagues, an inhibition in myelin protein expression was observed after 7 days of 50 µM sildenafil treatment. The myelination-promoting effects of sildenafil in organotypic cerebellar brain slices were observed after 1µM treatment for 10 days. Furthermore, the diminished expression of myelin proteins after sildenafil treatment was observed in pure primary rat OPC cultures, while organotypic cerebellar brain slices contain multiple cell types. Therefore, an indirect effect of sildenafil for promoting remyelination

cannot be ruled out. This difference in treatment regimens is a potential explanation for the observed differences and underscore the importance of cGMP fine-tuning. Altogether, both cAMP and cGMP specific PDE inhibitors have been shown to be promising stimulators for OPC differentiation that boosts CNS repair in MS. However, validating these findings in multiple *in vitro* and *in vivo* models for remyelination is essential before further clinical development.

Neurons

The lack of myelin in both acute and chronically demyelinated lesions has profound pathophysiological consequences. For instance, Na+ channels are redistributed over the demyelinated axolemma as a final compensatory mechanism of neurons in order to maintain nerve conduction although the myelin sheath is lost (271). Progressive axonal and neuronal loss associated with MS eventually causes weakening of neural circuits leading to cognitive and motor impairments (272). Therefore, neuroprotection or repair of neuronal damage may delay, halt or counter disease progression.

Stimulation of cyclic nucleotide signaling has been shown to increase neuronal resilience by promoting neuroplasticity. Inhibition of PDEs may therefore be an appropriate strategy to induce neuroprotection in MS. Inhibition of specific PDEs is found to enhance neuroplasticity, subsequently increasing neuronal resilience. Vinpocetine, a selective PDE1 inhibitor, can limit oxidative stress and neuronal damage in a model of vascular dementia (273). PDE2 inhibition was found to improve neuronal plasticity, as observed by an increase in hippocampal long term potentiation (LTP), which is regarded as the underlying physiological correlate of memory (274). The increase in LTP was accompanied by improved object memory performance, both in rats and mice (275). After induction of brain ischemia (276) or in animal models using chronic unpredictable stress (277), the PDE2 inhibitor Bay 60-7550 attenuated the pathological decrease in neuroplasticity related proteins (e.g. BDNF), thereby enhancing neuroplasticity and subsequently neuroprotection. Cilostazol, a PDE3 inhibitor, mediates neuronal repair after induced neuronal loss in the dentate gyrus through an increase in pCREB-mediated hippocampal neural stem cell proliferation (278). The potential of PDE4 inhibition to stimulate neuroplasticity has been studied extensively in the context

of learning and memory (163, 279, 280); both non-specific inhibition of the PDE4 gene family (281), as well as targeting of individual PDE4 genes (282) or isoforms (283) are able to increase neuroplasticity and memory functioning. Moreover, neuroprotective and neuroregenerative effects by inhibition of PDE4 have been shown after different types of insults, including SCI (157, 284, 285), striatal neurotoxicity (286-288) and mouse models of Huntington's disease (288, 289). Similarly, PDE5 inhibition by sildenafil and vardenafil can not only improve object memory (290, 291), but also protect against striatal degeneration by stimulation of neuronal surviving pathways, including BDNF and p-CREB expression (292). Interestingly, sildenafil treatment (15 mg/kg administered orally) reduces oxidative stress in mice exposed to noise stress through an increase in free radical scavengers such as super oxide dismutase (SOD) 1, SOD2 and SOD3 (293). Additionally, PDE7 inhibition was found to induce neuroprotective and anti-inflammatory activities in a rat model of Parkinson's disease (294). A reduction in hippocampal apoptosis was also observed after PDE7 inhibition in an Alzheimer mouse model (295). Alzheimer-associated decreases in dendritic spines and plasticity can be counteracted by PDE9 inhibition (296). Finally, PDE10 inhibition increases neuronal survival in a transgenic mouse model of Huntington's disease (297).

As described above, neuroprotective treatment strategies can be achieved by targeting distinct PDE families or isoforms, given the wide applicability of PDE inhibitors to suppress damaging signals such as neuronal apoptosis and oxidative stress, but also to stimulate neuronal survival and repair. Furthermore, inhibition of these PDEs is primarily associated with an improvement in cognitive performance including memory and learning. This latter aspect makes PDE inhibition even more interesting, considering cognitive decline is one of the major symptoms of disease progression in MS (298). However, while inhibition of different types of PDE enzymes has been shown to be beneficial in several models, the exact mechanisms underlying its neuroprotective effects are yet to be elucidated in the context of MS.

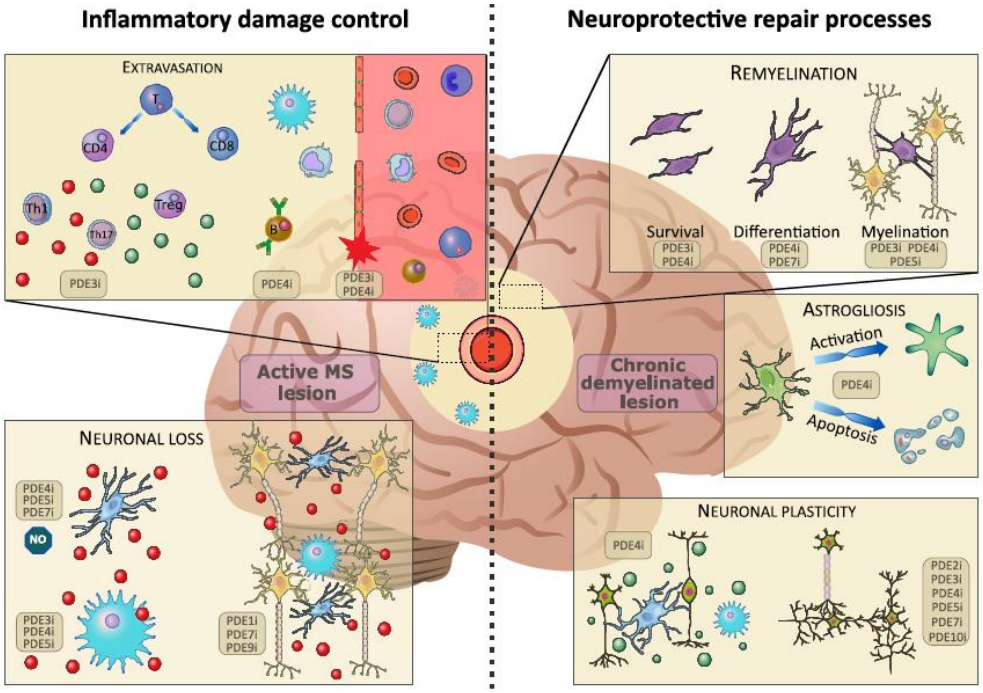

FIG 2.1: The effects of PDE inhibition on different cell types in inflammatory damage control (active lesion) and neuroprotective repair processes (chronic demyelinated lesion). Upon disruption of the blood-brain-barrier (BBB), patrolling immune cells (monocytes, T- and B-lymphocytes) extravasate into the central nervous system. Here, the immature cells differentiate and elicit their functions in the inflammatory environment. A broad spectrum of pro- (red) and anti-(green) inflammatory cytokines are found in the active lesion. Inhibition of PDEs has been found to positively influence BBB integrity, B-cell functioning and T-cell expression patterns, skewing them towards an anti-inflammatory phenotype. The inflammatory environment causes activation of microglia and infiltrating macrophages, which contributes to excessive neuronal loss. Inhibition of PDEs counteracts this inflammatory activation and promotes neuronal survival. In chronic demyelinated lesions, the inhibition of PDEs has been found to ameliorate remyelination, thus supporting endogenous repair mechanisms. Furthermore, PDE inhibition counteracts astrogliosis by halting activation and apoptosis of astrocytes. Finally, inhibition of a multitude of PDEs has been found to promote neuronal plasticity and skew microglia and infiltrating macrophages towards an anti-inflammatory phenotype. Images were modified from Reactome icon library and Servier Medical Art, licensed under a Creative Common Attribution 3.0 Generic License (299).

PDE inhibitors in clinical trials as a therapy for MS

It is clear that PDEs are involved in numerous and different processes in MS. Currently, the majority of MS therapies are focused on reducing disease severity by preventing the infiltration or activation of immune cells in the CNS (table 2.1). However, these therapeutics are unable to halt or reverse disease progression. Therefore, there is an urgent need for the development of new therapeutic strategies. The multimodal effects of PDE inhibitors makes them highly interesting for clinical use to treat MS patients. However, most research regarding PDE inhibitors to date has been performed at the preclinical level and very few clinical trials have been conducted to assess their clinical potential (table 2.2).

In early 2001, a Phase I/Early Phase II clinical trial was designed to test the dose, tolerability and efficacy of the PDE4 inhibitor, rolipram as a treatment against CNS inflammation for MS patients (300). In the first stage of the study, six MS patients were enrolled to assess the optimal and safe dose of the compound. Two additional patients with moderate inflammatory brain activity were recruited for the second stage of the study. Even though no difference in clinical disability was observed, rolipram was not well tolerated by the patients. Adverse events such as nausea, vomiting, gastroesophageal reflux and insomnia were common during the therapy. Moreover, rolipram treatment was accompanied by the unexpected side-effect of an increase in the total amount of contrast enhanced lesions (CEL) per patient when compared to their baseline state demonstrating it has no clinical benefit. As this was the predetermined primary outcome of the study, the trial was terminated in an early phase (300).

Similarly, a double blind, placebo-controlled phase II trial was conducted to evaluate the safety and effects of Ibudilast as a treatment strategy for RRMS patients (301). As discussed above, ibudilast is a non-selective PDE inhibitor that also inhibits the macrophage migration inhibitory factor and toll-like receptor 4 (302, 303). Patients who enrolled in the study received either 30 mg, 60 mg ibudilast or a placebo every day for one year. No difference in lesion activity was observed between the different groups, resulting in an unmet primary endpoint. However, ibudilast treatment seemed to slow brain atrophy, a measure of permanent tissue injury and disease progression in MS (301). Consequently in

2013, the SPRINT-MS phase II clinical trial was established to assess the efficacy and tolerability of ibudilast as a treatment for progressive MS patients (304). Both PPMS and SPMS patients were recruited in the study and received either 50 mg ibudilast or a placebo, twice daily for 96 weeks. The recently published results show that upon ibudilast treatment, the rate of brain atrophy was slowed by 48%. However, as with rolipram, treatment with ibudilast was accompanied by adverse events such as gastrointestinal symptoms, headaches and depression (304).

In 2004, a pilot study was initiated to investigate whether the PDE5 inhibitor, sildenafil citrate, improves cerebral blood perfusion in MS patients (305). MS patients frequently experience a compromised cerebral blood flow which can lead to neuronal cell death. Therefore, it was hypothesized that blood flow perfusion can be increased in these patients through treatment with sildenafil citrate. Both MS patients and healthy volunteers were recruited for this study. MRI scans of the cerebral arteries were taken at baseline prior to treatment, as well as one hour after sildenafil citrate administration (305). Even though the study was completed within two years, the results and outcomes of the trial are yet to be disclosed.

At present, ibudilast is the only PDE inhibitor that has yielded positive results in a clinical setting. The ongoing SPRINT-MS study will validate whether the observed effects of ibudilast on brain atrophy are reproducible, and if it is associated with slower disease progression (304). However, even though ibudilast targets different PDE families, it preferentially targets PDE4 (306). As seen with rolipram, targeting PDE4 in humans is associated with strong adverse effects such as nausea and vomiting, which can compromise the potential use of such inhibitors in clinical settings. There is therefore an urgent need to develop and assess the beneficial effects of PDE isoform inhibitors for their beneficial effects in clinical trials for MS.

Table 2.1: Overview of marketed drugs for the treatment of MS

Drug name	Indication	Route of administration	Mode of action
Alemtuzumab	RRMS	IV	Immune modulation
Cladribine	RRMS/SPMS	Oral	Cellular energy depletion
Daclizumab (withdrawn)	RRMS	SC	T lymphocyte inactivation
Dimethyl fumarate	RRMS	Oral	Anti-inflammatory; neuroprotective
Fingolimod	RRMS/SPMS	Oral	Reduced infiltration of pathogenic lymphocytes into the CNS
Glatiramer acetate	RRMS	SC; IM; IV	Immune modulation
Interferon beta-1a	RRMS/PPMS	IM; SC; IV	Immune modulation
Interferon beta-1b	RRMS/PPMS/SPMS	SC	Immune modulation
Lemtrada	RRMS	IV	T lymphocyte depletion
Mitoxantrone	RRMS	IV	Immune suppressive
Monomethyl fumarate	RRMS/SPMS	Oral	Immune modulation; diminish neurodegeneration
Natalizumab	RRMS	IV	Immune modulation; anti-inflammatory; antineoplastic
Ocrelizumab	RRMS/PPMS	IV	Prevention B lymphocyte activation
Ofatumumab	RRMS	SC	Immune modulation (B lymphocyte)
Ozanimod	RRMS/SPMS	Oral	Immune modulation
Peginterferon beta-1a	RRMS/PPMS	SC	Immune modulation
Ponesimod	RRMS	Oral	Reduced infiltration of pathogenic lymphocytes into the CNS
Siponimod (fumarate)	RRMS/SPMS	Oral	Immune modulation
Teriflunomide	RRMS/PPMS	Oral	Immune suppression

MS multiple sclerosis; RRMS relapse remitting MS; PPMS primary progressive MS; SPMS secondary progressive MS; IM intramuscular; IV intravenous; SC subcutaneous (GlobalData extraction 22/12/2022)

Table 2.2: Overview of (pre-)clinical studies with PDE inhibitors for the treatment of MS

Drug name	Indication	Route of administration	Mode of action	Target	Status
AP-1	MS	Oral	Immune modulation	PDE7 and GSK3B	Preclinical
Ibudilast	PPMS; SPMS	Oral; ophthalmic	Anti-inflammatory; neuroprotective	Non-selective PDE inhibitor	Phase II
Revamilast	MS	Oral	Immune modulation	PDE4	inactive
Rolipram	MS	Oral	Facilitates neural transmission; immune modulation	PDE4	Inactive
Sildenafil	RRMS/SPMS	Oral	Increase blood flow	PDE5	Phase II
Small molecules to inhibit PDE7	MS	Oral	Immune modulation	PDE7	Inactive
TDP-101	MS	/	Immune modulation	PDE4B	Preclinical

MS multiple sclerosis; RRMS relapse remitting MS; PPMS primary progressive MS; SPMS secondary progressive MS; PDE phosphodiesterase; GSK3B glycogen synthase kinase 3 beta (GlobalData extraction 25/05/2019)

PDE inhibitors in other neurodegenerative disorders

Neuroinflammation and neurodegeneration are central processes involved in a wide range of CNS disorders. Based on the aforementioned cellular effects, it is not surprising that PDE inhibitors have been extensively studied in the context of disorders other than MS. Therefore, multiple lessons can be drawn from studies conducted in other disorders and may be implemented when devising therapeutic applications of PDE inhibitors in MS. Although neuroinflammatory and neurodegenerative processes are identical in many disorders, the underlying pathological causality is highly diverse. Therefore, relevant findings supporting the role of PDE inhibitors in other CNS disorders do not provide conclusive results, but rather show the potential of PDE inhibitors in treating MS. Here we will briefly discuss the potential of PDE inhibitors for treating CNS trauma , stroke and peripheral nerve repair, and their relevance for treating MS.

PDE inhibition following CNS trauma – spinal cord injury

After CNS trauma such as SCI, a chronic neuroinflammatory response occurs that impairs neuroregeneration. PDE4 inhibition has been shown to reduce inflammatory processes in monocytes and lymphocytes (307). Considering the role of these infiltrating immune cells in the pathophysiology of SCI, there have been many studies further investigating the effect of PDE4 inhibition. It was demonstrated that PDE4 inhibition increases axonal regeneration using the PDE4 inhibitor rolipram (266). Moreover, Whitaker et al. found that rolipram protected oligodendrocytes against secondary cell death. Furthermore, it was shown that spinal cord oligodendrocytes express PDE4A, B and D, while microglia predominantly express PDE4B (266). Bao et al. have also demonstrated that PDE4 inhibition decreased white matter damage, oxidative stress and leukocyte infiltration, resulting in cellular protection and locomotor improvements after SCI (307). In addition to PDE4, PDE7 inhibition was also studied in the context of SCI. PDE7 is expressed on both macrophages and neurons (308, 309). *Paterniti et al.* sought to determine the effect of PDE7 inhibition on secondary processes after SCI. Their data demonstrated that PDE7 reduced spinal cord inflammation, tissue injury, neutrophil infiltration, oxidative stress, and apoptosis after SCI (309). Cognitive impairment is an additional effect of neurodegeneration. PDE4 inhibition

can also affect cognitive behavior after trauma. This was demonstrated after traumatic brain injury (TBI), where rolipram rescued the cognitive impairment in rats with TBI, an effect that might be attributable to increased CREB activation during learning (310).

PDE inhibition following CNS trauma – stroke

Two major hallmark in stroke are neuroinflammation and neurodegeneration. Depending on the type of CNS lesion, stroke can be classified into two types: ischemic stroke (70-85% of the cases) and hemorrhagic stroke (15-30% of the cases) (75, 77, 311). In ischemic stroke, the severely impaired cerebral blood flow deprives neurons from nutrients and oxygen, leading to neuronal free radical production, mitochondrial dysfunction and oxidative stress (75, 120, 312). The resulting neuronal apoptosis and necrosis results in massive neuronal cell death, which subsequently activates a downstream neuroinflammatory cascade by activating resident microglia and recruiting leukocytes towards the infarct region (81). Therefore, modulation of neuroprotective and/or neuroinflammatory processes by targeting PDEs may hold therapeutic potential in light of treating (ischemic) stroke. Inhibition of PDE4 was shown to diminish neuroinflammation, thereby reducing infarct size and improving neurological deficit scores by directly affecting innate immunity during the acute phase of ischemic stroke (173, 313-318). Both PDE7 and PDE8 inhibition lower T cell responses, thereby affecting the adaptive immune reactions and potentially be of therapeutic interest during a more chronic phase of the disease (120, 319). The role of PDE inhibition to diminish neuroinflammation as a therapeutic strategy for ischemic stroke is more elaborative described in a review by Ponsaerts et al. (120).

Besides diminishing the neuroinflammatory response following stroke, stimulating neuroregenerative processes using PDE inhibition could improve stroke outcome. Indeed, enhancing axonal projection regeneration by inhibiting PDE2A stimulated peri-infarct neuronal connectivity, thereby enhancing motor recovery (320). Moreover, inhibiting PDE10A regulated long-term post-infarct brain remodelling and plasticity by enhancing neuronal survival and neurogenesis (321). Via stimulating the cGMP/PKG/CREB pathway, the PDE9A inhibitor LW33 decreased

SH-SY_5Y neuronal apoptosis and improved cognitive functioning in a stroke animal model (322).

The promising results of PDE inhibition in CNS trauma are consistent with the previously described potential of these inhibitors in MS treatments. Reduced neuroinflammatory responses, increased axonal regeneration and decreased oxidative stress levels upon PDE inhibition can all halt or prevent disease progression of MS. Furthermore, PDE4 inhibition additionally rescued cognitive impairment in pathological circumstances. Given that 40-65% of MS patients experience cognitive impairments (323), PDE4 inhibition would not only reduce pathological hallmarks in the CNS of MS patients, but would also directly reduce a prominent MS-related symptom.

PDE inhibition to induce peripheral remyelination

Little is known about the therapeutic role of PDE inhibition in stimulating peripheral nerve (PN) repair and Schwann-cell mediated (re)myelination. In the peripheral nervous system (PNS), cAMP regulation via PDE4 activity plays a crucial role, particularly in the events involved in nerve repair (324). The therapeutic efficacy of PDE4 inhibition for stimulating PN regeneration was demonstrated as 0.4µmol/kg/h rolipram infusion stimulated peripheral nerve guide after surgical nerve transection, which resulted in faster regrowth of both motor and sensory nerve fibers across the lesion site in rats (325). Regarding myelination, 8 weeks of 5mg/kg rolipram administration restored the peripheral myelination pattern in Rac1 conditional KO mice (326). However, no decisive conclusions of the therapeutic property of PDE4 inhibition on Schwann cell functioning directly can be drawn from these findings as no *in vitro* experiments have been conducted before directly evaluating the effect of PDE inhibition on Schwann cells. Based on the abovementioned findings of PDE inhibition on oligodendrocyte differentiation in the CNS, it, however, is worthwhile further exploring the therapeutic potential of PDE(4) inhibition on Schwann cell maturation and subsequently PNS myelination in peripheral nerve repair or peripheral neuropathies (e.g. Charcot-Marie-Tooth (CMT) disease).

Concluding remarks

The role of PDE inhibitors to modulate neuroinflammatory and neuroreparative processes has gained tremendous interest over the last several years. It is becoming clear that targeting of PDE families can modify multiple cellular key players involved in a variety of processes involved in MS pathogenesis. Due to this multifactorial effect, inhibiting a single PDE family is often accompanied with severe side effects, hampering their translation for a clinical application. Nevertheless, different PDE families are shown to be beneficial in different phases of MS. For example, in the initial phase of MS when BBB integrity is lost, not cGMP but rather cAMP-specific PDE inhibitors are considered a viable therapeutic strategy. Elevating cAMP levels in endothelial cells increased the expression of tight junctions, while elevating cAMP levels in astrocytes decreased the expression of adhesion molecules, subsequently creating a synergistic effect that prevents peripheral lymphocyte infiltration into the CNS via the BBB. During RRMS, there is already an ongoing active pro-inflammatory response. Therefore, disease progression may be halted through the use of cAMP-specific PDE inhibitors to either directly modulate Th1 and Th17 responses or to increase Treg populations to regulate immune homeostasis. Elevating cAMP levels in phagocytes diminishes the secretion of pro-inflammatory cytokines and subsequently lowers the pro-inflammatory phenotype of these cells. Before CNS repair can be initiated in MS patients, myelin debris needs to be internalized at the lesion site by these phagocytes. However, the phagocytic properties of these cells are not stimulated by the increase of intracellular cAMP levels, but rather by the increase of cGMP levels specifically. Therefore, cGMP-specific PDE inhibitors are considered a potential therapeutic strategy for promoting repair processes in later stages of MS. In the context of OPC differentiation, both cAMP and cGMP specific PDE inhibitors have shown their potential. However, these findings require replication be validated and the potential of the inhibitors should be explored further in the context of progressive MS. Finally, enhancing neuroplasticity is considered a possible strategy for promoting functional recovery in MS patients. Multiple PDE inhibitors have been shown to be neuroprotective and to enhance neuroplasticity *in vitro* and *in vivo*, however their efficacy in the context of MS remains unexplored.

Although promising results were obtained in pre-clinical studies, contradictory results were observed in PDE KO animals compared to pharmacological inhibition. However, directly comparing these findings is difficult given the developmental differences in these animals due to the permanent absence of the PDE enzyme throughout the animal's life. Compensatory mechanism are potentially being activated early in the life of PDE KO animals causing an increased expression of other PDE families, genes or isoforms. The development of conditional KO animals can therefore lead to new promising results to confirm the involvement of specific PDEs in pathological conditions. Furthermore, clinical studies using PDE inhibitors often show severe side effects due to the multifactorial effects of PDE inhibitors on multiple cellular processes. PDE isoforms show specific cellular compartmentalization, creating distinct signalosomes within different cells. Therefore, identifying which PDE genes and isoforms underlie distinct pathogenic processes in MS can create a more targeted approach for modifying specific key players during different phases of MS. As such, targeting specific PDE isoforms can further lower the occurrence of adverse events. Taken together, identifying the key PDE families, genes and isoforms involved in specific phases and processes may lead to the development of a tailor-made approach for treating MS.

Acknowledgments

MS, JP and TV have a proprietary interest in selective PDE4D inhibitors for the treatment of MS. The authors sincerely thank Joanna Randall for editing the paper.

CHAPTER 3

Inhibiting PDE4 subtypes in multiple sclerosis

Based on:

Selective PDE4 subtype inhibition provides new opportunities to intervene in neuroinflammatory versus myelin damaging hallmarks of multiple sclerosis

Melissa Schepers, Dean Paes, Assia Tiane, Ben Rombaut, Elisabeth Piccart, Lieve van Veggel, Pascal Gervois, Esther Wolfs, Ivo Lambrichts, Chiara Brullo, Olga Bruno, Ernesto Fedele, Roberta Ricciarelli, Charles ffrench-Constant, Marie E. Bechler, Pauline van Schaik, Wia Baron, Evy Lefevere, Kobi Wasner, Anne Grünewald, Catherine Verfaillie, Paulien Baeten, Bieke Broux, Paul Wieringa, Niels Hellings, Jos Prickaerts* and Tim Vanmierlo*

*Equally contributing senior authors

Published in Brain, Behavior and Immunity

Declaration of own contribution:

M.S. contributed to the experimental design, data generation (with support of co-authors) and analysis, interpretation and manuscript writing

Graphical abstract

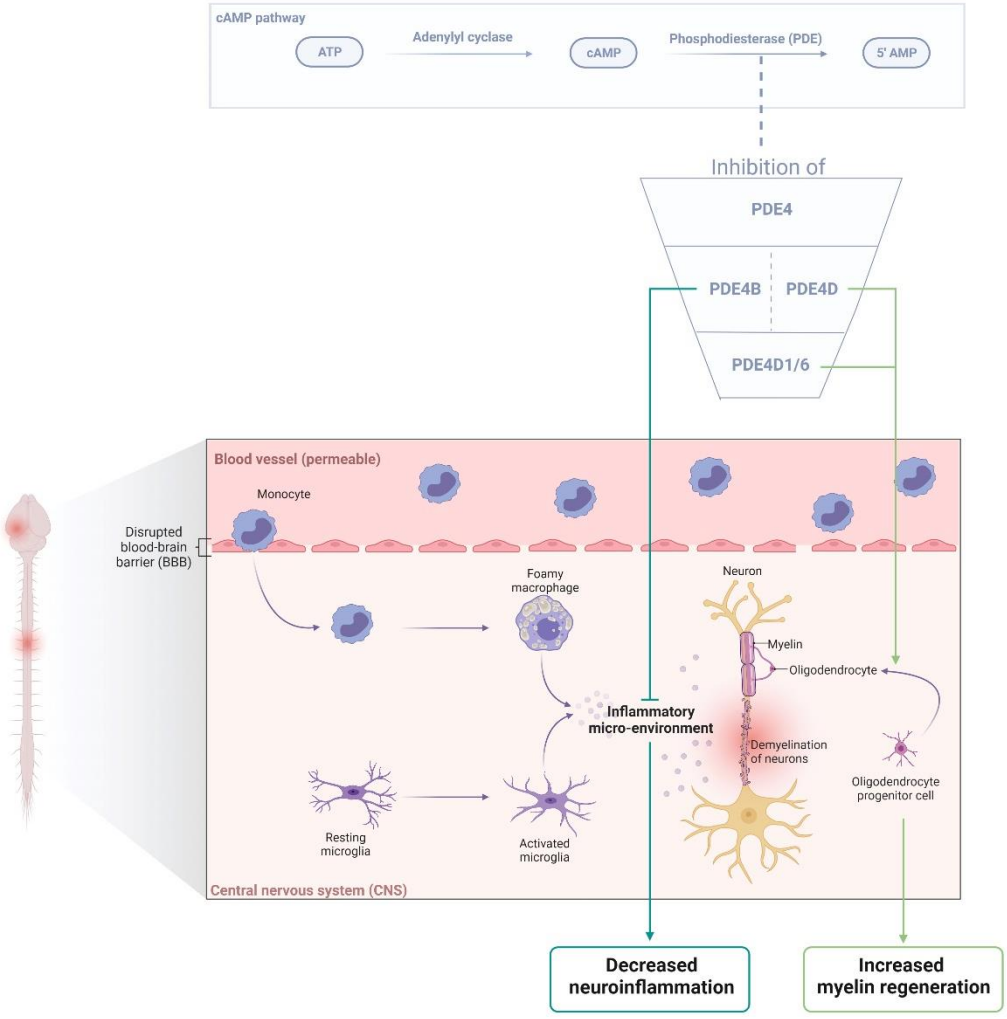

Graphical abstract. Figure created in BioRender.

Abstract

Multiple sclerosis (MS) is a chronic autoimmune disease of the central nervous system (CNS) characterized by focal inflammatory lesions and prominent demyelination. Even though the currently available therapies are effective in treating the initial stages of disease, they are unable to halt or reverse disease progression into the chronic progressive stage. Thus far, no repair-inducing treatments are available for progressive MS patients. Hence, there is an urgent need for the development of new therapeutic strategies either targeting the destructive immunological demyelination or boosting endogenous repair mechanisms. Using *in vitro*, *ex vivo,* and *in vivo* models, we demonstrate that selective inhibition of phosphodiesterase 4 (PDE4), a family of enzymes that hydrolyzes and inactivates cyclic adenosine monophosphate (cAMP), reduces inflammation and promotes myelin repair. More specifically, we segregated the myelination-promoting and anti-inflammatory effects into a PDE4D- and PDE4B-dependent process respectively. We show that inhibition of PDE4D boosts oligodendrocyte progenitor cells (OPC) differentiation and enhances (re)myelination of both murine OPCs and human iPSC-derived OPCs. In addition, PDE4D inhibition promotes *in vivo* remyelination in the cuprizone model, which is accompanied by improved spatial memory and reduced visual evoked potential latency times. We further identified that PDE4B-specific inhibition exerts anti-inflammatory effects since it lowers *in vitro* monocytic nitric oxide (NO) production and improves *in vivo* neurological scores during the early phase of experimental autoimmune encephalomyelitis (EAE). In contrast to the pan PDE4 inhibitor roflumilast, the therapeutic dose of both the PDE4B-specific inhibitor A33 and the PDE4D-specific inhibitor Gebr32a did not trigger emesis-like side effects in rodents. Finally, we report distinct *pde4d* isoform expression patterns in human area postrema neurons and human oligodendroglia lineage cells. Using the CRISPR-Cas9 system, we confirmed that PDE4D1/2 and PDE4D6 are the key targets to induce OPC differentiation. Collectively, these data demonstrate that gene specific PDE4 inhibitors have potential as novel therapeutic agents for targeting the distinct disease processes of MS.

Introduction

The chronic autoimmune disease multiple sclerosis (MS) is characterized by the infiltration of myelin-reactive T-cells, B-cells, and infiltrating macrophages in the central nervous system (CNS) (30-32). Subsequent pathological processes encompass chronic inflammation, demyelination of the axons, and loss of myelin producing oligodendrocytes (29, 35). In relapse-remitting MS (RRMS), spontaneous remyelination occurs by differentiation of recruited oligodendrocyte progenitor cells (OPCs) into myelin-producing oligodendrocytes (36, 37, 327, 328). Although abundantly present in many CNS lesions, OPCs eventually fail to differentiate into mature myelinating oligodendrocytes. This failure and incomplete remyelination are features of progressive MS (PMS) (38, 39, 327). Early disease activity in RRMS patients is suppressed by immunomodulatory treatment strategies that aim to suppress the autoimmune-induced demyelination (329, 330). Yet, in spite of treatment, about 50% of the RRMS patients will develop into secondary PMS patients within a time frame of 10 to 15 years following disease onset (43, 139). Additionally, approximately 10-15% of MS patients endure gradual accumulation of disability from disease onset, without experiencing an initial relapsing course. These patients are classified as primary PMS patients (43). During the early stages of PMS, treatments such as ocrelizumab and siponimod are still effective as they suppress the overactive immune system (54, 55). However, as the disease progresses, no approved therapy has been shown effective in restoring the damaged myelin or neurons in the CNS (56).

3’-5’-cyclic adenosine monophosphate (cAMP) has been described to possess prominent immunomodulatory and myelin regenerative functions (331, 332). Phosphodiesterases (PDEs) catalyze the hydrolysis of second messengers such as cAMP and cGMP to regulate the spatiotemporal presence and activity of second messengers intracellularly. PDEs comprise eleven enzyme families (PDE1-11) that hydrolyze the cyclic nucleotides cAMP and/or cGMP. The PDE4 family is the most prominently expressed cAMP-specific PDE family in immune cells and oligodendrocytes. The four different PDE4 subtypes (PDE4A, B, C and D) each encodes for multiple transcriptional variants (e.g., PDE4D1-PDE4D9) (108, 266, 333-336). The generated PDE4D isoforms share a particular amino acid similarity

(upstream conserved region (UCR) 1, UCR2 partially and the catalytic domain), but can be distinguished based on their unique N-terminal amino acid sequence (337, 338). PDE4 isoforms can be categorized as long, short or supershort based on the inclusion of both the UCR1 and UCR2, UCR2 only or a truncated UCR2 region as regulatory domains (123). The molecular biology of the different PDE4 enzymes is described and visualized extensively by Paes et al. (108). Indeed, several preclinical studies have shown the efficacy of different pan PDE4 inhibitors for diminishing neuroinflammation in experimental autoimmune encephalitis (EAE) and enhancing remyelination in the cuprizone model, which are two well-established animal models of MS (118, 300, 339). Recently, a phase II double-blinded clinical trial with the small molecule ibudilast, which inhibits PDE4 as well as PDE10, toll-like-receptor-4 (TLR4) and the macrophage migration factor (MIF), demonstrated a 48% reduction in brain parenchymal fraction in PMS patients indicating a reduction in brain atrophy (304, 340). Although generally well tolerated, patients treated with ibudilast did report a higher incidence of gastrointestinal disorders (304, 340). In line, clinical studies with pan PDE4 inhibitors were prematurely terminated due to adverse events such as vomiting, nausea, and gastroesophageal reflexes (158, 300). Interestingly, PDE4 genes (e.g. *PDE4A-D*) and isoforms (e.g. *PDE4B1-PDE4B5* and *PDE4D1-PDE4D9*) show distinct cellular expression patterns and intracellular compartmentalization, and can therefore offer a more targeted approach for controlling neuro-inflammation, neuro-regeneration, and remyelination, thereby enhancing the therapeutic potential and diminishing side effects accompanied with pan PDE4 inhibition (108, 341).

To overcome the emetic effects of full PDE4 inhibitors, yet maintain the anti-inflammatory and regenerative potential, PDE4 subtype inhibition can be considered unique therapeutic targets. PDE4B has been described to be primarily related to the modulation of inflammatory responses (158, 192, 219, 226). As such, *pde4b* expression is highly increased in monocytes upon inflammatory stimulation. PDE4B inhibition has been shown to promote phosphorylation and thus mediate activation of STAT3 (signal transducer and activator of transcription 3) (220). In infiltrated regulatory T cells, the negative correlation found between *pde4b2, FoxP3* and TGF-β levels, suggest an immunomodulatory role of PDE4B2 (158, 182, 192). On the contrary, the PDE4D-sparing PDE4 inhibitor ABI-4 did not

affect inflammatory processes in murine microglia cultures, excluding a direct role for PDE4D in inflammation (240). Alternatively, PDE4D-specific inhibition has been largely related to improved memory and neuroplasticity (342-348). However, despite being a therapeutic target, it is hypothesized that especially PDE4D is responsible for the emetic side effects upon pan PDE4 inhibition since *PDE4D* is highly expressed in the area postrema, the chemoreceptor trigger zone for emesis in the brainstem, compared to other PDE4 genes (349). In line, complete *PDE4D* gene deletion resulted in increased emetic-like behavior in rodents (129, 349). Yet, the second generation PDE4 inhibitor roflumilast showed less emetic side effects compared to the first generation PDE4 inhibitor rolipram, and, interestingly, PDE4D-specific inhibitors such as Gebr7b, Gebr32a and BPN14770 did not result in emesis up to 100-fold of their effective memory enhancing dose (281, 282, 350, 351). The reduced emetogenic potential in these new generation PDE4(D) inhibitors is likely due to the different affinity for the individual *PDE4D* isoforms expressed in the area postrema, as distinct isoforms show specific intracellular localization indicating different biological roles (108).

Consequently, we hypothesized that by selectively targeting PDE4 gene products, i.e., specifically PDE4D and PDE4B, the therapeutic potential of PDE4 inhibition in relation to MS can be specifically directed towards remyelination or inflammation, without triggering emetic side effects. In this study, we show that selective inhibition of PDE4D increased OPC differentiation and remyelination. We further demonstrate distinct *pde4d* isoform expression profiles in human area postrema neurons and human MS oligodendroglia lineage cells. Moreover, we demonstrate that targeting PDE4B halts inflammatory damage by suppressing neuro-inflammatory responses in the EAE animal model of MS without affecting remyelination. Interestingly, the therapeutic dosage of both the PDE4B inhibitor (A33) or PDE4D inhibitor (Gebr32a) did not show emetic side effects in the xylazine-ketamine wake-up test, a surrogate test for emesis in rodents, nor did it increase the *ex vivo* action potential firing rate of neurons in the murine area postrema. To our knowledge, this is the first study demonstrating that selective PDE4D and PDE4B inhibition provides new opportunities to safely intervene in either the myelin damaging or the neuro-inflammatory hallmarks of MS to induce CNS repair.

Materials and methods

Animals

For EAE induction, 10-week old female C57BL/6J OlaHsd mice were obtained from Envigo (the Netherlands) and were housed in groups upon arrival. For the cuprizone experiment, eight-week old male C57BL/6J OlaHsd mice were obtained from Envigo (the Netherlands) and were housed individually. All animals were housed in a controlled temperature environment (21-22°C) with an inverse day-night rhythm (lights off 7a.m., lights on 7p.m) and ad libitum access to food and water. A radio, which was playing softly, provided background noise in the room. The experiments were conducted in accordance to the guidelines of EU Directive 2010/63/EU on the protection of animals used for scientific purposes. All experiments were approved by the local ethical committee at Hasselt University for animal experiments (matrix ID: 201551; 201652; 201836; 201976; 202035).

Cuprizone

After one week of acclimatization, male C57BL/6J OlaHsd mice were subjected to a cuprizone or control diet. Cuprizone (Bis(cyclohexanone)oxaldihydrazone) (Sigma- Aldrich, United States) was mixed at an 0.3% w/w end concentration in crushed chow. Weight changes were monitored daily throughout the experiment. Treatment was initiated two days preceding the cuprizone stop, and continued for 9 additional days. At the end of the experiment, animals were sacrificed via transcardial perfusion (PBS/heparin) after lethal dolethal injection (200mg/kg). Brains were collected and post-mortem fixated via overnight 4% PFA immersion. After immersion, a sucrose gradient was used for cryoprotection (10%, 20%, 30%) after which brains were frozen in liquid nitrogen.

Roflumilast, A33 and Gebr32a treatment

Where indicated, animals received a twice a day subcutaneous injection containing roflumilast (1 mg/kg or 3 mg/kg) (BioLeaders)(IC_{50} PDE4: 0.2-4.3 nM (352)), Gebr32a (0.1 mg/kg or 0.3 mg/kg) (University of Genova) (IC_{50} PDE4D isoforms: 1.16-4.97 µM (351)), or A33 (3mg/kg) (Sigma-Aldrich) (IC_{50} PDE4B: 27 nM (353)) dissolved in DMSO (1:1000; vehicle) (VWR prolabo) (223, 351). Compounds were further diluted in 0.5% methylcellulose and 2% Tween80.

Functional readout

Object location task

The object location task (OLT) was performed during the pre-motoric phase of the EAE (4 and 10 d.p.i) and during the cuprizone experiment (during demyelination phase (6 weeks cuprizone) and remyelination phase (5 days post cuprizone)). Baseline performance was assessed following acclimatization and preceding the start of the experiments. The OLT was performed as described previously (354). Briefly, animals were placed in a circular arena with a diameter and height of 40 cm. The back-half of the arena wall was made of polyvinyl chloride covered with white paper. Testing was performed during two trials of 4 minutes (trial 1 with symmetrically placed objects; trial 2 with one stationary and one moved object). The exploration time for the two objects was measured manually using self-designed object location task software. The measures were used to calculate the discrimination index (d2 = (time spent on moved object – time spent on object on former place)/time spent exploring in trial 2). A d2>0 indicates a preference for the moved object, while a d2 that is not significantly different from 0 indicates no preference. All behavioral experiments were performed in a randomized blinded setup.

Visual evoked potential

Epidermal visual evoked potentials (VEPs) were measured at the end of the cuprizone-induced demyelination phase (6 weeks of cuprizone) and during remyelination (4 days post cuprizone). Animals were dark-adapted for at least 3h prior to the start of VEP to increase sensitivity and to provide a larger dynamic range. Any light sources in the room (laptop, digital scale) were covered with infrared filters. Animals were anesthetized by intraperitoneal (i.p.) injection with xylazine (20mg/kg) and ketamine (80mg/kg). Pupils were dilated using 1% tropicamide for 5 minutes, and subsequently 2.5% phenylephrine hydrochloride for 1 minute. Next, mice were placed on a heating pad and an active electrode was placed subdermal at the visual cortex, a ground electrode was inserted at the base of the tail to prevent electromagnetic noise from the environment, and finally, a reference electrode was inserted in the tongue. Lastly, the eyes were moistened with saline and the flash electrodes were placed on the eyes. Impedance measurement was used to evaluate electrode connection before

starting the VEP. Next, mice were presented with 200 white light flashes, each with a duration of 310ms. The stimulus frequency was set at 1Hz and stimulus intensity was set at 0.5cd.s/m^2. Latency time (i.e. time between visual flash stimulus and the arrival of the signal in the visual cortex) was given in milliseconds (ms) being reflective of the myelination status of the visual tract.

Experimental autoimmune encephalomyelitis (EAE)

Mice were immunized subcutaneously with an emulsion containing 300µg myelin oligodendrocyte glycoprotein 35–55 peptide (MOG35–55) in complete Freund's adjuvant (CFA) (0.5-1.5 mg killed mycobacterium tuberculosis) (EK-2110) and received two intraperitoneal (i.p.) injections of pertussis toxin (PTX) directly after immunization and 24 h later (100ng/injection) (Hooke). For the bone marrow transplantation EAE experiment, only one PTX injection was administered (40ng/injection) (Hooke). Animal welfare was monitored daily while being clinically scored by blinded investigators using a standard 5-point scale (0: no symptoms; 1: limp tail; 2: hind limp weakness; 3: complete hind limp paralysis; 4: complete hind limp paralysis and partial front leg paralysis; 5: moribund). Animals were sacrificed at EAE onset (n=5/group), peak (n=5/group) and at the end of the experiment (n=≥8/group) by transcardial perfusion following a lethal Dolethal injection (200mg/kg). The brain, spinal cord, spleen and lymph nodes were harvested from each animal. The lymph nodes, spleen and CNS (1 brain hemisphere and half of the spinal cord) were further processes for flow cytometry analysis. The remaining part of the spinal cord was imbedded in Tissue-Tek optimal cutting temperature (OCT) compound (IHC) and together with the brain (qPCR) snap-frozen using liquid nitrogen.

Bone marrow transplantation

Chimeric mice were generated by whole body irradiation (eight Gy) of C57BL/6 females. Femurs and tibias were removed from female *pde4b*$^{+/+}$, *pde4b*$^{+/-}$ and *pde4b*$^{-/-}$ mice (*pde4b*$^{-/-}$ mice kindly provided by Prof. Dr. Viacheslav). *Pde4b*$^{-/-}$ is generated by homologous recombination, as described previously (355). Bone marrow was flushed with sterile PBS (phosphate buffered saline, pH: 7.5). Mice were reconstituted with 10^7 cells into the tail vein of recipients within 4h post-irradiation. Bone marrow was allowed to engraft for 9 weeks before EAE induction.

During recovery, mice were treated with Neomycin (FSA Chemicals) and Polymyxini B sulphate (Fagron) added to the drinking water.

Human derived cell culture

Human monocyte derived macrophages

Human-derived monocytes were sorted using the MojoSortTM Streptavidin Nanobeads Column Protocol and positive selection. The positively sorted $CD14^+$ cells were re-suspended in RPMI 1640 medium (Lonza) supplemented with 10% fetal bovine serum and 50 U/ml penicillin and 50 mg/ml streptomycin (all Life technologies). Cells were plated at a density of 1.4×10^5 cells per well in 24-well plates and placed in a humidified CO_2 incubator at 5% CO_2/ 37°C for 7 days. Thereafter, cells were treated with vehicle (0.1% DMSO), the PDE4 inhibitor roflumilast (1μM), the PDE4B inhibitor A33 (1μM) or the PDE4D inhibitor Gebr32 (1μM), and exposed to isolated human myelin (100μg/ml). Subsequently, after 24h, macrophages were treated with pro-inflammatory stimuli (10ng/ml IL-1β and 100ng/ml IFN-γ) (PeproTech) for another 24h.

iPSC-derived OPCs

Inducible SOX10 overexpressing iPSCs were generated from the human iPSC Sigma line (iPSC EPITHELIAL-1 IPSC0028, purchased from Sigma-Aldrich, ECACC cat. no. 66540499) and used to obtain $O4^+$ and MBP^+ oligodendrocyte culture as described previously (356, 357). After differentiating iPSCs towards oligodendrocytes, cells were frozen in liquid nitrogen until thawing of the cells for the microfiber myelination assay. Throughout the myelination assay, cells were kept in iPSC oligodendrocyte differentiation medium (see Supplementary table S3.1 for medium composition).

Primary murine cell isolation

Oligodendrocyte precursor cells

Primary mouse oligodendrocyte precursor cells (OPCs) were isolated from p0 C57bl6 pups using the shake off method as described previously (358). Primary OPCs were plated on a glass coverslip at a density of 1.5×10^5 cells per well in a 24-well plate (ICC) or 1.5×10^6 cells per well in a 6-well plate (Western blot) and cultured at 8.5% CO_2. Cells were maintained in SATO differentiation medium unless stated otherwise (see Supplementary table S3.1 for medium composition).

After allowing the cells to attach (1h), OPCs were treated with vehicle (0.1% DMSO), the PDE4 inhibitor roflumilast (1μM, 5μM or 10μM) or the PDE4D inhibitor Gebr32a (0.5μM, 1μM or 5μM). Treatment was repeated on day 2 and day 4, applying a 50% medium change. Cells were fixed with 4% PFA (ICC) or lysed using RIPA buffer (WB) at day 6 to evaluate OPC differentiation. Importantly, Gebr32a was administered at a non-toxic and non-proliferative concentration (**Supplementary Fig S3.1**).

Bone marrow derived macrophages

Mouse bone marrow derived macrophages were obtained from 12-week old C57Bl/6J OlaHsd mice and isolated as described previously (359). Briefly, tibial and femoral bone marrow suspensions were plated at a concentration of $10x10^6$ cells/10 cm culture plate. Bone marrow cells were differentiated into macrophages by culturing them in RPMI 1640 medium (Invitrogen), supplemented with 50 U/ml penicillin (Invitrogen), 50U/ml streptomycin (Invitrogen), 10% heat inactivated fetal calf serum (Gibco) and 15% L929 conditioned medium.

Microglia

Primary microglia were isolated from p0 C57bl6 pups using the shake off method. Meninges-free cerebral cortices were mechanically dissociated and chemically digested using 3U/ml papain to obtain a cell suspension. After 4 days in cultures, culture medium was enriched with 1/3 L929 conditioned medium to generate microglia-enriched glial cultures. Microglia were obtained by using orbital shaking and seeded on a 24-well plate (250.000 cells/well). Microglia were treated with 0.1% DMSO, 1μM roflumilast, 1μM A33 or 1μM Gebr32a, while simultaneously being stimulated with myelin (100μg/ml), for 24h. Next, 10 ng/ml IL-1β (PeproTech) and 100ng/ml IFN-γ (PeproTech) was added to inflammatory activate microglia. After 24h, the medium was collected and processes for nitrite assessment using the Griess assay.

Brain microvasculature endothelial cells

Murine brain microvascular endothelial cells (BMECs) were isolated from adult 10-week-old mice. After the whole brains were isolated, meninges were removed and cortical tissue was homogenized. Next, the meninges-free brains were digested using a 0.7mg/ml collagenase and 39 U/ml DNase I mixture for 75 minutes,

followed by a 1h incubation with a mixture of 1mg/ml Collagenase/Dispase and 39 U/ml DNase I. Using a 33% continuous Percoll gradient, the microvessel cells were collected and plated on a Collagen Type IV coated 6-well plate (1 brain per well). After 5 days, BMECs were inflamed using 10 ng/ml TNF-α (PeproTech) and 10 ng/ml IFN-γ (PeproTech) while the treatment with 0.1% DMSO, 1μM roflumilast, 1μM A33 or 1μM Gebr32a was simultaneously started. After 48h, cells were processed by means of flow cytometry to evaluate the expression of adhesion molecules.

Cerebellar organotypic slice cultures

C57Bl/6J OlaHsd mouse pups (postnatal day 10) were used to generate organotypic cerebellar brain slices. Sagital sections (350μm) were made from pup cerebellum using a tissue chopper and cultured onto Millicell hydrophilic PTFE cell culture inserts with a pore size of 0.4μm (Sigma-Aldrich) in a 24-well plate at 3 slices per insert. Media was composed of 50% minimal essential media (Gibco), 25% Earle's balanced salt solution (Gibco), 25% heat inactivated horse serum (Thermo Fisher), 6.5 mg/ml glucose (Sigma-Aldrich), 1% penicillin-streptomycin (Life technologies) and 1% glutamax (Thermo Fisher). After allowing a recovery period of 3 days, slices were demyelinated by incubation in lysolecithin (0.5 mg/ml; Sigma-Aldrich) for 16h. After demyelination, slices were washed in media for 10 minutes and treatment was initiated 24h later (vehicle of 0.1% DMSO, 1μM roflumilast or 1μM Gebr32a). Treatment was repeated every other day and continued for 14 days. At the end of the experiment, slices were fixed in 4% PFA.

Microfiber myelination assay

A neuron-free 3D microfiber assay was used to evaluate myelination (360). Aligned PLLA 2μm diameter fiber scaffold substrates (AMS.TECL-006-1X; Amsbio) were coated with poly-L-Lysine (PLL) and seeded with murine OPCs, or coated with PLO/laminin and seeded with human iPSC-dervied OPCs, both at a density of 50.000 cells/scaffold (12 well plate crown insert) in their respective culture medium described above. One hour after plating, cells were treated with the respective compound. Treatment was repeated every two days with a 50% medium change and continued for 14 days. At the end of the experiment, scaffolds were fixed in 4% PFA.

Mapping of OPCs, oligodendrocyte and neurons for isolation from human brain tissue using LCM

Human post-mortem area postrema and chronic inactive MS lesion samples were obtained through the Netherlands Brain Bank (www.brainbank.nl) and were sectioned into 10µm sections on a cryostat (Leica) and mounted on glass cover slides (demographic data in table 3.1). Next, neurons (NeuN: 1/200; Millipore MAB377) were stained for in area postrema sections, while oligodendrocytes (GalC: 1/500; Millipore MAB342) and OPCs (NG2: 1/200; Abcam Ab101807) were stained for in MS lesion samples. Briefly, before starting the staining, all containers, jars and working area were rinsed with RNaseZap and nuclease free water (Ambion). Sections were first fixed in ice-cold acetone for 4 minutes and washed for 5 seconds in TBS/TBS-T/TBS before endogenous peroxidase was neutralized with 1.5%H_2O_2 in TBS for 10 seconds. Next, sections were rinsed with TBS and blocked with 1%BSA in TBS-T for 10 minutes. Primary Antibodies were incubated for 30 minutes followed by a 7-minute horseradish peroxidase (HRP)-linked secondary antibody (vector laboratories) incubation. After rinsing the secondary antibody with TBS, sections were incubated with an avidin-biotinylated horseradish peroxidase complex for 5 minutes after which visualization of the staining was accomplished using 0.3% ammonium nickel sulphate and 0.025% diaminobenzidine (pH 7.8) in TBS. After dehydration (30 second sequential wash in 75%-95%-100% ethanol and 5 minutes xylene), sections were ready for proceeding to the laser capture microdissection (LCM). Neurons of the area postrema, oligodendrocytes from normal appearing white matter and OPCs from chronic inactive MS lesions were located in the human tissue, isolated using a PALM MicroBeam (Zeiss), and 50 cells per sample per cell type were captured into 0.1-ml tube cap with 10µl lysis buffer (RNeasy picopure kit, Qiagen).

Table 3.1. Demographic data of human post-mortem tissue

Characteristic	Area postrema samples	MS patient samples
Sex (male/female)	4/6	4/6
Age, mean (SD)	78.5 (11.54)	64.7 (9.64)
PMI, mean (SD)	7.288 (2.246)	9.72 (4.09)
Diagnosis (PRMS/SPMS/PPMS/Unspecified)	n.a.	1/4/3/2

ABBREVIATIONS: MS = multiple sclerosis; SD = standard deviation; PMI = post-mortem interval; PRMS = primary relapsing MS; SPMS = secondary progressive MS; PPMS = primary progressive MS; n.a. = not applicable.

CRISPR-Cas9

Guide RNA design, cloning and transformation

N-terminal specificity between *pde4d* isoforms was defined using NCBI and Ensembl databases. Using the Zhang-lab online webtool (http://crispr.mit.edu), specific single guide RNAs (sgRNAs) were designed against the N-terminal of each mouse *pde4d* isoform. For each sgRNA, the lowest off-target prediction was chosen and the frameshift-inducing frequency was determined using the InDelphi algorithm (361) (table 3.2). The synthesized oligo sgRNAs included an additional guanine nucleotide for increasing its transcriptional efficiency and an overhang to fit into the BbsI restriction gap. Next, 1µg of plasmid DNA was incubated overnight with 40U BbsI restriction enzyme (Bioké) at 37°C, which was followed by an enzyme inactivation step were the DNA was incubated at 65°C for 20 minutes. After enzyme inactivation, the DNA sample was immediately loaded on a 1% agarose gel from which the restricted vector was extracted according to the manufacturer's instructions (PCR and gel clean-up kit, Macherey-Nagel, Düren, Germany). A 5:1 insert to vector molar ratio was used to ligate annealed sgRNAs into the linearized vector using T4 DNA Ligase (Bioké) according to the manufacturer's protocol. NEB® 5-alpha competent E. coli cells (Bioké) were used for transforming by means of heathshock and the ligated product and cells were plated on ampicillin (Amp; 100 mg/ml) supplemented LB-agar plates. Single colonies were picked and cultured after overnight propagation, followed by plasmid extraction and purification using a NucleoBond Xtra Midi EF kit (Macherey-Nagel). Correct incorporation of the sgRNA was validated by means of SANGER sequencing.

Table 3.2. Oligonucleotide sequences to be annealed and ligated in the PX458 vector as gRNA against PDE4D isoforms.

Isoform	**Forward gRNA (5'-3')**	**Reverse gRNA (5'-3')**	**Frameshift frequency** (based on inDelphi algorithm)
pde4d1	CACCGCATCCGAGCATGGCGGGGTA	AAACTACCCCGCCATGCTCGGATG	67.7%
pde4d3	CACCGTACATGCAACATAGGAGACG	AAACCGTCTCCTATGTTGCATGTAC	89.4%
pde4d4	CACCGCCCGGGCGGTCAGCGAAGA	AAACTCTTCGCTGACCGCCCGGGC	61.6%
pde4d5	CACCGAAGTGGATAATCCGCATGT	AAACACATGCGGATTATCCACTTC	61.5%
pde4d6	CACCGTATTTATTGTCAGTGTCTTG	AAACCAAGACACTGACAATAAATA	80.5%
pde4d7	CACCGATCTCGTACGGCGACTTTCT	AAACAGAAAGTCGCCGTACGAGAT	85.9%
pde4d8	CACCGAGAACTAGAACAAGATTGCG	AAACCGCAATCTTGTTCTAGTTCTC	73.7%
pde4d9	CACCGGTCTACAAGTTCCCTGAGG	AAACCCTCAGGGAACTTGTAGACC	57.5%

Transfection

The pSpCas9(BB)-2A-GFP plasmid was a gift from Feng Zhang (Addgene plasmid #48138; http://n2t.net/addgene:48138; RRID:Addgene_48138). 24h after seeding, primary mouse OPCs were transfected with the plasmid using the OZ Biosciences NeuroMag Transfection Reagent (Bio-connect). Briefly, 1.75µl Neuromag reagent was incubated for 20 minutes (room temperature) with 500ng plasmid and 50µl DMEM 6429 medium to allow DNA/Neuromag complex formation. Next, the formed complexes were added dropwise to primary OPC cultures (150 000 cells/well) which were maintained in P/S free SATO medium. The cells were then placed on a magnetic plate in an 8.5% CO_2 incubator for 30 minutes to allow magnetofection. After removing the magnetic plate, cells were kept in standard SATO differentiation medium to allow differentiation for a period of six days. The PX458 plasmid (not manipulated) with no target specificity was used as a control.

Quantitative qPCR

Total RNA was isolated using the RNeasy mini kit (tissue samples; Qiagen) or the RNeasy picopure kit (laser captured cells; Qiagen) according to the manufacturer's instructions with the use of Qiazol lysis reagent (Qiagen). RNA concentration and purity were determined using a Nanodrop spectrophotometer (Isogen Life science). Consequently, cDNA synthesis was performed using the qScript cDNA SuperMix (Quanta Biosciences). Quantitative PCR was conducted on a StepOnePlus™ Real-Time PCR system (Applied biosystems). The SYBR green master mix (Applied biosystems), 10µM of forward and reverse primers, nuclease free water and 12.5ng template cDNA in a total reaction volume of 10 µl. For mouse brain samples, a relative quantification of gene expression was accomplished by using the comparative Ct method with data normalization for to the most stable reference genes. For laser-captured cells, qPCR was performed on paired oligodendrocytes and OPCs and area postrema neurons using verified primer couples for the different *pde4d* splice variants. The proportional contribution of each splice variant was calculated for each sample (sum isoforms per sample = 1). Details of the primers are shown in table 3.3.

Table 3.3. Primers sequences

GENE	SPECIES	FORWARD PRIMER (5'-3')	REVERSE PRIMER (5'-3')
Il-27	*Mus musculus*	CACTCCTGGCAATCGAGATTC	CACTCCTGGCAATCGAGATCC
actb	*Mus musculus*	GGCTGTATTCCCCTCCATCG	CAGTTGGTAACAATGCCATGT
gapdh	*Mus musculus*	ACCACAGTCCATGCCATCAC	TCCACCACCCTGTTGCTGTA
PDE4D1	*Homo sapiens*	AGAACTGAGTCCCCCTTTCC	TGAGCTCCCGATTAAGCATC
PDE4D3	*Homo sapiens*	CCACGATAGCTGCTCAAACA	GTGCCATTGTCCACATCAA
PDE4D4	*Homo sapiens*	TCTGGCGCCTTCAAGTGAG	CAGAGATGCTTGGGGGCTTT
PDE4D5	*Homo sapiens*	TGTTGCAGCATGAGAAGTCC	ATGTATGTGCCACCGTGAAA
PDE4D6	*Homo sapiens*	ATTCGATGGGAAGACGGCTG	CCACAAGCCACGCAGAGTAT
PDE4D7	*Homo sapiens*	GAACATTCAACGACCAACCA	TTCCGGGACATAGACTTTGG
PDE4D8	*Homo sapiens*	CGCACCAGCTCTGACTTCTC	CGCAATCTTGATTTGGCTCT
PDE4D9	*Homo sapiens*	ATGCTGGTTTCCCTTGTGAC	ATGGGCAAGGTTCTAACACG

Nitric oxide (NO) assessment

Griess assay

NO was indirectly measured from inflamed mouse monocyte medium (24h, 10 ng/ml IL-1β and 100ng/ml IFN-γ) (PeproTech) using the Griess reagent nitrite measurement kit (Abcam). Briefly, N-(1-naphthyl)ethylenediamine dihydrochloride and sulphanilamide react with the released nitrite present in the culture medium and produce a pink azo dye. Consequently, absorbance of the pink azo dye was measured using a microplate reader (iMark, Bio-Rad) at 540nm.

DAF assay

DAF-FM (ab145295) was used to directly detect low concentrations of NO. DAF-FM (5μM) was added 24h following inflammatory stimulation. After fixation, cells were mounted on Superfrost Plus glasses to initiate the analysis. Images of immunostainings were acquired using a Digital sight DS-2MBWc fluorescence camera adapted on a Nikon Eclipse 80i microscope. Images (1600 × 1200) were analyzed with ImageJ 1.45e software (NIH; available at: http://rsb.info.nih.gov/ij/). The background was subtracted and the mean fluorescence intensity of the cells was measured for each condition.

Western Blot

OPC differentiation was determined using MBP-targeted western blot. Total protein content was extracted from treated primary OPC cultures ($1.5x10^6$ cells/well) by homogenization in RIPA buffer (150 mM sodium chloride, 1.0% Triton X-100, 0.5% sodium deoxycholate, 0.1% SDS, 50 mM Tris, pH 8.0) supplemented with a protease (complete Ultra tablets, Roche) and phosphatase (PhosSTOP EASYpack, Roche) inhibitor cocktail. The total protein concentrations were assessed using the Pierce™ BCA Protein Assay Kit (Thermo Fisher Scientific) according to manufacturer's guidelines. Next, 40μg of protein sample was separated by 10% sodium dodecyl sulfate polyacrylamide gel electrophorese and blotted onto a PVDF membrane (GE Healthcare, Buckinghamshore, UK). The membrane was transferred into blocking buffer (4 % non-fat dry milk, Tris-buffered saline with 0.1% Tween-20) for 1 hour at room temperature. Primary antibodies were incubated: rat anti-MBP (1/500, MAB386 Millipore) and Mouse Anti-β-actin (1/1000, Santa Cruz Biotechnology) for 2 hours at room temperature. After washing with TBS-T (Tris-buffered saline with 0.1% Tween-20) membranes

were incubated with secondary antibodies: horseradish peroxidase-conjugated rabbit-anti mouse and goat anti- rat antibodies (Dako, 1:2000) for 1 hour at room temperature. An ECL Plus detection kit (Thermo Fisher Scientific) was used and the generated chemiluminescent signal was detected by a luminescent image analyzer (ImageQuant LAS 4000 mini; GE Healthcare).

Flow cytometry

The profile of inflammatory cells present in the lymph nodes, spleen or CNS of EAE animals was analyzed by flow cytometry. All analyzed tissues were dissociated into single cells by mashing the tissue through a 70µm cell strainer. Red blood cells from the spleen were additionally lysed using 0.83 (w/v) ammonium chloride and myelin was removed from CNS samples by using a Percoll gradient. The Zombie NIR Fixable Viability kit (Biolegend, 423105) was used to gate for viable cells. Next, cells were incubated with 10% rat serum prior to incubating the cells with surface staining antibodies. The Transcription Factor Staining Buffer Set (Thermo Fisher Scientific) was used according to the manufacturer's instructions for fixing and permeabilizing the cells prior to the intracellular staining. Immune cell subtypes were detected using the following antibodies: Pacific Blue anti-mouse CD4 (100427), Brilliant Violet 510 anti-mouse CD8a (100751), FITC anti-mouse CD3 (100203), Brilliant Violet 650 anti-mouse CD19 (115541), Alexa Fluor 700 anti-mouse CD45 (103127), PE/Dazzle 594 anti-mouse IL-17A (506937), PE/Cy7 anti-mouse IFN-γ (505825), PE anti-mouse IL-4 (504103), Alexa Fluor 647 anti-mouse FoxP3 (126407), PerCP/Cy5.5 anti-mouse CD11b (101227) and Brilliant Violet 785 anti-mouse Ly-6c (128041) (all from BioLegend). Samples were acquired using the LSRF Fortessa (BD Biosciences) and analyzed using FlowJo 10.8.0 (BD Biosciences) (**Supplementary Fig S3.2**).

The expression of the adhesion molecules VCAM-1 and ICAM-1 on inflamed BMECs was analyzed using flow cytometry. FVD eFI506 (eBioscience) was used to gate for viable cells. Next, cells were stained for VCAM-1 using a FITC-labeled antibody (Biolegend, 105705) and ICAM-1 using an AF647-labeled antibody (Biolegend, 322718). Both the percentage of positive cells and mean fluorescent intensity was used as a read-out for further analysis.

Immunofluorescence

Immunocytochemistry

Organotypic brain slices and both murine and human OPC were fixed in 4% paraformaldehyde. A 1% bovine serum albumin (BSA) block was used for 30 min at room temperature. Primary antibodies were incubated for 4 hours at room temperature: rat anti-MBP (1:500, MAB386 Millipore), Mouse Anti-O4 (1:1000, MAB1326 R&D systems) and/or Rabbit Anti-Neurofilament (1:750, Ab8135, Abcam). The glass cover slips, microfiber samples, or MilliPore inserts were then incubated for 1 hour in the dark at room temperature with Alexa 488- or Alexa 555-conjugated secondary antibodies (1:600, Invitrogen). Nuclear staining was performed using 4,6'-diamidino-2-phenylindole (DAPI; Invitrogen) for 10 minutes. The glass cover slides, microfiber samples and organotypic brain slice membranes were mounted onto cover glasses with Fluoromount-G. OPC differentiation analysis using the Leica DM2000 LED microscope (20x magnification pictures; 5 random pictures per cover slide) and Fiji, ImageJ (manual threshold of MBP and O4 positive area corrected for the number of cells per picture). The microfiber and organotypic brain slices samples were imaged under a Zeiss LSM880 confocal microscope (0.42µm z-steps with a 40x/1.1 water objective). The number of complete myelin sheaths, and the average and complete length of complete myelin sheaths per cell were determined in the microfiber myelination assay. The myelination index was calculated for the brain slice experiment, which is the volume of MBP and neurofilament colocalization corrected for the area of neurofilament present per z-layer. 3D rendering images were made afterwards using the VAA3D software (VAA3D-Neuron2_Autotracing) (362).

Immunohistochemistry

Frozen coronal brain sections (bregma -2mm; 10µm; cuprizone study) and both transversal and longitudinal spinal cord sections (10µm; EAE study) were generated via cryosectioning (Leica) and were stained for MBP or F4/80 and Arginase respectively. Briefly, sections were air-dried and fixed in acetone for 10 minutes. Non-specific binding was blocked using 10% DAKO protein block in PBS for 1h. Cuprizone brain sections were incubated overnight with rat anti-MBP (1:500, MAB386 Millipore) or anti-CC1 (1:50) (Calbiochem), longitudinal spinal

cord sections with both rat anti-F4/80 (1:100, MCA497G, Serotec) and mouse anti-arginase 1 (1:100, 610708, BD Trasnduction lab), and transversal spinal cord sections with both rat anti-MBP (1:500, MAB386 Millipore) and rabbit-anti neurofilament (1:750, Ab8135, Abcam) at 4°C. Next, after three washing steps with PBS, sections were incubated with Alexa 488- or Alexa 555-conjuagted secondary antibodies (1:600, Invitrogen) for 1h. Nuclei were counterstained with DAPI and coverslips were mounted using fluorescent mounting medium (DAKO). For the cuprizone experiment, 3 images per animal per region (corpus callosum and dentate gyrus) were collected (between anterior posterior coordinates -1.5mm and -1.9mm relative to Bregma). For the EAE experiment, 5 random images within each longitudinal spinal cord section (3 sections per animal) were taken, thereby comprising the cervical, thoracal and lumbar spinal cord regions. The cervical spinal cord region was used for generating transversal sections and 3 random images per section were collected (5 sections per animal). Images were taken using the Leica DM2000 LED microscope and quantified with Fiji, ImageJ. MBP quantification was performed in a blinded manner and was based on the area percentage positive for MBP in the corpus callosum by means of a manual threshold adjustment. For the spinal cord sections, the double positive area for F4/80 and Arginase 1 was determined using the colocalization plugin of Fiji, ImageJ. The results obtained were averaged to obtain one representative value per animal.

Transmission electron microscopy

The sample preparation for TEM was performed as described previously (363) with minor modifications. For the corpus callosum analysis of the cupizone studies, a coronal brain block (1 mm thick) within the anteroposterior coordinates from -0.3 to -1.5 mm was cut in the midsagittal plane. For assessing remyelination in the EAE model, the optic nerve was isolated. The collected tissues were fixed with 2% glutaraldehyde and post-fixated with 2% osmiumtetroxide in 0.05M sodium cacodylate buffer (pH=7.3) for 1 hour at 4°C. Tissues were then stained with 2% uranyl acetate in 10% acetone for 20 min, dehydrated through graded concentrations of acetone and embedded in epoxy resin (araldite). Semithin sections (0.5 µm) were stained with a solution of thionin and methylene blue (0.1% aqueous solution) for light microscopic examination to delineate the region

of interest. Subsequently, ultrathin sections (0.06 µm) were cut and mounted on 0.7% formvar-coated grids and contrasted with uranyl-acetate followed by lead citrate and examined on a Philips EM 208 transmission electron microscope (Philips, Eindhoven, The Netherlands) operated at 80 kV.2.9. G ratios (=diameter axon/diameter axon with myelin sheath) were measured to evaluate myelin thickness using Fiji, Image J.

Emesis indicators

Patch clamp

Acute coronal brain slices were made from 12-16 week old male C57Bl6 mice using a Leica vibratome. Putative area postrema neurons were identified based on location relative to the central canal and electrophysiological characteristics. Pipettes of 4-6 MOhm resistance filled with a Na HEPES-based solution were used for extracellular recordings using the loose cell attached method as described by (364). Baseline firing rate was recorded for four minutes, after which either Gebr-32a or roflumilast (blinded) was bath perfused for six minutes.

Xylazine/ketamine anesthesia test

The duration of anesthesia induced by the combination of xylazine (10 mg/kg i.p) and ketamine (60 mg/kg i.p) was determined in C57Bl6 mice. Fifteen minutes following the induction of anesthesia, mice were treated with different doses of A33, Gebr32a or roflumilast. The duration of anesthesia was assessed by the return of the righting reflex (365).

Statistical analysis

GraphPad Prism 9.0.0 software (GraphPad software Inc) was used to perform statistical analyses. The sample size of each experiment was determined using G*Power based power analysis. Outlier values were determined based on the Dixon test for extreme values (significance level of 0.05) and excluded for further analysis. Differences between groups were evaluated using a non-parametric Kruskal-Wallis test with Dunn's post-hoc analysis against the vehicle group when the sample size was $n \leq 5$. When the sample size was $n \geq 6$, normality was checked using the Shapiro-Wilk test for normality. Normally distributed data were subsequently analyzed with a one-way ANOVA with Tukey's (*in vivo* and post-mortem analysis) or Dunnett's (*in vitro* editing experiment) multiple comparison.

Differences between EAE scores were evaluated using a non-parametric Friedman test with Dunn multiple comparison against vehicle group. Subsequently, differences of the AUC calculated from EAE scores over time were evaluated using a non-parametric Kruskal-Wallis test with Dunn's post-hoc analysis against the vehicle. Differences over time within the VEP experiment were evaluated using a repeated measure two-way ANOVA with Šídák's multiple comparisons test. Behavioural experiments were evaluated for differences compared to chance level using one-sample t test. All data are displayed as mean ± SEM, *P≤0.05, **P≤0.001, P≤0.005, #P≤0.05, ##P≤0.01.

Results

PDE4D inhibition stimulates OPC differentiation and enhances remyelination in cerebellar organotypic brain slices

To decipher the myelin-promoting effects of PDE4 (roflumilast), PDE4B (A33) and PDE4D (Gebr32a) inhibition, we treated primary mouse OPCs with either one of the inhibitors at different concentrations to subsequently evaluate cellular differentiation. By analyzing the number of myelin basic protein (MBP) positive cells to assess OPC differentiation, together with the $O4^+$ area (pre-mature oligodendrocyte marker) and MBP^+ area (terminally differentiated oligodendrocyte marker), we demonstrated an increase of OPC maturation upon 6 days of 1µM roflumilast (Kruskal-Wallis test with Dunn's post-hoc analysis; $F(3,12)=10.70$;**$P\leq0.01$) (**Fig 3.1A-D)** or either 1µM or 5µM Gebr32a treatment (Kruskal-Wallis test with Dunn's post-hoc analysis; $F(3,18)=17.77$;**$P\leq0.01$) (**Fig 3.1E-H**). Differentiated oligodendrocytes show clear morphological complexity and extensive process formation, which precedes axonal ensheathment. Furthermore, total MBP levels were measured by Western blotting and confirmed the immunocytochemical observations of increased MBP protein levels upon PDE4/PDE4D inhibition (two-tailed Mann-Whitney test, *$P\leq0.05$) (**Fig 3.1I and 3.1J**). Importantly, A33-induced PDE4B inhibition did not enhance OPC differentiation (**Fig 3.1K and 3.1L**). Furthermore, similar morphological complexities were observed when culturing primary OPCs on the differentiation inhibiting coating fibronectin **(Fig 3.2A-C).**

To assess the role of PDE4/PDE4D inhibition on myelination and remyelination, we made use of electrospun microfibers and organotypic cerebellar brain slice cultures as they both are able to demonstrate myelination along definable fibers or axons respectively. We found that PDE4 and PDE4D inhibition led to significantly more longer and complete myelin sheaths per oligodendrocyte in both murine-derived primary oligodendrocytes (Kruskal-Wallis test with Dunn's post-hoc analysis; $F(2,18)=10.78$; $F(2,18)=11.52$; $F(2,18)=14.03$; *$P\leq0.05$; **$P\leq0.01$; ***$P\leq0.005$) (**Fig 3.3A-D**) or human iPSC-derived oligodendrocytes (Kruskal-Wallis test with Dunn's post-hoc analysis; $F(2,15)=11.61$; $F(2,15)=10.86$; $F(2,15)=12.07$; *$P\leq0.05$; **$P\leq0.01$) (**Fig 3.3E-H**). Brain slice cultures were demyelinated by means of lysophosphatidylcholine (LPC) and

remyelination was allowed for 14 days with or without a PDE4 or PDE4D inhibitor. Kruskal-Wallis analysis of the slice cultures at the end of the experiment showed a clear increase in axonal myelin ensheathment upon PDE4D inhibition compared to vehicle treated slices (Dunn's multiple comparison analysis, $F(2,15)=15.16$; $^{*}P \leq 0.05$) (**Fig 3.3I-J).**

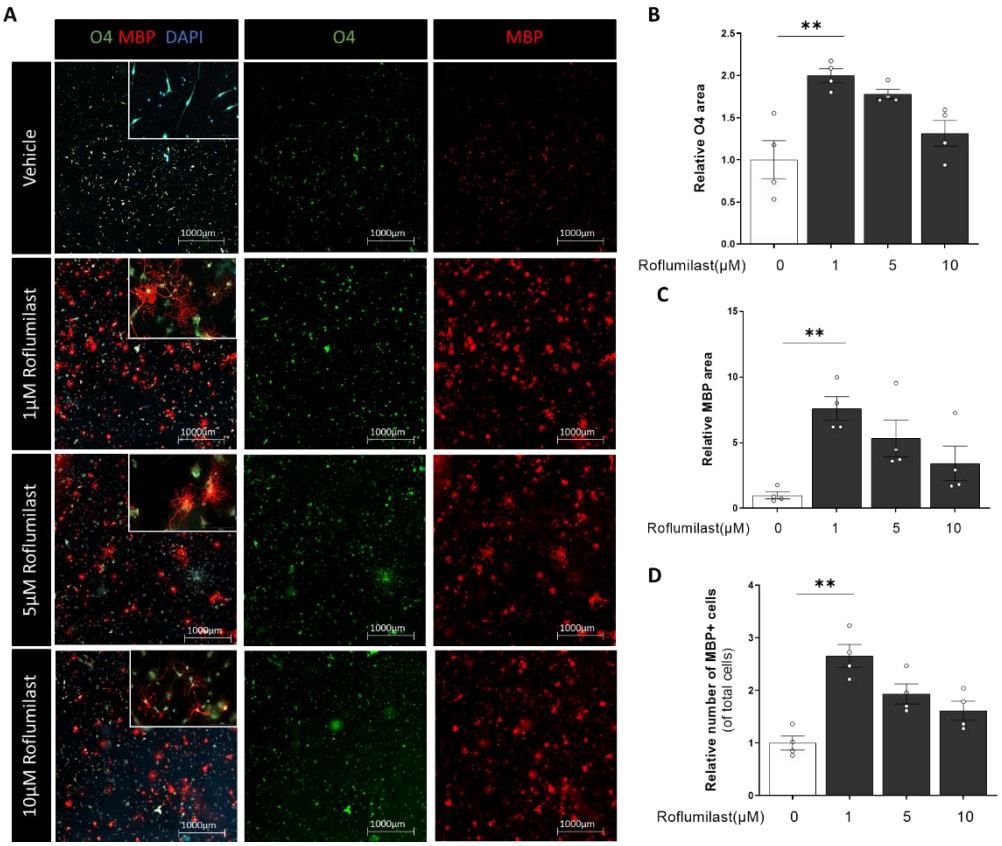

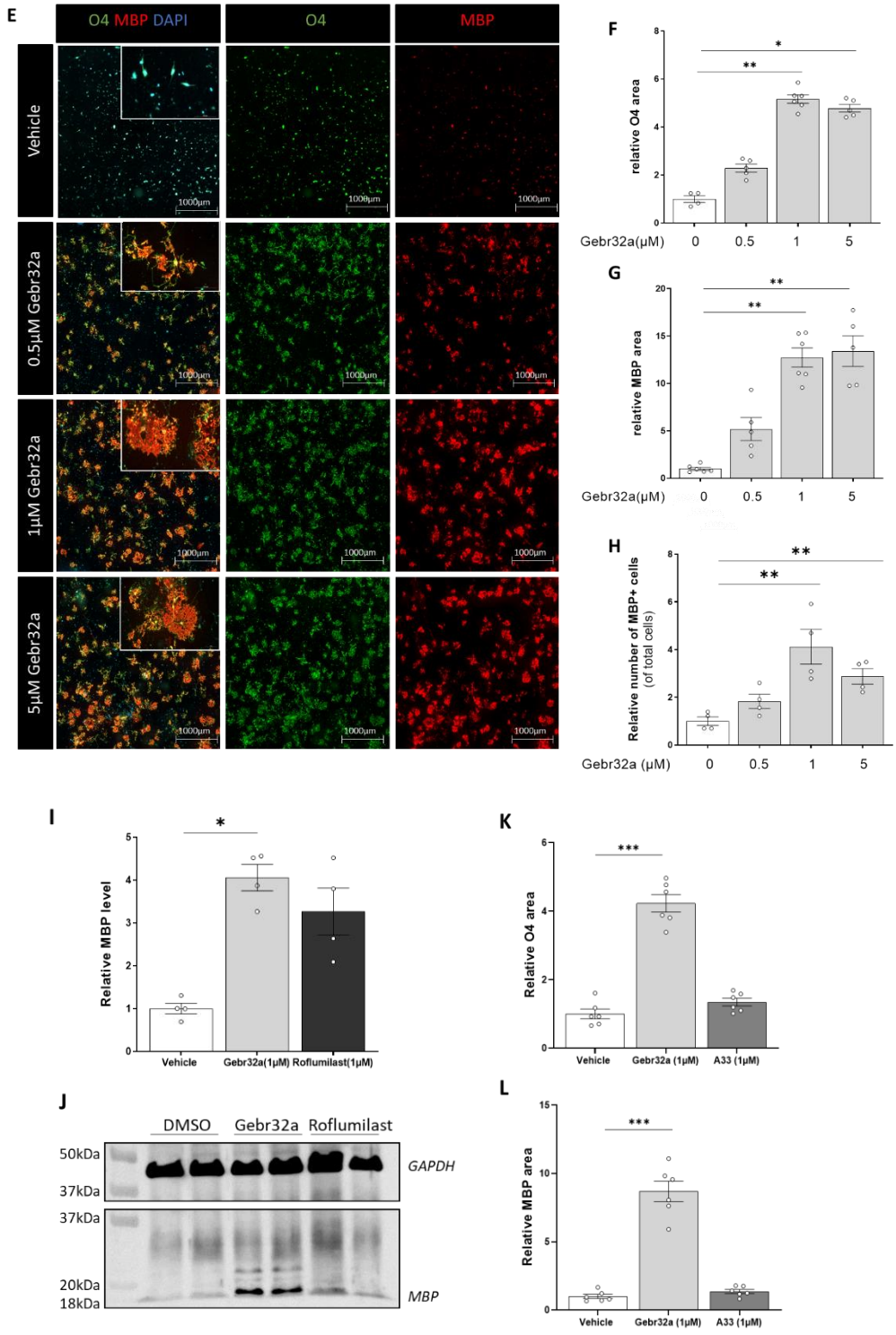
E
O4 MBP DAPI
O4
MBP
Vehicle
0.5μM Gebr32a
1μM Gebr32a
5μM Gebr32a
1000μm
F
relative O4 area
Gebr32a(μM) 0 0.5 1 5
G
relative MBP area
Gebr32a(μM) 0 0.5 1 5
H
Relative number of MBP+ cells
(of total cells)
Gebr32a (μM) 0 0.5 1 5
I
Relative MBP level
Vehicle Gebr32a(1μM) Roflumilast(1μM)
J
DMSO Gebr32a Roflumilast
50kDa
37kDa
GAPDH
37kDa
20kDa
18kDa
MBP
K
Relative O4 area
Vehicle Gebr32a (1μM) A33 (1μM)
L
Relative MBP area
Vehicle Gebr32a (1μM) A33 (1μM)

FIG 3.1: Inhibition of PDE4D by Gebr32a induces OPC differentiation, while PDE4B inhibition by A33 does not alter OPC differentiation. Primary mouse OPCs were allowed to differentiate for 6 days and were treated on day 0, 2 and 4 with different concentrations of **(A)** roflumilast (1µM, 5µM, 10µM) or **(D)** Gebr32a (0.5µM, 1µM, 5µM) or A33 (1µM). After 6 days of culture, cells were stained for O4 (late OPC marker) and MBP (oligodendrocyte marker). **(D and H)** The number of MBP^+ cells, **(B, F and K)** $O4^+$ area and **(C, G and L)** MBP^+ area was measured and corrected for the amount of cells (n≥4/group) **(I-J)** The total level of MBP and β-actin protein expression upon roflumilast (1µM) or Gebr32a (1µM) treatment was determined by means of western blotting and the ratio of MBP to β-actin is displayed (n=4/group)**.** The sample size 'n' represents the number of wells obtained from minimally three independent cell culture experiments. Data were analyzed using a non-parametric Kruskal-Wallis test with Dunn's multiple comparisons. Data are displayed as mean +/-SEM. (*p≤0,05; **p≤0,001; ***p≤0,005).

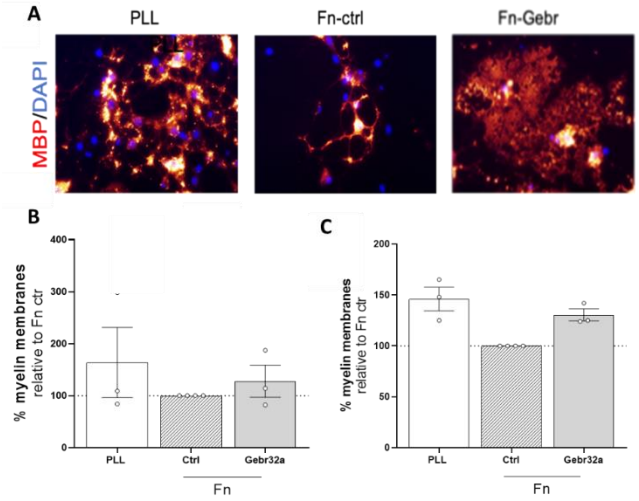

FIG 3.2: Exposure to PDE4D-inhibitor Gebr32a overcomes inhibition of myelin membrane formation by fibronectin. (A) Representative images of MBP immunocytochemistry of OPCs treated from day 3 onwards. **(B and C)** Quantitative analysis of the percentage of MBP-positive cells and the percentage of MBP-positive oligodendrocytes (OLGs) bearing myelin membranes treated from day 3 onwards. Each bar represents the mean±SEM of the relative percentages of 3 independent experiments. In each independent experiment, the percentages of untreated cells grown on a Fn substrate were set at 100% (horizontal line, black bar). Exposure to Gebr32a at day 3 of differentiation overcomes Fn-mediated inhibition (compared to positive control PLL) of myelin membrane formation in primary oligodendrocyte monocultures. No statistical analysis was conducted due to the low sample size.

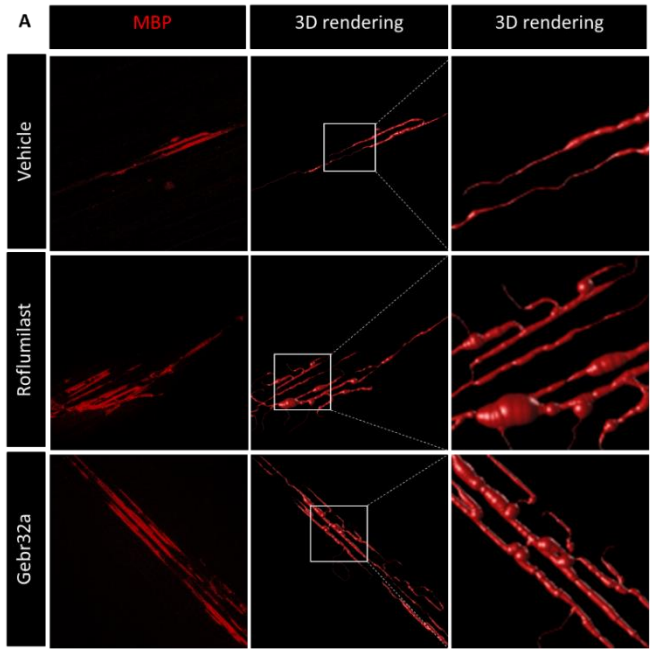
A
MBP
3D rendering
3D rendering
Vehicle
Roflumilast
Gebr32a

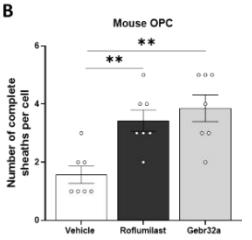
B
Mouse OPC
Number of complete sheaths per cell
Vehicle
Roflumilast
Gebr32a

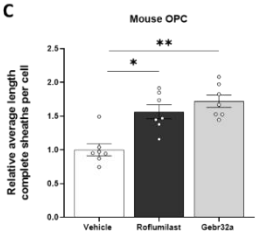
C
Mouse OPC
Relative average length complete sheaths per cell
Vehicle
Roflumilast
Gebr32a

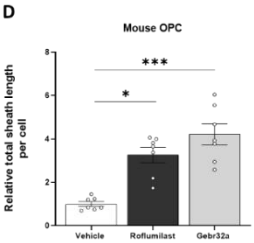
D
Mouse OPC
Relative total sheath length per cell
Vehicle
Roflumilast
Gebr32a

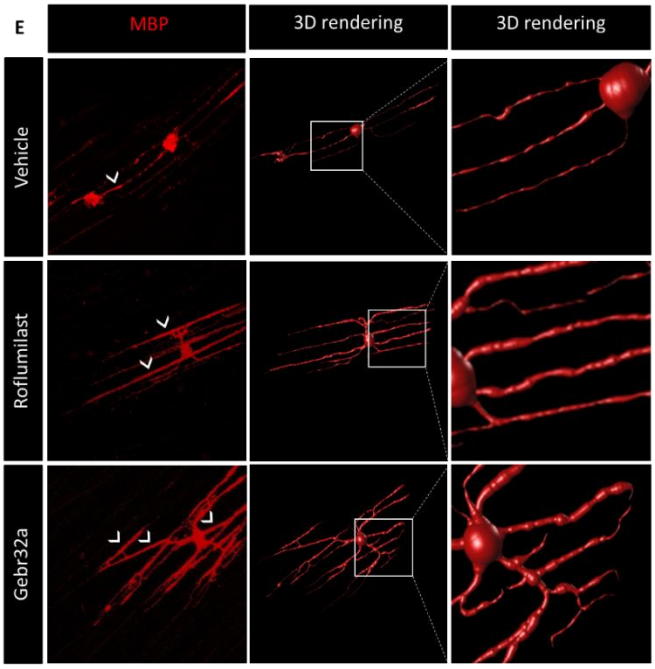
E
MBP
3D rendering
3D rendering
Vehicle
Roflumilast
Gebr32a

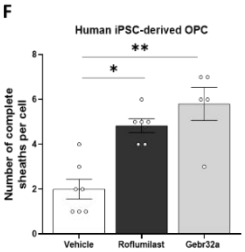
F
Human iPSC-derived OPC
Number of complete sheaths per cell
Vehicle
Roflumilast
Gebr32a

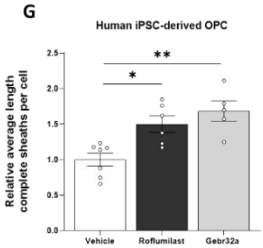
G
Human iPSC-derived OPC
Relative average length complete sheaths per cell
Vehicle
Roflumilast
Gebr32a

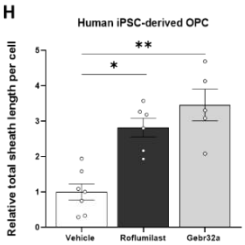
H
Human iPSC-derived OPC
Relative total sheath length per cell
Vehicle
Roflumilast
Gebr32a

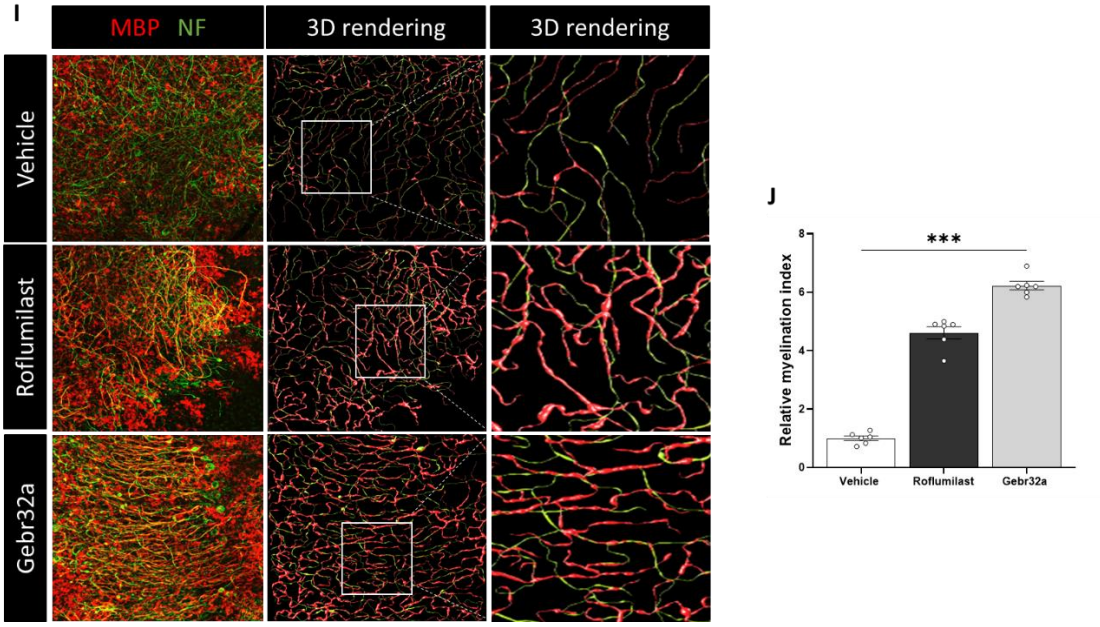

Fig 3.3: Inhibition of PDE4D by Gebr32a increases (re)myelination of mouse OPCs, human iPSC-derived OPCs, and organotypic brain slices. Confocal and 3D rendered images showing the formation of myelin-like extensions on microfibers by **(A)** primary mouse OPCs and **(E)** human iPSC-derived OPCs. Quantitative data analysis shows a higher number of complete myelin sheath formation, an increased average length of the formed complete myelin sheaths, and an increased total length of complete myelin sheaths per cell upon 1µM roflumilast or 1µM Gebr32a treatment of both **(B-D)** primary mouse OPCs and **(F-H)** iPSC-derived OPCs (n≥5/group). **(I-J)** Mouse brain slices (350µM) were demyelinated using lysolecithin (16h) and subsequently treated for 14 days with vehicle (0,1%DMSO), 1µM roflumilast or 1µM Gebr32a. After 14 days of remyelination, slice cultures were stained for MBP and neurofilament. The relative myelination index is determined on the level of MBP and neurofilament co-localization, corrected for the amount of neurofilament positive axons (n=6/group). For the microfiber myelination assay, the sample size 'n' represents the number of wells obtained from minimally three independent cell culture experiments (mouse OPCs) or from three iPSC-derived differentiations in which minimally 5 cells per insert were quantified and averaged. For the brain slice experiment, the sample size 'n' represents the number of inserts obtained from minimally three independent brain slice isolations. Data were analyzed using a non-parametric Kruskal-Wallis test with Dunn's multiple comparisons. Data are displayed as mean +/-SEM (*p≤0,05; **p≤0,001; ***p≤0,005).

PDE4D inhibition enhances remyelination, and thereby promotes functional recovery, after cuprizone-induced demyelination

The effect of PDE4/PDE4D inhibition on remyelination was further examined *in vivo* using the acute cuprizone model (0.3% w/w for 6 weeks). After cuprizone administration, animals were returned to a normal chow diet to allow spontaneous remyelination (**Fig 3.4A**). At the end of the demyelination period, spatial memory assessment in the OLT demonstrated an impairment upon cuprizone intoxication (two-tailed one sample t-test against d2≠0;** P<0.01; *** P<0.005) (**Supplementary Fig S3.3**). To make sure sufficient compound concentrations accumulated in the brain to immediately initiate remyelination, we started the treatment regimen two days before ceasing the cuprizone diet. Following cuprizone withdrawal and upon treatment during the remyelination period, the roflumilast-treated group (3 mg/kg, s.c.) and the Gebr32a-treated group (0.3 mg/kg, s.c.) showed recovery of spatial memory performances (two-tailed one sample t-test against d2≠0; *P<0.05; ***P<0.005) (One-way ANOVA with Tukey's multiple comparisons; F(3,74)=4.894; #P≤0.05; ##P≤0.01) (**Fig 3.4B and C**). As VEP latency time is correlated with optic nerve de- and remyelination, we implemented epidermal flash VEP measurements (3 trains of 20 stimuli, 10µs duration, 1Hz frequency) of both eyes during both de- and remyelination (366). Significantly increased latency times were observed at the end of cuprizone administration indicating demyelination of the optic nerve, and they were significantly decreased upon PDE4D inhibition during remyelination, indicating functional remyelination (repeated measure two-way ANOVA with Sidak's multiple comparison test; F(2,18)=63.27; **P≤0.01; ***P≤0.005) (**Fig 3.4D**).

Post-mortem analysis revealed a significantly increased MBP^+ area upon PDE4 or PDE4D inhibition in both the corpus callosum and hippocampal dentate gyrus after 10 days of treatment (One-way ANOVA with Tukey's multiple comparisons, F(3,33)=15.34; F(3,31)=36.15; F(3,32)=6.281; F(3,32)=5.743; *P≤0.05; **P≤0.01; ***P≤0.005) (**Fig 3.4E-J)**. This increase in MBP^+ area was accompanied with an increased number of CC1+ oligodendrocytes in the corpus callosum (Kruskal-Wallis test with Dunn's multiple comparison; F(3,20)=14.52; ***P≤0.005) **(Fig 3.4K-L)**. In line, PDE4 and PDE4D inhibition during remyelination significantly decreased the G ratios in the corpus callosum (Kruskal-

Wallis test with Dunn's multiple comparison; F(3,26)=13.19; F(3,16)=12.90) and increased the number of myelinated axons (Kruskal-Wallis test with Dunn's multiple comparison; F(3,26)=15.38; F(3,16)=13.26) (*P≤0.05; **P≤0.01) (**Fig 3.4M-T**). Collectively, these results show that PDE4D inhibition establishes functional remyelination in the acute cuprizone model.

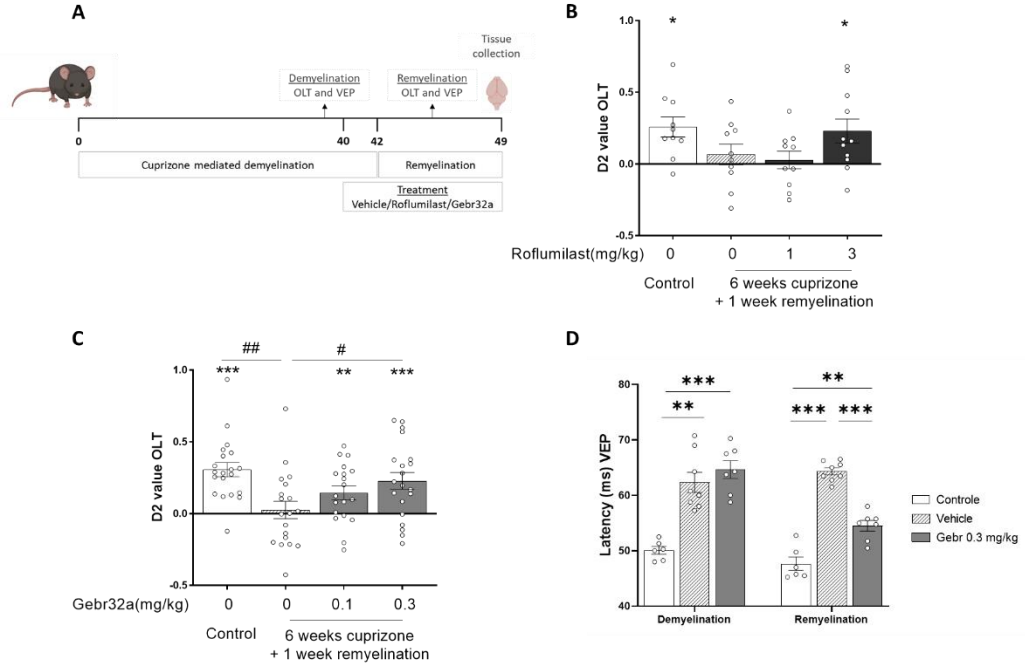

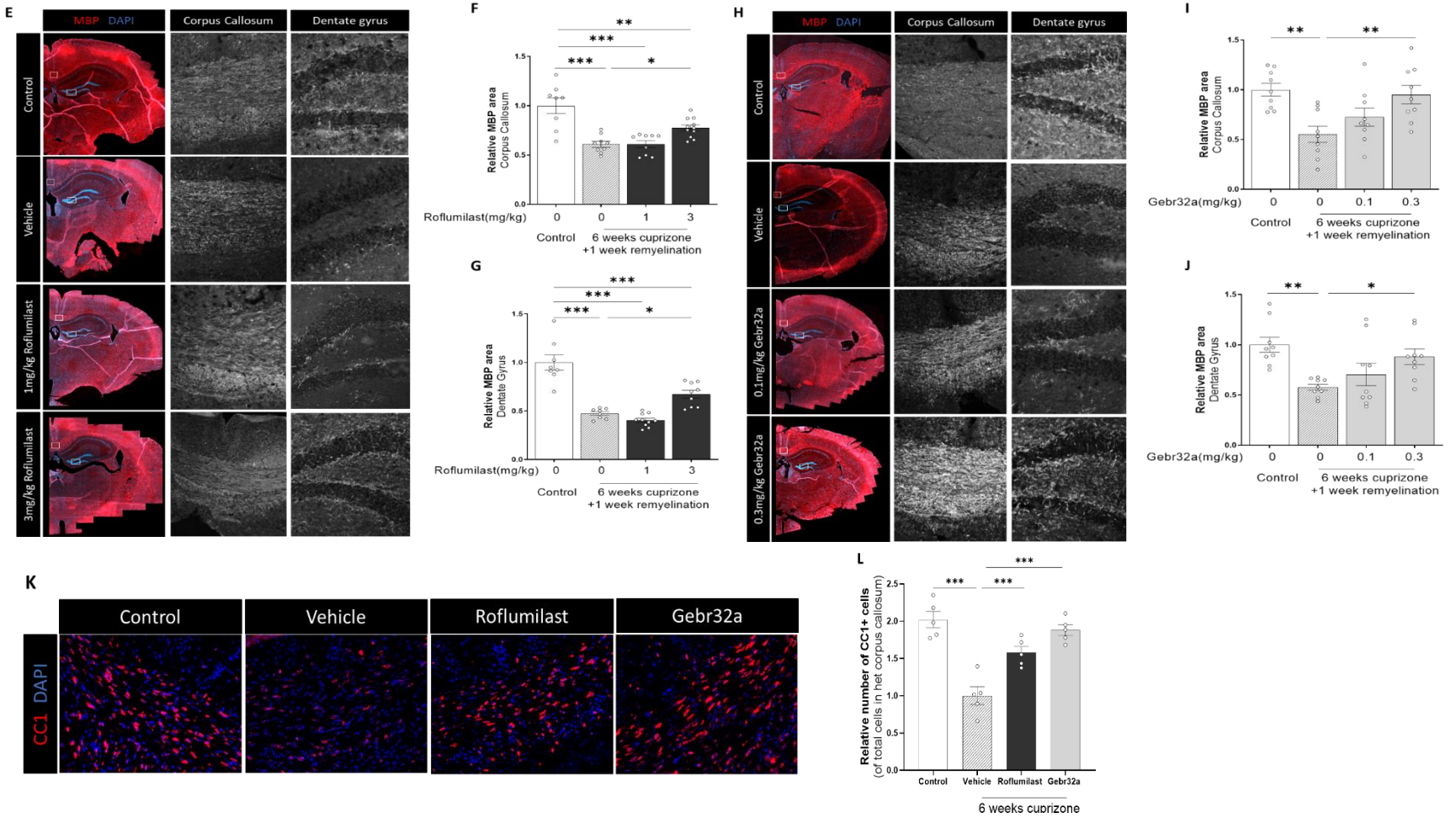
E
MBP DAPI
Corpus Callosum
Dentate gyrus
Control
Vehicle
1mg/kg Roflumilast
3mg/kg Roflumilast
F
Relative MBP area
Corpus Callosum
Roflumilast(mg/kg) 0 0 1 3
Control
6 weeks cuprizone
+1 week remyelination
G
Relative MBP area
Dentate Gyrus
Roflumilast(mg/kg) 0 0 1 3
Control
6 weeks cuprizone
+1 week remyelination
H
MBP DAPI
Corpus Callosum
Dentate gyrus
Control
Vehicle
0.1mg/kg Gebr32a
0.3mg/kg Gebr32a
I
Relative MBP area
Corpus Callosum
Gebr32a(mg/kg) 0 0 0.1 0.3
Control
6 weeks cuprizone
+1 week remyelination
J
Relative MBP area
Dentate Gyrus
Gebr32a(mg/kg) 0 0 0.1 0.3
Control
6 weeks cuprizone
+1 week remyelination
K
Control
Vehicle
Roflumilast
Gebr32a
CC1 DAPI
L
Relative number of CC1+ cells
(of total cells in net corpus callosum)
Control
Vehicle
Roflumilast
Gebr32a
6 weeks cuprizone

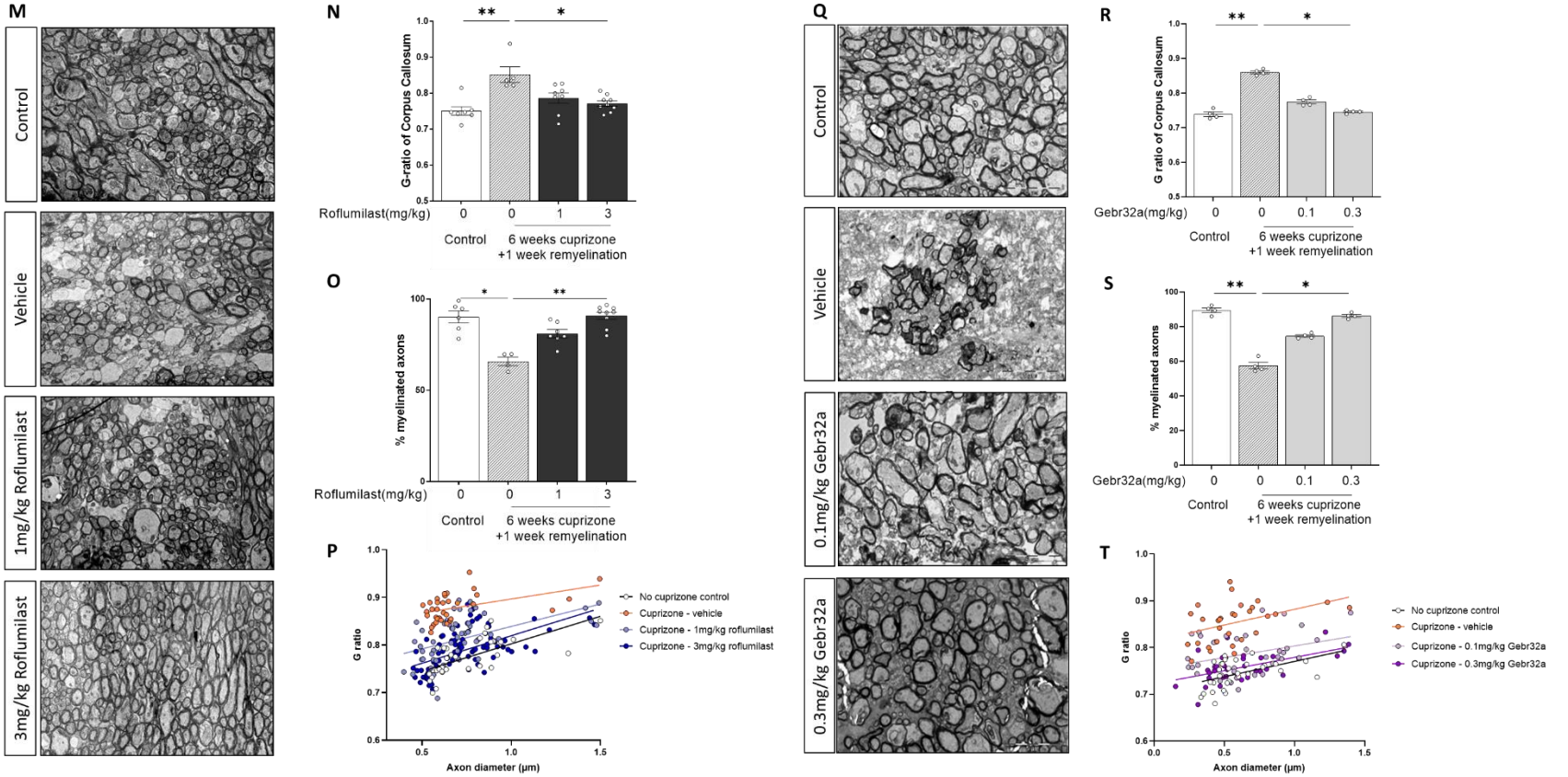
M
Control
Vehicle
1mg/kg Roflumilast
3mg/kg Roflumilast
N
G-ratio of Corpus Callosum
**
*
Roflumilast(mg/kg)
0
0
1
3
Control
6 weeks cuprizone
+1 week remyelination
O
% myelinated axons
*
**
Roflumilast(mg/kg)
0
0
1
3
Control
6 weeks cuprizone
+1 week remyelination
P
G ratio
Axon diameter (µm)
No cuprizone control
Cuprizone - vehicle
Cuprizone - 1mg/kg roflumilast
Cuprizone - 3mg/kg roflumilast
Q
Control
Vehicle
0.1mg/kg Gebr32a
0.3mg/kg Gebr32a
R
G ratio of Corpus Callosum
**
*
Gebr32a(mg/kg)
0
0
0.1
0.3
Control
6 weeks cuprizone
+1 week remyelination
S
% myelinated axons
**
*
Gebr32a(mg/kg)
0
0
0.1
0.3
Control
6 weeks cuprizone
+1 week remyelination
T
G ratio
Axon diameter (µm)
No cuprizone control
Cuprizone - vehicle
Cuprizone - 0.1mg/kg Gebr32a
Cuprizone - 0.3mg/kg Gebr32a

FIG 3.4: Inhibition of PDE4D by Gebr32a improves functional remyelination, as measured by means of the spatial memory performances and visual evoked potential latency times. (A) Schematic representation of the cuprizone experiment. **(B-D)** Functional remyelination was evaluated by means of the OLT at the 3h inter-trial-interval to evaluate spatial memory performances, and while visual evoked potential latency times were determined to assess optic tract and central nervous system signaling (n≥6/group). At the end of the experiment, all animals were sacrificed and brains were isolated. At anteroposterior coordinates from -0.3 to -1.5 mm (midsagittal slice), the brain was used for TEM analysis. The remaining posterior part of the brain was used for slicing and immunohistochemistry against MBP. **(E and H)** Representative pictures of MBP staining in the corpus callosum and dentate gyrus. The MBP+ area in both the **(F and I)** corpus callosum and **(G and J)** dentate gyrus of the hippocampus were analyzed (n≥8/group). **(K-L)** While cuprizone diet reduced the number of oligodendrocytes in the corpus callosum, 3mg/kg roflumilast and 0.3mg/kg Gebr32a treatment caused a robust increase in CC1+ oligodendrocytes (n=5/group). **(K-P)** G ratios and the amount of myelinated axons were measured based on corpus callosum TEM pictures (n≥4/group). A one sample t-test was performed to test for spatial memory (e.g. D2≠0). A one-way ANOVA with Tukey's multiple comparison test was performed to evaluate significances among groups in the OLT (#p<0,05; ##p<0,01). A two-way ANOVA with Sidak's multiple comparison test was performed to test for significances in the VEP latency times. MBP+ area differences were analyzed with a one-way ANOVA with Tukey's multiple comparison test. Significant differences for the amount of $CC1^+$ cells, G ratio measurements and percentage of myelinated axons were evaluated with a non-parametric Kruskal-Wallis test with Dunn's multiple comparisons. Data are displayed as mean +/-SEM (*p<0.05; **p<0.01; ***p<0.005).

PDE4D isoforms show distinct expression patterns indicative for their functional contribution

Next, we determined the different *PDE4D* isoform expression profiles in laser capture micro-dissected neurons of the human area postrema, the primary CNS area involved in emesis. We showed a particularly high mRNA expression of the long *PDE4D7* isoform in these neurons, while *PDE4D1/2, PDE4D4* and *PDE4D6* were very lowly expressed (**Fig 3.5A and 3.5B**). Interestingly, when comparing these expression profiles to laser capture micro-dissected OPCs derived from chronic inactive human MS lesions, abundantly present in progressive MS stages, and NAWM oligodendrocytes, we saw a clear distinction between isoform expressions (**Fig 3.5A and 3.5B**). Especially *PDE4D6*, and to a lesser extent *PDE4D1/2* expression levels were more abundantly present in OPCs and to a lesser extent in oligodendrocytes. As no isoform-specific PDE4D inhibitors exist, and we aimed to validate the role of the different PDE4D isoforms in OPC differentiation, we made use of a CRISPR-Cas9 system to specifically knock down selected isoforms. Guide RNAs were designed to the N-terminus of each unique PDE4D isoform specifically. In this way, an in/del can be created at the targeted location, creating a frameshift and therefore a non-functional enzyme. Six days post-transfection (transfection efficiency of 55%), a higher number of primary mouse OPCs transfected with either *pde4d1/2* or *pde4d6* targeting CRISPR/Cas9 plasmids was MBP^+, indicating an induction of OPC differentiation (One-way ANOVA with Dunnett's multiple comparison; $F(8,36)=64.56$; ***$P \leq 0.005$) (**Fig 3.5C and 3.5D**). These data indicate that the short PDE4D1 and PDE4D6 isoforms might skew differentiation in OPCs, while their expression is mostly lacking in neurons in the area postrema, which are responsible for emesis.

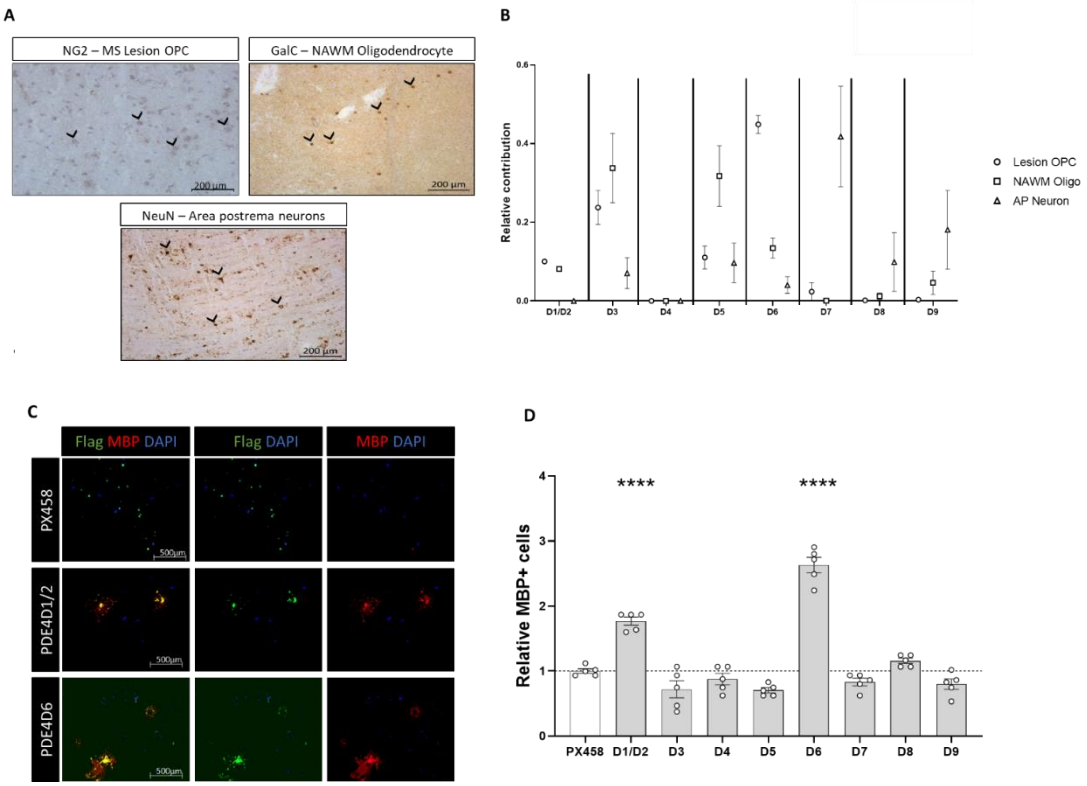

FIG 3.5: Gene expression profiles of the *PDE4D* isoforms in human area postrema (AP) neurons and MS patient oligodendrocyte precursor cells (OPC) and oligodendrocytes (OLg) is indicative for biological functionality as shown by targeted isoform knockdown. (A) MS lesion OPCs, NAWM oligodendrocytes and area postrema neurons were mapped using NG2, GalC or NeuN respectively for laser capture microdissection (LCM). **(B)** Using LCM, 50 individually cells collected per cell type and pooled for mRNA extraction and gene expression. Oligodendrocytes and OPCs were pairwise collected in the same samples. Area postrema neurons were derived from non-neurological CNS donor samples. The proportional contribution of each splice variant was calculated for each sample (sum isoforms per sample = 1) (n=10/group). **(C-D)** Primary mouse OPCs were transfected with a CRISPR/Cas9 construct (PX458 backbone with cloned gRNAs designed for specific isoform) by means of magnetofection. Fluorescence analysis showed more MBP positive oligodendrocytes within the transfected population of cells upon PDE4D1 or PDE4D6 knockdown (n=5/group). For the LCM experiment, the sample size 'n' represents the number of donors used to isolate the belonging cell type. For the CRISPR/Cas9 experiment, the sample size 'n' represents the number of wells obtained from minimally three independent cell culture experiments Data were analyzed using a non-parametric Kruskal-Wallis test with Dunn's multiple comparisons test (***p<0,001).

The PDE4B inhibitor A33 diminishes neuro-inflammation, while the PDE4D inhibitor Gebr32a increased CNS myelin content in EAE

To understand whether PDE4D and PDE4B inhibition shows differential effects on neuroinflammation versus myelination, we studied the therapeutic potential of the pan PDE4 inhibitor roflumilast, the PDE4B inhibitor A33 and the PDE4D inhibitor Gebr32a in the chronic EAE model. During the early acute phase of the model, neuroinflammation is prominent, while the level of myelination can be studied during the chronic phase of the disease. Therefore, as a readout, we assessed clinical scores, cognitive performance pre-onset of neurological symptoms, immune cell phenotype, and the level of de- and remyelination of the animals.

At four and ten days after EAE induction, pre-onset of the clinical symptoms, spatial memory was assessed in the OLT and the average performance was taken for further analysis. Mice treated with the roflumilast (3mg/kg) or A33 (3mg/kg) displayed intact spatial memory (two-tailed one sample t-test against d2≠0; ** P≤0.01; *** P≤0.005) whereas the vehicle and Gebr32a-treated groups displayed impaired spatial memory following induction of the EAE (**Fig 3.6A**). In line with this, roflumilast and A33 suppressed EAE clinical scores (area under curve; AUC) during the inflammatory phase of the disease from (Friedman test with Dunn's multiple comparison F(3,59)=64.44; ***P≤0.005) (non-parametric Kruskal-Wallis test with Dunn's post-hoc analysis for AUC). In contrast, Gebr32a (3mg/kg) did not affect the neurological disabilities in this phase (**Fig 3.6B**). During a 10-day washout period (d34 - d44 d.p.i.), clinical symptoms increased in roflumilast and A33-treated groups. Restarting the treatment regimen in the chronic stage of EAE at 45 days post induction showed a reversal in efficacy of the inhibitors. While roflumilast and Gebr32a significantly reduced clinical symptoms, A33 was no longer effective at this chronic stage of the disease (Friedman test with Dunn's multiple comparisons; F(3,20)=29.17; *P≤0.05, ***P≤0.005) (non-parametric Kruskal-Wallis test with Dunn's post-hoc analysis for AUC) (**Fig 3.6B**).

Flow cytometry was performed at peak of the disease (day 20 p.i.) and at the end of the chronic stage (day 65 p.i.)(**Supplementary Fig S3.2**). At peak, the CNS of the A33 and roflumilast treated-animals exhibited a reduced percentage of pathogenic T cells ($CD45^+CD3^+CD4^+IFN\gamma^+$) (non-parametric Kruskal-Wallis test with Dunn's post-hoc analysis; F(3,16)=10.67; *P≤0.05), and a relative increase

of non-pathogenic T cells ($CD45^+CD3^+CD4^+IFN\gamma^-IL17^-$) (non-parametric Kruskal-Wallis test with Dunn's post-hoc analysis; $F(3,16)=10.24$; $^*P\leq0.05$), whereas no differences were noted at the end stage (day 65 p.i.) (**Fig 3.6C-I**). A non-parametric Kruskal-Wallis test revealed a significant reduction of inflammatory monocytes ($CD45^+CD11^+Ly6c^{High}$) (Dunn's post-hoc analysis; $F(3,16)=14.79$;$^{**}P\leq0.01$) and an increased *Il-27* mRNA expression in the brain (Dunn's post-hoc analysis; $F(3,13)=12.26$; $^*P\leq0.05^{**}P\leq0.01$) of A33 and roflumilast, but not Gebr32 treated animals (**Fig 3.6J**). No differences in regulatory T cells were observed, nor at peak or at the end of the experiment (**Supplementary Fig S3.4**). Additionally, the spinal cord of roflumilast or A33 treated animals showed an increased presence of $Arginase^+$ infiltrated monocytes, indicating a shift towards $Arg1^+$ macrophages (Kruskal-Wallis test; Dunn's post hoc analysis; $F(3,16)=14.79$; $^*P\leq0.05$; $^{**}P\leq0.01$) (**Fig 3.6K and L**). The total number of infiltrating lymphocytes or monocytes did not differ over the complete EAE disease course (**Supplementary Fig S3.5**), nor were any differences detected in peripheral tissues including lymph nodes and spleen in any of the treatment groups. At the end of the disease course, an MBP staining on transversal sections of the spinal cord of these animals displayed a significantly increased MBP^+ area upon roflumilast and Gebr32a, but not upon A33 treatment (non-parametric Kruskal-Wallis test with Dunn's multiple comparisons; $F(3,16)=16.71$; $^*P\leq0.05$; $^{***}P\leq0.005$) (**Fig 3.6M and N**). Ultrastructural myelin imaging using TEM confirmed the immunohistochemical observations displaying decreased G ratios and an increased number of myelinated axons in the optic nerve of the animals treated with roflumilast and Gebr32a treatment, but not when treated with A33 (day 65 d.p.i.) (non-parametric Kruskal-Wallis test with Dunn's multiple comparisons; $F(3,16)=15.34$; $^*P\leq0.05$; $^{**}P\leq0.01$) (**Fig 3.6O-R**). These data indicate an increase in myelin content during the chronic stage of the disease.

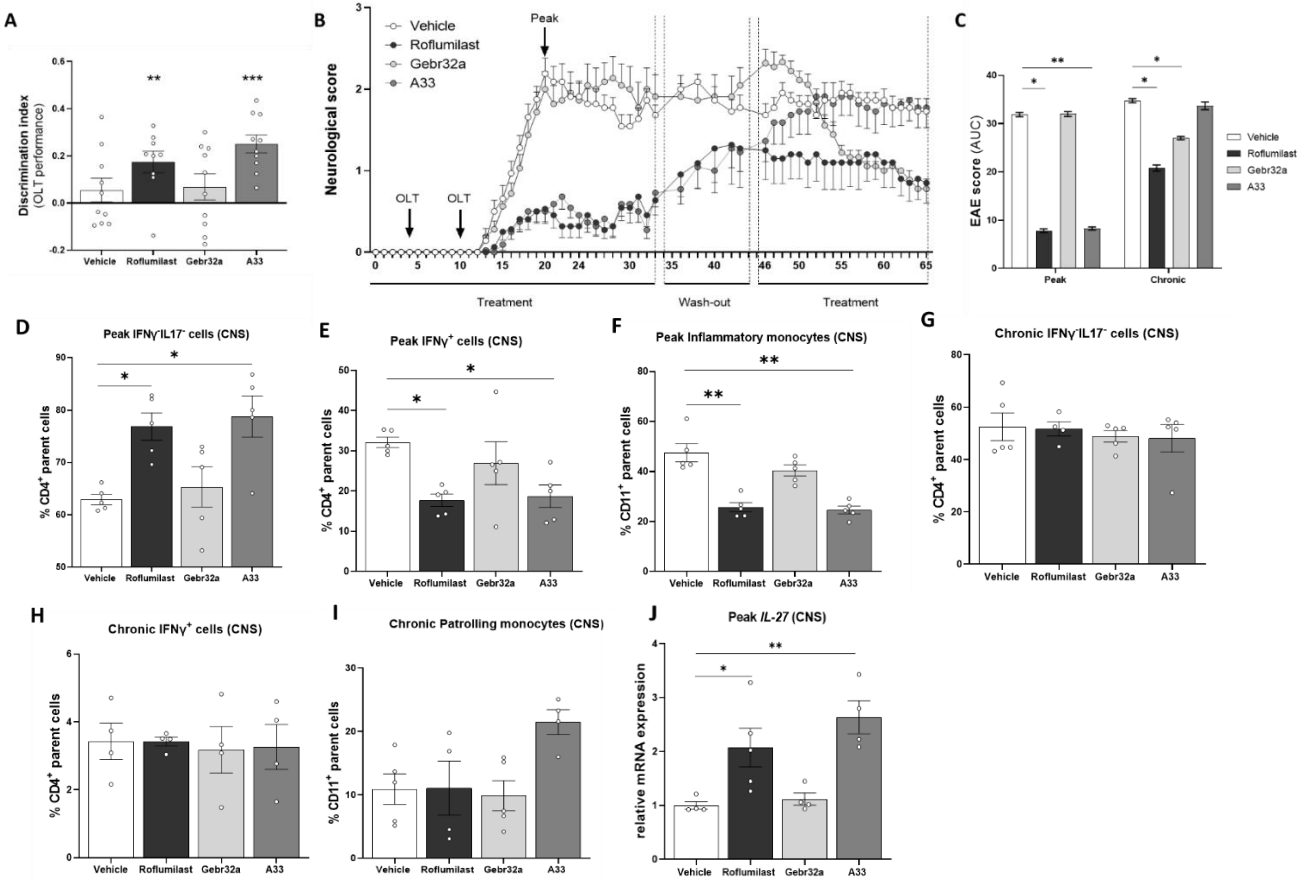
A
Discrimination index
(OLT performance)
Vehicle
Roflumilast
Gebr32a
A33
B
Vehicle
Roflumilast
Gebr32a
A33
Peak
Neurological score
OLT
OLT
Treatment
Wash-out
Treatment
C
EAE score (AUC)
Peak
Chronic
D
Peak IFNγ-IL17- cells (CNS)
% CD4+ parent cells
E
Peak IFNγ+ cells (CNS)
% CD4+ parent cells
F
Peak Inflammatory monocytes (CNS)
% CD11+ parent cells
G
Chronic IFNγ-IL17- cells (CNS)
% CD4+ parent cells
H
Chronic IFNγ+ cells (CNS)
% CD4+ parent cells
I
Chronic Patrolling monocytes (CNS)
% CD11+ parent cells
J
Peak IL-27 (CNS)
relative mRNA expression

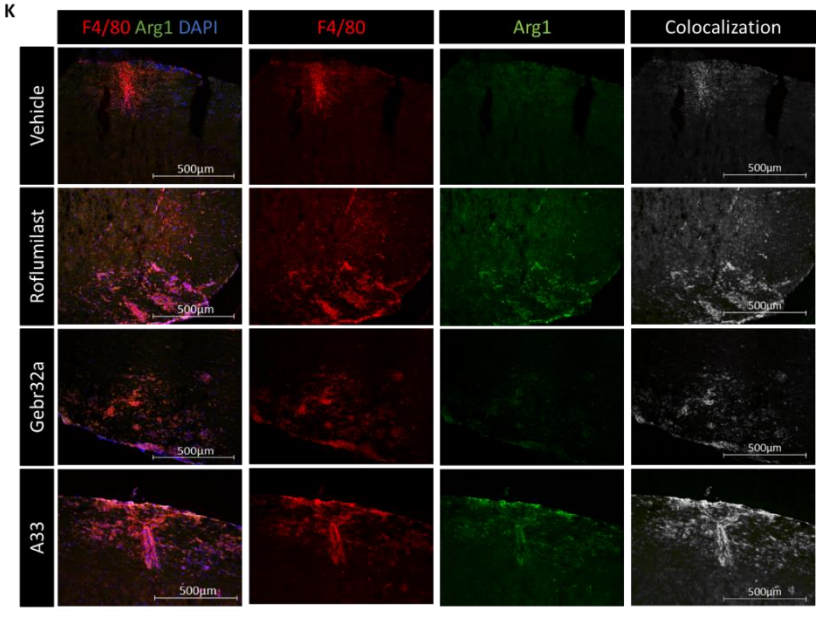
K
F4/80 Arg1 DAPI
F4/80
Arg1
Colocalization
Vehicle
Roflumilast
Gebr32a
A33
500µm

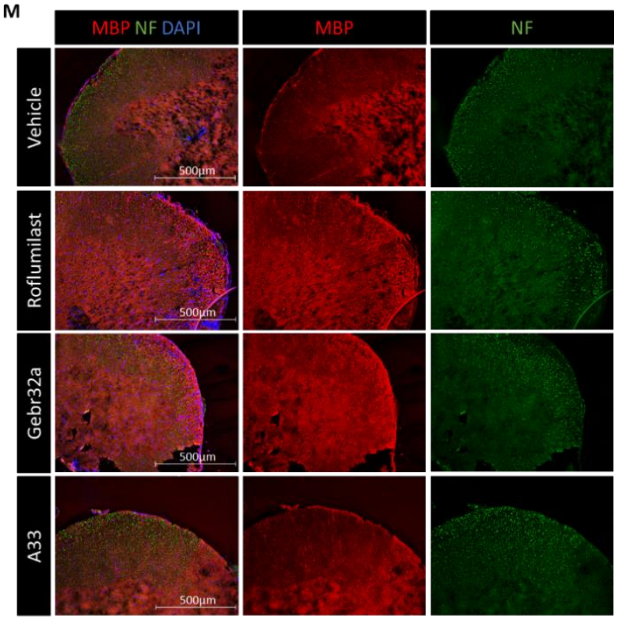
M
MBP NF DAPI
MBP
NF
Vehicle
Roflumilast
Gebr32a
A33
500µm

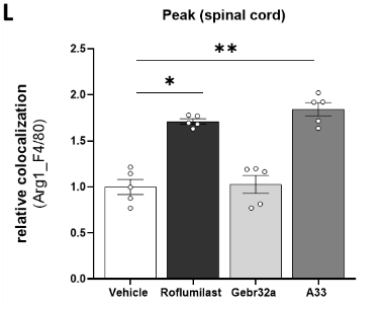
L
Peak (spinal cord)
relative colocalization
(Arg1_F4/80)
2.5
2.0
1.5
1.0
0.5
0.0
**
*
Vehicle
Roflumilast
Gebr32a
A33

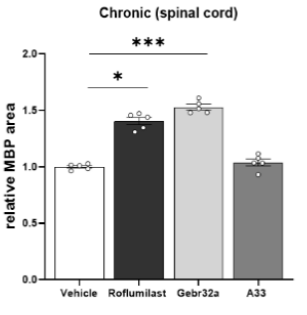
N
Chronic (spinal cord)
relative MBP area
2.0
1.5
1.0
0.5
0.0
***
*
Vehicle
Roflumilast
Gebr32a
A33

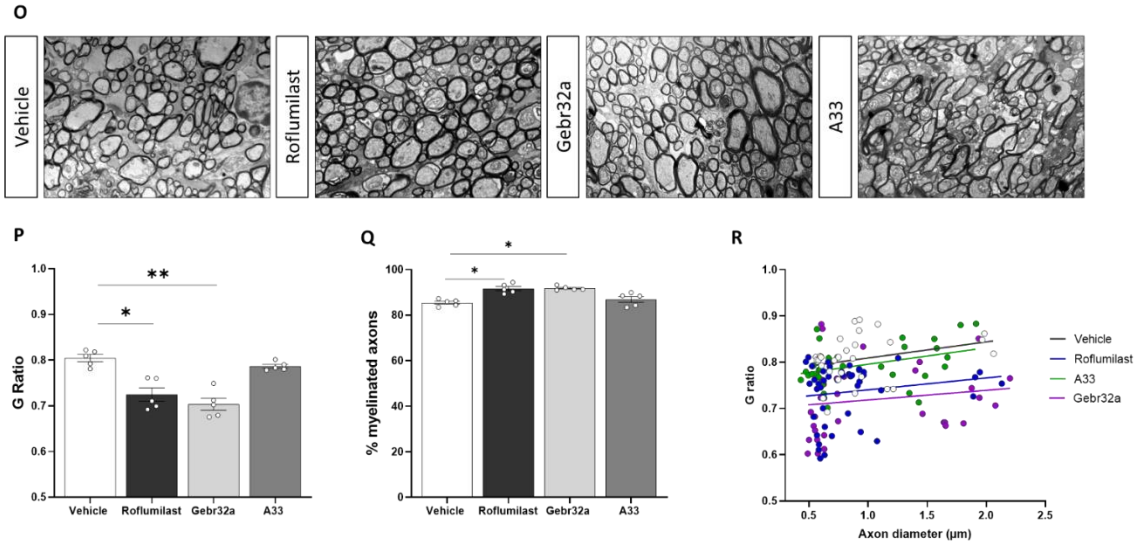

FIG 3.6: Inhibition of PDE4B by A33 has immunomodulatory effects and therefore ameliorates acute clinical scores, while inhibition of PDE4D by Gebr32a reduces neurological scores in the chronic phase of the disease and enhanced the proportion of myelinated axons. (A) Four groups consisting of each 21 10-weeks old female mice were immunized with MOG_{35-55} peptide and treated with 0.1% DMSO, roflumilast (3mg/kg), A33 (3mg/kg) or Gebr32a (0.3mg/kg) by subcutaneous injections starting from the day of immunization until day 65 with a drug wash out period included from day 34-45. Preceding EAE induction, 44 out of 84 animals were trained for the object location task (OLT). After EAE induction, the 44 trained animals were subdivided among the 4 treatment groups (n= 11/group). At four and ten days post induction, preceding motor impairment, spatial memory performances were assessed using the OLT (n≥8/group) **(B)** Animals were neurologically scored daily in a blinded manner for clinical signs on a 0-5 scale (n≥9/group). **(C)** AUC of EAE scores were analyzed to determine significances in neurological scores (n≥9/group). **(D-I)** At disease peak (20dpi) and at the end of the experiment (65dpi), 5 animals per group were sacrificed for flow cytometry and immunohistochemical analysis. The percentage of nonpathogenic/pathogenic T cells and inflammatory/patrolling phagocytes in the CNS are displayed in relation to the parental cells (absolute T lymphocyte and monocyte number) (n=5/group). **(J)** mRNA expression analysis of *il-27* in the brain of EAE animals sacrificed at peak (n≥4/group) **(K-L)** Longitudinal sections of the spinal cord were made at disease peak and evaluated for Arginase and F4/80 colocalization (n≥4/group). **(M-N)** Transversal sections of the spinal cord were made at the chronic end phase of the disease where the MBP^+ area was evaluated and correct for the number of neurofilament positive axon**s** (n≥4/group)**. (O-R)** Optic nerves were isolated at the end of the experiment and further processed for TEM analysis (n=5/group)**.** A one sample t-test was performed to test for spatial memory (e.g. D2≠0). A non-parametric Friedman tests with Dunn's multiple comparison against vehicle group was performed to evaluate differences in clinical scores during the EAE course. The AUC of EAE scores over time, flow cytometry, IHC and TEM results were analyzed with a non-parametric Kruskal-Wallis test with Dunn's multiple comparison (*p≤0,05; **p≤0.01; ***p≤0.001). Data shown are mean +/- SEM.

pde4b$^{-/-}$ bone marrow transplantation promotes clinical recovery in EAE by diminishing neuro-inflammation

Since pharmacological inhibition of PDE4B by means of A33 diminished neuro-inflammation, we next aimed to further determine the involvement of Pde4b during EAE disease course by performing a bone-marrow transplantation of *pde4b$^{-/-}$, pde4b$^{+/-}$, and pde4b$^{+/+}$* mice into lethally irradiated wild type acceptor mice preceding EAE induction (**Fig 3.7A**). The onset of the disease (day 10 p.i.) was not affected, but, based on a non-parametric Kruskal-Wallis test, knockout *pde4b$^{-/-}$* and *pde4b$^{+/-}$* heterozygous bone marrow receivers displayed a significant gene dose-dependent reduction in the clinical scores (Tukey's multiple comparison test, $F(2,27)=12.73$; ***P≤0.005) (**Fig 3.7B-C**). In line with pharmacological PDE4B inhibition, the CNS at disease peak of *pde4b$^{-/-}$* bone marrow receivers showed an increased percentage of anti-inflammatory or patrolling phagocytes ($CD45^+CD11^+Ly6c^{low}$) (Kruskal-Wallis test with Dunn's multiple comparisons; $F(2,12)=9.454$; *P≤0.05) and non-pathogenic T lymphocytes ($CD45^+CD3^+CD4^+IFN\gamma^-IL17^-$) (Kruskal-Wallis test with Dunn's multiple comparisons; $F(2,12)=10.66$;**P≤0.01), while inflammatory monocytes ($CD45^+CD11^+Ly6c^{High}$) (Kruskal-Wallis test with Dunn's multiple comparisons; $F(2,12)=8.637$;**P≤0.01) and pathogenic T lymphocytes ($CD45^+CD3^+CD4^+IFN\gamma^+$) were significantly decreased (**Fig 3.7D-G**).

To study whether PDE4B inhibition directly skews the phagocyte phenotype shift, thereby affecting the inflammatory activity, both murine BMDMs and microglia were exposed to mouse myelin (48h) and an inflammatory trigger (IFNγ and IL-1β; 24h). We observed that PDE4B inhibition by 1μM A33 significantly suppressed the murine phagocytic nitrite release in the medium, which is an indicator of nitric oxide production (Kruskal-Wallis test with Dunn's multiple comparisons; $F(3,16)=16.28$; $F(3,21)$; *P≤0.05)(**Fig 3.8A and 3.8B**). Furthermore, ICAM-1 and VCAM-1 adhesion molecule levels were measured on primary brain microvasculature endothelial cells (BMEC) using flow cytometry. Following PDE4 or PDE4B inhibition, mean fluorescent intensity levels of ICAM-1 were significantly reduced indicated a reduced ICAM-1 protein abundance (Kruskal-Wallis test with Dunn's multiple comparisons; $F(3,23)=9.388$;*P≤0.05) (**Fig 3.8C-F**).

To evaluate whether PDE4B inhibition is also able to skew the human macrophage phenotype shift, human MDMs were exposed to human myelin (48h) and an inflammatory trigger (IFNγ and IL-1β; 24h). A33 attenuated the NO production in human macrophages, as measured by a decrease in DAF fluorescent signal (Kruskal-Wallis test with Dunn's multiple comparisons; F(3,20)=18.22;*P≤0.05; ***P≤0.005) **(Fig 3.8G and 3.8H)**. These findings, together with the *in vivo* immunomodulatory actions position PDE4B as an important target for reducing the neuroinflammatory status in MS.

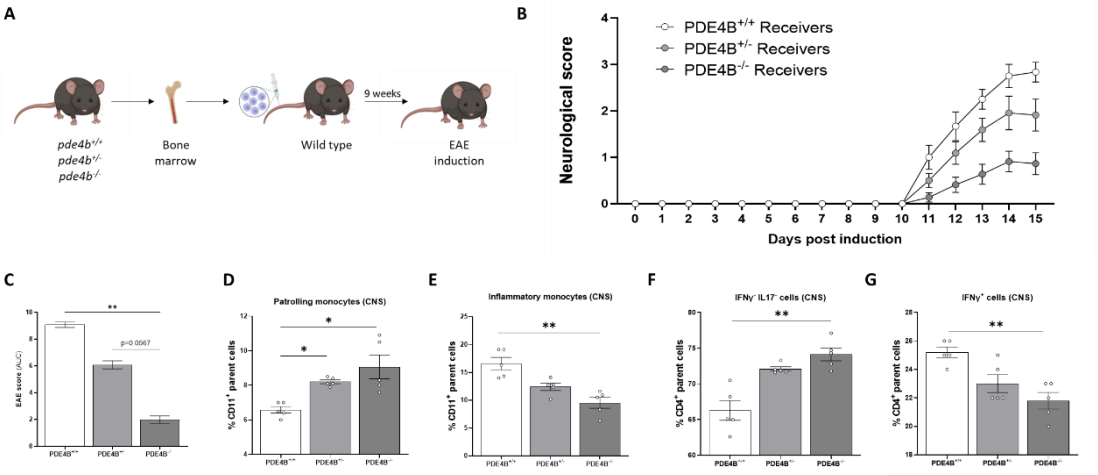

FIG 3.7: Bone marrow transplantation of PDE4B$^{+/-}$ or PDE4B$^{-/-}$ donors reduces neurological scores in the EAE model. (A) Schematic representation of the bone marrow transplantation followed by EAE experiment. **(B)** Following bone marrow transplantation and engraftment, 28 female C57bl6 OlaHsd mice were immunized in the flank and neck with MOG_{35-55} peptide emulsified in Complete Freund's Adjuvant containing Mycobacterium tuberculosis. Animals were neurologically scored for clinical signs on a daily basis (n≥7). **(C)** AUC of EAE scores were analyzed to determine significances in neurological scores (n≥7/group). **(D-G)** At the peak of the disease (15 dpi), all animals were sacrificed for flow cytometry analysis. The percentage of nonpathogenic as well as pathogenic monocytes and T lymphocytes are displayed in relation to the parental cells ($CD11b^+$ monocytes or $CD4^+$ T lymphocytes in the CNS) (n≥4). Difference in AUC clinical scores and flow cytometry results were analyzed with a non-parametric Kruskal-Wallis test with Dunn's multiple comparison. Changes in immune cell subsets were analyzed using a non-parametric Kruskal-Wallis test with Dunn's multiple comparisons test. Data are displayed as mean +/-SEM. (*p≤0,05; **p≤0,01; ***p≤0,005).

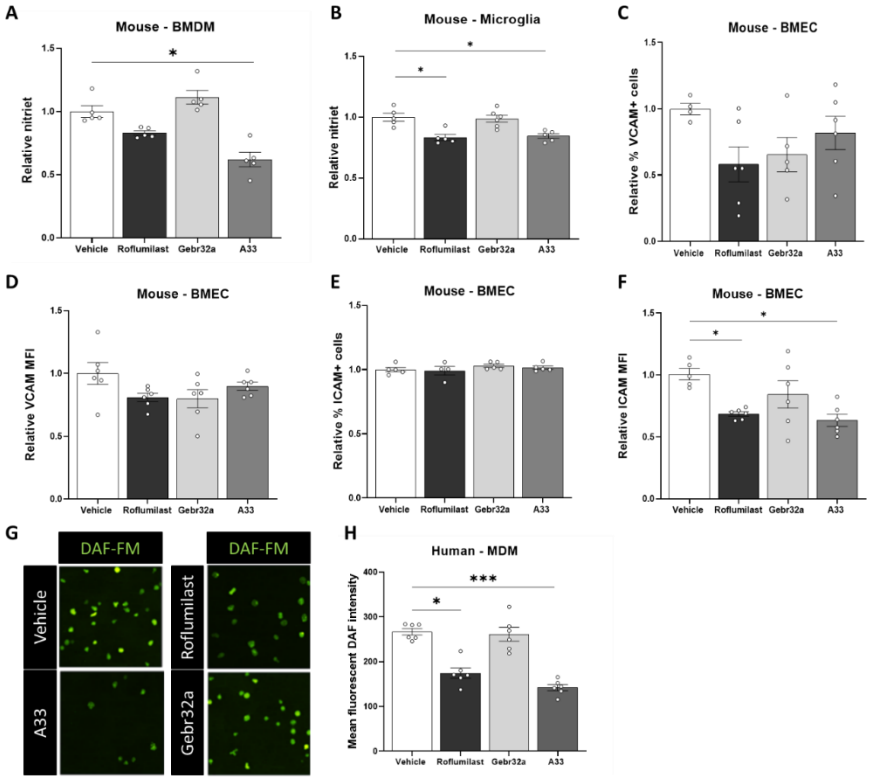

FIG 3.8: inhibition of PDE4 by roflumilast and PDE4B by A33 alters mouse and human phagocyte activation and lowers the mean fluorescent intensity of ICAM on murine endothelial cells. (A) Mouse bone marrow derived macrophages (BMDMs) or **(B)** microglia were stimulated with mouse myelin (100µg/ml) for 24h and simultaneously treated with 0.1% DMSO, 1µM roflumilast, 1µM Gebr32a or 1µM A33. After 18h, medium was processed for NO secretion using a Griess assay (n≥5/group). Furthermore, brain microvasculature endothelial cells were inflamed with TNFα (10ng/ml) and IFNγ (10ng/ml) and treated with the PDE4/B/D inhibitor for 48h. Cells were harvested and adhesion molecule expression were analyzed using flow cytometry. The percentage of **(C)** $VCAM^+$ or **(E)** $ICAM^+$ positive cells and the **(D and F)** mean fluorescent intensity of the cells for either one of the adhesion molecules were quantified (n≥4/group).**(G-H)** Human monocyte derived macrophages (MDMs) were stimulated with human myelin (100µg/ml) for 24h and simultaneously treated with 0.1% DMSO, 1µM roflumilast, 1µM Gebr32a or 1µM A33. After 18h, human MDM cells were processed for intracellular NO production measurement using DAF-FM (n=6/group). For the mouse BMDM, microglia and endothelial cell experiment, the sample size 'n' represents the number of wells obtained from minimally three independent cell culture experiments. For the human MDM experiment, the sample size 'n' represents the number of donors used to isolate MDMs. Data were analyzed using a non-parametric Kruskal-Wallis test with Dunn's multiple comparisons test. Data are displayed as mean +/-SEM. (*p≤0,05; ***p≤0,005).

The therapeutic dose of Gebr32a and A33 is not accompanied with emetic-like side effects

Given the emetic potential pan PDE4 inhibitors possess, the duration of the xylazine/ketamine α2-adrenergic receptor-mediated anesthesia was measured upon roflumilast, Gebr32a or A33 treatment (**Fig 3.9A)**. While the known emetic dosage of roflumilast (3mg/kg, s.c.) significantly reduced the anesthesia duration, neither tested concentration of A33 or Gebr32a altered the time until the righting reflex compared with the vehicle condition (non-parametric Kruskal-Wallis test with Dunn's post-hoc analysis; $F(14,131)=52.79$; $^{**}P\leq0.01$). In line with this finding, only 1µM of roflumilast bath perfusion increased electrical activity in neurons of the murine area postrema while this effect was not observed for 1µM Gebr32a (**Fig 3.9B**).

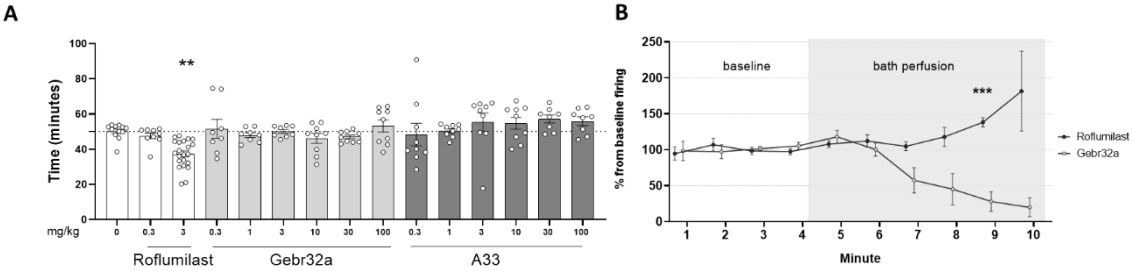

FIG 3.9: The xylazine/ketamine anesthesia time and action potential firing rate of mouse area postrema neurons show no signs of emetic side effects upon PDE4B or PDE4D inhibition by means of A33 or Gebr32a. (A) Fifteen minutes following anesthesia induced by a xylazine (10 mg/kg, i.p)/ketamine (60 mg/kg, i.p) combination, mice were treated by subcutaneous injections with different doses of roflumilast (0.3 or 3 mg/kg), A33 (0.3-100mg/kg) or Gebr32a (0.3-100mg/kg). The time until the return of the righting reflex was used as a measure for anesthesia duration (n≥8/group). **(B)** Putative area postrema neurons were identified based on location relative to the central canal and electrophysiological characteristics. Pipettes of 4-6 MOhm resistance filled with a Na HEPES-based solution were used for extracellular recordings using the loose cell attached method as described by Branch and Beckstead (2012). Baseline firing rate was recorded for four minutes. A non-parametric Kruskal Wallis test was used to evaluate significance. Data are shown as mean +/- SEM ($^{**}p\leq0.01$;$^{***}p\leq0.005$).

Discussion

Targeting the destructive immunological interplay in MS and promoting endogenous remyelination are key goals in developing novel MS therapeutics. In line with previous studies, we confirmed that full PDE4 inhibition by means of roflumilast supports neuro-regenerative responses and suppresses neuroinflammation in different animal models of MS (104, 118, 158, 190, 367, 368). Next, we segregated the myelination-promoting role of PDE4 inhibition into a PDE4D-dependent process, while selective PDE4B inhibition accounted for the anti-inflammatory effects. However, the major drawback in translating PDE4 inhibitors towards clinical applications are the predicted emetic side effects ascribed to *PDE4D* expression in the *area postrema* in the medulla oblongata (349). Interestingly, we show here for the first time that short and super-short *PDE4D* isoforms are hardly expressed in the neurons of human *area postrema*, while highly expressed in human OPCs. These findings render the (super-)short PDE4D isoforms an interesting target to safely enhance remyelination. Therefore, by selectively and complementary inhibiting PDE4 genes, we provide a new opportunity to enhance remyelination without triggering the emetic side effects linked to full PDE4 inhibition.

In our study, we identified that PDE4D inhibition in particular is sufficient to stimulate OPC differentiation by inducing MBP protein levels in primary OPCs, both on PLL coated substrate as well as in the presence of fibronectin. Both primary murine OPCs and human iPSC-derived OPCs significantly increased their number and length of myelin sheaths surrounding electro-spun microfibers upon PDE4D inhibition. Consequently, in an *ex vivo* cerebellar brain slice model, PDE4D inhibition increased the level of remyelination after LPC-induced demyelination. The enhanced differentiation of OPCs and the consecutive induction of (re)myelination upon roflumilast treatment is consistent with previous studies reporting beneficial effects of both cAMP analogous (e.g. dibutyryl cAMP and 8-bromo cAMP) and pan PDE4 inhibitors (rolipram) on *in vitro* and *in vivo* oligodendroglial differentiation (118, 263). Moreover, it has been shown that downstream of cAMP, the PKA-CREB axis is crucial for OPC differentiation, and its activation is sufficient to overcome the inhibition of myelination by fibronectin, reflective of a pathological demyelinated MS lesion (118, 263, 369).

Next, we investigated the effects of PDE4D inhibition in an *in vivo* cuprizone model. After ceasing the cuprizone diet, both roflumilast and Gebr32a treatment were shown to enhance both molecular and functional remyelination. Both, roflumilast and Gebr32a have previously been ascribed to have pro-cognitive effects in healthy mice and an Alzheimer mouse model (281, 351). However, the doses applied in the current study are not within the range of the reported spatial memory-enhancing dosages (i.e., 100-fold higher) (281, 351). Besides spatial memory performances, we implemented the highly translational VEP measurements in our cuprizone animal model. VEP measurements are among of the most important electrophysiological tests for diagnosing and measuring progression during MS pathogenesis (370). Abnormal latency times of VEP recordings are indicative of demyelination of the central nervous system and are highly complementary to clinical outcomes of somatosensory functions. Six weeks of cuprizone treatment significantly prolonged the latency of the VEP recordings due to the cuprizone-induced demyelination. We showed that subcutaneous treatment of 0.3 mg/kg Gebr32a successfully reduces VEP latency time in the cuprizone model. These data further support the remyelination-boosting capacity of PDE4D inhibition. Due to the lack of OPC differentiation promoting effects of the PDE4B inhibitor A33, we have not investigated its therapeutic role in the cuprizone model. However, the abovementioned finding that PDE4B inhibition skews phagocyte polarization might implicate that an indirect remyelination promoting effect of A33 could positively influence cuprizone outcome (371, 372). Nevertheless, controversy exists concerning the role of macrophages for promoting repair in the cuprizone model which can be attributed, among others, to the specific therapeutic window in which compound have to be administered to observe phagocyte-mediated remyelination (373).

On an isoform level, we demonstrate here that especially short and super-short *PDE4D* isoforms (*PDE4D1/2* and *PDE4D6*) are highly present in human MS lesion OPCs and to a lesser extent in myelinating oligodendrocytes, indicating a clear difference in cell type specific isoform expression abundancy. To assess the biological relevance of the individual PDE4D isoforms on OPC differentiation, we made use of a CRISPR-Cas9 genetic editing system to create isoform-specific knockdown cultures. We applied a commercially available plasmid (374), which uses a FLAG- and GFP-TAG to trace transfected cells and a Cas9 endonuclease to

create a gRNA guided in/del. Transfection of primary mouse OPCs with gRNAs targeting either the short *pde4d1/2* or the super-short *pde4d6* isoform led to more MBP-positive oligodendrocytes within the transfected pool of cells, indicating that knockdown of one of the two isoforms is sufficient for boosting OPC differentiation. Importantly, no other *pde4d* isoform knockdown could significantly affect the differentiation rate of primary transfected OPCs.

As a second and more pathologically complex animal model for MS, we made use of the chronic EAE model where neuro-inflammation is the driving force of CNS demyelination. Interestingly, while lacking efficacy in the early stage of the disease, PDE4D inhibition in the chronic phase improved motor functioning and therefore lowered neurological EAE scores to the level of roflumilast-treated mice. MOG-induced neuro-inflammatory processes have been described to cause optic nerve demyelination and therefore allow remyelination assessment in the EAE model (375-377). Our findings confirm a remyelination-boosting potential of PDE4/PDE4D inhibition as lower G ratios of the optic nerve were detected, independent of the axonal diameter, in both roflumilast- and Gebr32a-treated mice at the end of the EAE experiment.

In contrast to PDE4D inhibition, PDE4B inhibition significantly reduced neuroinflammation and coinciding memory deficits and neurological scores in the acute phase of the MOG_{35-55}-induced EAE model. The cognitive deficits observed in the EAE model have previously been attributed to the up-regulation of inflammatory cytokines, dysregulation of the HPA-axis, disruption of hippocampal synapses and/or downregulation of choline acetyltransferase, all which can be influenced by altering intracellular cAMP levels (378-380). Post-mortem, we demonstrated a reduction in CNS-infiltrating inflammatory Th1 cells and inflammatory monocytes at EAE peak upon PDE4B inhibition. Our data corroborated these findings, as we showed an increased expression of *Arginase-1* and the anti-inflammatory cytokine *Il-27*, which additionally exerts an inhibitory function on IFN-γ production by activated $CD4^+$ T cells (381-383). In line with this, PDE4B inhibition has previously been held responsible for anti-inflammatory actions (219, 384). Upon inflammatory stimulation, *Pde4b* expression is paralleled with an increase in key inflammatory markers (e.g., TNF-α and IL-1β) in immune cells including microglia, astrocytes and $CD11b^+$ macrophages (226, 229). In

mouse macrophages, pharmacological PDE4 inhibition by rolipram (10μM) has been shown to lower LPS-induced TNF-α production, an effect that is exclusively mediated through PDE4B-specific inhibition as demonstrated by using *Pde4b* null-macrophages (219). In line with these observations, *Pde4b*$^{-/-}$ mice highlight the crucial role of PDE4B in neuroinflammatory responses as these mice showed reduced glial cell activation upon systemic LPS-induced endotoxemia and decreased inflammatory protein markers (e.g. *GFAP, CD11b, Iba1, Cox2*) following spinal cord injury (226, 229). Furthermore, intraperitoneal administration of the PDE4B inhibitor 2-(1H-indol-3-yl)-quinoxaline (derivative 3b) halted MS disease progression in the EAE zebrafish model starting from a 3mg/kg dose (226, 385).

In line with our post-mortem results, both the pan PDE4 inhibitor rolipram and the cAMP-specific PDE7 inhibitor TC3.6 have been reported to decrease the pro-inflammatory IL-17 production and reduce the extravasation of immune cells in the CNS (190). Even though both cAMP-modulating PDE inhibitors alter the final immune response similarly, Gonzalez-Garcia et al. showed distinct pathways to achieve this immunomodulatory effect (190). The PDE7 inhibitor TC3.6 directly suppressed IL-17 production by $CD4^+$ lymphocytes, while the PDE4 inhibitor rolipram only achieved this decreased production of IL-17 when CD11b+ monocytes were co-cultured or when the supernatant of rolipram treated-$CD11b^+$ cells was transferred to the $CD4^+$ lymphocyte cultures (190). The indirect effect of rolipram on IL-17 production is thought to be mediated by monocytes' elevated production of IL-27 (190, 386, 387). Previously, it has also been shown that the expression of the cAMP-specific PDE8A is induced in activated T lymphocytes, and inhibition of the complete PDE8 family by PF-04957325 (10 mg/kg) has been shown to suppress neuroinflammation, thereby reducing the inflammatory lesion load in the EAE animal model (388, 389). The therapeutic potential of the cAMP-specific PDE4, PDE7 and PDE8 inhibitors highlights the crucial role of cAMP in modulating the anti-inflammatory responses.

Since the inhibitors used in this study have been administered systemically, we aimed to exclude potential non-inflammatory actions because PDE4B inhibition has also been ascribed to stimulate neurogenesis, neural plasticity, synaptic strengthening and coordination of peripheral endotoxemia and gut dysbiosis - all

processes which have been shown to affect inflammation and EAE outcome (226, 229, 390). Therefore, we performed a BMT preceding EAE induction to target PDE4B in specifically immune cells. As with the use of a PDE4B inhibitor in the acute phase of the EAE model, selective absence of PDE4B in *pde4b*$^{-/-}$ bone marrow-transferred mice displayed a gene dosage-dependent protective effect on the neurological EAE score. Inflammatory monocytes and IFNγ^{+} CD4^{+} T cells decreased in *pde4b*$^{-/-}$ bone marrow acceptor mice, whereas patrolling phagocytes and IFNγ^{-}IL17^{-}CD4^{+} T cells significantly increased during EAE.

In vitro, we have seen that phagocytes are affected by PDE4B inhibition. Human monocyte-derived macrophages and murine BMDMs, and murine microglia, which is in line with the previously reported phagocyte polarization effects of roflumilast (236, 391). In primary brain microvasculature endothelial cells, a reduced protein abundance was detected at the level of ICAM-1 and subtle to no differences were detected at the level of VCAM-1 adhesion molecules, two endothelial leukocyte integrin counterreceptors that enable leukocyte transmigration to the brain (192). The sole significant effect on ICAM-1 protein abundance and not on VCAM-1, nor on the percentage of cells expressing the adhesion molecules, reduces but does not exclude, the possibility of their contribution to the effects seen in the different models. Yet, since the total number of lymphocytes and monocytes were not altered in the CNS upon PDE4B inhibition, this relatively small decrease in adhesion molecule presence did not result in less immune cell infiltration and therefore contributed minimally to the PDE4B-driven protection against EAE pathology. Important to note is that we have not investigated the direct role of inhibiting PDE4B using A33 in lymphocytes. Previous research reported an essential role for cAMP modulation to alter T lymphocyte activation (124, 186). Whereas activated T lymphocytes display an enzymatic increase of PDE7, inhibiting PDE7 decreased T lymphocyte polarization and increased FoxP3 levels and anti-inflammatory IL-10 secretion (189-191). In line, inhibiting PDE4 displayed similar results as it reduced pro-inflammatory cytokine secretion and T lymphocyte polarization, and increased anti-inflammatory cytokine production (104, 190). Regarding the PDE4 subtypes, even though activated T lymphocytes showed an increase in enzymatic PDE4A and PDE4D levels, and not PDE4B, PDE4B was demonstrated to play an essential role in Th2 lymphocyte activation and dendritic cell recruitment (112, 192). However, the exact effect of inhibiting

PDE4B specifically to alter T lymphocyte responses or polarization remains to be investigated.

The emetic side effects are a major drawback of the translation potential of pan PDE4 inhibitors into clinical applications. However, still a lot of controversy exists about the exact underlying mechanism of such emetic side effects. Recently, it was suggested that a reduced gastric emptying in mice upon full PDE4 inhibition was due to concurrent inhibition of more than one single PDE4 subtype since selective ablation of any PDE4 subtype did not impaired gastric emptying which was observed upon full PDE4 inhibition (128). Nevertheless, other studies have used *pde4b*- or *pde4d*-deficient mice to determine the specific contribution of distinct subtypes in the emetic response. In contrast to *pde4b*-deficient mice, *pde4d*-deficient mice showed signs of emetic side effects since their anesthesia time was reduced in the xylazine/ketamine induced anesthesia test, a surrogate marker for measuring emesis in rodents (129). Furthermore, the full PDE4 inhibitor PMNPQ (0.3 mg/kg) significantly reduced anesthesia time in both wild type and *pde4b* deficient mice but did not reduce anesthesia time further in *pde4d*-deficient mice, indicating a crucial role for PDE4D in PDE4 inhibition-mediated emetic side effects (129). In this study, we show for the first time the *PDE4D* isoform expression profile in laser-captured neurons of the human post-mortem area postrema. Our data show that especially long PDE4D isoforms are highly concentrated in area postrema neurons and hereby highlights the importance of selectivity towards PDE4D isoforms in order to minimally alter cAMP levels in the area postrema to avoid emetogenic effects of the inhibitors. In fact, the PDE4 gene-specific inhibitors used in this study showed no emetic side effects up to 300-fold the therapeutic dose in the *in vivo* xylazine/ketamine anesthesia test, nor did they increase the action potential firing rate of mouse area postrema neurons assessed by path-clamp electrophysiology. These data already indicate a level of isoform specificity in existing inhibitors (392).

Collectively, we demonstrated that specific PDE4 inhibition can orchestrate key processes in MS, such as neuroinflammation and myelin regeneration. Since full PDE4 inhibitors have been described to coincide with severe side effects, such as nausea and vomiting, new strategies should be implemented to rule out side effects while retaining potential therapeutic effects. Our data provide more insight into PDE4B inhibition to diminish neuroinflammation and isoform-specific PDE4D inhibition to stimulate remyelination. By identifying downstream isoform target specificity, non-emetogenic therapeutics can be identified and developed, since area postrema neurons show distinct expression profiles compared to oligodendroglial cells. Furthermore, as the therapeutic dose of A33 and Gebr32a used in this study already lacked emetic side effects based on murine *in vitro* and *in vivo* tests, this highlights their potential for further exploration in the context of MS and other neurodegenerative disorders.

Supplementary material and methods

Supplementary table S3.1. iPSC oligodendrocyte and SATO differentiation medium composition

Medium	Component	End concentration	Supplier
iPSC oligodendrocyte medium	DMEM/F-12 with GlutaMAX™	n.a.	Sigma-Aldrich
	Penicillin/streptomycin	1%	Invitrogen
	N2 supplement	1x	Sigma-Aldrich
	B27 supplement	1x	Sigma-Aldrich
	2-mercaptoethanol	0.5µM	Sigma-Aldrich
	human insulin	25µg/ml	Sigma-Aldrich
	MEM nonessential amino acids (NEAA)	1x	Sigma-Aldrich
	PDGF-AA	10ng/ml	PeproTech
	HGF	5ng/ml	PeproTech
	IGF-1	10ng/ml	PeproTech
	NT-3	10ng/ml	PeproTech
	T3	60ng/ml	Sigma-Aldrich
	Biotin	100ng/ml	Sigma-Aldrich
	db-cAMP	1µM	Sigma-Aldrich
SATO differentiation medium	DMEM high glucose medium (D6429)	n.a.	Sigma-Aldrich
	Penicillin/streptomycin	0.5%	Invitrogen
	Heat inactivated horse serum	2%	Sigma-Aldrich
	Putrescin	0.1mM	Sigma-Aldrich
	Transferrin	0.3mM	Sigma-Aldrich
	Sodium selenite	0.2µM	Sigma-Aldrich
	Progesterone	0.02mM	Sigma-Aldrich
	Bovine insulin	0.8mM	Sigma-Aldrich
	triiodothyronine	0.5µM	Sigma-Aldrich
	B27 supplement	2%	In house protocol

ABBREVIATIONS: n.a. = not applicable.

Supplementary figures

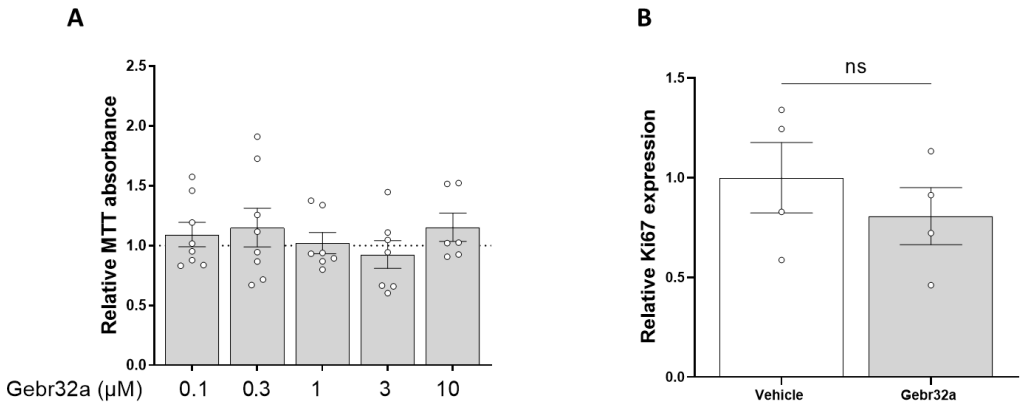

FIG S3.1: Inhibition of PDE4D by Gebr32a is not toxic up to 20μM, nor did it affect the proliferation rate of oligodendrocyte precursor cells. Primary mouse OPCs were treated for 48h with the PDE4D inhibitor Gebr32a. After 48h, cells were processed for mitochondrial activity using an **(A)** MTT assay**,** or were stained for **(B)** Ki67 to evaluate proliferation (n≥4/group)**.** MTT results were analyzed using a non-parametric Kruskal-Wallis test with Dunn's multiple comparisons. ICC data were analyzed using a non-parametric Mann-Withney test. Data are displayed as mean +/-SEM.

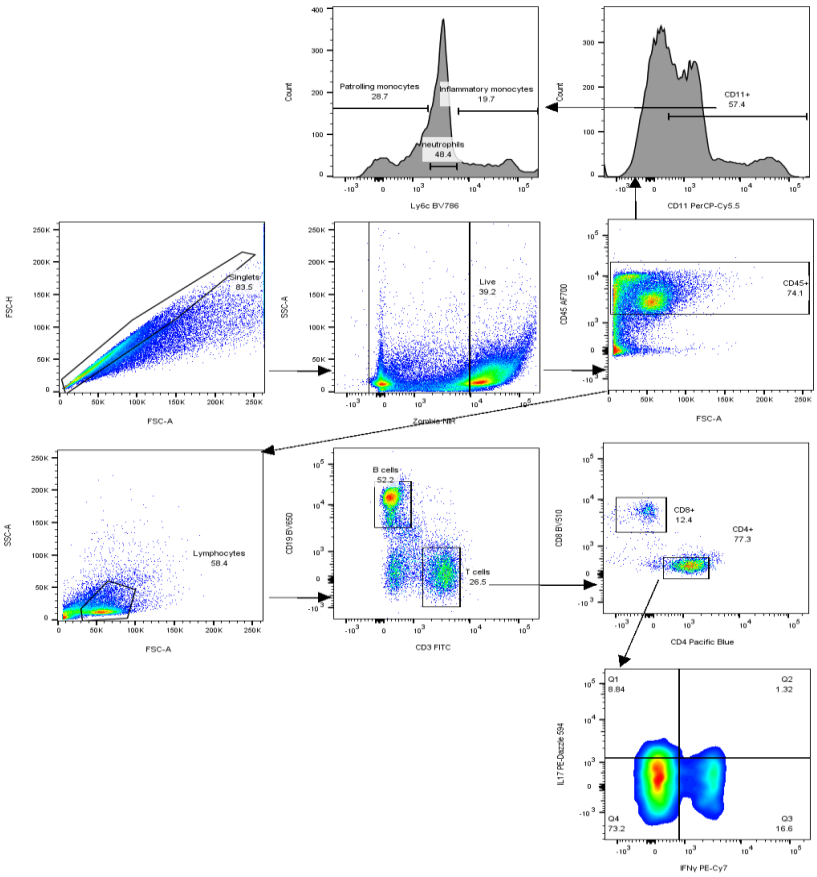

FIG S3.2: Flow cytometry gating strategy for identifying immune cell subsets.

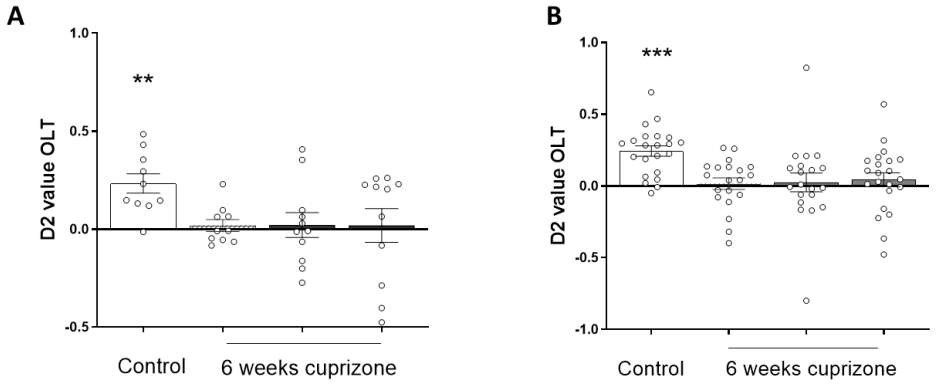

FIG S3.3: Cuprizone induced demyelination impairs spatial memory performances. (A and B) Nine-week old male C57bl6 mice were trained for the OLT as described previously (Sierksma et al 2014). Subsequently, animals were fed a 0.3% cuprizone diet for 6 weeks to induce demyelination, while the control group received a regular chow diet. The OLT was performed at the 3h inter-trial-interval to evaluate spatial memory performances and conducted at the end of the cuprizone intoxication (demyelination) preceding the start of the treatment. The cuprizone groups are displayed according to the different treatment groups. However, no treatment was initiated when testing during the demyelination phase, rendering no differences between the different cuprizone groups. A one sample t-test was performed to test for spatial memory (e.g. D2≠0) (***p<0,01; ***p<0,005).

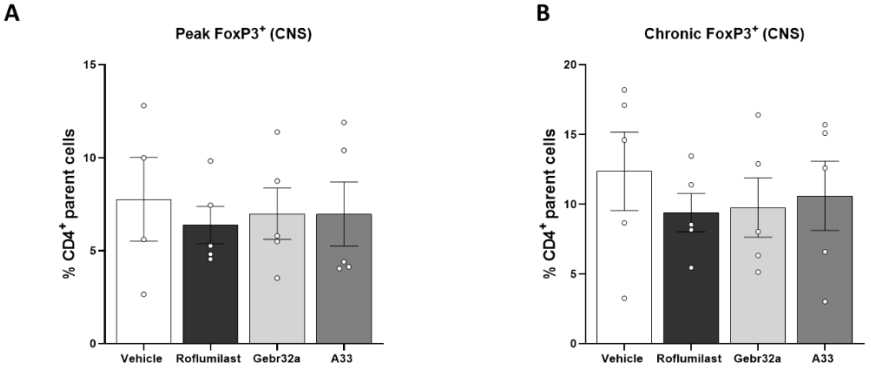

FIG S3.4: The percentage of regulatory T cell subsets in the CNS following EAE is not altered upon PDE4 or PDE4 subtype specific inhibition. (A) At EAE disease peak or at the **(B)** end of the experiment, animals were sacrificed for flow cytometry analysis for immune cell subsets phenotyping. The percentages of regulatory T cells in relation to their parent cell (CD4 T lymphocytes) are displayed here. Results were analyzed with a non-parametric Kruskal-Wallis test with Dunn's multiple comparison. Data shown are mean +/- SEM.

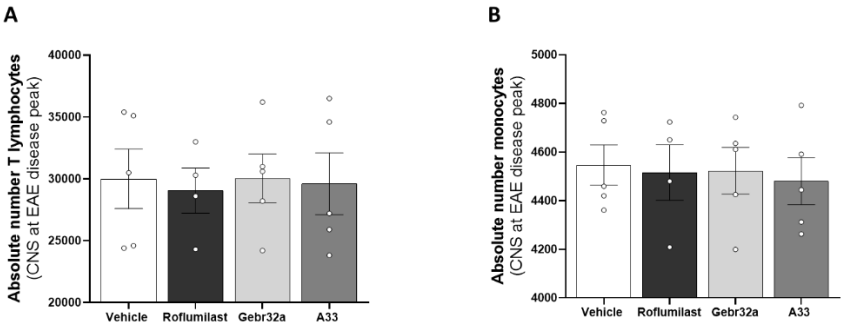

FIG S3.5: total numbers of T lymphocytes and monocytes do not differ in the CNS at EAE disease peak. (A) At EAE disease peak, animals were sacrificed for flow cytometry analysis for immune cell subsets phenotyping. The absolute number of T lymphocytes and monocytes are displayed here. Results were analyzed with a non-parametric Kruskal-Wallis test with Dunn's multiple comparison. Data shown are mean +/- SEM.

Acknowledgements

MS, EP, JP and TV have a proprietary interest in selective PDE4D inhibitors for the treatment of demyelinating disorders and neurodegenerative disorders. JP has a proprietary interest in the PDE4 inhibitor roflumilast for the treatment of cognitive impairment as well as PDE4D inhibitors for the treatment of Alzheimer's disease.

We thank Prof. Dr. O.N. Viacheslav (University Medical Center Hamburg-Eppendorf, German Center for Cardiovascular Research) and Prof. Dr. M. Conti (University of California), for providing the PDE4B KO animals. Furthermore, we thank Rewind Therapeutics for providing the visual evoked potential equipment.

This work was supported by FWO [Grant: 12G0817N and 1S57521N], Fondation Charcot Stichting [Grant: ID2020-0019], MS Liga Vlaanderen and MS stichting Nederland [Grant: 18-1016 MS].

CHAPTER 4

Inhibiting PDE4 subtypes in spinal cord injury

Based on:

Inhibition of phosphodiesterase 4D (PDE4D) improves functional and histopathological outcome after hemisection spinal cord injury

Melissa Schepers*, Sven Hendrix*, Elise van Breedam, Peter Ponsaerts, Stefanie Lemmens, Roberta Ricciarelli, Ernesto Fedele, Olga Bruno, Chiara Brullo, Niels Helings, Jos Prickaerts, Jana Van Broeckhoven#, Tim Vanmierlo#

* Equally contributing first authors

# Equally contributing senior authors

Manuscript in preparation

Declaration of own contribution:

M.S. contributed to the experimental design, data generation (with support of co-authors) and analysis, interpretation and manuscript writing

Abstract

Spinal cord injury (SCI) is a life-changing event that occurs when the spinal cord is damaged. To improve clinical outcomes in SCI, two key strategies are currently being considered: modulation of the neuroinflammatory response elicited by the SCI which impedes regeneration, and stimulation of the body's own neuro-regenerative repair mechanism. Upon SCI, neuronal levels of the second messenger cyclic adenosine monophosphate (cAMP) are known to reduce over time and maintaining intracellular levels of cAMP has been shown to be effective in reducing the damage caused by SCI. cAMP is known to play a crucial role in anti-inflammatory and repair promoting processes and its intracellular levels are controlled by enzymes called phosphodiesterases (PDEs). The PDE4 family is the most abundant in the central nervous system (CNS) and immune cells and its inhibition has been shown to be therapeutically relevant for managing SCI pathology. However, unfortunately, the use of full PDE4 inhibitors at therapeutic doses can cause severe emetic side effects, severely hampering their translation towards a clinical application. Therefore, in this study, we evaluated the effect of inhibiting specific PDE4 subtypes (PDE4B and PDE4D) on inflammatory and regenerative processes in the CNS following SCI, as these subtype specific inhibitors have been demonstrated to be well tolerated. We demonstrate that administration of the PDE4D inhibitor Gebr32a (0.3 mg/kg), but not the PDE4B inhibitor A33 (3 mg/kg), improved functional and histopathological outcome after SCI, comparable to treatment with the full PDE4 inhibitor roflumilast (3 mg/kg). Furthermore, using a luminescent human iPSC-derived neurosphere model, we demonstrated that PDE4D inhibition stabilizes neural viability by preventing apoptosis and stimulating neuronal differentiation. These findings suggest that gene-specific PDE4D inhibition offers a novel therapeutic approach for SCI.

Introduction

Spinal cord injury (SCI) is characterized by a complex secondary injury phase that causes further permanent damage and yields neurological dysfunction (66). To date, regeneration and recovery of function remain limited after SCI (73). Neuroinflammation and the limited endogenous regeneration hamper potential recovery of neural tissue. Despite efforts, current treatments suppress the inflammatory processes but remain ineffective to promote repair. Therefore, there is an urgent need to develop new therapeutic strategies that tackle both neuroinflammatory and regenerative processes.

Cyclic adenosine monophosphate (cAMP) is a crucial molecule involved as second messenger in multiple signaling pathways and exerts broad modulatory effects on various cell types (124, 393). In the context of central nervous system (CNS) injury, cAMP has been shown to exhibit anti-inflammatory and neuroregenerative functions. In the adult CNS, neuronal cAMP levels are relatively low and will further decrease over time following SCI (394). Therefore, maintaining or elevating the intracellular cAMP levels to direct the immune responses or to stimulate neuroregeneration can be considered a valuable approach to temper SCI pathogenesis. Phosphodiesterases (PDEs) are a class of enzymes responsible for the degradation of cyclic nucleotides, such as cAMP. In the CNS, the PDE4 family is the most expressed enzyme responsible for the inactivation of cAMP (108, 393). As such, the wide range of beneficial actions due to PDE4 inhibition was previously demonstrated in an SCI mouse model (157, 266, 284, 307). The golden standard, first generation PDE4 inhibitor rolipram was found to act anti-inflammatory, neuroprotective and regenerative (157, 266, 284). Whereas a continuous and controlled mini osmotic pump mediated release of rolipram (0.4 µmol/kg/hour) attenuated astrogliosis and enhanced axonal outgrowth following SCI, administration of a single dose of 0.5 mg/kg or 1 mg/kg rolipram per day appeared to be sufficient to enhance neuronal survival and simultaneously protect oligodendrocytes, thereby CNS myelination (157, 266, 284). Additionally, the PDE4 inhibitor IC486051 further confirmed the anti-inflammatory properties observed upon rolipram administration as 0.5 mg/kg or 1.0 mg/kg IC486051 bolus doses decreased oxidative stress markers and leukocyte infiltration into the lesion size, thereby reducing the resulting tissue damage (307). However, despite these promising findings, the clinical translation of full PDE4 inhibitors have been

hampered due to tolerability problems (e.g., emesis). Therefore, to mitigate the side effects and increase tolerability, PDE4 subtype specific inhibitors have been developed. The PDE4 family consists of four different subtypes (PDE4A-PDE4D). Inhibition of the PDE4D subtype has been shown to successfully boost myelin regeneration and neuroplasticity, while PDE4B subtype inhibition suppresses the neuroinflammatory responses of macrophages and microglia (219, 235, 345, 347). Interestingly, targeting these individual genes circumvented the emetic side-effects accompanied with full PDE4 inhibitors such as roflumilast and rolipram (chapter 3).

Consequently, in this study, we aimed to disentangle the role of PDE4B and PDE4D inhibition in SCI. Using the hemisection animal model, we show that, in contrast to the PDE4B inhibitor A33, the PDE4D inhibitor Gebr32a improved functional and histopathological outcome after SCI to a similar extend as the full PDE4 inhibitor roflumilast. Furthermore, neuronal apoptosis was prevented by inhibiting PDE4D, as demonstrated with primary neuronal mouse cultures, iPSC-derived neuronal precursor cultures and luminescent iPSC-derived neurospheres. Furthermore, more neural differentiation was observed in these iPSC-derived neurospheroids. Overall, these findings underline the therapeutic potential of specific PDE4D inhibition to act neuroprotective and consequently improve neural plasticity, leading to functional recovery after SCI.

Material & methods

Animals

In vivo experiments were performed with female 10-12-week-old WT C57BL/6j mice (Janvier Labs). Mice were group housed at the conventional animal facility of Hasselt University under stable conditions (temperature-controlled room, 12 h light/dark cycle, food, and water ad libitum). Experiments were approved by the local ethical committee (ethical ID 202060) and were performed according to the guidelines of Directive 2010/63/EU on the protection of animals used for scientific purposes.

Spinal cord injury model

A T-cut spinal cord hemisection injury was performed as previously described (2, 3). Briefly, mice were anesthetized with 2-3% isoflurane and underwent a partial laminectomy at thoracic level 8. Iridectomy scissors were used to transect left and right dorsal funiculi, the dorsal horns, and the ventral funiculus, resulting in a T-cut hemisection injury. The back muscles were sutured, and the skin was closed with wound clips (Bioconnect). Post-operative treatment included blood-loss compensation by glucose (20%, i.p.) and pain relief by buprenorphine (0.1 mg/kg bodyweight, s.c.)(Temgesic). Mice were placed in a recovery chamber (33 °C) until they regained consciousness. Bladders were voided daily until animals were able to urinate independently. The *in vivo* experiments were conducted in two independent cohorts. Table 4.1 provides a sample size overview for each experimental animal group for both cohorts. Since both cohorts showed similar outcomes (**Supplementary Fig S4.1**), results were pooled for statistical analysis.

Administration PDE4 inhibitors

Starting 1 h after SCI, mice were injected twice daily subcutaneously with either (1) vehicle (DMSO, VWR prolabo), (2) the PDE4 inhibitor roflumilast (3 mg/kg, Xi'an leader biochemical engineering co., LTD), (3) a PDE4B inhibitor A33 (3 mg/kg, Sigma-Aldrich), and (4) the PDE4D inhibitor Gebr32a (0.3 mg/kg, university of Genoa (351)). The final experimental animal group (5) received a timed treatment regimen where the A33 (3mg/kg) administration was changed to a Gebr32a (0.3mg/kg) at 10 days post injury (dpi). All inhibitors were dissolved in a 0,1% DMSO + 0,5% methylcellulose + 2% Tween solution.

Locomotion test

Following SCI, functional recovery was assessed daily using the standardized Basso Mouse Scale (BMS) score for locomotion (0 = complete hind limb paralysis, 9 = normal motor function) (5). Scores are based on hind limb movements in an open field during a 4 min testing window. The evaluation was done by an investigator blinded to the treatment groups and was performed daily from 1 until 7 days post-injury (dpi), followed by a scoring every 2nd or 3rd day. For the analysis, the mean BMS score of the left and right hind limb was used for each animal. Mice who did not display any increase in BMS score or abnormally high BMS scores at day 1 post injury were excluded for further analysis (table 4.1).

Table 4.1: Overview of the number of animals receiving a hemisection induced SCI which were included or excluded for functional and histopathological analysis based on locomotor functionality. The sequential PDE4B followed by PDE4D inhibitor treatment group were not included in cohort 2 due to the lack of additional effectiveness compared to continuous PDE4D inhibition.

Treatment group	Cohort 1		Cohort 2		Total
	Included	Excluded	Included	Excluded	
Vehicle	6	6	9	1	**15**
Roflumilast (3mg/kg)	7	7	7	3	**14**
A33 (3 mg/kg)	6	7	10	0	**16**
Gebr32a (0.3 mg/kg)	8	6	6	4	**14**
A33 followed by Gebr32a	10	4	0	0	**10**

Primary mouse neuronal cultures

Fetal mice brains (E17-19) were used to obtain primary cortical neuron cultures (395). Meninges-free cerebral cortices were chemically dissociated for 15 minutes using trypsin. Next, to stop the chemical dissociation, cortices were washed with minimal essential medium (MEM) supplemented with 1% heat inactivated horse serum (Thermo Fisher), 0.6% glucose (Sigma-Aldrich) and 100 U/ml penicillin/streptomycin (Life Technologies). The cortical tissue was subsequentially mechanically dissociated with a P1000 pipette to generate single cell suspensions. Primary mouse neurons were seeded at a density of 8×10^4 cells per well in a 96-well plate (flat bottom, Greiner) in MEM supplemented medium. After allowing attachment for 4h, plating MEM medium was replaced by neurobasal medium supplemented with 1x B27 supplement (Thermo Fisher), 2mM L-glutamine (Thermo Fisher) and 100 U/ml penicillin/streptomycin (Life Technologies). Cells were maintained at 37°C with 5% CO_2 culture conditions. Treatment (vehicle: 1/1000 DMSO; roflumilast: 1µM, A33: 1µM, Gebr32a: 1µM) was started 24h post isolation while cultures were simultaneously deprived of the B27 growth factor in order to induce neuronal cell death (for an additional 48h).

PI viability assay

In the primary mouse neuron culture viability was assessed using a propidium iodide (PI) viability assay as described previously (396, 397). Briefly, 48 hours following B27 growth factor depletion and PDE inhibitor treatment, culture medium was replaced with Lysis buffer A100 (ChemoMetec), after which the lysis reaction was halted by adding equal amounts of stabilization buffer B (ChemoMetec), supplemented with PI (10µg/ml, Sigma). After 15 min incubation in the dark, fluorescent emission was measured using the FluoStart OPTIMA plate reader (Excitation: 540 nm, Emission, 612nm).

Luminescent iPSC-derived neural spheroid cultures

Neurospheroids were formed as described previously (398). Briefly, eGFP/Luc human iPSC-NSCs were seeded at equal densities of 1.6 x 10^4 cells per well in a Geltrex (Life Technologies) coated ULA 96-well plate (Corning) in neural expansion medium (NEM, Gibco). Neurospheroids were maintained at 37°C, 5% CO_2 culture conditions under constant orbital shaking (85 rpm). Two days after plating, fresh NEM was added. A 50% medium change was conducted every other day. Additionally, the luminescent signal was measured weekly by adding 1.5 mg/ml Beetle luciferin (E1601, Promega) for 48h to the neurosphere cultures. The luminescent signal was measured using Clariostar Plus plate reader, after which a complete medium change was performed to eliminate remaining luciferin. PDE inhibition treatment (1/1000 DMSO as vehicle, 1µM roflumilast, 1µM A33 or 1µM Gebr32a) was initiated following 1 week of culturing (after the first luminescent signal measurement). At the end of the experiment (6 weeks of culturing), neurospheres were fixed with 4% paraformaldehyde for 150 min at room temperature, incubated in 20% sucrose (w/v in PBS) overnight and consecutively used for cryosectioning and immunocytochemical analysis.

Immunofluorescence

Immunohistochemistry (post mortem spinal cord tissue)

At 28 dpi, mice received an overdose of dolethal (200 mg/kg) (Vetiquinol B.V.) and were transcardially perfused with Ringer solution containing heparin, followed by a 4% paraformaldehyde (PFA) in PBS perfusion (399). Longitudinal spinal cord cryosections of 10 µm thick were obtained. Immunofluorescent stainings were performed as described previously (2, 3). In brief, to investigate lesion size, demyelinated area, astrogliosis, immune cell infiltration, and neuronal apoptosis, sections were blocked using 10% protein block (Dako) in PBS containing 0.5% Triton-X-100 for 1 h at RT. For evaluating oligodendrocyte differentiation, an antigen retrieval step using a sodium citrate buffer (10mM Sodium citrate, 0.05% Tween20, pH 6.0) was conducted. Primary antibodies were diluted in PBS with 1% protein block and 0.5% Triton-X-100 and were incubated overnight at 4°C (Table 4.2). Following washing, secondary antibody incubation was done for 1 h at RT. The following secondary antibodies were used: goat anti-rat Alexa fluor 488 (1:250, A11006, ThermoFisher Scientific), goat anti-mouse Alexa fluor 568

(1:250, A11004, ThermoFisher Scientific), goat anti-rat Alexa fluor 568 (1:250, A11077, Invitrogen), and goat anti-rabbit Alexa 488 (1:250, A11008, Invitrogen). The specificity of secondary antibodies was tested by omitting the primary antibody. Counterstaining with DAPI (1:1000, Sigma-Aldrich) was performed for 10 min. Pictures were taken using a LEICA DM4000 B LED microscope and LAS X software (Leica).

Immunocytochemistry (neurospheroids)

After fixation, neurospheroids were processed as described previously to allow high-throughput staining (398). Briefly, a 3D printed mold maker (Molecular Spectroscopy research group, University of Antwerp) was used to make a silicone mold with 66 wells each corresponding to the size of the neurospheroids. Tissue-Tek-OCT (VWR) was used to cover the bottom of the wells, after which single neurospheroids were loaded into separate wells of the silicone mold. Next, the neurospheroid were covered with additional OCT and the molds were subsequently snap-frozen in isopentane at a fixed temperate (-50°C), after which cryosections of 10µm were obtained on poly-L-lysine (Sigma) coated glass slides. For immunohistochemical analysis, neurospheroid sections were permeabilized for 30 minutes (0.1% Triton-X in TBS) and blocked with 10% protein block in TBS (DAKO). Primary antibodies were incubated overnight at 4°C in 10% milk solution (table 4.2). Following washing, secondary antibody incubation was done for 1 h at RT. The following secondary antibodies were used: donkey anti-rabbit Alexa fluor 488 (1:600, A11006, ThermoFisher Scientific), donkey anti-rabbit Alexa fluor 555 (1:600, A11004, ThermoFisher Scientific), and goat anti-guinea pig Alexa fluor 555 (1:600, A11077, Invitrogen). DAPI was used to counterstain cellular nuclei. Pictures were taken using a Axioscan 7 microscope slide scanner (Zeiss).

Table 4.2: List of primary antibodies used for immunohistochemistry (post mortem tissue) and immunocytochemistry (neurospheroids)

Immunofluorescence	Antibody	Host	Source	Dilution factor
Immunohistochemistry	Glial fibrillary acid protein (GFAP)	Mouse	Sigma Aldrich (**G3893**)	1/500
	Myelin basic protein (MBP)	Rat	Merck Millipore (**MAB386**)	1/250
	CD4	Rat	BD Biosciences (**553043**)	1/250
	Cleaved caspase 3	Rabbit	Cell Signaling (**9661**)	1/100
	NeuN	Mouse	Millipore (**MAB377**)	1/1000
	Olig2	Goat	Biotechne R&D (**AF2418**)	1/50
	APC (CC1)	Mouse	Calbiochem (**OP80**)	1/50
Immunocytochemistry	NeuN	Guinea-pig	Millipore (**ABN90P**)	1/100
	Cleaved caspase 3	Rabbit	Cell Signaling (**9661**)	1/400
	Doublecortin (DCX)	Rabbit	Abcam (**ab18723**)	1/500

Immunohistochemical quantification

Quantification was carried out on the original, unedited pictures. Representative images displayed in the figures were digitally enhanced to improve visibility. Quantification of histopathological parameters was performed as described previously and was performed by investigators blinded to experimental groups (2, 3). To quantify lesion size ($GFAP^-$ area) and demyelinated area (MBP^- area), 5-7 sections per animal containing lesion center and consecutive rostral and caudal area were analyzed. To determine astrogliosis (GFAP expression) an intensity analysis using ImageJ was performed (2). T helper cells were identified by being $CD4^+Iba\text{-}1^-$ and quantified by counting the number of T cells in 1 microscope field both rostral and caudal of the lesion site (400). Differences in cleaved caspase, NeuN, and DCX positive cells within the neurospheroids was determined using an intensity analysis using ImageJ, after which the positive area was corrected for the number of nuclei present in the pictures.

IncuCyte live-cell imaging of cleaved caspase 3/7

eGFP/Luc human iPSC-NSCs were seeded at a density of 1×10^4 cells per well in a Geltrex coated 96 well plate (flatt bottom, Greiner). After allowing attachment for 24h, cells were treated with the PDE4 inhibitors (vehicle: 1/1000 DMSO, 1µM roflumilast, 1µM A33 or 1µM Gebr32a) and apoptosis was induced by depriving oxygen (1% O_2 for 4h. Simultaneously, the IncuCyte Caspase-3/7 Red apoptosis reagent (1.5µM; #4704, Sartorius) was supplemented to the cultures. Cell plates were placed into the IncuCyte live-cell analysis system and 5 images were taken per well. End-point apoptosis was measured 6h after oxygen deprivation. The IncuCyte integrated analysis software was used to quantify the total level of apoptosis.

Statistics

Data analysis was performed using GraphPad Prism version 9 (GraphPad Software). D'Agostino and Pearson omnibus test was used to assess normality. The BMS and neurospheroid chemiluminescent results were analyzed using a two-way ANOVA for repeated measurements. GFAP intensity was analyzed using a two-way ANOVA with a Bonferroni post hoc test. All other data was checked for normality using the Shapiro-Wilk test. Normally distributed data were subsequently analyzed with a one-way ANOVA with Dunnett's multiple

comparisons (compared to vehicle). Not normally distributed data were analyzed using the non-parametric Kruskal-Wallis test with Dunn's multiple comparison (compared to vehicle). Data are presented as mean ± standard error of the mean (SEM). Differences with P values < 0.05 were considered significant.

Results

PDE4 and PDE4D inhibition improve functional recovery and histopathological outcome after SCI, whereas PDE4B inhibition did not

In an initial experiment, we examined whether PDE4B or PDE4D subtype specific inhibitors are capable of improving functional recovery in a hemisection model for SCI. As a positive control, we included roflumilast, a second-generation pan PDE4 inhibitor. Starting 1h post SCI injury, mice received either vehicle or the different PDE4 inhibitors: (1) full PDE4 inhibitor roflumilast, (2) specific PDE4B inhibitor A33, (3) specific PDE4D inhibitor Gebr32a, (4) or a sequential administration of A33 followed by Gebr32a. Due to the previously described involvement of PDE4B in neuroinflammation and PDE4D in CNS regeneration, we additionally included the sequential treatment regimen where animals first received A33, followed by Gebr32a treatment initiated 10 days post injury. Functional recovery was measured for 4 weeks using the BMS score. Both roflumilast and Gebr32a significantly improved functional recovery compared to vehicle-treated mice, whereas A33 treatment did not had an effect on functional outcome (**Fig 4.1**). BMS scores among Gebr32a and roflumilast treatment were not significantly different (**Fig 4.1**). The A33 treatment preceding Gebr32a treatment was of no additional benefit, since, starting from day 10, functional recovery mimicked those of continuous Gebr32a treatment (**Fig 4.1**). Therefore, the sequential treatment group was not taken along for further post mortem analysis.

In line, histological GFAP and MBP analyses indicated significantly reduced lesion size and demyelinated areas respectively in roflumilast and Gebr32a-treated mice compared to the vehicle group whereas, A33 did not (**Fig 4.2A-J**). Next, the level of astrogliosis was determined by analyzing GFAP intensity at varying distances to lesion center. Whereas roflumilast and Geb32a treatment did not altered GFAP intensities, A33 exacerbated astrogliosis, especially at the rostral lesion site. As an additional neuroinflammatory outcome measurement, we determined the number of infiltrated CD4+ T lymphocytes in the perilesional area. Neither of the PDE4 or PDE4 subytpe inhibitors pointed towards differences between treatment groups (**Supplementary Fig S4.2**).

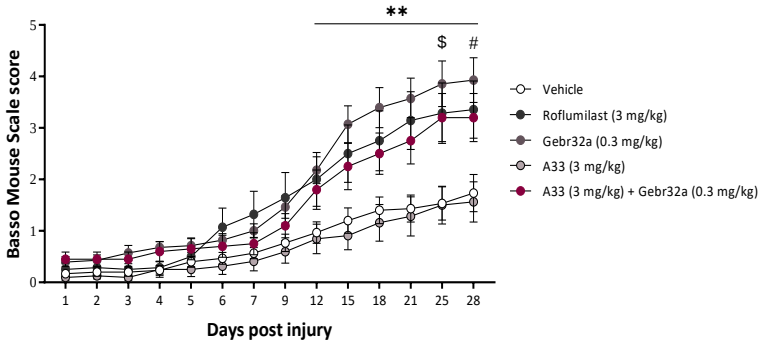

FIG 4.1: The PDE4 inhibitor roflumilast and the PDE4D inhibitor Gebr32a treatment improve functional recovery after spinal cord injury, whereas the PDE4B inhibitor A33 had no effect.

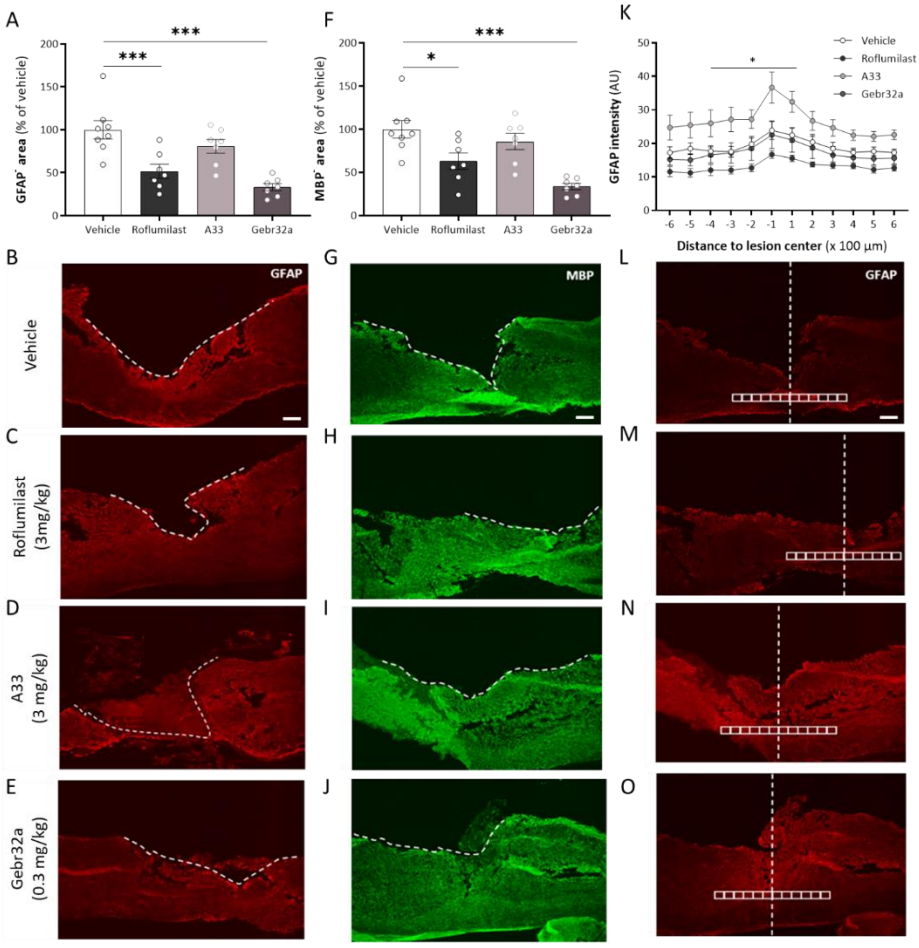

FIG 4.2: Roflumilast and Gebr32a treatment reduce the lesion size and demyelinated area after spinal cord injury, whereas A33 exacerbates astrogliosis.

FIG 4.1: The PDE4 inhibitor roflumilast and the PDE4D inhibitor Gebr32a treatment improve functional recovery after spinal cord injury, whereas the PDE4B inhibitor A33 had no effect. Immediately after injury, mice were treated with vehicle, a general PDE4 inhibitor roflumilast (3 mg/kg), or gene-specific PDE4 inhibitors, A33 (3mg/kg) and Gebr32a (0.3 mg/kg). In contrast to A33, roflumilast and Gebr32a significantly improved functional outcome compared to vehicle-treated mice over time. Data were analyzed using a two-way ANOVA with Dunnett's multiple comparison test (compared to vehicle). Data are displayed as mean +/-SEM ($p≤0.05 vehicle versus roflumilast; **p≤0.001 vehicle versus Gebr32a, #p≤0.05 vehicle versus A33+Gebr32a).

FIG 4.2: Roflumilast and Gebr32a treatment reduce the lesion size and demyelinated area after spinal cord injury, whereas A33 exacerbates astrogliosis. A-O) Immediately after injury, mice were treated with vehicle, a general PDE4 inhibitor roflumilast, or gene-specific PDE4 inhibitors, A33 and Gebr32a. **(A)** Quantification of lesion size, determined by the GFAP negative area, showed that this was reduced in the mice treated with roflumilast or Gebr32a compared to the vehicle group. No difference between the vehicle and A33 groups was observed. Data were normalized to vehicle and are shown as mean ± SEM. *n* = 4-6 mice/group. **(B-E)** Representative images from the spinal cord sections are shown. Lesion size ($GFAP^-$) was determined as depicted by the dotted white line. Scale bar = 250 µm. **(F)** Quantification of the demyelinated area, determined by the MBP negative area, showed that this was reduced in mice treated with roflumilast or Gebr32a compared to the vehicle group. No difference between vehicle and A33 groups was observed. Data were normalized to vehicle and are shown as mean ± SEM. *n* = 7-8 mice/group. **(G-J)** Representative images from the spinal cord sections are shown. Demyelinated are (MBP^-) was determined as depicted by the dotted white line. Scale bar = 250 µm. **(K)** Quantification of astrogliosis by GFAP intensity analysis showed that, in contrast to other treatment groups, A33 application exacerbated astrogliosis compared to vehicle-treated mice. Data are shown as mean ± SEM. *n* = 4-6 mice/group. *A33 versus vehicle**. (L-O)** Representative images from the spinal cord sections are shown. All analyses were quantified within square areas of 100 µm x 100 µm perilesional placed as indicated in the figure, extending 600 µm rostral to 600 µm caudal from the lesion center (white line). Scale bar = 500 µm. Demyelination area and lesion size were analyzed using a one-way ANOVA with Dunnett's multiple comparison test (compared to vehicle). GFAP intensity was analyzed using a two-way ANOVA with a Bonferroni post hoc test. Data are displayed as mean +/-SEM (*p<0.05; ***p<0.005).

PDE4 and PDE4D inhibition acts neuroprotective and stimulates 5-HT serotonergic regeneration

Next, we investigated whether the abovementioned decreased lesion size observations were accompanied by neuroprotection and neuroregeneration. First, the neuroprotective effects of PDE4 or PDE4 subtype inhibition were determined based on cleaved caspase 3 and NeuN double positivity at the lesion size to evaluate the number of apoptotic neurons. Mice treated with the PDE4 inhibitor roflumilast or PDE4D inhibitor Gebr32a displayed a reduced number of $NeuN^+$ Cleaved $Caspase3^+$ double positive cells compared to vehicle treated animals at the (peri-) lesion (**Fig 4.3A-E**). Furthermore, A33 treated animals displayed a non-significant trend ($p=0.08$) towards reduced neuronal cell death (**Fig 4.3A-E**).

Next, to determine the spinal dendritic plasticity of serotonin fiber projections, the number and length of descending 5-HT positive tracts were determined. In contrast to A33, both roflumilast and Gebr32a-treated animals significantly increased the mean number and length of descending 5-HT dendrites, indicating serotonergic neuroregeneration or -protection (**Fig 4.4A-C**).

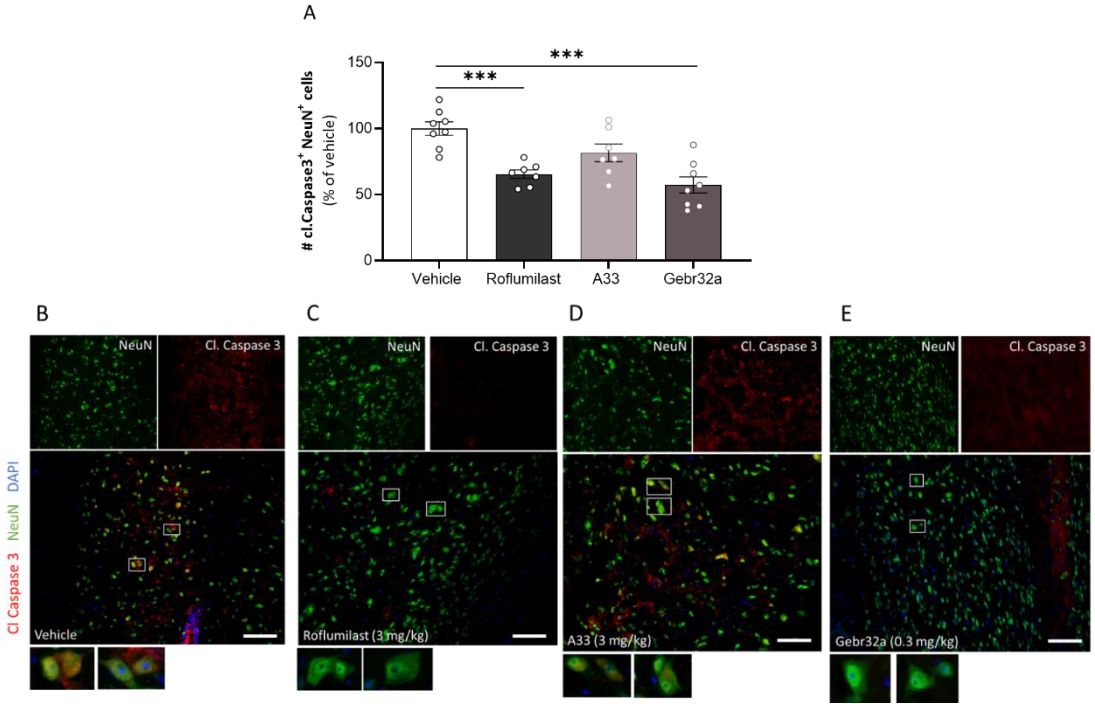

FIG 4.3: PDE4 and PDE4D inhibition acts neuroprotective at the lesion site. (A) Quantification of the number of Cleaved Caspase $3^{+}NeuN^{+}$ neurons at the (peri) lesion site indicated a neuroprotective feature of both PDE4 and PDE4D inhibition as reduced neuronal apoptosis was observed. Dara are normalized to vehicle and are shown as mean ± SEM. *n* = 7-8 mice/group. **(B-E)** Representative images of the Cleaved Caspase 3-NeuN staining at the lesion site. Single stainings are shown above the merged image. The white boxed regions are shown at higher magnification (40x) underneath the merged image. Scale bar = 100 µm. Results were analyzed using a one-way ANOVA with Dunnett's multiple comparison test (compared to vehicle). Data are displayed as mean +/-SEM (***p<0.005).

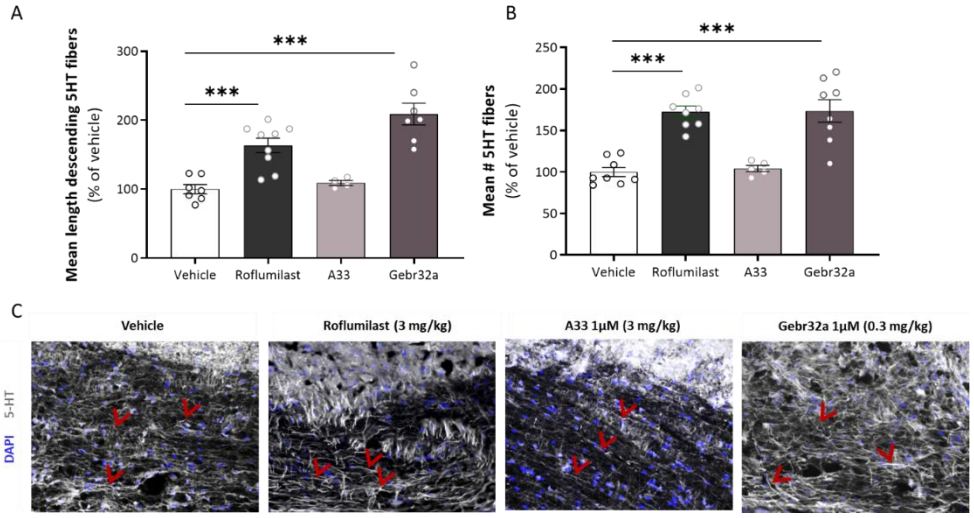

FIG 4.4: Roflumilast and Gebr32a increase 5-HT serotonergic regeneration or preservation following SCI as indicated by the increased number and length of descending 5-HT tracts over the lesion site. Quantification of the 5-HT serotonergic staining showed both an **(A)** increase in the number and **(B)** length of descending 5-HT tracts over the SCI lesion site upon PDE4 (roflumilast) and PDE4D (Gebr32a) inhibition. Data were normalized to vehicle and are shown as mean ± SEM. *n* = 4-9 mice/group. **(C)** Representative images of the 5-HT staining at the lesion site. The red arrows indicate examples of 5-HT descending tracts. Results were analyzed using a one-way ANOVA with Dunnett's multiple comparison test (compared to vehicle). Data are displayed as mean +/-SEM (***p<0.005).

Oligodendrocyte differentiation is enhanced by PDE4 and PDE4D inhibition at the (peri) lesion site following spinal cord injury

Due to the reduced demyelinated area observed at the lesion site upon both PDE4 and PDE4D inhibition, we next aimed to investigate the presence of differentiated oligodendrocytes (CC1+) present at the lesion size. The total number of oligodendrolineage cells was first determined based on Olig2 positivity at the lesion site, of which no differences were observed upon either full PDE4 or PDE4 subtype specific inhibition compared to control treated animals (**Supplementary Fig S4.3**). However, mice treated with the PDE4 inhibitor roflumilast or the PDE4D inhibitor Gebr32a did display a significant increase in the number of mature oligodendrocytes (Olig2^{+}CC1^{+}) compared to vehicle or A33 treated animals (**Fig 4.5A-E**).

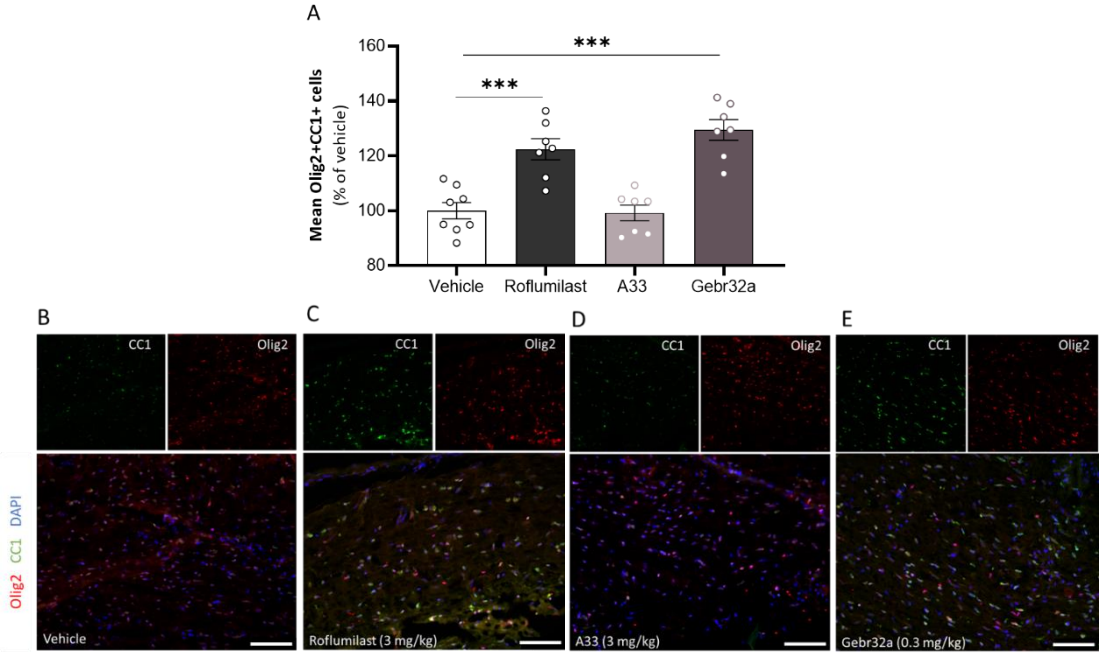

FIG 4.5: Roflumilast and Gebr32a treatment increase oligodendrocyte differentiation. (A) Using a double staining for Olig2 (oligodendrolineage marker) and CC1 (mature oligodendrocyte marker) we showed a significantly increased percentage of mature oligodendrocytes at the lesion site following PDE4 (roflumilast) and PDE4D (Gebr32a inhibition). Data were normalized to vehicle and are shown as mean ± SEM. *n* = 7-8 mice/group. **(B-E)** Representative images of the Olig2-CC1 double staining at the lesion site. Single stainings are shown above the merged image. Scale bar = 100 µm. Results were analyzed using a one-way ANOVA with Dunnett's multiple comparison test (compared to vehicle). Data are displayed as mean +/-SEM (***p<0.005).

PDE4 and PDE4D inhibition both prevent apoptosis of primary murine and human iPSC derived neurons

To evaluate whether the neuroprotective feature of roflumilast and Gebr32a observed *in vivo* can be attributed to direct neuronal protection, we evaluated neuronal apoptosis in both primary mouse derived neurons and human iPSC-derived NSCs. **Figure 4.6A** demonstrate the level of neuronal apoptosis of mouse neurons following 48h of B27 growth factor deprivation. Both roflumilast mediated PDE4 inhibition and Gebr32a mediated PDE4D inhibition partly prevented the stress-induced neuronal apoptosis as observed by a higher PI signal compared to vehicle treated cultures. In line, human iPSC-derived neuronal stem cell cultures subjected to oxygen deprivation for 4h and treated with either roflumilast or Gebr32a displayed a significant reduction of cleaved caspase3/7 positivity 6h post stress-induced neuronal apoptosis (**Fig 4.6B**).

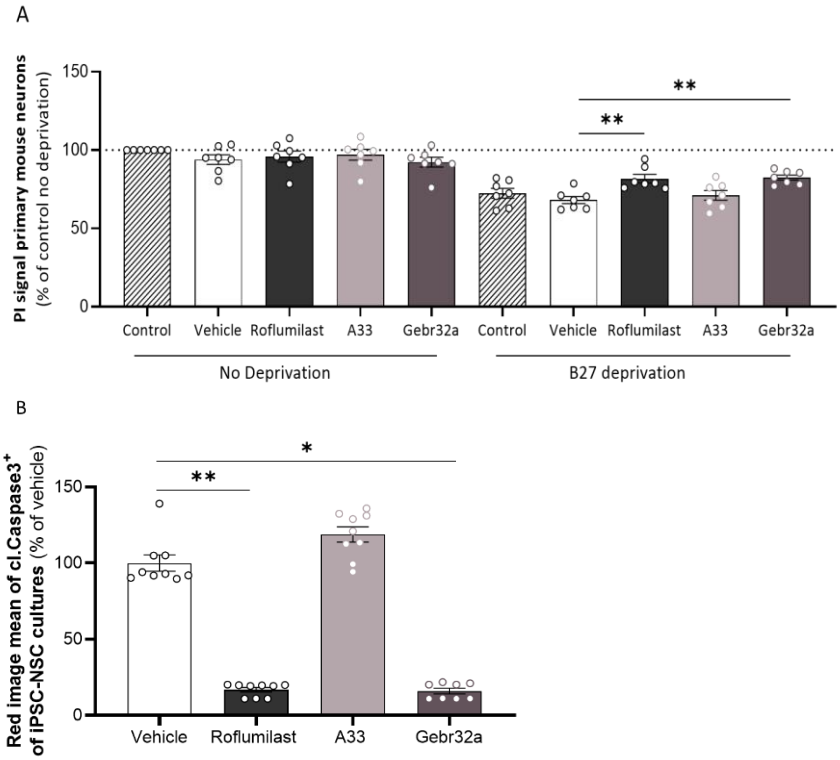

FIG 4.6: Apoptosis of primary mouse neurons and human iPSC-derived NSCs was prevented by both roflumilast and Gebr32a. (A) Primary mouse neurons deprived from the growth factor B27 for 48h showed a decreased neuronal viability at the end of the experiment, which was partly prevented by inhibiting PDE4 (roflumilast) or PDE4D (Gebr32a). Data were normalized to vehicle and are shown as mean ± SEM. *n* = 6-7/group with an 'n' representative for one well **(B)** Human iPSC neuronal stem cells showed increased levels of Cleaved Caspase 3/7 upon oxygen deprivation, which was significantly reduced upon PDE4 (roflumilast) and PDE4D (Gebr32a) inhibition. *n* = 8-9/group with an 'n' representative for one well. Results from PI measurements of primary mouse neurons were analyzed using a one-way ANOVA with Dunnett's multiple comparison test (compared to vehicle). Results of Cleaved Caspase 3 signal measurements were analyzed using a non-parametric Kruskal-Wallis test with Dunn's multiple comparison test (compared to vehicle). Data are displayed as mean +/-SEM (*p<0.05; **p<0.01).

Bioluminescence real-time monitoring of human neurospheroids demonstrates the neuroprotective feature of both PDE4 and PDE4D inhibition, which is accompanied with increased neuronal differentiation

To enable real-time read-out of neurospheroids, eGFP/Luc human iPSC derived neuronal stem cells stably expressing the firefly luciferase reporter were used to generate neurospheroids. Over time, decreased viability was observed in the neurospheroids reflecting core oxygen/nutrient deprivation and therefore gradual cell loss. However, in contrast to the PDE4B inhibitor A33, treatment with either the PDE4 inhibitor roflumilast or the PDE4D inhibitor Gebr32a stabilized neurospheroid viability when stress-induced core cell loss occurred (**Fig 4.7A**). At the end of the 6 week culture period, neurospheroids were characterized for the level of apoptosis (Cleaved Caspase 3), neuronal differentiation (NeuN), and neurogenesis. Quantification of the Cleaved Caspase 3^+ cells revealed a significant reduction of apoptosis when inhibiting PDE4 or PDE4D (**Fig 4.7B, E**). Furthermore, both roflumilast and Gebr32a treatment significantly increased neuronal differentiation as more $NeuN^+$ cells were present at the end of the experiment (**Fig 4.7C, E**). No significant differences were found in DCX^+ cells, nor for A33 treatment within any marker evaluated (**Fig 4.7B-E**).

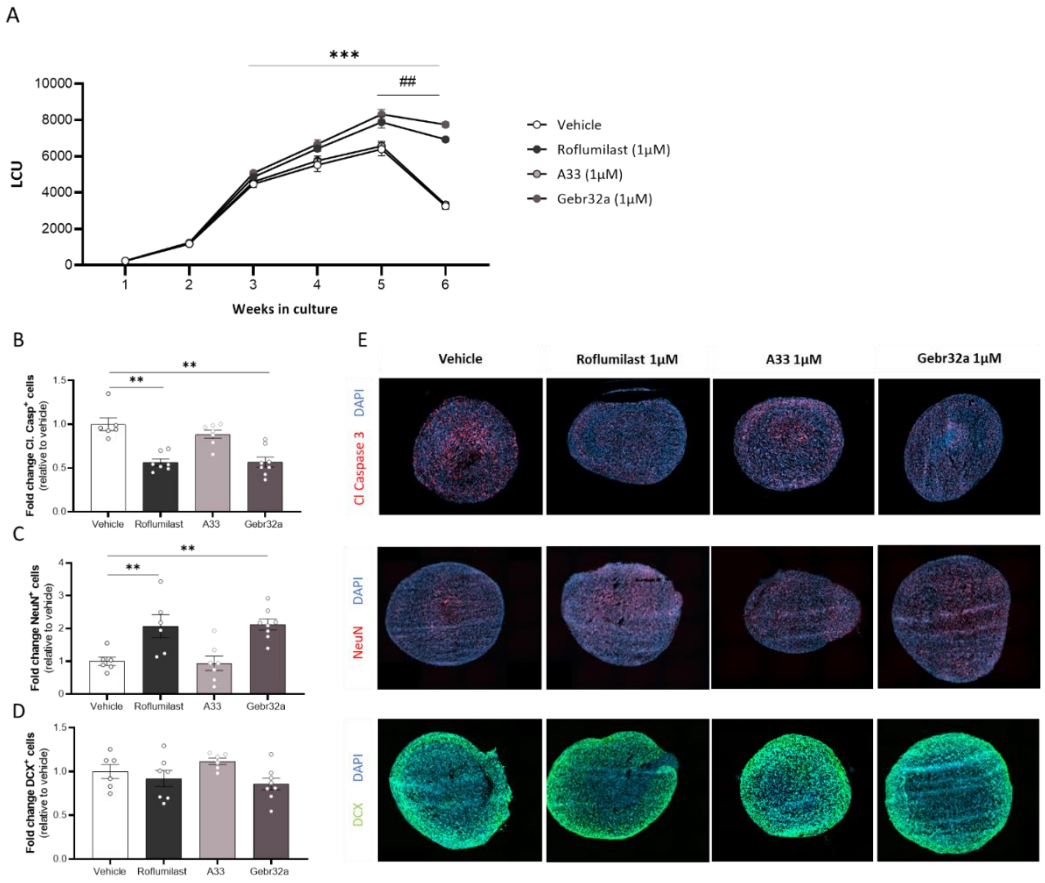

Figure 4.7: Roflumilast and Gebr32a treatment protected human iPSC derived neurospheroids from neural apoptosis and stimulated neuronal differentiation, while not affecting neurogenesis. (A) Weekly luminescence measurement of neurospheroids showed a stabilized viability over time. Data are shown as mean ± SEM. *n* = 24 spheroids/group. At the end of the culture experiment, the 6 week old neurospheroids were stained and quantified for its number of **(B)** Cleaved Caspase 3 (apoptosis), **(C)** NeuN (neuronal differentiation), or **(D)** DCX (neurogenesis) positive cells with respect to the total number of nuclei. Data were normalized to vehicle and are shown as mean ± SEM. *n* = 6-8 spheroids/group. **(E)** Representative immunofluorescent images of the human iPSC-derived neurospheroids. The amount of cleaved caspase positive cells were analyzed using a non-parametric Kruskal-Wallis test with Dunn's multiple comparison (compared to vehicle). The amount of NeuN or DCX positive cells were analyzed using a one-way ANOVA with Dunnett's multiple comparison test (compared to vehicle). Data are displayed as mean +/-SEM (**p<0.01).

Discussion

In SCI research, PDE4 inhibition has yielded promising results due to its broad effects on different secondary injury-related possesses, such as immune cell infiltration and inflammation (157, 266, 284, 307). However, the translation of pan-PDE4 inhibitors remains limited due to their poor tolerability in patients at doses required for clinical effectiveness to suppress inflammation and stimulate repair (103). In order to circumvent this pitfall, we investigated the potential of specific non-emetic PDE4B and PDE4D inhibitors, respectively A33 and Gebr32a. The PDE4 inhibitor roflumilast (3 mg/kg), PDE4B specific inhibitor A33 (3 mg/kg) and the PDE4D inhibitor Gebr32a (0.3 mg/kg) were administered at a dose previously demonstrated to diminish neuroinflammation or enhance myelin regeneration upon CNS pathology (chapter 3). We now show that the PDE4D inhibitor Gebr32a significantly improved functional recovery after SCI similar to the pan PDE4 inhibitor roflumilast, whereas the PDE4B inhibitor A33 did not. In addition, both roflumilast and Gebr32a reduced the lesion size, demyelinated area, neuronal apoptosis while boosting 5-HT serotonergic tract regeneration, and oligodendrocyte differentiation. Furthermore, the neuroprotective feature of both full PDE4 inhibition and PDE4D subtype inhibition can, at least partially, be attributed to a direct neuronal effect as we demonstrated a decreased neuronal apoptosis *in vitro.* Using human iPSC-derived neurospheroids, we further demonstrated neuroprotection in a 3D culture model, which was accompanied with increased neuronal differentiation. These results support the use of the PDE4D inhibitor Gebr32a for SCI therapy.

Roflumilast has been shown to induce recovery in a contusion SCI model via modulating phagocyte polarization (401). Here, we confirm the beneficial effect on the locomotion of this new-generation PDE4 inhibitor in a hemisection SCI model. In general, pan-PDE4 inhibitors block most PDE4 subfamilies but in particular the B and D gene products (281, 402). Studies have shown that these two subfamilies exert different functions. Whereas PDE4B orchestrates the inflammatory immune response, PDE4D contributes to adult neurogenesis, neuroplasticity and myelin regeneration (chapter 3)(403). As SCI is characterized by a robust neuroinflammatory response and limited to no axonal regeneration, we focused on PDE4B and PDE4D inhibition. In this study, we used the PDE4B

inhibitor A33 and PDE4D inhibitor Gebr32a, both lacking an emetic response up to 100 mg/kg (chapter 3).

After SCI, PDE4B is acutely upregulated in the damaged spinal cord (226). The PDE4B subfamily is an important modulator of the intracellular cAMP levels in inflammatory cells, including macrophages and microglia (124, 235). In a mouse model of multiple sclerosis, the PDE4B expression in antigen-presenting cells, such as phagocytes, was correlated with the disease severity (158). Pharmacological inhibition of PDE4 using A33 (dosis) induced anti-inflammatory markers (e.g., Arginase-1) in phagocytes (214, 223, 404). Complete PDE4B knockdown had beneficial effects on recovery in a contusion SCI model (226). Based on these data, it was somewhat surprising that PDE4B inhibition by A33 did not improved functional recovery in our study. Another study has reported beneficial actions of A33 by limiting inflammation and lesion size in traumatic brain injury (223, 403). In contrast, our histological analysis did not show an effect of A33 on the damaged area despite using the same dosage. Besides the crucial role in phagocytes, PDE4B is mainly expressed by astrocytes (124). In response to SCI, astrocytes undergo phenotypic changes referred to as reactive astrogliosis (68, 405-407). Reactive astrocytes located in the perilesional area are considered to be detrimental after SCI due to their role in the formation of a glial scar, which is a physical barrier for regenerating axons, and their secretion of chemical mediators, which block repair or damage tissue (68, 408). A previous study showed that PDE4B knockdown significantly reduced astrocyte activation (229). In contrast, we observed that A33 administration exacerbated astrogliosis, which may explain the absence of improved functional outcome. Importantly, it has been previously shown that treatment protocol and dose are important determinants for beneficial effects (409). Hence, we cannot exclude that elevating the dose of A33 could still provide long-term benefits after SCI. However, additionally, it remains possible that the PDE4B inhibitor A33 lacks effectivity for treating transection SCI.

PDE4D is responsible for memory- and cognition-enhancing effects via, for example, stimulating hippocampal neurogenesis (335). Full PDE4 inhibition using rolipram treatment after SCI was previously shown to attenuate oligodendrocyte apoptosis and promote axonal growth and plasticity (chapter 3) (393, 409). We have found that selective PDE4D inhibition by Gebr32a boosts oligodendrocyte precursor cell differentiation *in vitro* and stimulated remyelination in an *ex vivo* demyelinated cerebellar brain slice model (chapter 3). In the current study, we show that Gebr32a administration improved functional recovery after SCI and reduced lesion size and decreased demyelinated area, which was accompanied with increased numbers of mature oligodendrocytes. Moreover, Gebr32a acts neuroprotective following SCI as demonstrated by the decreased number of apoptotic neurons. Since the loss of locomotor function following SCI correlates to the damage of 5-HT serotonergic projections in the spinal cord, we aimed to evaluate neuroregeneration by quantifying the descending 5-HT tracts over the lesion site. Treatment of Gebr32a increased both the number and length of descending 5-HT tracts, indicating either a 5-HT sparing feature or neuroregenerative feature of PDE4D inhibition. The effects observed after Gebr32a treatment were comparable to roflumilast.

Due to the hypothesized anti-inflammatory properties of PDE4B inhibition, and the previously observed regenerative properties of PDE4D inhibition, we evaluated whether a sequential treatment regimen where, during the initial phase of SCI, the PDE4B inhibitor A33 was administered which was subsequently substituted by the PDE4D inhibitor Gebr32a from day 10 onwards, would even further improve SCI outcome compared to monotreatment strategies. The neuro-inflammatory response itself is an essential defense mechanisms with contradictory effects. While inflammatory processes are essential for removing cellular debris, their benefits are overshadowed by the accumulation of inflammatory cytokines in the CNS upon inflammatory immune cell infiltration (69, 410). These secondary inflammatory-mediated damage processes severely impair regenerative processes and glial functioning (411). Therefore, by diminishing the neuroinflammatory response by inhibiting PDE4B, we aimed to create a favorable micro-environment thereby allowing regeneration to occur more efficiently. By inhibiting PDE4D in a later phase, the regenerative process could be further enhanced an functional outcome would be improved even more compared to

continuous PDE4B or PDE4D subtype inhibition throughout the disease course. However, unfortunately, inhibiting PDE4B by means of A33 during the early phase of the disease did not provided an additional benefit on functional outcome following hemisection SCI compared to continuous PDE4D inhibition by means of Gebr32a. Based on post mortem analysis, the absence of the hypothesized add-on effect could be explained due to the lack of efficacy of the PDE4B inhibitor itself, which in turn could be due to the dose, timing or route of administration as discussed above. Therefore, it cannot be excluded that sequential PDE4 subtype specific treatment can be even more efficient and clinically relevant compared to only PDE4D inhibition to treat SCI.

Finally, we aimed to evaluated whether the observed neuroprotective features *in vivo* were mediated by a direct action of Gebr32a on neurons. In SCI, both direct and indirect neuroprotective actions can be considered an interesting therapeutic strategies. Following the initial injury, a wide variety of secondary injury processes are provoked of which the neuroinflammatory response is the most complex and important one (66). Local factors at the injury site, including apoptotic cells, cytokines present in the micro-environment and cellular debris, skew the phenotypic properties of immune cells such as macrophages and microglia (66, 412). Therefore, modulating neuro-inflammatory responses could also be considered an indirect neuroprotective therapeutic strategy. Furthermore, oligodendrocytes surrounding the lesion site can provide structural protection and metabolic support to neurons (413). Making oligodendrocytes more resilient can therefore act indirectly neuroprotective as well. Although we cannot exclude any indirect neuroprotective effects of Gebr32a so far, we demonstrated here, at least partially, that the observed decrease in neuronal apoptosis can be attributed to direct neuronal protection. In both murine and human iPSC-derived neurons, Gebr32a treatment diminished neuronal cell death. Similarly, Gebr32a stabilized the human neurospheroid viability, which was accompanied with decreased apoptosis and increased neuronal differentiation. These data suggest that PDE4D inhibition directly affects the survival of neurons following SCI.

Taken together, despite the promising preclinical findings of PDE4 inhibition, the accompanied severe side effects at the therapeutic dose have hindered their clinical translation so far. In this study, we exploited the impact of A33 and Gebr32a, a PDE4B and PDE4D inhibitor, respectively, upon SCI. In contrast to A33, Gebr32a improved functional and histopathological outcomes to a comparable level as the non-specific PDE4 inhibitor roflumilast. However, whereas roflumilast is associated with emetic-like behavior at its repair-inducing dose, Gebr32a is not (chapter 3). These data strongly support the notion that neuroprotective compound Gebr32a is a more refined approach to raise cAMP levels and, therefore, holds great potential as a novel therapeutic approach for SCI treatment.

Supplemental figures

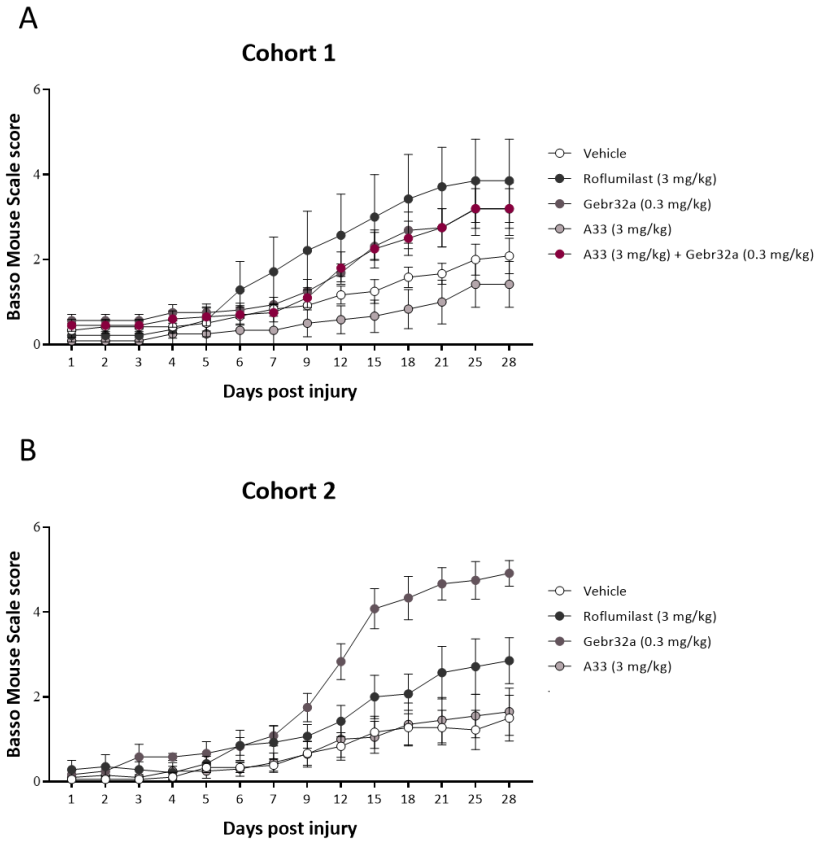

FIG S4.1: Two independent cohorts of hemisection SCI demonstrate an improved functional recovery upon either PDE4 or PDE4D inhibition using roflumilast or Gebr32a respectively. Immediately after injury, mice were treated with vehicle, a general PDE4 inhibitor roflumilast (3 mg/kg), or gene-specific PDE4 inhibitors, A33 (3mg/kg) and Gebr32a (0.3 mg/kg). In contrast to A33, roflumilast and Gebr32a significantly improved functional outcome compared to vehicle-treated mice over time in both **(A)** animal cohort 1 and **(B)** animal cohort 2.

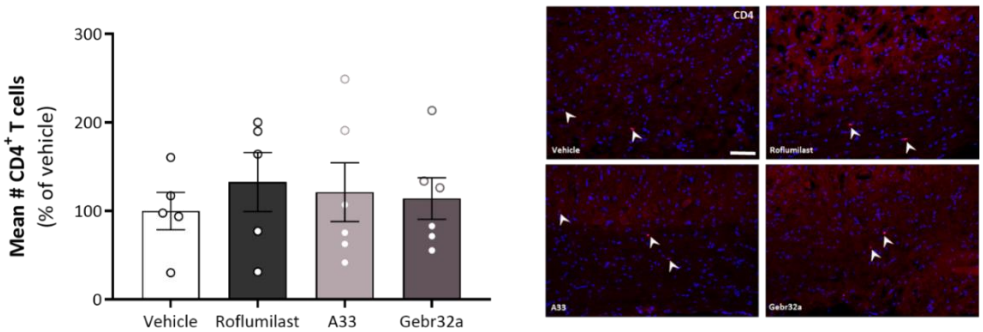

Fig S4.2: After spinal cord injury, the number of CD4$^+$ T cells in the spinal cord does not change upon treatment with roflumilast, A33, or Gebr32a. Immediately after injury, mice were treated with vehicle, a general PDE4 inhibitor roflumilast (3 mg/kg), or gene-specific PDE4 inhibitors, A33 (3 mg/kg) and Gebr32a (0.3 mg/kg). **(A)** CD4 staining in spinal cord sections revealed no changes in the number of CD4$^+$ T cells between the different groups. *n* = 5-6 mice/group. **(B-E)** Representative images of the CD4$^+$ cells in the spinal cord sections of mice treated with the different PDE4 inhibitors. White arrows indicate the cells. Scale bar = 75 µm. Results were analyzed using a one-way ANOVA with Dunnett's multiple comparison test (compared to vehicle). Data are displayed as mean +/-SEM.

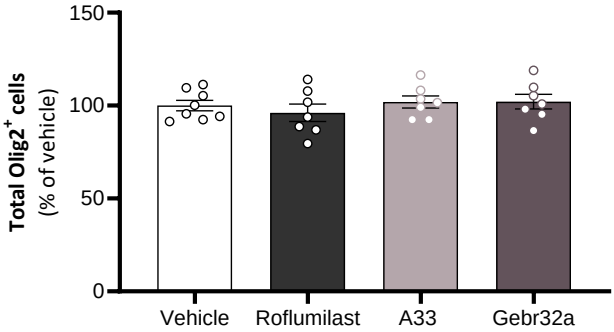

Fig S4.3: After spinal cord injury, the total number of Olig2$^+$ oligodendrolineage cells does not change upon roflumilast, A33 or Gebr32a. Immediately after injury, mice were treated with vehicle, a general PDE4 inhibitor roflumilast (3 mg/kg), or gene-specific PDE4 inhibitors, A33 (3 mg/kg) and Gebr32a (0.3 mg/kg). Olig2 staining in spinal cord sections revealed no differences in total number of oligodendrolineage cells between the different treatment groups. *n* = 7-8 mice/group. Results were analyzed using a one-way ANOVA with Dunnett's multiple comparison test (compared to vehicle). Data are displayed as mean +/-SEM.

Acknowledgements

TV, JP and MS have proprietary interest in selective PDE4D inhibitors for the treatment of demyelinating disorders.

This work was supported by FWO [Grant: 12G0817N and 1S57521N].

CHAPTER 5

Inhibiting PDE4 subtypes in ischemic stroke

Based on:

Phosphodiesterase 4B subtype inhibition to diminish neuroinflammation following ischemic stroke

Melissa Schepers[*], Laura Ponsaerts[*], Hannelore Kemps, Mirre De Bondt, Niels Hellings, Jos Prickaerts, Annelies Bronckaers[#], Tim Vanmierlo[#]

* Equally contributing first authors
# Equally contributing senior authors

Declaration of own contribution:

M.S. contributed to the experimental design, data generation (with support of co-authors, except figure 5.3) and analysis, interpretation and manuscript writing

CHAPTER 6

Inhibiting PDE4 in peripheral Schwann cell mediated nerve-repair

Based on:

Phosphodiesterase (PDE) 4 inhibition boosts Schwann cell myelination in a 3D regeneration model

Melissa Schepers*, Afonso Malheiro*, Adrián Seijas Gamardo, Niels Hellings, Jos Prickaerts, Lorenzo Moroni, Tim Vanmierlo#, Paul Wieringa#

* Equally contributing first authors

# Equally contributing senior authors

Published in European Journal of Pharmaceutical Science

Declaration of own contribution:

M.S. contributed to the experimental design, data generation (with support of co-authors, except figure 6.1A-B and 6.3F) and analysis, interpretation and manuscript writing

Abstract

Phosphodiesterase 4 (PDE4) inhibitors have been extensively researched for their anti-inflammatory and neuroregenerative properties. Despite the known neuroplastic and myelin regenerative properties of nonselective PDE4 inhibitors on the central nervous system, the direct impact on peripheral remyelination and subsequent neuroregeneration has not yet been investigated. Therefore, to examine the possible therapeutic effect of PDE4 inhibition on peripheral glia, we assessed the differentiation of primary rat Schwann cells exposed *in vitro* to the PDE4 inhibitor roflumilast. To further investigate the differentiation promoting effects of roflumilast, we developed a 3D model of rat Schwann cell myelination that closely resembles the *in vivo* situation. Using these *in vitro* models, we demonstrated that pan-PDE4 inhibition using roflumilast significantly promoted differentiation of Schwann cells towards a myelinating phenotype, as indicated by the upregulation of myelin proteins, including MBP and MAG. Additionally, we created a unique regenerative model comprised of a 3D co-culture of rat Schwann cells and human iPSC-derived neurons. Schwann cells treated with roflumilast enhanced axonal outgrowth of iPSC-derived nociceptive neurons, which was accompanied by an accelerated myelination speed, thereby showing not only phenotypic but also functional changes of roflumilast-treated Schwann cells. Taken together, the PDE4 inhibitor roflumilast possesses a therapeutic benefit to stimulate Schwann cell differentiation and, subsequently myelination, as demonstrated in the biologically relevant *in vitro* platform used in this study. These results can aid in the development of novel PDE4 inhibition-based therapies in the advancement of peripheral regenerative medicine.

Introduction

Schwann cells play a crucial role in nerve regeneration following PNS neuropathies as they actively support nerve repair by secreting trophic factors and cytokines that promote neuroregeneration and axonal outgrowth (92). However, upon aging and disease, Schwann cell dysfunction limits its regenerative capacity, hampering PNS repair (92). Hence, there is a growing need to identify novel pharmacological targets capable of restoring Schwann cell function and, thereby nerve repair.

The second messenger cyclic adenosine monophosphate (cAMP) has been shown to be crucially involved in Schwann cell biology (430). Both Schwann cell differentiation and the subsequent myelination processes are positively regulated by cAMP, where prolonging or elevating intracellular cAMP signalling has been demonstrated to increase both the expression of myelin proteins (e.g. MAG, MBP and O1) and the Krox-20/c-Jun transcription factor ratio towards favouring Schwann cell differentiation and myelination (92, 105, 326, 431-437). The importance of cAMP in Schwann cell biology is reinforced by the results obtained with forskolin, a potent agonist of the cAMP anabolic membrane-bound catalyst adenylyl cyclase. Depending on the concentration of forskolin, and therefore cAMP, either Schwann cell proliferation or differentiation was stimulated (438-440). In line, following peripheral transection and crush injuries *in vivo*, cAMP levels are reduced up to 10% in Schwann cells and only start to normalize upon the initiation of remyelination, rendering the spatiotemporal control of cAMP signalling essential for proper Schwann cell functioning (324).

The tight control of intracellular cAMP levels is accomplished by a family of cAMP-degrading enzymes called phosphodiesterases (PDEs). In neural tissue, the PDE4 family actively limits cAMP levels in both neural and glial cells, accounting for 70 to 80% of the complete PDE expression profile (284, 441). In the CNS, inhibiting PDE4 enhances oligodendrocyte precursor cell (OPC) differentiation and subsequent remyelination, indicating a central role for PDE4 in the (re)myelination process (118, 367, 442). In the PNS, regulating intracellular cAMP levels via inhibition of PDE4 has been mainly investigated for its potential neuroregenerative properties. Despite the inhibitory microenvironment following PNS nerve damage, elevating cAMP with the PDE4 inhibitor rolipram promoted *in vivo* axonal outgrowth across the lesion site (325). However, the effect of PDE4 inhibition on

Schwann cells remains speculative and is based on *in vivo* results or findings with cAMP analogues.

In this study, we aimed to determine the therapeutic potential of the PDE4 inhibitor roflumilast on Schwann cell differentiation and myelination. Using primary rat Schwann cells, we first evaluated and confirmed the importance of cAMP in promoting cellular differentiation in a 2D culture model. Furthermore, by indirectly increasing intracellular cAMP using roflumilast, Schwann cell differentiation could be promoted as well. Next, to mimic the *in vivo* environment following PNS neuropathies, primary rat Schwann cells were seeded on a 3D peripheral nerve model scaffolds. This creates an analogue of the bands of Büngner, which are longitudinally aligned Schwann cells tracks that are formed in the initial stages of PNS repair to guide axonal regrowth (443). In line with the 2D culturing conditions, roflumilast promoted Schwann cell differentiation within the 3D model as indicated by the increased gene expression and protein levels of myelin-related proteins. Finally, to evaluate myelination and axonal growth, we co-cultured rat Schwann cells with human iPSC-derived neurons in a newly established and validated 3D culture platform (444). Schwann cells treated with roflumilast positively influenced nerve repair reflected by an accelerated axonal growth. Furthermore, roflumilast treated Schwann cells demonstrated an increased differentiation and subsequent myelination of newly formed iPSC-derived nociceptive neurons. The findings of this study demonstrate for the first time the therapeutic potential of PDE4 inhibition on PNS remyelination and nerve repair, and can therefore aid in the development of novel regenerative therapeutic strategies.

Material and methods

3D Scaffold fabrication for Schwann cell culturing

The 3D scaffolds were fabricated via a two-step electrospinning (ESP) process with a custom-built apparatus. First, a release layer was produced by electrospraying a solution of 50% polyethyleneoxide (PEO, Mn = 3350, Sigma-Aldrich, Catalog #P5413) in Milli-Q onto aluminium foil. For this, the solution flowed through a 0.8 mm inner diameter stainless steel needle (Unimed S.A.) at 2 ml/hr, while subjected to 20 kV and at a distance of 10 cm from a 60 mm diameter mandrel rotating at 5000 rpm. Afterwards, a nonwoven polyurethane mesh (6691 LL (40 g/m2), a kind gift from Lantor B.V., The Netherlands) was prepared by punching an array of 12 mm circular holes and placed on the mandrel, covering the PEO sprayed-foil. Next, the scaffolds were produced by ESP of 300PEOT55PBT45 (PolyVation) in 75:25 Chloroform/1,1,3,3-hexafluoroisopropanol solution onto the mesh support structure. For this process, the solution flowed through a 0.5 mm inner diameter stainless steel needle (Unimed S.A.) at 0.75 ml/hr, while applying a voltage of 12 kV and at a distance of 10 cm from a rotating mandrel (at 5000 rpm). During both processes, the humidity remained at 35-40% and the temperature at 22-24 °C. Finally, individual scaffolds were generated from the polyurethane mesh by punching 15 mm-outer diameter sections concentric to the 12 mm holes, resulting in a thin ESP membrane supported by a polyurethane mesh ring. Next, scaffolds were dipped in deionized water to allow detachment of the scaffolds and stored in PBS. Preceding the cell seeding, scaffolds were sterilized by immersing them in 70% ethanol for 1h, followed by a repeated PBS washing step.

Primary Schwann cells harvesting, purification and culture

Primary Schwann cells were harvested from the sciatic nerves of neonatal Wistar rat pups, following local and Dutch animal use guidelines, and were based on previously described protocols (443-445). Briefly, nerve segments were extracted and digested in a 0.05% collagenase solution (60 min, 37°C, 5% CO_2)(Sigma-Aldrich, Catalog #C9697). Cell suspensions were passed through a 40 µm cell strainer, washed and seeded on 35mm poly-L-lysine (0.01%; Sigma-Aldrich, Catalog #P1666) and 1 µg/ml laminin (R&D systems, Catalog #3400-010-02) pre-

coated petridishes in proliferation and purification medium (DMEM D-valine (Cell Culture Technologies), 2 mM L-glutamine (ThermoFisher Scientific, Catalog #25030081), 10% (v/v) fetal bovine serum (FBS)(Catalog #F3297), 1x N2 supplement (R&D Systems, Catalog #AR003), 20 µg/ml bovine pituitary extract (Catalog #P1476), 5 µM forskolin (Catalog #93049), 100 U/ml penicillin and 100 µg/ml streptomycin (Catalog #P4458), and 0.25 µg/ml amphotericin B (Catalog #PHR1662)(all Sigma-Aldrich unless stated otherwise). Fresh medium was added at day 7 of culture and changed every two days until confluency. Cells were used between passage number 3 and 6 (P3-P6).

2D Schwann cell culture

Schwann cells were seeded at 25 x 10^3 cells/cm^2 on glass coverslips (12 mm; in a 24 well plate) (immunocytochemistry) or 24-well plates (qPCR), both pre-coated overnight with 1 µg/ml laminin-1 (R&D systems, Catalog #3400-010-02) and 2 µg/ml poly-D-lysine (Sigma-Aldrich, Catalog #A-003-E). The seeding medium was composed of DMEM supplemented with 10% FBS (v/v) (Sigma-Aldrich, Catalog #F3297). After 24 h of culture, the medium was changed to serum deprivation medium (1% FBS (v/v)). To evaluate the effect of cAMP supplementation on Schwann cell differentiation, medium was changed after 24h to serum-deprived DMEM medium containing 250 µM of 8-(4-Chlorophenylthio)adenosine 3',5'-cyclic monophosphate sodium salt (CPT-cAMP, water soluble, Sigma-Aldrich, Catalog #C3912). Cells were cultured in these conditions for 3 days and either fixated with 4% PFA for 20 minutes (immunocytochemistry) (Sigma-Aldrich, Catalog #158127) or lysated with Qiazol (qPCR)(Qiagen, Catalog #79306). To evaluate the effect of the PDE4 inhibitor roflumilast on Schwann cell differentiation, roflumilast (DMSO soluble, BioLeaders) was supplemented instead of CPT-cAMP 24h following serum deprivation (1/1000 final DMSO fraction in cultures) at a concentration of 5µM or 10µM (IC50 ranges between 0.2 and 4.3nM in cell free assay) (352). For downstream signalling pathway analysis, Schwann cells were treated with 250µM db-cAMP (Bio-techne, Catalog #1141) or 10µM roflumilast, with or without the EPAC inhibitor ESI-09 (10µM) (Bio-techne, Catalog #4773) or the PKA inhibitor H-89 (10µM) (Bio-techne, Catalog #2910). Cells were kept in culture for six days and treatment was repeated on day 2 and 4 (with a 50% medium change). Cells were fixated with 4% PFA for 20 minutes

(immunocytochemistry) or lysated with Qiazol (qPCR). Based on DAPI counts, roflumilast did not affected cell survival or proliferation at the used dosages (data not shown).

3D Schwann cell culture

Schwann cells were seeded at 100 x 10^3 cells per scaffold (abovementioned) and cultured in Schwann cell medium composed of DMEM supplemented with 4 mM L-glutamine (ThermoFisher Scientific), 100 U/ml penicillin and 100 µg/ml streptomycin (ThermoFisher Scientific, Catalog #25030081), 10% (v/v) FBS (Sigma-Aldrich, Catalog #F3297), 20 µg/ml bovine pituitary extract (Sigma-Aldrich, Catalog #P1476), 5 µM forskolin (Sigma-Aldrich, Catalog #93049) and 1x N2 supplement (R&D systems, Catalog #AR003). After 7 days of culturing, treatment was initiated by supplementing Schwann cell medium with either vehicle (1/1000 DMSO) or roflumilast. Treatment was repeated every other day after which cells were fixated with 4% PFA for 20 minutes (immunocytochemistry) or lysated with Qiazol (qPCR) at day 6 of the experiment. Throughout the experiment, cells were kept at 37°C with 5% CO_2.

Agarose microwell platform fabrication

A 3% (w/v) sterile agarose (ThermoFisher Scientific, Catalog #16500500) solution was prepared in PBS (ThermoFisher Scientific, Catalog #10010001). Next, 8 mL of the prepared agarose solution was poured onto an in-house produced PDMS stamp with the negative template of 1580 microwells with a diameter of 400 µM. A short centrifugation step removed the air bubbles, after which the agarose plate was allowed to solidify for 45 minutes at 4°C. Upon solidification, the agarose blocks were removed and cut in the appropriate size (12 well plate) and subsequently covered with PBS for storage at 4°C. The day before cell seeding, PBS was replaced by culture media containing Advanced RPMI 1640 media supplemented with 1x Glutamax (ThermoFisher Scientific, Catalog #35050061) and kept at 37°C with 5% CO_2 overnight.

iPSCs-derived nociceptive neurons

Human iPSC line LUMC0031iCTRL08 (Provided by the LUMC iPSC core facility) was cultured on Geltrex (ThermoFisher Scientific, Catalog #A1569601) coated dishes at a density of 10 x 10^3 /cm^2 in mTESR1 medium (Stem Cell Technology, Catalog #100-1130). To induce iPSC differentiation into nociceptive neurons, a modified protocol published by *Chambers et al* was used (446). Briefly, 200 undifferentiated iPSCs are seeded onto 400 µm agarose microwells (described above) and forced to settle by introducing a centrifugation step of 2 min at 1200 rpm. Seeding medium was composed of mTESR1 medium supplemented with 10 µM Y-27632 (Stem Cell Technology, Catalog #72303) and 0.5% Geltrex (ThermoFisher Scientific, Catalog #A1569601) in suspension. The cellular spheroid is formed after 24h and a complete medium change was conducted with mTESR1 medium supplemented with 1% DMSO to initiate cell synchronisation. The cells were maintained for 72 h in the synchronisation medium. Post synchronisation, nociceptor differentiation was initiated by changing the medium into dual SMAD inhibition media containing Advanced RPMI 1640 (Thermofisher Scientific, ThermoFisher Scientific, Catalog #12633012) supplemented with Glutamax (ThermoFisher Scientific, Catalog #35050061), 100 nM LDN-193189 (Tocris, Catalog #6053) and 10µM SB431542 (Tocris, Catalog #1614). The spheres were maintained for 48 h in the dual SMAD inhibition media. Following this, neural crest commitment was induced via media containing Advanced RPMI 1640 supplemented with Glutamax, 3 µM CHIR99021 (Tocris, Catalog #4423) and 1 µM retinoic acid (Tocris, Catalog #0695). The spheres were maintained in the neural crest induction media for 5 days with a full medium change every other day. Following the neural crest induction, spheres were incubated in notch inhibition media, consisting of Advanced RPMI supplemented with Glutamax, 10 µM SU5402 (Tocris, Catalog #3300) and 10 µM DAPT (Tocris, Catalog #2634), for 48 h. Finally, the neurospheres, composed of trunk neural crest cells, were collected and seeded on the scaffolds. Herein, cells were cultured in neural maturation medium for at least 5 days to reach the nociceptor phenotype. The neural medium is composed of Neurobasal Medium (ThermoFisher Scientific, Catalog #21103049), 0.5 mM Glutamax (ThermoFisher Scientific, Catalog #35050061), 100 U/ml penicillin and 100 µg/ml streptomycin (ThermoFisher Scientific, Catalog #P4458), 100 ng/ml human nerve growth factor (NGF; Sigma-Aldrich, Catalog

#H9666), 50 µg/ml ascorbic acid (Sigma-Aldrich, Catalog #BP461), 25 ng/ml human neuregulin-1 type III (NRG-1 SMDF; R&D systems, Catalog #378-SM) and 1x N21 supplement (R&D systems, Catalog #AR008).

iPSCs-Schwann cell co-culture on 3D scaffolds

Schwann cells were seeded on the 3D scaffolds and cultured with the PDE4 inhibitors as described above. For this experiment, Schwann cells were first exposed to vehicle (1/1000 DMSO) or roflumilast before introducing the iPSC-derived nociceptive neurons. At day 14 of culture in the scaffolds, the iPSCs-derived neurospheres were collected from the agarose mold and seeded on the scaffolds (one neurosphere per scaffold). The cells were cultured in neural medium composed as described above.

Quantitative polymerase chain reaction (qPCR)

For gene expression analysis, Schwann cells were lysated using Qiazol (Qiagen, Catalog #79306) from which total RNA was isolated using the isopropanol precipitation method. Next, cDNA synthesis was conducted using the qScript cDNA synthesis kit (Quanta, Catalog #95048) according to the manufacturer's instructions. Gene expression analysis was performed using a StepOnePlus detection system (Applied Biosystems, USA). The reaction mixture consisted of SYBR Green master mix (Applied Biosystems, Catalog #A25742), 10 µM forward and reverse primers (IDT), nuclease free water and cDNA template (5 ng/µl), up to a total reaction volume of 10 µl. The primer pairs used for amplification are listed below (table 1). Results were analysed by the comparative Ct method and were normalised to the most stable housekeeping genes, determined by Genorm (*YWHAZ* and *ACTB* for gene expression analysis within CPT-cAMP and roflumilast experiments, *RPL13a* and *PGK1* for the EPAC and PKA inhibitor experiments).

Table 6.1 : Primer sequences for qPCR.

GENE	SPECIES	FORWARD PRIMER (5'-3')	REVERSE PRIMER (5'-3')
Sox10	*R. Norvegicus*	GCACGCAGAAAGTTAGCC	TGTCACTCTCGTTCAGCAAC
PLP	*R. Norvegicus*	TCTGCAAAACAGCCGAGTTC	TGGCAGCAATCATGAAGGTG
cJUN	*R. Norvegicus*	TCCACGGCCACGGCCAACATGCT	CCACTGTTAACGTGGTTCATGAC
MAG	*R. Norvegicus*	GCTACAACCAGTACACCTTCTC	TGACCTCTACTTCCGTTCCTG
MBP	*R. Norvegicus*	ACGCGCATCTTGTTAATCCG	AAGTTTCGTCCCTGCGTTTC
Krox20	*R. Norvegicus*	GCCCCTTTGACCAGATGAAC	GGAGAATTTGCCCATGTAAGTG
BCL2	*R. Norvegicus*	ATCGCTCTGTGGATGACTGAGTAC	AGAGACAGCCAGGAGAAATCAAAC
Bax	*R. Norvegicus*	CCAGGACGCATCCACCAAGAAGC	TGCCACACGGAAGAAGACCTCTCG
BDNF	*R. Norvegicus*	ATAGGAGACCCTCCGCAACT	CTGCCATGCATGAAACACTT
NGF	*R. Norvegicus*	TGCATAGCGTAATGTCCATGTTG	CTGTGTCAAGGGAATGCTGAA
GDNF	*R. Norvegicus*	TTGCATTCCTGCTACAGTGC	TGTAGCTGGGCCTCCTTCTA
PGK1	*R. Norvegicus*	ATGCAAAGACTGGCCAAGCTAC	AGCCACAGCCTCAGCATATTTC
RPL13a	*R. Norvegicus*	GGATCCCTCCACCCTATGACA	CTGGTACTTCCACCCGACCTC
YWHAZ	*R. Norvegicus*	GATGAAGCCATTGCTGAACTTG	GTCTCCTTGGGTATCCGATGTC
ACTB	*R. Norvegicus*	TGTCACCAACTGGGACGATA	GGGGTGTTGAAGGTCTCAAA

Immunostaining

Samples were fixed with 4% paraformaldehyde (PFA) for 20 minutes at room temperature and subsequently permeabilized for 30 minutes with 0.1% Triton X-100 dissolved in PBS. Next, a blocking step was conducted with a blocking buffer composed of 5% goat serum, 0.05% Tween-20, and 1% bovine serum albumin (Sigma-Aldrich, Catalog #9048-46-8). Primary antibodies were subsequently dissolved in blocking buffer and samples were incubated overnight at 4°C. Following washing, secondary antibody incubation was done for 2h at room temperature. DAPI (1:1000, Sigma-Aldrich, Catalog #28718-90-3) was used to counterstain the nuclei. The primary antibodies used were the following: anti-βIII tubulin (Sigma-Aldrich, Catalog #T8578, 1:500), anti-myelin basic protein, MBP (Thermo Fisher Scientific, Catalog #PA1-46447, 1:50) and anti-myelin associated glycoprotein, MAG (Abcam, Catalog #ab89780, 1:100), anti-oligodendrocyte marker 1, O1 (Novus Biologicals, Catalog #MAB1327, 1:100), anti-Krox20 (Sigma-Aldrich, Catalog #ABE1374, 1:100), anti-cJun (Cell Signaling Technologies, Catalog #9165S, 1:300), anti-p75 (Alomone Labs, Catalog #ANT-007, 1:50). The used secondary antibodies were the following: goat anti-mouse conjugated with Alexa Fluor 488; goat anti-mouse conjugated with Alexa Fluor 568 and goat anti-rabbit conjugated with Alexa Fluor 568 (all used at 1:1000).

Microscopy

Images were acquired using either a fluorescence microscope (Leica DM2000 LED microscope; 2D Schwann cell cultures), inverted epifluorescence microscope (Nikon Eclipse Ti-e; 3D Schwann cell cultures) or a confocal laser scanning microscope (Leica TCS SP8; iPSC-Schwann cell coculture). Images were prepared and analysed using Fiji software. To quantify marker expression, we measured the mean area of each marker and corrected this for the total number of cells present. At least 10 images were taken per sample (5 replicates per condition). The VAA3D software was used to create 3D rendered images (VAA3D-Neuron2_Autotracing) (362).

Image analysis

Images were prepared and analysed using Fiji software (https://fiji.sc/). Results were analyzed in a blinded manner. To quantify marker expression in 2D samples (coverslips and well-plates) and 3D scaffolds, the positive area covered by each marker was determined by manually setting the threshold. The total area was subsequently corrected by the total number of cells in the image. Cell count was performed using the standard Analyze Particles function to DAPI + objects. At least 10 images per sample, and 5 replicates per conditions were analyzed.

To measure the axonal area, the βIII tubulin positive area occupied by the neurites was determined, thereby excluding cell bodies. Next, for the myelinated are, the MBP positive are was measured within the same area excluding the central segment of the scaffold.

Statistics

The GraphPad Prism 9.0.0 software (GraphPad software Inc) was used to analyse the data and build the subsequent graphs. All data are shown as mean ± standard error mean (SEM). If the sample size was $n \leq 4$, differences between groups were assessed by a non-parametric Mann-Whitney or Kruskal-Wallis test along with Dunn's post-hoc analysis, with the vehicle group serving as the reference. For sample sizes of $n \geq 5$, normality was verified using the Shapiro-Wilk test before conducting the analysis. Normally distributed data were subsequently analyzed with a t-test or one-way ANOVA with Tukey's multiple comparison. A p-value of 0.05 was considered statistically significant (*$p \leq 0.05$, **$p \leq 0.01$, ***$p \leq 0.005$, ****$p \leq 0.001$).

Results

CPT-cAMP stimulates Schwann cell differentiation

Since PDE4 inhibitors indirectly elevate intracellular cAMP levels, we first aimed to validate the role of cAMP itself on Schwann cell differentiation. Exposing primary rat Schwann cells to a cell membrane-permeable CPT-cAMP analogue (250µM 8-(4-Chlorophenylthio)adenosine 3',5'-cyclic monophosphate sodium salt) led to a significant enhancement of Schwann cell differentiation into a myelinating phenotype. After 3 days of CPT-cAMP administration, Schwann cells adapted a shift in both morphology and phenotype. While vehicle treated cells remained elongated, CPT-cAMP-treated Schwann cells adopted a flattened shape with a large cytoplasmic-to-nuclei ratio (**Fig 6.1A-B**). Gene expression analysis revealed a significant upregulation of the myelin gene MBP (**Fig 6.1C**) and a trend towards upregulation of PLP (**Fig 6.1D**). The transcription factor Krox20, which controls Schwann cell myelination by suppressing the cJun pathway, was significantly upregulated upon CPT-cAMP treatment (**Fig 6.1E**). Accordingly, cJun expression was significantly reduced in CPT-cAMP treated Schwann cells (**Fig 6.1F**). The phenotypic consequences of these changes in gene expression were confirmed using immunocytochemistry (**Fig 6.1G**). Schwann cells treated with CPT-cAMP displayed a significant upregulation of the glycolipid marker for mature myelinating cells 01, and the myelin protein MBP and MAG (**Fig 6.1H-J**), and an increased expression of Krox20 (**Fig 6.1K**), while cJun expression was significantly reduced (**Fig 6.1L**).

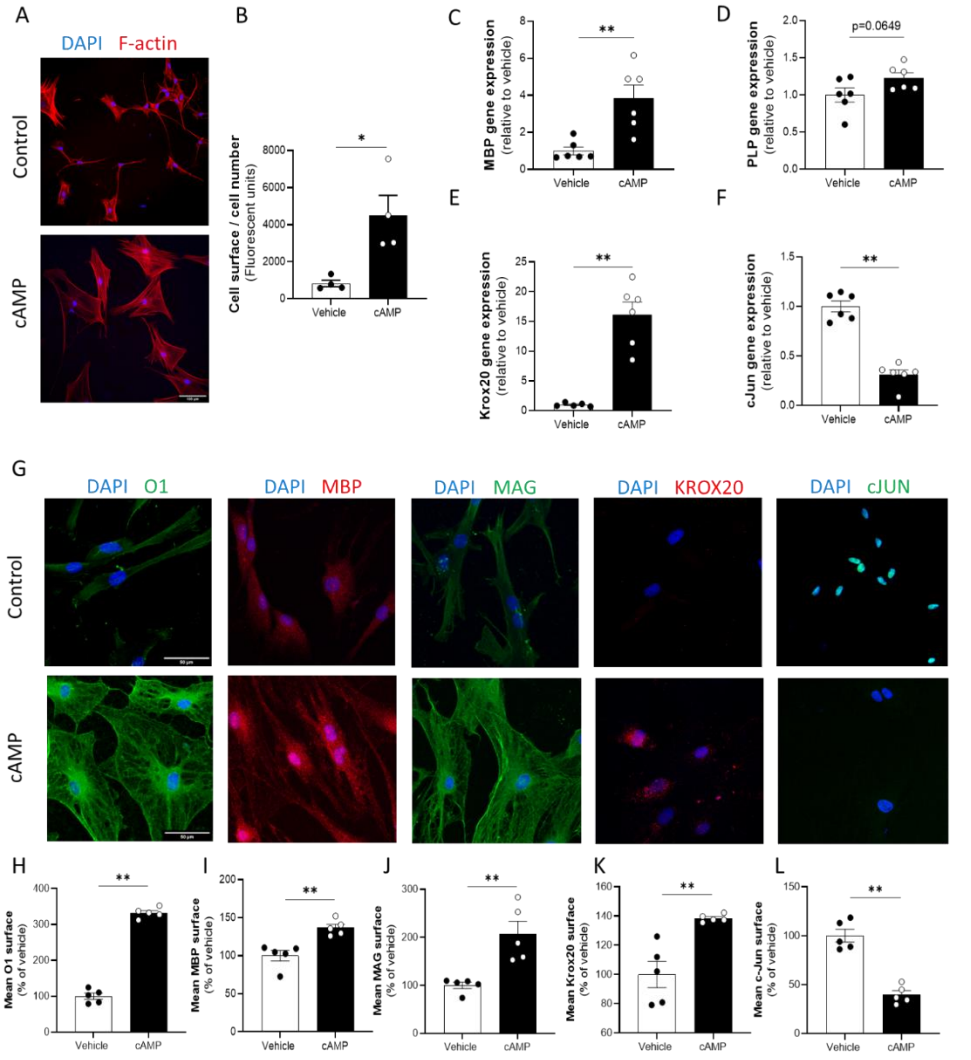

FIG 6.1: CPT-cAMP boosts Schwann cell differentiation into a myelinating phenotype. Schwann cells were treated for 3 days with a CPT-cAMP analogue and subsequently evaluated for their morphology and phenotype. (A-B) Schwann cell morphology was assessed using a cytoskeletal F-actin staining which demonstrates a flattened and significantly increased cell surface upon CPT-cAMP treatment. Scale bar indicates 100µm. (C-F) Gene expression analysis reveals a significant upregulation of the myelin gene (C) MBP, a trend towards upregulation for the myelin gene (D) PLP, a significant upregulation of the transcription factor (E) Krox20 and a significant downregulation of the transcription factor (F) cJun. (G) Immunocytochemical staining analysis demonstrates a significant upregulation of the myelin protein (H) O1, (I) MBP, and (J) MAG upon CPT-cAMP treatment. Furthermore, the (K) Krox20 protein levels were significant increased, while (L) cJun protein levels were significantly decreased. Scale bar indicates 50µm. Data are presented as mean ± SEM (n=5/group). Data were analysed using a non-parametric Mann-Whitney test. (*p<0.05; **p<0.01)

PDE4 inhibition by roflumilast stimulates Schwann cell differentiation in both a 2D and 3D culture condition

To evaluate the effect of the PDE4 inhibitor roflumilast on cellular differentiation, primary rat Schwann cells were exposed to roflumilast (5μM or 10μM) for 6 days and subsequently analysed for their myelination phenotype. Similar to exogenous cAMP supplementation, roflumilast stimulated Schwann cell differentiation at both 5μM and 10μM exposure led to a significant upregulation of the myelin protein MBP and the glycolipid O1 (**Fig 6.2A-C**).

Next, to assess the differentiation promoting potential of Schwann cells in a more biologically relevant model, we cultured primary Schwann cells on a 3D scaffold that induces Schwann cell alignment, mimicking the initial stages of PNS regeneration (**Fig 6.3A**). Both 5μM and 10μM of roflumilast treatment significantly increased myelin gene expression (MBP, PLP and MAG) (**Fig 6.3B-D**) and SOX10 expression, a key transcription factor of Schwann cell lineage cells (**Fig 6.3E**). With regard to myelin protein expression (**Fig 6.3F**), both 5μM and 10μM roflumilast induced a significant upregulation of both MAG and MBP on the 3D Schwann cell bands compared to the vehicle condition (**Fig 6.3G-H**).

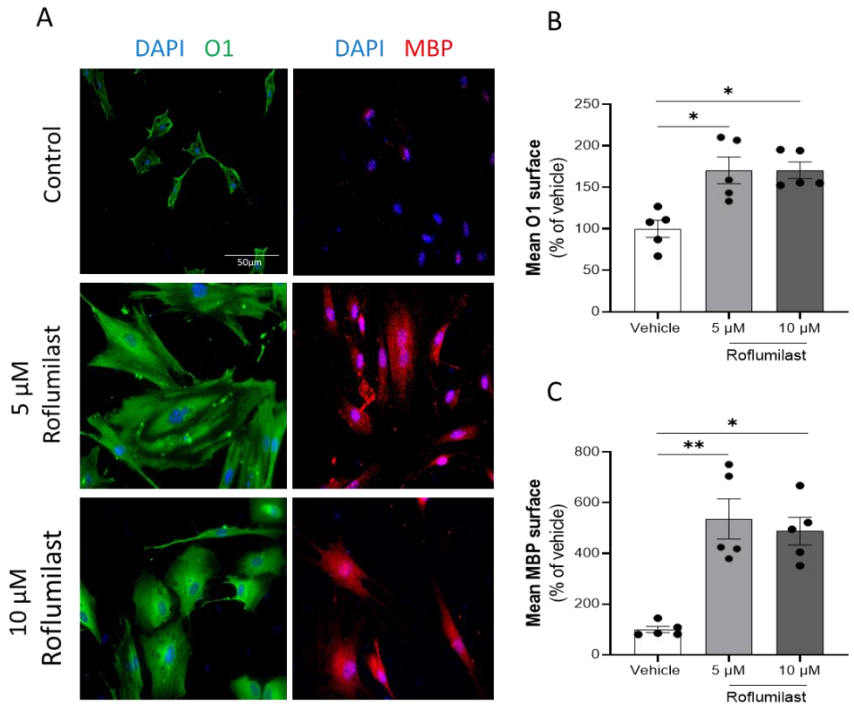

FIG 6.2: Roflumilast boosts Schwann cell differentiation into a myelinating phenotype. Schwann cells were treated for 6 days with either 5µM or 10µM roflumilast (treatment repeated every other day) and subsequently analysed for their differentiation promoting capacity. (A) Immunocytochemical analysis revealed a significant upregulation of both (B) O1 and (C) MBP protein levels upon roflumilast treatment. Scale bars are 50µm. Data are presented as mean ± SEM (n=5/group). Data were analysed using a non-parametric Kruskal-Wallis test with Dunn's post-hoc analysis (compared to vehicle). (*p<0.05; **p<0.01)

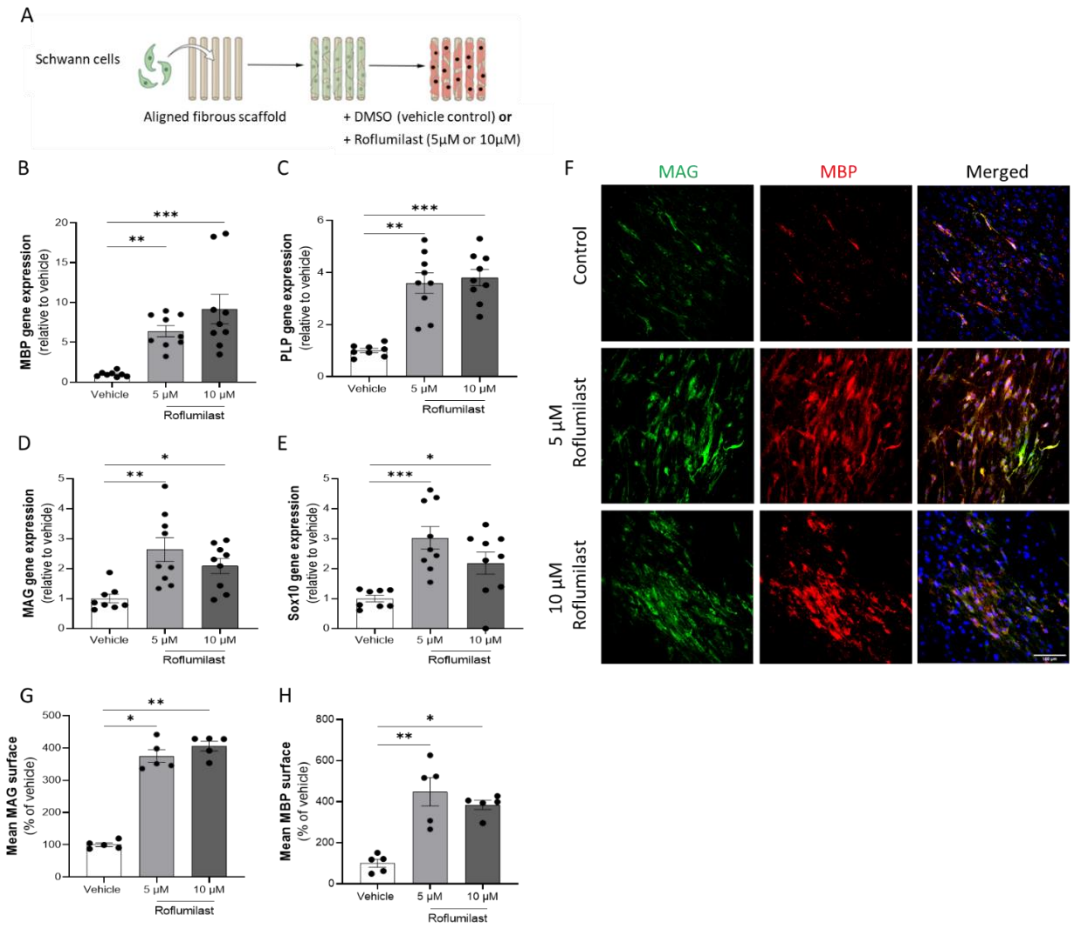

FIG 6.3: Roflumilast boosts Schwann cell differentiation into a myelinating and nerve repair promoting phenotype. (A) Primary rat Schwann cells were seeded onto a 3D aligned scaffold to generate Schwann cell composed bands of Büngner mimicking regeneration bands. Cells were treated with either 5μM or 10μM roflumilast for 6 days (treatment repeated every other day). (B-E) Both 5μM and 10μM roflumilast treatment led to a significant upregulation of (B) MBP, (C) PLP, (D) MAG, and (E) SOX10 gene expression compared to vehicle treated cells. (F) Immunohistochemical analysis demonstrate a significant increase in myelin protein surface of both (G) MAG and (H) MBP. Scale bars are 100μm. Data are presented as mean ± SEM (n=5/group). Data were analysed using a non-parametric Kruskal-Wallis test with Dunn's post-hoc analysis (compared to vehicle). (*p<0.05; **p<0.01; ***p<0.005)

Roflumilast treated Schwann cells showed an increased myelination speed of iPSC-derived nociceptive neurons

To evaluate whether the differentiation promoting capacity of roflumilast translates into a higher myelination capacity, we co-cultured rat Schwann cells with human iPSC-derived nociceptive neurons. First, Schwann cell alignment was accomplished by culturing cells on the 3D scaffolds and subsequently treated with 10µM roflumilast for 6 days (**Fig 6.3A**). Next, iPSC-derived neurospheres were added to the Schwann cell cultures, which were maintained for 14 or 21 days in neural medium, and subsequently axonal region and myelinated area were analysed. After 14 days of coculture, roflumilast-treated Schwann cells significantly promoted axonal outgrowth of iPSC-derived neurons (**Fig 6.4A-B**), which was accompanied with an increased myelinated area (**Fig 6.4A-C**). After 21 days of coculture, no difference in both axonal area or myelinated area were observed (**Fig 6.4D-F**).

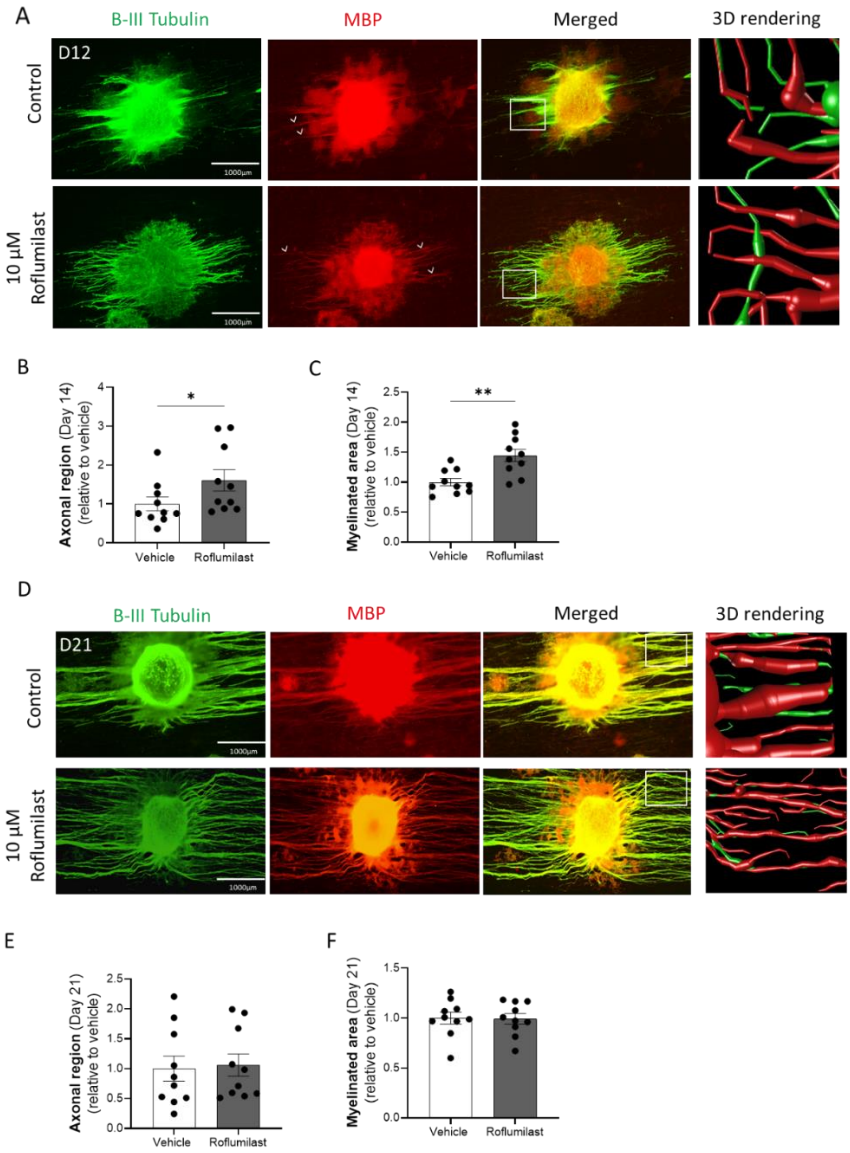

Figure 6.4: Roflumilast treated Schwann cells accelerate axonal outgrowth and myelination of iPSC-derived nociceptive neurons. Schwann cells were cultured on 3D scaffolds and treated for 6 days with 10µM roflumilast (treatment repeated every other day). Subsequently, iPSC-derived neurospheres were added to the treated Schwann cells and maintained for an additional 14 or 21 days. (A) Immunocytochemical analysis demonstrate an increased (B) axonal growth and (C) myelination of iPSC-derived neurons cultured with roflumilast treated Schwann cells after 14 days. (D) Immunohistochemical analysis showed no differences in either (E) axonal growth, nor (F) myelination following 21 days of co-culture. Arrowheads highlight myelinated axon structures. White squares indicate the 3D rendered image location. Scale bars are 1000µm. Data are presented as mean ± SEM (n=10/group). Data were analysed using a non-parametric Mann-Whitney test. (*p<0.05; **p<0.01).

The EPAC inhibitor ESI-09 inhibits myelin gene expression, while the PKA inhibitor H-89 prevents neurotrophic factor gene expression following roflumilast treatment

As demonstrated above, both cAMP and roflumilast treatment increases the maturation of primary rat Schwann cells. The expression of myelin genes, including MBP, PLP and MAG, was significantly upregulated in Schwann cells treated with db-cAMP or roflumilast compared to the control group (**Fig 6.5A-C**). Similarly, the expression of neurotrophic factors, including brain-derived neurotrophic factor (BDNF), nerve growth factor (NGF), and glial-derived neurotrophic factor (GDNF), was significantly increased as well upon db-cAMP or roflumilast treatment (**Fig 6.5D-F**).

To further investigate the downstream signalling pathways involved in the roflumilast-induced upregulation of myelin genes and neurotrophic factors, Schwann cells were treated with the EPAC inhibitor ESI-09 or the PKA inhibitor H-89 simultaneously with roflumilast. Co-treatment of Schwann cells with roflumilast and the EPAC inhibitor ESI-09 significantly inhibited the increase in myelin gene expression (**Fig 6.5A-C**), whereas co-treatment with roflumilast and the PKA inhibitor H-89 significantly inhibited the increase in neurotrophic factor expression (**Fig 6.5D-F**).

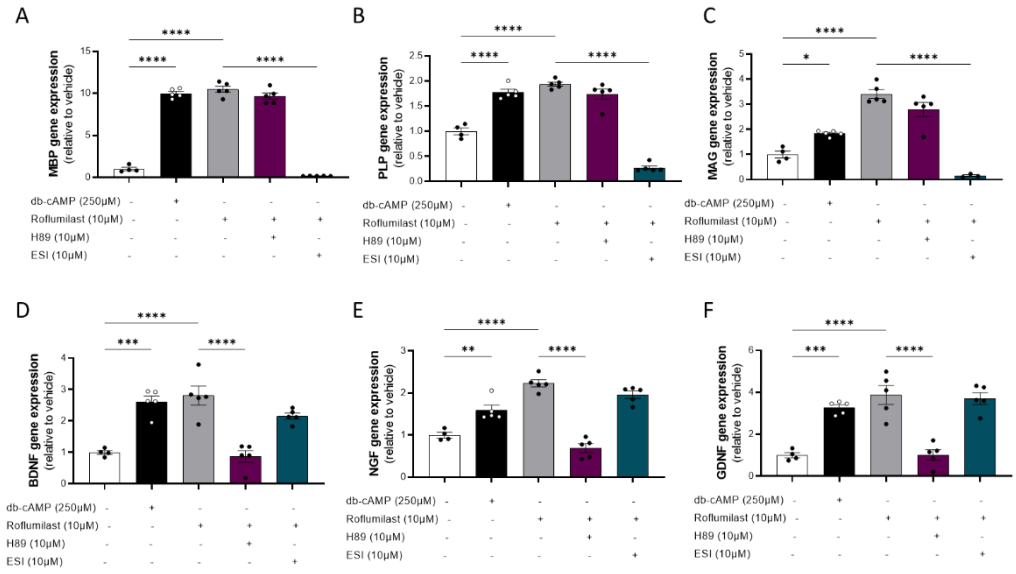

FIG 6.5: Roflumilast increase myelin gene expression and neurotrophic factor gene expression via downstream EPAC and PKA signalling respectively. Schwann cells were treated for 6 days with either 250μM db-cAMP or 10μM roflumilast with or without 10μM ESI-09 (EPAC inhibitor) or 10μM H-89 (PKA inhibitor). Gene expression analysis reveals a significant upregulation of the myelin genes (A) MBP, (B) PLP and (C) MAG upon db-cAMP or roflumilast treatment, which is inhibited upon ESI-09 treatment. Additionally, neurotrophic factor gene expression, including (D) BDNF, (E) NGF and (F) GDNF was significantly upregulated following db-cAMP and roflumilast treatment which was prevented when co-treated with H89. Data are presented as mean ± SEM (n≥4/group). Data were analysed using a one-way ANOVA with Tukey's multiple comparison (*p<0.05; **p<0.01; ***p<0.005; ****p<0.001).

Discussion

PDE4 inhibitors hold promise as therapeutics for the treatment of multiple disorders. With respect to the nervous system, most reports to date have focused on CNS disorders, thereby overlooking the therapeutic potential of PDE4 inhibitors on PNS repair. In this study, we demonstrate that PDE4 inhibition, by means of roflumilast, promotes Schwann cell differentiation into a myelinating phenotype. Furthermore, Schwann cells treated with roflumilast promote axonal outgrowth of human iPSC-derived nociceptive neurons while simultaneously enhancing their myelination capacity. The findings from this study support the use of PDE4-inhibitor based treatment strategies for the treatment of peripheral demyelinating neuropathies.

It has been shown that enhancing intracellular cAMP signalling promotes Schwann cell differentiation (105, 326, 431-433). To first validate these findings, we treated primary rat Schwann cells with 250µM of a membrane-permeable cAMP analogue, a concentration known to cause a fast and robust change in the cellular phenotype (431, 447). Indeed, cAMP-treated Schwann cells enlarged up to 5-times compared to vehicle treated cells and increased their gene expression and protein levels of myelin genes and Krox20, while exhibiting lower levels of cJun. With regards to PDE4 inhibition in Schwann cells, the main findings so far focused on *in vivo* administration of the PDE4 inhibitor rolipram to stimulate peripheral nerve regeneration and remyelination. After surgical repair of transected nerves, a 0.4 µmol/kg/h infusion of rolipram promotes axonal outgrowth over the lesion size in rats (325). Furthermore, a daily intraperitoneal injection of 5mg/kg rolipram has shown to rescue peripheral myelin deficiencies in Rac1-CKO mice after 8 weeks (326). Nevertheless, no compelling conclusions of PDE4 inhibition on Schwann cells specifically can be drawn from these *in vivo* findings since PDE4 inhibition has shown to also directly influence neuroregeneration and neuroplasticity (120, 124, 429). In the CNS, exogenous cAMP dosing or the application of PDE4 inhibitors, such as rolipram and roflumilast, have shown to improve oligodendrocyte precursor cells (OPCs) differentiation and oligodendrocyte-mediated *de novo* myelin formation after injury (118). In this study, we show now that primary rat Schwann cells trceated with the PDE4 inhibitor roflumilast

significantly increase O1 and MBP levels, indicating a phenotypical shift towards promoting myelination.

Following PNS injury, Schwann cells guide axonal outgrowth by forming aligned cellular tracks called bands of Büngner (90, 91). These bands of Büngner provide a favourable cellular and molecular environment (e.g. laminin and collage IV secretion) that conduces regrowing axons via haptotaxis back to their target during early PNS regeneration (90). Therefore, in a next step, a biologically relevant 3D platform was applied that topographically guides cellular alignment and promotes anisotropic Schwann cell band formation similar to the *in vivo* bands of Büngner (443, 444). To test the potential of PDE4 inhibition on Schwann cell alignment, we seeded primary rat Schwann cells on the scaffold and treated them with roflumilast for 6 days. Both 5μM and 10μM of roflumilast demonstrated to significantly enhance myelin gene expression (MAG, MBP and PLP) and SOX10 expression, this latter being a transcription factor that confirms the Schwann cell lineage fate (448).No significant difference was observed between both roflumilast concentrations used within this study. This indicates a non-linear dose-effect relationship between the PDE4 inhibitor and the Schwann cell differentiation, likely displaying an inverted U-shaped response. The inverted U-shape correlation creates an "area of best performance" comprising a (small) range of biologically effective dosages. Since no significant differences were observed between both 5μM and 10μM concentration, both roflumilast concentrations are likely to be within the "area of best performance". Importantly, the upregulation in gene expression was accompanied with an elevated protein level of the myelin proteins MAG and MBP, further confirming the increase in myelinating phenotype of Schwann cells obtained upon PDE4 inhibition.

As demonstrated in this study, the ubiquitously expressed second messenger cAMP significantly promotes Schwann cell differentiation. In addition, we demonstrate here that PDE4 inhibition, by means of roflumilast, boosts Schwann cell differentiation and promotes both myelination and axonal outgrowth of iPSC-derived neurons, this latter likely due to mitogenic growth factor secretion. Previously, it was shown that the presence and abundance of myelinated MBP positive segments positively correlated with compacted myelin layers and myelinated area as observed with transmission electron microscopy, indeed

indicating a functional myelination phenotype of Schwann cells when stimulated with roflumilast (444). Interestingly, after 21 days of co-culture, no differences were observed in either axonal or myelinated area, indicating mainly an accelerated neurite outgrowth and myelination promoting effect of PDE4 inhibition. Besides myelination, Schwann cells have been reported to support axonal growth directly via the secretion of mitogenic growth factors (e.g. neuregulin), another process controlled by cAMP signalling (432, 436, 449, 450). The outcome of cAMP signalling in Schwann cells highly depends on the set of downstream effectors activated. Increasing intracellular cAMP levels activates a downstream signalling cascade involving, among others, protein kinase A (PKA), cyclic nucleotide-gated ion channels and exchange protein directly activated by cAMP (EPAC) (110, 451). These downstream effectors are involved in regulating several physiological processes, including immunomodulation, glial cell differentiation and neural regeneration (110, 325, 441). In Schwann cells, the mitogenic activity of cAMP exclusively relies on downstream PKA signalling, while the differentiation boosting action relies on a PKA-independent mechanism partially involving EPAC signalling (440, 447). By preventing the degradative action of PDE4 enzymes, intracellular levels of cAMP can be raised, activating both PKA and EPAC downstream signalling. In this study, we demonstrated that both db-cAMP and the PDE4 inhibitor roflumilast were effective in boosting the expression of myelin genes (MBP, PLP, and MAG) and genes related to neurotrophic factors (BDNF, NGF, and GDNF) in primary rat Schwann cells. Interestingly, when downstream EPAC was inhibited, the expression of myelin genes was hindered after PDE4 inhibition, while the inhibition of PKA significantly impeded the expression of neurotrophic factor genes. The difference in downstream EPAC and PKA signaling provides valuable insights into how stimulation of the cAMP pathway can support both neurite outgrowth and myelination simultaneously.

Unfortunately, high levels of PDE4 inhibition *in vivo* coincide with emetic side effects such as vomiting and nausea, hampering their direct translation towards a clinical application (108). However, current research in the area of PNS repair has involved the creating of nerve guidance conduits (NGCs) which are pre-seeded with Schwann cells to enhance the regenerative process (452). The results we show here suggest that PDE4 inhibition could be applied *ex vivo* to SC-laden NGCs

in order to prime their regenerative phenotype further, thereby achieving enhanced nerve repair in the first critical days after injury, while avoiding a systemic application of inhibitors that can lead to emesis. Alternatively, the PDE4 family comprises four PDE4 subtypes, PDE4A-D, and selective ablation of any of the PDE4 subtypes did not result in emetic side effects, rending PDE4 subtype inhibition a novel and safe therapeutic avenue to explore (128). Identifying and targeting the specific PDE4 subtype responsible for Schwann cell differentiation can therefore hold the key for comprising therapeutic benefits, without inducing emetic side effects (442). Whether or not the remyelination and mitogenic growth factor secretion of PDE4 inhibition to boost PNS regeneration is within the emetic dose range of a drug remains to be elucidated. However, based on previous *in vivo* studies evaluating the effect of the PDE4 inhibitor rolipram, of which the emetogenic profile is known, it is highly likely that the therapeutic dose is accompanied with emetic side effect (281). Identifying the PDE4 subtype responsible for the regenerative therapeutic properties can therefore lower the occurrence of potential adverse side effects and therefore increase their therapeutic potential.

Taken together, our data demonstrate that pharmacological PDE4 inhibition by roflumilast promotes Schwann cell differentiation into a myelinating phenotype. Furthermore, roflumilast-treated Schwann cells increase axonal outgrowth of iPSC-derived nociceptive neurons. These *in vitro* findings provide a new incentive for future *in vivo* studies investigating the potential of PDE4 inhibitors to treat PNS neuropathies, thereby further aiding drug development for pursuing new and improved PNS regenerative therapies.

Acknowledgements

TV, JP and MS have proprietary interest in selective PDE4D inhibitors for the treatment of demyelinating disorders.

We thank the Microscopy CORE Lab (M4I Maastricht University), especially Hans Duimel and Kevin Knoops for their help in confocal imaging. We thank the province of Limburg for the project funding. This work was partly supported by the research programme VENI 2017 STW- project 15900 financed by the Dutch Research Council (NWO), the FWO (12G0817N and 1S57521N) and the Fondation Charcot Stichting.

CHAPTER 7

Inhibiting PDE4 subtype in Charcot-Marie Tooth disease type 1A

Based on:

Increasing cAMP levels by inhibiting phosphodiesterase 4D improves nerve conduction and both functional and molecular outcome in a mouse model for Charcot Marie Tooth disease type 1A

Melissa Schepers[*], Tim Vangansewinkel[*], Karen Libberecht[*], Darren Jacobs, Elisabeth Piccart, Hanne Jeurissen, Robert Prior, Roberta Ricciarelli, Chiara Brullo, Ernesto Fedele, Olga Bruno, Jos Prickaerts, Ludo Van Den Bosch, Ivo Lambrichts[#], Tim Vanmierlo[#], Esther Wolfs[#]

* Equally contributing first authors

# Equally contributing senior authors

Manuscript in preparation

Declaration of own contribution:

M.S. contributed to the experimental design, data generation (with support of co-authors, except figure 7.1) and analysis, interpretation and manuscript writing

Abstract

Charcot-Marie-Tooth disease type 1A (CMT1A) is the most common inherited neuropathy of the peripheral nervous system for which no therapy is currently available. It is caused by a duplication of the *peripheral myelin protein 22* gene (PMP22), primarily causing Schwann cell dedifferentiation and demyelination leading to decreased nerve conduction and subsequent motor and sensory deficits. Cyclic adenosine monophosphate (cAMP) is an important second messenger molecule involved in Schwann cell maturation and differentiation. Increasing cAMP by inhibiting its natural regulators, phosphodiesterases (PDE), may be an interesting target. In this study, the therapeutic potential of the specific PDE-4D inhibitor Gebr32a was tested in C3-PMP22 mice, an animal model for CMT1A. 4-month-old C3-PMP22 mice were injected subcutaneously twice a day with Gebr32a (0.3mg/kg) or vehicle control for 7 weeks (n=9 mice/group). Wildtype littermates (n=12) were included as controls and received vehicle injections. All mice were functionally tested at baseline and at the end of the treatment. Electrophysiological recordings showed that axonal functions were comparable between Gebr32a treated mice and controls. In contrast, nerve conduction in the sciatic nerve of treated mice was significantly increased compared to controls, indicating improved myelination. In addition, treated C3-PMP22 mice traversed a 7mm wide beam significantly faster compared to controls. These mice also made significantly less foot slips on the grid walk test compared to untreated animals, indicating improved sensorimotor functions. Gebr32a treated mice were also able to run longer on an accelerating rotarod compared to untreated mice, not reaching significance. Furthermore, we observed that the grip strength of all limbs was significantly increased in treated C3-PMP22 mice. Finally, post mortem analysis revealed in an increase in myelination of the sciatic nerve. To conclude, we found that inhibition of PDE-4D with Gebr32a can be used to improve the functional and molecular outcome in an animal model for CMT1A disease, highlighting its potential as a new therapeutic strategy for CMT1A disease management.

Introduction

Charcot-Marie-Tooth disease (CMT) is the most common hereditary motor and sensory neuropathy with an estimated worldwide prevalence of 1 in 2500 (94-97). CMT is a clinically and genetically heterogeneous disease, affecting both children and adults. Patients typically exhibit a slowly progressive and length-dependent degeneration of their peripheral nerves resulting in muscle weakness, atrophy in the feet and legs which extend later to the hands, causing reduced tendon reflexes and slight to moderate distal sensory impairment. Foot deformities like *pes cavus* and hammer toes are among the frequently reported manifestations of CMT, with patients sometimes also exhibiting hearing loss and hip dysplasia. These and other additional symptoms that mark the different CMT subtypes may cause a significant decrease in the quality of life of affected individuals (453). Based on electrophysiological criteria and the cell type affected, CMT is broadly classified into two major subgroups, CMT1 and CMT2 but also intermediate types exist. CMT1 is a demyelinating peripheral neuropathy affecting primarily the myelinating Schwann cells and is further characterized by slow nerve conduction velocities (NCVs) (<38 m/s in patients). CMT2, on the other hand, is characterized by axonal degeneration and NCVs are within the normal (>40–45 m/s) or occasionally in the mildly abnormal range (30–40 m/s). However, it is important to note that axonal loss is a feature of both CMT2 and CMT1 and it is the major determinant of disability in patients with CMT, even when axonal loss is secondary to demyelination. Mutations in over 100 genes have been found to be associated with the pathogenesis of CMT and related neuropathies (99).

Axon myelination in the PNS is essential to attain rapid saltatory impulse conduction. The multi-layered myelin sheath structure is achieved by wrapping the plasma membrane of Schwann cells around large-caliber axons. This precise arrangement and its integrity are disrupted in CMT type 1 causing malformation or deterioration of the myelin sheath or even demyelination. CMT1 is caused by mutations or copy-number variations in several genes (98, 99). The most common form of the disease is CMT1A (prevalence ranges from 20-64%), an autosomal dominant form caused by a tandem duplication of a chromosome region containing the *PMP22* gene; resulting in a higher dosage of PMP22 expression (454). PMP22 is an integral membrane glycoprotein of compact myelin and comprises 2-5% of the total myelin proteins in the PNS (455). The functional

importance is highlighted by the fact that genetic alterations in the *PMP22* gene are the cause of the most common inherited nerve disorders (455). Although significant progress has been made in the field, as of to date, no effective treatments have been developed for CMT patients. Therapeutic compounds that have been tested are ascorbic acid, onapristone, and antisense oligonucleotides (ASOs), amongst others (456-459).

Key for developing new and effective treatment strategies for managing CMT1A pathophysiology is correcting the molecular derangements causing the Schwann cell CMT1A phenotype. The intracellular second messenger cyclic adenosine monophosphate (cAMP) has previously been shown to play a key role in orchestrating Schwann cell functioning. Balancing intracellular cAMP levels, and therefore its downstream signaling cascade activation (e.g. MEK-ERK kinase cascade, PI3K-AKT pathway), is crucial for maintaining a proper balance between Schwann cell proliferation and myelination (460). While low concentration of cAMP favor Schwann cell proliferation, elevating cAMP levels demonstrated to positively regulate Schwann cell differentiation and subsequently myelination (326, 432, 433, 461). Interestingly, a transgenic Sprague-Dawley rat model overexpressing *PMP22*, thereby mimicking CMT1A pathophysiology, display a decrease in intracellular cAMP levels in CMT1A Schwann cells compared to wild type cells, highlighting the potential of elevating cAMP levels as a novel therapeutic strategy for correcting Schwann cell functioning in CMT1A (462).

Intracellular cAMP signaling is positively regulated by adenylyl cyclase (AC) while being rapidly degraded by a class of enzymes called phosphodiesterases (PDEs). The superfamily of PDEs can be classified into 11 families (PDE1-11) and classification is based on substrate specificity (cAMP and/or cGMP), mechanisms of regulation, kinetic properties and subcellular distribution (108). Each of these families consist of several genes (e.g. PDE4A-4D) and each gene product can have multiple isoforms (e.g. PDE4D1-9), which yields a cell type-specific PDE expression signature (108, 124). In neural tissue, PDE4 is the predominant enzyme expressed limiting cAMP signaling, and inhibiting its enzymatic activity, thereby increasing intracellular cAMP levels, has demonstrated to act neuroregenerative in the PNS (284, 325, 441). However, emetic and gastrointestinal side effects accompanied with PDE4 inhibitors at their repair

inducing dose significantly decreases their clinical relevance for treating peripheral neuropathies (129). Interestingly, in the CNS, inhibiting the PDE4D subtype using the small molecule Gebr32a has recently shown to enhance oligodendrocyte precursor cell differentiation and subsequently remyelination at a non-emetic dose, indicating a crucial role for PDE4D in orchestrating (re)myelination processes (chapter 3). However, the effect of the PDE4D inhibitor Gebr32a on Schwann cell functioning to restore the derangements in CMT1A Schwann cells remains unknown.

In this study, we aimed to determine the therapeutic potential of the PDE4D inhibitor Gebr32a on the peripheral neuropathy CMT1A using the C3-PMP22 mouse model. Gebr32a-mediated PDE4D inhibition was capable of improving both functional and molecular outcome following CMT1A-induced Schwann cell neuropathology as demonstrated by an increased grip strength, prolonged motor endurance on the rotarod, improved motor coordination, enhanced sciatic nerve conduction and an enhanced molecular myelination. The findings of the study demonstrate for the first time the therapeutic potential of PDE4D inhibition on correcting CMT1A-induced Schwann cell dysfunction thereby aiding in CMT1A disease management.

Material and methods

Animals and treatment

C3-PMP22 mice were kindly provided by Prof. Dr. Frank Baas (Amsterdam University) and maintained in a C57BL6/J genetic background. Mice were housed in a conventional animal facility at Hasselt University under standardized conditions (i.e., in a temperature-controlled room (20 6 3°C) on a 12 h light-dark schedule and with food and water ad libitum). All experiments were approved by the Hasselt University Ethics Committee and they were performed according to the guidelines described in Directive 2010/63/EU on the protection of animals used for scientific purposes.

C3-PMP22 animals were divided into two groups based on their baseline performances. The vehicle treated group received 0.1% DMSO (VWR prolab) diluted in 2% Tween80 (Merck) and 0.5% methyl cellulose (Sigma-Aldrich). The Gebr32a treated group received 0.3 mg/kg Gebr32a (University of Genova) dissolved in a final concentration of 0.1% DMSO and diluted in 2% Tween80 (Merck) and 0.5% methyl cellulose (Sigma-Aldrich). Treatment was administered twice a day via subcutaneous injections which lasted for a total of 10 weeks.

Two different animal cohorts were simultaneously treated and phenotypically characterized. Within the first cohort of animals treatment was initiated between 15-20 weeks of age and comprised both male and female littermates (WT control n=5; C3-PMP22 vehicle n=4; C3-PMP22 Gebr32a n=4). Within the second cohort, treatment was initiated between 30-35 weeks of age and solely comprised male littermates (WT control n=7; C3-PMP22 vehicle n=5; C3-PMP22 Gebr32a n=5).

Genotyping

Genotyping was conducted using digital droplet PCR (ddPCR) (see below) until heterozygous animals were identified, and then these mice were crossbred with wild-type (Wt) mice, resulting in either heterozygous or Wt offspring. The genotyping from these litters was done by standard PCR to distinguish between C3 mice and littermate Wt mice. For PCR analysis, genomic DNA was purified from a small section of mouse ear or tail by lysing the tissue overnight at 55 °C with proteinase K (20 mg/ml; Roche, Basel, Switzerland) in a lysis buffer composed of 0.2% SDS, 200 mM NaCl, 100 mM Tris–HCl (pH 8.5), and 5 mM EDTA. Samples were then centrifuged, and DNA was precipitated using isopropanol and pelleted by centrifugation. Pellets were subsequently washed in 75% ethanol and dissolved in Tris–EDTA buffer containing 0.1 mM EDTA and 10 mM Tris–HCl (pH 7.5). Primers used for genotyping were purchased from IDT solutions (Leuven, Belgium) (table 7.1).

PCR program cycle conditions were as follows: (1) 3 min at 94 °C, (2) 10 s at 94 °C, (3) 10 s at 53.8 °C, (4) 10 s at 72 °C, and (5) 5 min at 72 °C, and then the run was held at 15 °C until the plate was removed from the PCR thermal cycler. Steps 2–4 were set to a cycle of 30 times. The subsequent PCR product was ran on a 2% agarose gel, stained using SYBR Safe DNA Gel Stain (Thermo Fisher Scientific, Waltham, MA, USA) and visualized using a transilluminator (UVP Visi-Blue™ Transilluminator, Thermo Fisher Scientific).

Table 7.1 : Primer sequences for qPCR.

Gene	Species	Forward primer (5'-3')	Reverse primer (5'-3')
PMP22	*Mus musculus*	TGGTGATGAGAAACAGT	TGATTCTCTCTAGCAATGGA
IL	*Mus musculus*	CTAGGCCACAGAATTGAAAGATCT	GTAGGTGGAAATTCTAGCATCC

Motor phenotyping

All behavioral assessments were performed in a randomized order and scored blind.

Beam walk

Motor coordination was analyzed using beams with a width of 7, 12 or 18 mm, 1m long and 3 cm. Beams were suspended 1m above the ground with a black end goal box. Mice were allowed to traverse the beam and the time to cross the inner 80cm of the beam was measured. For each mouse, 3 successful runs were recorded. A successful run was defined as one continuous movement (no stopping or turning around).

Rotarod

An accelerating mouse-sized Rotarod (Ugo Basile, Italy) was used to evaluate evoked voluntary motor function. Four trials were performed using 4 – 40 RPM acceleration over the course of 5 min, with a minimum of 5 min rest between trials.

Grip strength tests

Forelimb grip strength was assessed using a grid connected to a LabQuest® Newton meter (Vernier, USA). As a mouse grasped the grid, the pull force was recorded by slowly pulling the animal backwards by the tail until it released grip. For each animal, 3 grip strength trials were conducted with a minimum of five minutes rest period between each trial and the average maximum pull force was determined.

Hanging wire

Mice were placed on a cage lid and turned upside down until approximately 10cm above the cage. The latency to fall was recorded with a maximal cutoff time of 2 min. For each mouse, 3 measurements were recorded with at least 5 min of rest between trials to avoid fatigue.

Grid walk

For the grid walk test, a grid walkway of 1m long (10 cm width) with a grid size of 2 cm x 2 cm was used. The grid walkway was suspended 1m above the ground with a black end goal box. A camera was mounted underneath, filming the inner 80 cm of the walkway. Each animal crossed the walkway 3 times. Recording were

analyzed to determine the number of foot slips. Foot slips were defined as a hind paw completely passing through the plane of the wire grid. The average number of foot slips was calculated for each mouse.

Pellet retrieval

The training protocol for evaluating forelimb dominance using the pellet retrieval test was modified from Chen et al. 2014 (463). Briefly, on the first day, mice were shaped by placing them individually inside the training chamber after which they were subsequently food-restricted. Next, animals gained access to food for 2h per day for the remainder of the training period. On the second day, mice were placed inside the training chamber with 10 pellets. From the third day onwards, forelimb dominance was determined as previously described (463). After forelimb dominance was determined for each animal, animals were scored on the final day as described previously (463). 30 attempts or 20 min (whichever came first) were recorded and scored (1, success; 2, dropped; 3, fail). From these data, the success rate was calculated per animal. After initial training, no re-training was needed. After treatment, mice were immediately scored in the same way as the final day of training.

Electrophysiology

Compound Muscle Action Potentials (CMAP) of the sciatic nerve were recorded using a NIM-Eclipse® System (Medtronic), following the protocol as described previously (464). Briefly, after anesthetizing the animal, the mouse is placed on a heating pad in the prone position. Stimulating electrodes are subsequently subcutaneously placed with a distance of approximately 1 cm on both sides of the sciatic notch. Next, the gastrocnemius muscle is located and the recording electrode is placed subcutaneously in alignment. The reference electrode is placed subcutaneously next to the Achilles tendon (30° angle) and the ground electrode is placed subcutaneously on the side of the mouse. Supramaximal stimulation was used to evoke the CMAPs (5-20 mA, up to 60 mA in demyelinating conditions).

Immunohistochemistry

At the end of the treatment, mice received an overdose of dolethal (200mg/kg) and were transcardially perfused with Ringer solution containing heparin, followed by 4% paraformaldehyde in PBS (pH 7.4). Sciatic nerves were dissected and post fixed for 24h in 4%PFA and 5% sucrose in PBS. Next, 10 µm thick frozen coronal tissue sections were cut via cryosectioning (Leica) and immunohistochemical stainings were performed. Briefly, nerve sections were air dryed and heat induced antigen retrieval was performed using sodium citrate buffer (10mM, pH 6.0). Sections were blocked with 100% protein block (DAKO) and incubated overnight with mouse-anti-β-tubulin (1:250, T8578 Sigma) and rat-anti-MBP (1:500, MAB386 Millipore) at 4°C in a humidified chamber. Following repeated washing steps with PBS, nerve sections were subsequently incubated with Alexa 488- or Alexa 555 conjugated secondary antibodies (1:600, Invitrogen). A DAPI (Life Technologies) counterstain was performed to reveal cellular nuclei whereafter sections were mounted. Images were taken with a Zeiss LSM880 confocal microscope. Quantitative image analysis was performed on original unmodified photos using the ImageJ open source software with which integrated densities were analysed for both β-tubulin and MBP.

Statistical analysis

All statistical analyses were performed using GraphPad Prism 9.4.1 software (GraphPad Software, Inc.). Data sets were analyzed for normal distribution using the Shapiro-Wilk normality test. Normally distributed data were analysed with an unpaired t-test between vehicle and Gebr32a treated C3-PMP22 mice. Not normally distributed data were statistically analysed using the nonparametric Mann-Whitney test. Data were presented as means ± SEM. Differences were considered statistically significant when $P \leq 0.05$ (*p≤0.05, **p≤0.01, ***p≤0.005, ****p≤0.001). Whereas no differences were observed between both animal cohorts in motor function evaluation or electrophysiological measurements, results were pooled to increase statistical power.

Results

Gebr32 significantly improves nerve conduction and the functional outcome in C3-PMP22 mice

To evaluate sciatic nerve functioning and myelination, electrical nerve conduction was evaluated using electrophysiological measurements. Upon proximal sciatic nerve stimulation, compound muscle action potentials (CMAPs), were recorded in the distal hind limb muscle tissue (**Fig 7.1A**). Axonal integrity was assessed by quantifying the amplitude of the measured CMAPs (**Fig 7.1B**), while the level of myelination was reflected by the nerve conduction speed or latency time of the CMAPs (**Fig 7.1C and 7.1D**). Although not demonstrating any significant differences in axonal functioning as reflected by the amplitude, Gebr32a treatment significantly reduced sciatic nerve conduction as reflected by the latency time (**Fig 7.1A-D**).

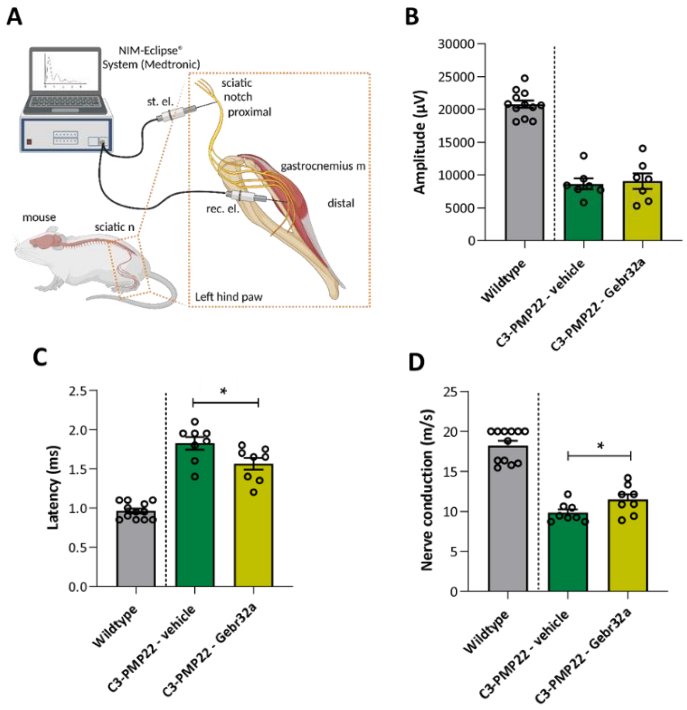

FIG 7.1: PDE4D inhibition by means of Gebr32a significantly improves electrophysiological outcome measurements. (**A**) Illustration compound motor action potential recordings (CMAPs) on the sciatic nerve of WT and C3-PMP22 mice. (**B**) The amplitude (as a measure for axonal functions) was comparable between treated and untreated C3-PMP22 mice. (**C, D**) The latency, and therefore also the nerve conduction speed, was significantly improved in Gebr32a treated C3-PMP22 mice, compared to untreated controls. (n≥7/group). Data were analysed using a non-parametric Mann-Whitney test (*p≤0.05).

Next, the therapeutic effect and clinical relevance of Gebr32a was assessed *in vivo* by performing multiple motor function evaluation tasks. Motoric phenotyping of the animals was conducted prior to initiating the treatment regimen, to randomize the different treatment groups, and repeated after ten weeks of treatment. Motor coordination was assessed using the beam walk test. C3-PMP22 animals took significantly longer to pass both a 12 mm and 7 mm wide beam compared to WT animals. However, upon Gebr32a treatment, C3-PMP22 mice were able to pass the 7 mm wide beam walk significantly faster (**Fig 7.2A**). Endurance, motor balance and evoked voluntary motor movement was assessed using the Rotarod. While WT animals were capable of staying significantly longer on the Rotarod, C3-PMP22 mice showed a reduced latency to fall. Even though not significantly ($p=0.06$), Gebr32a mediated PDE4D inhibition showed a trend to increase the latency to fall in C3-PMP22 animals (**Fig 7.2B**).

For assessing the grip strength, mice were subjected to the grip strength test and the hanging wire test. To prevent fatigue, a minimum of five minutes rest was implemented between each trial and three independent trials were conducted for each test. While forelimb grip strength is reduced upon CMT1A pathology, PDE4D inhibition by means of Gebr32a significantly increased grip strength in C3-PMP22 mice (**Fig 7.2C**). Additionally, the latency to fall in the hanging wire test was significantly increased upon Gebr32a treatment in C3-PMP22 animals (**Fig 7.2D**).

Motor coordination was subsequently further assessed using the grid walk test. After allowing the animals to transverse a wire grid, the number of hind paw slips through the grid were determined, which indicated an impaired sensorimotor function in C3-PMP22 animals. Upon Gebr32a treatment, C3-PMP22 mice displayed a reduced number of foot slips through the wire grid (**Fig 7.2E**).

Finally, forelimb dominance and coordination were evaluated using the pellet retrieval task. For each animal, 30 reaching attempts were recorded and the rate of successfully grabbing and feeding the pellet into the mouth was determined. While the C3-PMP22 genotype did affected forelimb coordination, as demonstrated by the significant lower success rate, Gebr32a treatment did not affected the pellet retrieval success rate (**Fig 7.2F**).

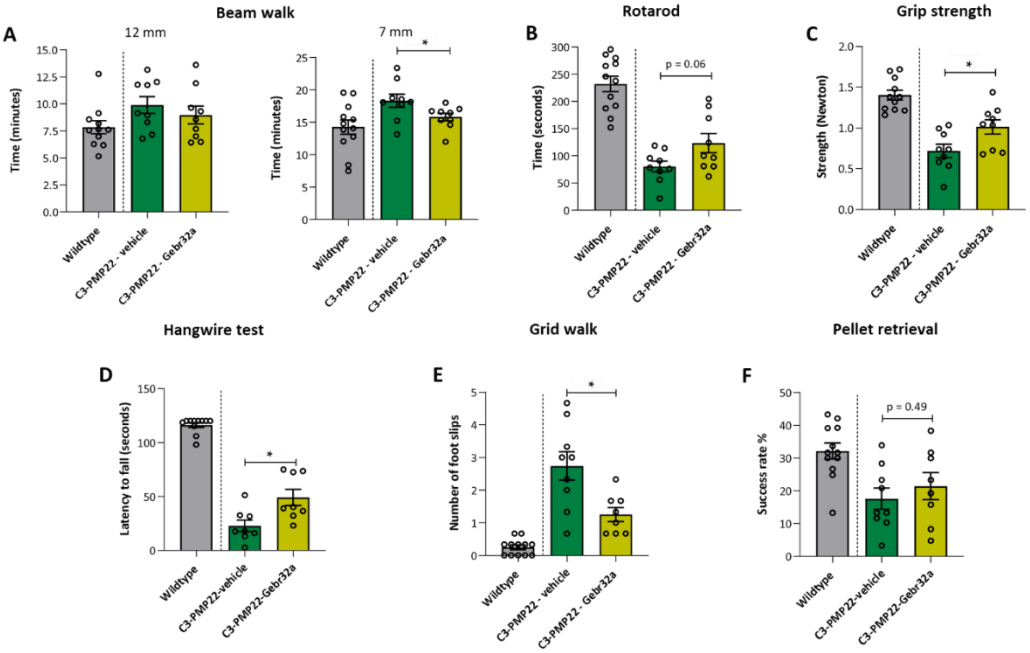

FIG 7.2: PDE4D inhibition by means of Gebr32a significantly enhances motor function. WT animals and C3-PMP22 animals either treated with a vehicle or the PDE4D inhibitor Gebr32a were motorically characterized. Gebr32a treatment demonstrates an increased (**A**) motor coordination as assessed using the beam walk, (**B**) rotarod evoked motor endurance, (**C-D**) grip strength, (**E**) sensorimotor functioning. (**F**) PDE4D inhibition by means of Gebr32a did, however, not alter pellet retrieval success rate. Data are presented as mean ± SEM (n≥7/group). Grip strength evaluation, rotarod performance, beam walk test and sciatic nerve amplitudes were analysed using a parametric unpaired t-test. The grid walk test, sciatic nerve latency and nerve conduction were evaluated using a non-parametric Mann-Whitney test (*p≤0.05).

Post mortem analysis reveals a myelination-promoting effect of Gebr32 in C3-PMP22 mice

As CMT1A disease affects Schwann cells and therefore the myelin amount, sciatic nerves were isolated at the end of the experiment to evaluate the amount of myelination. Nerve cross-sections were immunostained for the axonal marker β-tubulin and myelin marker MBP in order to confidently evaluate functional myelination surrounding axons (**Fig 7.3A-C**). While C3-PMP22 mice showed a lower level of both β-tubulin and MBP compared to WT mice, both protein levels were significantly increased upon Gebr32a-mediated PDE4D inhibition (**Fig 7.3A and 3B**).

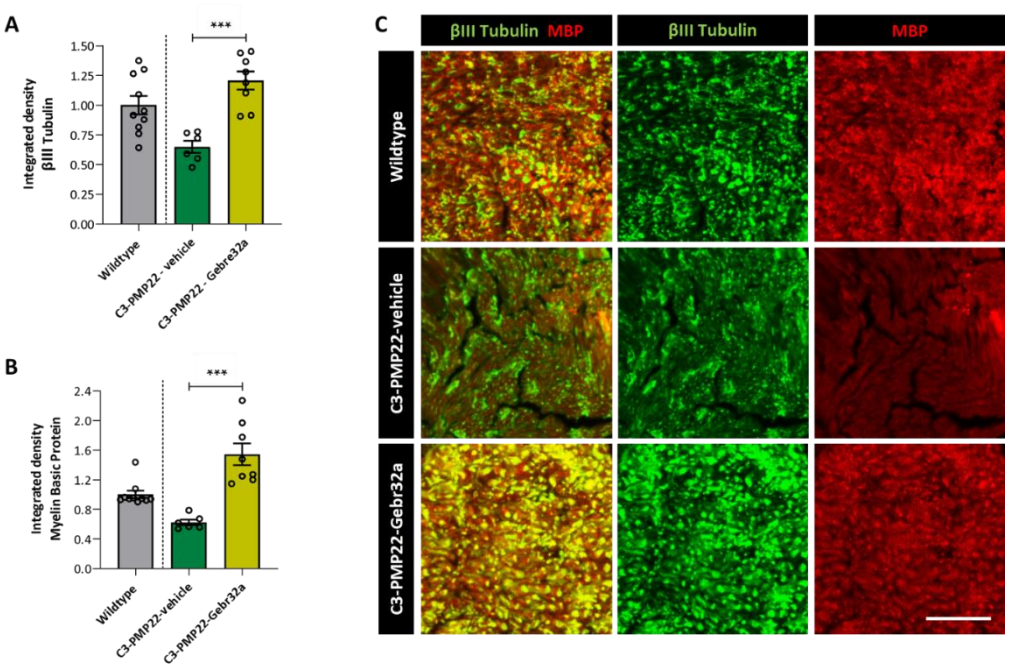

FIG 7.3: PDE4D inhibition by means of Gebr32a significantly increases β-tubulin and MBP levels in the sciatic nerve of C3-PMP22 animals. Sciatic nerves were isolated from all experimental animals at the end of the experiment and immunohistochemically analysed for their β-tubulin and MBP presence. PDE4D inhibition by means of Gebr32a significantly increased both (A) β tubulin and (B) MBP in the sciatic nerve of C3-PMP22 mice. (C) Representative images of the β-tubulin and MBP staining. Data are presented as mean ± SEM (n≥6/group). B-tubulin levels were analysed using a parametric t-test, while MBP levels were evaluated using a non-parametric Mann-Whitney test (***p≤0.005).

Discussion

The autosomal duplication of the *PMP22* gene in CMT1A results in a demyelinating peripheral neuropathy with clinical symptoms arising within the first two decades of life. The chronic demyelination throughout life leaves axons vulnerable ultimately leading to secondary neuroaxonal pathologies and neurodegeneration. However, no effective treatment exists restoring the CMT1A induced Schwann cell malformations and thereby myelination. Using the C3-PMP22 animal model for CMT1A, we demonstrated here that the PDE4D inhibitor Gebr32a significantly improved motor functioning demonstrated by an increased grip strength, motor coordination and sensorimotor functioning. Electrophysiological measurements revealed an enhanced sciatic nerve signal transduction following Gebr32a treatment, accompanied by an increase of myelination and β-tubulin levels. These data demonstrate the potential of PDE4D inhibition for restoring the CMT1A induced Schwann cell malformations, thereby highlighting its therapeutic potential for treating CMT1A pathology.

Developing (re)myelination therapies to correct the Schwann cell induced disease pathology has demonstrated to be a potent therapeutic strategy for treating CMT1A (460, 465-467). The full PDE4 inhibitor rolipram has previously been demonstrated to enhance myelination *in vivo* when administered simultaneously with transplanting Schwann cells following spinal cord injury (285, 468). Moreover, rolipram promoted oligodendrocyte differentiation and subsequently *in vivo* remyelination in an animal model for multiple sclerosis (118). In Schwann cells specifically, the PDE4 inhibitor roflumilast has shown to stimulate Schwann cell differentiation and roflumilast-treated Schwann cells additionally enhanced human iPSC-derived nociceptive axonal outgrowth (chapter 6). Unfortunately, PDE4 inhibition coincides with emetic adverse events hampering its clinical translation. Recently, the PDE4D subtype specific inhibitor Gebr32a has demonstrated to enhance CNS remyelination and oligodendrocyte differentiation similar to full PDE4 inhibition without preclinical indications of emetic side effects (chapter 3). Therefore, in this study, we investigated whether the PDE4D inhibitor Gebr32a could be a valuable therapeutic approach for correcting Schwann cell development in a C3-PMP22 mouse model for CMT1A.

To evaluate the therapeutic potential of the PDE4D inhibitor Gebr32a, we implemented several phenotypical motor function outcomes. We observed a disease induced phenotype in C3-PMP22 mice since their grip strength, muscle function, motor endurance on the rotarod, and motor coordination on the grid walk and beam walk were impaired compared to WT animals. However, motor function outcome could be significantly improved upon PDE4D inhibition. Gebr32a-mediated PDE4D inhibition significantly increased grip strength, motor coordination and evoked motor endurance. The only motoric task where a clear Gebr32a-mediated PDE4D inhibition effect was absent was the pellet retrieval task. While the pellet retrieval task allows researchers to evaluate fine motor movements from the forelimbs, it has also been demonstrated to highly rely on a motor-skill learning paradigm (463). Whereas the acquisition of a new motor skills with practice is categorized as motor learning, retention of the learn skills are considered motor memory (469). Forelimb training in rodents relies on functional and anatomical plasticity of peripheral nerve systems and the M1 motor cortex located in the CNS and the success of the pellet retrieval task indeed relies on an efficient learning phase preceding outcome evaluation (470-472). Therefore, in contrast to not learnable evoked motor behavior (e.g. hanging wire and grid walk), the pellet retrieval task not only evaluates motor behavior but rather evaluates the complex motor learning potential of the animals. The difference in underlying functional and anatomical structures involved potentially can explain the lack of efficacy of Gebr32a to improve pellet retrieval success rates.

Importantly, within this study, two animal cohorts, mainly differing in age were simultaneously treated and evaluated for functional outcome. Even though both cohorts differed 10-15 weeks of age when Gebr32a treatment was initiated, both cohorts responded in a similar way to treatment. Furthermore, the improved motor functions were accompanied by a reduced latency time of sciatic nerve stimulated CMAP measures, indicating an increased nerve conduction speed. The CMAP measurements were acquired using a minimally invasive electrophysiological measurement using subcutaneously place needle electrodes (464). To identify CMT neuropathies, it is recognized that supramaximal intensities are required potentially due to an increased electrical impedance present due to the endoneurial hypertrophic changes upon CMT pathogenesis (464, 473). Due to the high supramaximal intensities required for measuring CMAPs in demyelinating

neuropathies (up to 60 mA) compared to the supramaximal intensities used in WT animals (5-20 mA), we can conclude that PDE4D inhibition did not completely normalized sciatic nerve signal transduction. However the significantly improved nerve conduction observed here already correlated with enhanced motor functions, implicating that PDE4D inhibition can be considered as a powerful treatment strategy for improving CMT1A disease phenotype.

Post mortem analysis of the sciatic nerve revealed that PDE4D inhibition by means of Gebr32a was accompanied with an enhanced myelination in C3-PMP22 animals as higher levels of MBP were observed. Additionally, besides increased MBP levels, β-tubulin protein levels were found to be increased in the sciatic nerve of C3-PMP22 animals upon PDE4D inhibition. Beta tubulin III is a protein member specifically localized to neurons (474). Due to its correlation with neuronal differentiation, β-tubulin III has been implied to be crucially involved in peripheral axon regeneration (474-476). However, the observed increase in β-tubulin III in the sciatic nerve of C3-PMP22 animals here was somewhat unexpected as no differences were observed in the amplitude of the electrophysiological measurements. Further post mortem analysis, including transmission electron microscopy, is necessary to reveal and evaluate the myelin integrity in more detail upon PDE4D inhibition in C3-PMP22 mice.

Even though the exact underlying molecular mechanism remains to be elucidated, downstream key players within the cAMP signalling cascade have been described to be directly involved in Schwann cell functioning. Both the protein kinase A (PKA) and exchange protein activated by cAMP (EPAC) effector proteins were observed to directly increase the Krox-20 to c-Jun ratio in Schwann cells *in vitro*, thereby driving its differentiation and subsequent myelination, further supporting the role of modulating cAMP signalling to restore CMT1A induced Schwann cell malformation (431-433).

Taken together, our data demonstrate that pharmacological PDE4D inhibition by Gebr32a improves motor functioning in a C3-PMP22 mouse model for CMT1A. Furthermore, Gebr32a enhanced sciatic nerve conduction, which was accompanied by a corrected myelination pattern. The observed improved functional and molecular outcome upon Gebr32a-mediated PDE4D inhibition in an animal model for CMT1A disease highlights its potential as a new therapeutic strategy for CMT1A disease management.

Acknowledgements

TV, JP and MS have proprietary interest in selective PDE4D inhibitors for the treatment of demyelinating disorders.

This work was supported by FWO [Grant: 12G0817N and 1S57521N].

CHAPTER 8

General discussion

It has been suggested that PDE4 inhibitors can be used therapeutically in a range of disorders, as demonstrated preclinically, due to its role in controlling cAMP levels and intracellular signal transduction. However, adverse side effects (e.g. emesis) have significantly slowed down the clinical progress and translation of PDE4 inhibitors. In the current dissertation we now demonstrate that, by more precise targeting of PDE4 subtype or isoforms, adverse side effects can be overcome, while the therapeutic potential is retained or even improved.

PDE4 inhibitor induced emesis

There is still a lot of controversy about the exact underlying mechanism of PDE4 inhibitor mediated emetic side effects. Recently, it was suggested that a reduced gastric emptying in mice upon full PDE4 inhibition was due to concurrent inhibition of more than one single PDE4 subtype since selective ablation of any PDE4 subtype did not impair gastric emptying while full PDE4 inhibition did (128). Other studies have used pde4b- or pde4d-deficient mice to determine the specific contribution of distinct subtypes in the emetic response. In contrast to pde4b-deficient mice, pde4d-deficient mice showed signs of emetic side effects since their anesthesia time was reduced in the xylazine/ketamine induced anesthesia test, a surrogate marker for measuring emesis in rodents (129). Furthermore, the full PDE4 inhibitor PMNPQ (0.3 mg/kg) significantly reduced anesthesia time in both wild type and pde4b deficient mice but did not reduce anesthesia time further in pde4d-deficient mice, indicating a crucial role for PDE4D in PDE4 inhibition-mediated emetic side effects (129). In this study, we show for the first time the PDE4D isoform expression profile in laser-captured neurons of the human post-mortem area postrema. Our data show that especially long PDE4D isoforms are highly concentrated in area postrema neurons and hereby highlights the importance of selectivity towards the short PDE4D isoforms in order to minimally alter cAMP levels in the area postrema and thus avoid emetogenic effects of the inhibitors. In fact, the **PDE4 gene-specific inhibitors used in this dissertation showed no emetic side effects** up to 300-fold the therapeutic dose in the *in vivo* xylazine/ketamine anesthesia test, nor did they increase the action potential firing rate of mouse area postrema neurons assessed by path-clamp electrophysiology, indicating an underlying isoform preference of the PDE4D inhibitor Gebr32a. All together, these data already indicate a level of isoform

specificity in existing inhibitors, rendering the PDE4 subtype specific inhibitors used within this dissertation more clinically relevant (392).

PDE4 subtype specific inhibitors in the pathogenesis of MS

In our study, we identified that **PDE4D inhibition** is sufficient to stimulate OPC differentiation in primary OPCs, both on PLL coated substrates, as well as in the presence of the differentiation inhibiting glycoprotein fibronectin. Furthermore, we demonstrated that both primary murine OPCs and human iPSC-derived OPCs significantly increased their number and length of myelin sheaths surrounding electro-spun microfibers upon PDE4D inhibition indicating that enhanced OPC differentiation results in enhanced (re)myelination. In line with that, PDE4D inhibition increased the level of remyelination after LPC-induced demyelination in an *ex vivo* cerebellar brain slice model. Finally, using both the chronic EAE and cuprizone animal model of MS, we validate the *in vivo* myelination promoting properties of PDE4D inhibition as reflected by the increased MBP area (corpus callosum, dentate gyrus, spinal cord) and decreased G ratios (corpus callosum and optic nerve). Furthermore, spatial memory performances were improved and VEP latency times were decreased upon PDE4D inhibition, further supporting the remyelination-boosting capacity of PDE4D inhibition.

We are the first to show that PDE4D inhibition possess (re)myelination-promoting properties. Previous research related to cAMP signaling in oligodendrocytes was limited to the use of cAMP analogous (e.g. dibutyryl cAMP and 8-bromo cAMP) and pan PDE4 inhibitors (rolipram) on *in vitro* and *in vivo* oligodendroglial differentiation (118, 263). Furthermore, we demonstrated for the first time a clear difference in cell type specific isoform expression abundancies as especially short and super-short PDE4D isoforms were shown to be highly expressed in human MS lesion OPCs and to a lesser extent in myelinating oligodendrocytes isolated from the surrounding normal appearing white matter. As a next step, the biological relevance of the individual PDE4D isoforms on OPC differentiation was determined using CRISPR-Cas9 genetic editing. Transfection of primary mouse OPCs with gRNAs targeting either the short *pde4d1/2* or the super-short *pde4d6* isoform led to more MBP-positive oligodendrocytes within the transfected pool of cells, indicating that knockdown of one of the two isoforms is sufficient for boosting OPC differentiation. Importantly, no other *pde4d* isoform knockdown could significantly

affect the differentiation rate of primary transfected OPCs. These data provide an incentive for further developing PDE4D isoform specific inhibitors to even more selectively enhance remyelination.

In contrast to PDE4D inhibition, **PDE4B inhibition** significantly reduced neuroinflammation and coinciding memory deficits and neurological scores in the acute phase of the MOG_{35-55}-induced EAE model. We demonstrated that clinical improvement upon PDE4B inhibition was paralleled with a reduction in CNS-infiltrating inflammatory Th1 cells and inflammatory monocytes at EAE peak. Moreover, *pde4b*$^{-/-}$ bone marrow-transferred mice were gene dosage-dependent protected based on the neurological decline observed in EAE. The anti-inflammatory properties toward myeloid cells were further confirmed *in vitro* since PDE4B inhibition with A33 lowered phagocytic NO production and activation in murine phagocytes and human derived MDM.

The observed anti-inflammatory properties accompanied by PDE4B inhibition are not surprising since PDE4B inhibition has previously been held responsible for anti-inflammatory actions in other disease models (226, 229). Both inflammatory macrophage signaling and neutrophil recruitment was previously shown to be altered upon PDE4B inhibition (219, 384). Furthermore, even though activated T lymphocytes showed an increase in enzymatic PDE4A and PDE4D levels, and not PDE4B, PDE4B demonstrated to play an essential role in Th2 lymphocyte activation and dendritic cell recruitment *in vivo* (112, 192, 477). The exact effect of inhibiting PDE4B specifically to alter T lymphocyte responses or polarization remains to be further investigated. In our study, we observed a reduction in inflammatory Th1 cells in the CNS at EAE disease peak, however we have not investigated the direct role of inhibiting PDE4B using A33 in lymphocytes *in vitro*.

PDE4 subtype specific inhibitors in the pathogenesis of SCI

The PDE4 inhibitor roflumilast has previously been shown to induce recovery in a contusion SCI model via modulating phagocyte polarization (401). Furthermore, following a contusion mediated SCI in mice, PDE4B is acutely upregulated in the damaged spinal cord (226). These data, combined with the observed myelin regenerative effects of PDE4D inhibition and anti-inflammatory properties of PDE4B inhibition in the context of MS, highlights the therapeutic potential of PDE4 subtype specific inhibitors to treat SCI pathophysiology. In our study, the T-cut hemisection SCI mouse model was used which consists of a complete transection of the corticospinal tract by cutting the left and right dorsal funiculus, the dorsal horns and the ventral funiculus (478). Surprisingly, even though the T cut SCI model is accompanied by neuroinflammatory responses, **PDE4B inhibition** by A33 did not improve functional recovery. Furthermore, our histological analysis did not show an effect of A33 on the damaged area or glial scar formation. In contrast, Gebr32a mediated **PDE4D inhibition** improved functional recovery after SCI accompanied with a reduced lesion size, decreased demyelinated area, reduced number of apoptotic neurons, increased numbers of mature oligodendrocytes and enhanced 5-HT serotonergic neuroregeneration. Local factors at the injury site, including apoptotic cells, cytokines present in the micro-environment and cellular debris, skew the phenotypic properties of immune cells such as macrophages and microglia, towards a pro-inflammatory phenotype, which is reported to evoke secondary injury processes detrimental for neuronal survival and regeneration (66). Therefore, the observed neuroprotective actions observed upon PDE4D inhibition following SCI could be either via providing direct neuronal protection or by modulating the neuro-inflammatory responses, thereby indirectly providing neuroprotection. Although we cannot exclude any indirect neuroprotective effects of Gebr32a so far, we demonstrated here that the observed decrease in neuronal apoptosis can at least partially be attributed to direct neuronal protection. In both murine and human iPSC-derived neurons, Gebr32a treatment diminished neuronal cell death. Similarly, Gebr32a stabilized the human neurospheroid viability, which was accompanied with decreased apoptosis and increased neuronal differentiation. These data suggest that PDE4D inhibition directly affects the survival of neurons following SCI.

The unexpected finding that PDE4B inhibition does not improve either histopathological or functional outcome following SCI can be, among others, explained by the implemented treatment regimen within this study. The dose and treatment protocol used in this study is adapted and based on our findings within the EAE animal model of MS but are similar to previously conducted SCI studies with roflumilast (401). Previously, it has been shown already with PDE4 inhibitors that the treatment protocol and dose are important determinants of the beneficial therapeutic effect of the compound (409). Furthermore, preclinically, we have no signs that increasing the dose of A33 (up to 300 fold) is associated with (emetic) side effects, rendering a broad safe concentration range for *in vivo* dosing refinements. Another variable within this study is the type of SCI mouse model. While the abovementioned T-cut hemisection model has shown to be particular beneficial for the assessment of axonal regeneration and thereby regenerative medicine, the contusion model is characterized by a more profound neuroinflammatory process and axonal sparing and is the most common type of injury in human adults (70). The discrepancy in pathophysiology between the different types of SCI may reveal different therapeutic properties of the PDE4 gene specific inhibitors.

PDE4 subtype specific inhibitors in the pathogenesis of stroke

Nowadays, stroke treatment only includes recombinant tissue plasminogen activators and mechanical thrombectomy surgery (78). However, the narrow therapeutic window of the available treatment options limits their application potential, thereby highlights the need of novel therapeutic strategies for ischemic stroke. An underestimated player within stroke pathogenesis is the neuroinflammatory response. Following the ischemic stroke insult, resident microglia become activated in the penumbra while leukocytes, including monocytes, neutrophils and lymphocytes, are recruited to the lesion site (80). Therefore, due to the described anti-inflammatory properties of **PDE4B** subtype specific inhibition, a prophylactic proof of concept study was conducted with A33 to validate the potential of both PDE4 subtype specific inhibitors and interfering with the neuroinflammatory response for diminishing ischemic stroke pathophysiology. Within our study, we demonstrated that the prophylactic administration of the PDE4B inhibitor A33 reduces the infarct size while simultaneously decreasing the neuroinflammatory reaction 24 hours following

experimental dMCAO induced ischemic stroke. The observed decrease in neuroinflammation is attributed to a reduction in infiltrating neutrophils in the ipsilateral hemisphere, and an increase in M2 phenotype-like macrophages. In addition, PDE4B inhibition reduces neutrophil activation *in vitro*. Our results are in line with the previously described therapeutic potential of multiple PDE4 inhibitors for treating ischemic stroke. The majority of preclinical models, however, evaluated full PDE4 inhibitors such as roflumilast and rolipram in the transient MCAO (tMCAO) mouse model for ischemic stroke. From a clinical perspective, the dMCAO model used in this study represents the stroke patients that do not benefit from reperfusion therapies, while a transient ischemic stroke model rather represents the subset of stroke patients that benefit from reperfusion-based therapies including rtPAs and mechanical thrombectomy (425).

Our findings did not revealed any significant effects of **PDE4D** specific inhibition on ischemic stroke pathophysiology, neither *in vitro*, nor *in vivo*. However, a trend towards reduced lesion sizes upon Gebr32a following dMCAO surgery was observed. Based on the neuroactive properties of PDE4D inhibition, it remains possible that long term PDE4D inhibition would be therapeutically relevant for stimulating neuroregeneration and providing neuroprotection in the penumbra of the infarct, thereby reducing lesion size and promoting long term functional recovery following ischemic stroke (124, 281, 283, 429). This needs to be evaluated on future studies.

Important to note is the proof-of-principle nature of the *in vivo* experiment conducted within our study. Prophylactic PDE4B inhibition treatments are impossible to translate into a clinically interesting treatment regimen. However, our findings provide a mechanistic description of how PDE4B inhibitors are capable of diminishing or preventing neuroinflammatory insults in the context of ischemic stroke. Future follow-up studies focusing on the therapeutic potential of PDE4 subtype specific inhibitors will provide more insight into their clinical relevance.

PDE4 subtype specific inhibitors in the pathogenesis of peripheral nerve injury and CMT

With respect to PDE4 inhibitors and the nervous system, most reports to date have focused on CNS disorders, thereby overlooking the therapeutic potential of PDE4 inhibitors on PNS repair and neuropathies. In our studies, we demonstrated the therapeutic potential of the **PDE4 inhibitor** roflumilast in promoting Schwann cell differentiation into a myelinating phenotype, and additionally promoting axonal outgrowth of human iPSC-derived nociceptive neurons. These findings support the use of PDE4-inhibitor based treatment strategies for the treatment of peripheral demyelinating neuropathies and peripheral nerve injury. Furthermore, based on the CNS myelination promoting properties of **PDE4D specific inhibition**, we evaluated the therapeutic potential of the PDE4D inhibitor Gebr32a in an experimental model of the hereditary peripheral neuropathy CMT Type 1A (dysmyelinating form). Gebr32a-mediated PDE4D inhibition in a CMT1A animal model improved motoric functioning as reflected by an increased grip strength, motor coordination and sensorimotor functioning. Furthermore, sciatic nerve electrical conductance was improved as reflected by the decreased latency time upon sciatic nerve stimulation and subsequent CMAP analysis. The improved motoric functioning and electrical conductance was molecularly reflected by an increase in myelination of the sciatic nerve indicating the restoration of the molecular derangements causing the Schwann cell CMT1A phenotype.

Current research in the area of PNS repair has involved the creation of nerve guidance conduits pre-seeded with Schwann cells to enhance the neuroregenerative process (452). The results we obtained and discussed here, showing that roflumilast pre-treated Schwann cells are capable of stimulating human iPSC-derived nociceptive axonal outgrowth while simultaneously matching their myelination rate to the enhance outgrowth. These findings suggest that PDE4 inhibition could be applied *ex vivo* to Schwann cell-laden nerve guidance conduits to further prime there regenerative phenotype. Using this approach, systemic PDE4 inhibitor administration can be avoided, thereby circumventing potential PDE4 inhibition-mediated adverse events including emesis. Alternatively, selective PDE4 subtype inhibition could be considered to promote Schwann cell maturation *in vivo* since we demonstrated that the PDE4D inhibitor Gebr32a enhanced sciatic

nerve conduction and improved motor functioning in the Schwann cell neuropathy CMT1A at a non-emetic dose. Preliminary data indicate that this improved functional outcome is indeed attributed to a remyelination promoting effect of the PDE4D inhibitor since an enlarged MBP positive area was observed in the sciatic nerve upon treatment. However, these remyelination-promoting findings need to be confirmed using transmission electron microscopy by which g-ratios can be evaluated.

Taken together, within this dissertation, we have provided promising preclinical evidence for the effectiveness of specific PDE4B inhibition in an inflammatory animal model for MS, and as a prophylactic treatment strategy for combating ischemic stroke pathophysiology. Furthermore, inhibiting PDE4D can be considered a potent remyelination promoting therapeutic strategy for enhancing myelin regeneration in a demyelinating animal model for MS, enhancing myelin and neuroregeneration in a hemisection SCI model, and finally enhancing peripheral remyelination. Although unexpected, the absence of preclinical effectiveness of PDE4B inhibition for treating SCI, and PDE4D inhibition for enhancing neurorepair following ischemic stroke, might indicate a lack of effectiveness of the PDE4 gene specific inhibitors in the respective neurodegenerative disorders. Nevertheless, the lack of biologically significant results can be potentially explained by the experimental design (e.g. treatment regimen) as argued above.

Limitations and considerations

Preclinical work, and especially animal related work, unfortunately comes with some limitations. Neurodegenerative and demyelinating diseases rarely occur spontaneously in animals, making that researchers highly rely on genetically engineered or phenotype induced animal models. The predictive validity of animal models for humans has previously often been overestimated or misinterpreted. However, the predictive value of animal models can already be improved by a proper experimental design. By testing and validating findings in more than one experimental mouse model, external or predictive validity can highly be increased (479). More importantly, implementing relevant preclinical outcome measurements proven to be clinically relevant (e.g. VEP measurements) are recognized as a valid strategy to enhance translation to human disease (479).

Nevertheless, limitations of animal models in relation to PDE research still have to be acknowledged. The major drawback of clinical translation of PDE4 inhibitors is the evoked emetic response. Even though rodents are the most widely used and most extensively studied laboratory animal species, also in relation to the therapeutic evaluation of PDE4 inhibitors, they are unable to express an emetic response (480). Alternatively, surrogate marker tests have been developed, including the xylazine/ketamine anesthesia test, allowing researchers to assess emetic properties in rodents (365). The xylazine/ketamine anesthesia tests relies on the α2 adrenergic receptor agonism of xylazine leading to sedation. Interestingly, inhibition of the α2 receptor via α2 antagonism is involved in the initiation of the emetic response. Therefore, compounds, such as PDE4 inhibitors with α2 antagonistic properties will shorten the xylazine/ketamine-induced anesthesia time, thereby indicating an emetic potential of the evaluated compounds (481). In our study, we confirmed the previously described reduction in anesthesia time upon administration of the PDE4 inhibitor roflumilast, however, we did not observed any significant effect of the PDE4 subtype inhibitors A33 or Gebr32a up to 300 times their therapeutic dose. These results are indicative of their preclinical safety regarding emesis. Nevertheless, validation of the lack of an emetogenic reaction needs to be confirmed in higher level animal species such as ferrets.

Furthermore, a polymorphism has occurred within the PDE4D gene when comparing rodents to primates, rendering the expression of a tyrosine amino acid in rodents or a phenylalanine amino acid in primates within the regulatory UCR2 region (108). This difference in amino acid only occurs within PDE4D, distinguishing it from other primate PDE4 subtypes where the tyrosine amino acid remains present. The unique feature of phenylalanine presence in primate PDE4D has especially implications in the generation of PDE4D specific inhibitors since it can skew compound substrate specificity towards PDE4D (482). The PDE4D inhibitor used in this dissertation, Gebr32a, is a selective PDE4D inhibitor favoring PDE4D substrate binding over PDE4B as determined using human recombinant PDE4D isoforms (351). Structurally, the catecholic part of the Gebr32a molecule binds the catalytic domain of PDE4(D), leaving a protruding tail of Gebr32a which subsequently interacts with the regulatory domains UCR1 and UCR2 (392). Even though the selectivity of Gebr32a is not described to be dependent of the phenylalanine present in the UCR2, differences in selectivity magnitude between rodents and primates cannot be fully excluded. To cope with this, we confirmed the myelination promoting properties of the PDE4D inhibitor Gebr32a observed in primary mouse OPCs in human iPSC-derived OPCs. However, primate-based studies are required to fully evaluate the (re)myelination promoting potential of Gebr32a and its clinical relevance.

From a technical point of view, we implemented the challenging CRISPR/Cas9 technology to evaluate the effect of PDE4D isoform specific knockdown cultures as no PDE4D isoform specific inhibitors exist. The insertion/deletion repair mechanism was directed to occur in the isoform-specific N-terminus exons through specific guide RNA design, which was subsequently validated for its target specificity using BLAST. Based on the inDelphi algorithm, the type of mutation (e.g. number of base pairs inserted or deleted) was predicted which generated a non-sense coding frame shift mutation. Subsequently, the targeted isoform will not be expressed on a protein level. Unfortunately, in our study, the effectiveness and selectivity of the isoform knockdowns could not be assessed due to several reasons. Due to the lack of reliable, commercially available antibodies available, we were not able to measure the resulting PDE4D isoform protein amount following CRISPR/Cas9 mediated interference. On an mRNA level, detecting the generated insertion or deletion is unreliable since qPCR primers are not error proof

and might bind to the designed region even with a minor mismatch. Furthermore, the mRNA transcript and subsequent amplicon will be generated independent of the presence of a directed insertion or deletion mutation with the exception when the frame shift mutation leads to the transcription of a misplaced stop codon. Alternatively, single cell sorting based on the GFP tag present in the CRISPR/Cas9 plasmid and subsequent single cell sequencing would provide the most reliable validation of the CRISPR/Cas9 mediated mutation. In our study, we implemented several control measurements in order to guarantee a CRISPR/Cas9 mediated PDE4D isoform knockdown. As mentioned above, guide RNA design was validated for its target specificity using BLAST and the expected frameshift mutation frequencies following CRISPR/Cas9 mediated DNA cuts were predicted using the InDelphi algorithm. Furthermore, an unrestricted vector coding a scrambled guide RNA sequence was taken along and transfected, thereby providing a negative control and providing a control for the biological consequence of the transfection procedure. Finally, based on the PDE4D isoform expression profile generated in chapter 3 (human oligodendrolineage cells), we can expect that not all PDE4D isoforms are expressed in every cell type (e.g. PDE4D8 and PDE4D9 in OPCs). Nevertheless, we transfected CRISPR/Cas9 vectors encoding and targeting each PDE4D isoform separately, thereby including isoforms highly likely not leading to a biological action. In line, only the hypothesized PDE4D isoform knockdown of PDE4D1/2 or PDE4D6 led to an increase differentiation of OPCs and related MBP expression.

Regarding the effectiveness of the PDE4D isoform knockdowns, one might, correctly, argue that determining cAMP levels provides valuable information. However, due the dynamic nature of cAMP, determining its intracellular levels turns out to be technically challenging and time dependent. By means of a cAMP ELISA, we were able to validate the Gebr32a mediated increase in cAMP in a murine OPC cell line. For the CRISPR/Cas9 experiment, however, more high-end detection techniques would be required since PDE4D isoforms are part of specific intracellular nanodomains. Interfering within one specific PDE4D isoform would therefore cause very local nano-scaled cAMP alterations not necessarily reflected in the global intracellular cAMP levels measured using a cAMP ELISA. Currently, a lot of progress has been made regarding measuring cAMP changes on a nanoscale

level (e.g. nano-CUTie based FRET sensors) which will become indispensable for future PDE research (483).

Finally, whereas the research conducted within this dissertation focusses on preclinical animal models, it remains essential to further validate the observed biological effects in confirmatory studies. Preclinical animal models often comprise a controlled biological variance (in relation to age, sex, genetic background,..) and sustained environment in which experiments are being conducted. Therefore, generalization of preclinical findings regarding a heterogenous population remain difficult but crucial for having a societal impact.

Future opportunities

In this dissertation, we demonstrated that the neuroregenerative and anti-inflammatory properties of PDE4 inhibitors can be attributed to a PDE4D or PDE4B dependent process respectively. These findings opens new avenues for developing more targeted therapeutic strategies for treating different neurodegenerative and demyelinating disorders. Yet, although being able to specify which PDE4 subtype or isoform is responsible for a certain biological effect, which **downstream mechanism** is responsible for the observed therapeutically relevant processes remains unknown and rather speculative. Based on the literature, we know that multiple downstream effector proteins of cAMP signaling (e.g. protein kinase A (PKA) and exchange factor directly activated by cAMP (Epac)) are underlying the wide range of biological actions mediated by cAMP and therefore PDE signaling (12). Nevertheless, it remains poorly understood which exact signaling pathway is activated upon PDE4B or PDE4D inhibition in glia cells or neurons, rendering a scientific knowledge gap. Interestingly, it has recently been demonstrated that independent cell signaling units on the nanodomain scale exist comprising different PDE4D isoforms, causing cAMP concentration gradients throughout the cell, which are altered differently upon upstream signaling cues (13). Unravelling the underlying nanodomain signaling unit can therefore hold the key for understanding the distinct biological actions resulting from PDE4D inhibition, thereby bridging the knowledge gap and identifying new downstream druggable targets. Furthermore, based on the obtained PDE4D isoform expression profiles and the related biological consequences of these isoform distribution patterns, developing **PDE4D-isoform specific inhibitors** seem to be the next step for

increasing target specificity upon novel drug development. Yet unfortunately, due to the highly conserved regulatory and catalytic domains within PDE4D isoforms and between different genes, developing isoform-specific inhibitors has proven to be very difficult and pharmaceutically challenging. Currently, researchers in the field are developing and evaluating bifunctional protein degraders to accomplish targeted short isoform degradation. Even though these degraders target PDE4D short isoforms, they also degrade PDE4A, B and C short isoforms. Still, they provide a promising next step for developing more specific and potent PDE4 inhibitors. Taken together, the findings obtained within this dissertation open a door for developing new, more specific, more potent and clinically relevant PDE4 subtype based inhibitors for treating neurodegenerative and demyelinating disorders.

Summary

To allow proper nervous system functioning, glia cells must structurally and metabolically support electrical signal-conducting neurons. However, neurological disorders such as MS, SCI, stroke, and CMT disease severely impact nervous system functioning, leading to prominent disabilities. However, due to the limited regenerative potential of neurons, combined with the destructive micro-environment upon nervous tissue damage, endogenous repair mechanisms are limited in neurological disorders. Furthermore, despite recent progress being made in the development of new treatment strategies, no effective or curative treatment has been approved, capable of improving the patients quality of life. Therefore, the main aim of this dissertation is to evaluate the therapeutic potential of PDE4 subtype and isoform inhibition as a novel and more targeted approach to treat demyelinating and neurodegenerative disorders, while circumventing typical side effects seen upon on full PDE4 inhibition such as diarrhea, nausea and vomiting.

In the chronic demyelinating disorder MS, immune cell infiltration and subsequently neuroinflammation leads to focal demyelination and loss of myelinating oligodendrocytes. Once the inflammation is resolved, newly formed oligodendrocytes will regenerate myelin membranes, thereby remyelinating the nude axons. At later stages in the disease, remyelination becomes insufficient and less efficient, leading to prominent and persistent demyelination upon disease progression. Current treatment strategies for MS mainly include anti-inflammatory and immunosuppressive drugs. Unfortunately, even though currently available drugs are becoming more effective for treating the initial inflammatory phase of MS, disease progression cannot be halted, nor can repair be induced. As such, there is an urgent need for alternative treatment strategies capable of restoring the remyelination process, thereby inducing repair. Modulating second messenger (cAMP and cGMP) signaling has previously been demonstrated to control both inflammation and CNS repair. Therefore, in chapter 2, an overview is provided regarding the role of PDE inhibition in limiting pathological inflammation and stimulating repair in MS. Subsequently, chapter 3 addresses the therapeutic potential of specifically PDE4B and PDE4D inhibition in different (animal) models of MS. We demonstrated that the full PDE4 inhibitor roflumilast supports neuro-regenerative responses and suppresses neuroinflammation in both the cuprizone and EAE animal model of MS.

Importantly, we segregated the **myelination-promoting** role of PDE4 inhibition into a **PDE4D-dependent** process, while selective **PDE4B inhibition** accounted for the **anti-inflammatory effects**. A major drawback in translating PDE4 inhibitors towards clinical applications are the predicted emetic side effects. Importantly, we demonstrated that the subtype specific inhibitors A33 and Gebr32a used in this dissertation, did not showed preclinical signs of emetic-like behavior as determined via patch-clamp and the *in vivo* xylazine/ketamine anesthesia test. Nevertheless, since the predicted emetic side effects are ascribed to be related to *PDE4D* expression in the *area postrema* in the medulla oblongata, we additionally determined the *PDE4D* isoform expression profile specifically in neurons of the human *area postrema*. While short and super-short *PDE4D* isoforms are hardly expressed in the neurons, these isoforms are highly expressed in human OPCs isolated from human MS lesions. These findings render the (super) short PDE4D isoforms an interesting target to safely enhance remyelination.

Since attenuating neuroinflammation and initiating CNS repair are not processes limited and promising for the treatment of only MS, we further explored the therapeutic potential of PDE4 subtype specific inhibitors in other neurodegenerative disorders. Indeed, PDE4 inhibition has already yielded promising results in the context of SCI research due to its broad effects on different injury-related processes including neuroregeneration and immunomodulation. However, as mentioned above, the translation of full PDE4 inhibitors remains limited due to the dose-limiting emetic side effects, leading to poor tolerability in patients. Therefore, in chapter 4, we demonstrated that especially **PDE4D inhibition** by means of Gebr32a improved **functional recovery** after SCI. Comparable to the full PDE4 inhibitor roflumilast, Gebr32a-mediated PDE4D inhibition led to a reduced SCI lesion size, a reduced demyelinated area, decreased neuronal apoptosis, increased 5-HT serotonergic tract regeneration, and enhanced oligodendrocyte differentiation. Furthermore, using *in vitro* primary mouse neuronal cultures and human iPSC-derived neuronal precursor cell cultures, we demonstrated that the neuroprotective feature of PDE4D subtype inhibition can, at least partially, be attributed to a direct neuronal effect. Finally, using human iPSC-derived neurospheroids, we further demonstrated neuroprotection in a 3D culture model, which was accompanied with

increased neuronal differentiation, further supporting the use of the PDE4D inhibitor Gebr32a for the treatment of SCI.

Using a proof-of-concept study, the anti-inflammatory potential of PDE4B inhibition was further elucidated in chapter 5 in an animal model of ischemic stroke. By prophylactically administering the PDE4B inhibitor A33, cerebellar infarct size was significantly reduced 24 hours following experimental dMCAO induced ischemic stroke. The reduced lesion size could be attributed to a decreased neuroinflammation as a reduction in infiltrating neutrophils in the ipsilateral hemisphere, and an increase in $Arg1^+$ macrophages throughout the brain was observed. Furthermore, the immunomodulatory properties of PDE4B inhibition were highlighted *in vitro* since human neutrophil activation was significantly reduced upon PDE4B inhibition as demonstrated in a luminol-based ROS assay.

Finally, since demyelinating neurodegenerative disorders are not restricted to the CNS, we further explored the potential of PDE4 subtype inhibition to treat peripheral neuropathies. In the PNS, the myelin-producing glial support is provided by Schwann cells. Besides their myelinating properties, Schwann cells play a crucial role in nerve regeneration following PNS neuropathies as they secrete neurotrophic factors supportive of nerve repair. Interestingly, up to now, the direct effect of pan PDE4 inhibition or PDE4 subtype inhibition on Schwann cells has not been elucidated. In chapter 6, we therefore demonstrated for the first time that PDE4 inhibition, by means of roflumilast, promoted Schwann cell differentiation into a myelinating phenotype in both 2D and 3D culture models. Furthermore, roflumilast-treated Schwann cells promoted axonal outgrowth of human iPSC-derived nociceptive neurons while simultaneously enhancing their myelination capacity, thereby supporting the use of PDE4-inhibitor based treatment strategies for the treatment of peripheral demyelinating neuropathies. Finally, a hereditary peripheral neuropathy animal model for CMT1A disease was used in chapter 7 to evaluate the therapeutic potential of the PDE4D subtype inhibitor Gebr32a to stimulate peripheral remyelination. In line with the myelin regenerative properties observed in CNS pathologies, Gebr32a significantly enhanced sciatic nerve conduction in CMT1A animals, indicating improved myelination. Additional motor functioning phenotyping demonstrated improved motoric coordination, improved sensorimotor functions and increased grip

strength upon Gebr32a treatment in CMT1A animals. Finally, post mortem analysis confirmed a remyelination promoting effect of PDE4D inhibition by means of Gebr32a in the sciatic nerve of these animals, indicating the potential of PDE4D inhibition to functionally and molecularly enhance remyelination in the context of CMT1A pathology.

Taken together, the development of new and improved remyelinating enhancing and immunomodulatory therapies may prove beneficial for treating a wide range of neurodegenerative and demyelinating disorders including MS, SCI, stroke, peripheral nerve injury and CMT1A. In this dissertation, we provided an incentive for further developing PDE4 subtype specific inhibitors as a novel and clinically relevant drug-based strategy for treating both CNS and PNS related disorders.

Samenvatting

Zenuwcellen vertrouwen sterk op gliacellen om structurele en metabole steun te voorzien voor optimale signaaloverdracht. Echter gaan neurologische aandoeningen, zoals multiple sclerose (MS), een ruggenmergletsel, een beroerte en de ziekte van Charcot Marie Tooth (CMT) de werking van het zenuwstelsel sterk beïnvloeden, wat gaat leiden tot prominente beperkingen. De destructieve cellulaire omgeving die voorkomt bij deze neurodegeneratieve ziektes, samen met de niet-regeneratieve eigenschappen van zenuwcellen zelf, gaan het endogeen herstel van het zenuwstelsel beperken. Ondanks de recente vooruitgang bij het ontwikkelen van nieuwe behandelingsstrategieën voor deze neurodegeneratieve ziektes, is er nog steeds geen effectieve of curatieve behandeling beschikbaar die de levenskwaliteit van patiënten kan verbeteren. Het hoofddoel van de huidige dissertatie is dan ook om het therapeutische potentieel van PDE4-subtype- en -isovorminhibitie te evalueren als een nieuwe en gerichte aanpak om demyeliniserende en neurodegeneratieve aandoeningen te behandelen.

De infiltratie van immuuncellen, en de daaropvolgende ontstekingsreactie leidt in de chronische ziekte MS tot focale demyelinisatie en het verlies van myeliniserende oligodendrocyten. In de ontstane letsels zullen echter wel nieuw gevormde oligodendrocyten myelinemembranen regenereren, wat vervolgens zal leiden tot een proces genaamd remyelinisatie. Tijdens de progressie van de ziekte zal het remyelinisatieproces echter minder efficiënt en onvoldoende worden, hetgeen zal leiden tot prominente en aanhoudende demyelinisatie. Huidige behandelingsstrategieën voor MS omvatten voornamelijk ontstekingsremmende en immuunonderdrukkende medicijnen. Helaas kunnen zelfs de huidig beschikbare medicijnen de progressie van de ziekte niet afremmen, noch herstel bewerkstelligen. Er is dus een nood aan nieuwe en verbeterde ontstekingsremmende behandelingen die de ontstekingsreactie tijdens vroege stadia van de ziekte verminderen, terwijl regeneratieve therapieën dringend nodig zijn om het remyelinatieproces te herstellen en daarbij herstel te bewerkstelligen. Modulatie van de "second messenger" signalisatiecascades (cAMP en cGMP) werd reeds in het verleden aangetoond om zowel ontstekingsreacties als herstelprocessen in het centrale zenuwstelsel te controleren. Daarom biedt hoofdstuk 2 een overzicht van de rol van PDE-inhibitie bij het beperken van de pathologische ontstekingsreacties en het stimuleren van herstelprocessen bij MS. Vervolgens behandelt hoofdstuk 3 het therapeutische potentieel van specifieke

PDE4B- en PDE4D-inhibitie in verschillende diermodellen van MS. Wij hebben kunnen aantonen dat de volledige PDE4-remmer roflumilast zowel neuroregeneratie ondersteunt als ontstekingsreacties onderdrukt in zowel het cuprizone als EAE- diermodel voor MS. Belangrijk is dat we de myeliniserende rol van PDE4-inhibitie hebben kunnen terugleiden tot een PDE4D-afhankelijk proces, terwijl selectieve PDE4B-inhibitie verantwoordelijk was voor de anti-inflammatoire effecten. Een groot nadeel bij het vertalen van PDE4-remmers naar een klinische toepassing zijn echter de voorspelde emetische bijwerkingen (bijvoorbeeld misselijkheid en overgeven). Daarom hebben wij vervolgens via patch-clamp experimenten en de xylazine/ketamine anesthesie test in muizen aangetoond dat de subtypespecifieke PDE4B- en PDE4D-remmers A33 en Gebr32a die gebruikt werden in deze dissertatie geen preklinische tekenen vertonen van emetische bijwerkingen. Aangezien de voorspelde emetische bijwerkingen worden toegeschreven aan PDE4D-expressie in het area postrema in de hersenstam hebben wij bijkomend het PDE4D-isovorm expressieprofiel specifiek in neuronen van het menselijke area postrema bepaald. Terwijl korte en superkorte PDE4D-isovormen nauwelijks tot expressie komen in neuronen, zijn deze isovormen zeer aanwezig in humane oligodendrocytprecursorcellen (OPC's) afkomstig uit MS-letsels. Deze bevindingen maken de (super-)korte PDE4D-isovormen een interessant doelwit om remyelinatie veilig te versterken in MS.

Aangezien het onderdrukken van ontstekingsreacties in het zenuwstelsel en het initiëren van neuronaal herstel niet enkel kan toegepast worden voor voor de behandeling van MS, hebben wij verder het therapeutisch potentieel van specifieke PDE4-subtyperemmers onderzocht in andere neurodegeneratieve aandoeningen. Vanwege zijn vele beschreven herstelinducerende en ontstekingsremmende eigenschappen, heeft PDE4-inhibitie veelbelovende resultaten opgeleverd in het onderzoek naar ruggenmergletsels. Maar zoals hierboven vermeld, blijft de vertaling van volledige PDE4- remmers naar een klinische toepassing beperkt vanwege zijn dosisafhankelijke emetische bijwerkingen. In hoofdstuk 4 hebben we aangetoond dat vooral PDE4D-inhibitie door middel van Gebr32a functioneel herstel na een ruggenmergletsel verbeterde. Net als de volledige PDE4-remmer roflumilast leidde Gebr32a-gemedieerde PDE4D-inhibitie tot een kleinere letselgrootte, een verminderde gedemyeliniseerde regio, minder apoptotische neuronen, meer regeneratie van 5-

HT serotonergische zenuwbundels en een verbeterde oligodendrocytdifferentiatie. Verder hebben wij door middel van primaire muis celculturen en humane iPSC-afgeleide neuronale precursorculturen aangetoond dat de neuroprotectieve eigenschappen van PDE4D-subtype-inhibitie ten minste gedeeltelijk toegeschreven kunnen worden aan een direct neuronaal effect. Tenslotte hebben wij met behulp van humane iPSC-afgeleide neurosferen verder kunnen aantonen dat PDE4D-subtype-inhibitie zorgt voor neuroprotectief effect in een 3D-model, wat gepaard gaat met meer neuronale differentiatie, hetgeen verder het gebruik van de PDE4D-specifieke remmer Gebr32a ondersteunt voor de behandeling van een ruggenmergletsel.

Met een "proof-of-concept" studie in een diermodel voor ischemische beroerte werd het anti-inflammatoire potentieel van PDE4B-subtype-inhibitie geëvalueerd in hoofdstuk 5. Door de PDE4B-remmer A33 profylactisch toe te dienen, werd de cerebellaire infarctgrootte significant gereduceerd na experimentele dMCAO-geïnduceerde ischemische beroerte. De vermindering in letselgrootte kon worden toegeschreven aan een afname van de ontstekingsreactie, aangezien een afname van de infiltratie van neutrofielen in de ipsilaterale hersenhelft en een toename van M2-fenotype-achtige macrofagen in de hersenen werd waargenomen. Bovendien werden de immunomodulerende eigenschappen van PDE4B-inhibitie verder benadrukt *in vitro*, aangezien menselijke neutrofielactivatie significant verminderde na PDE4B-inhibitie, zoals aangetoond met een luminol-gebaseerde ROS-test.

Tenslotte, aangezien neurodegeneratieve en demyeliniserende ziektes niet enkel voorkomen in het centrale zenuwstelsel, hebben we verder het potentieel van PDE4- en PDE4-subtype-inhibitie onderzocht om perifere neuropathieën te behandelen. In het perifere zenuwstelsel (PZS) bieden de myelineproducerende Schwanncellen gliale ondersteunen aan de zenuwcellen. Maar naast hun myeliniserende eigenschappen spelen Schwanncellen ook een cruciale rol bij zenuwregeneratie bij PZS-neuropathieën door middel van de secretie van neurotrofische factoren. Opvallend is dat, tot nu toe, de directe effecten van PDE4- of PDE4-subtype-inhibitie bij Schwanncellen nog niet werden onderzocht. In hoofdstuk 6 hebben we daarom voor het eerst aangetoond dat PDE4-inhibitie door middel van roflumilast de differentiatie van Schwanncellen tot een myeliniserend fenotype stimuleert in zowel 2D- als 3D-celcultuurmodellen. Bovendien

bevorderen roflumilast behandelde Schwanncellen de axonale uitgroei van humane iPSC-afgeleide nociceptieve neuronen terwijl ze simultaan hun myeliniserende capaciteit verhoogden, hetgeen ondersteuning biedt voor het gebruik van PDE4- remmers voor de behandeling van perifere neuropathieën. Vervolgens, in hoofdstuk 7, werd een diermodel voor de erfelijke perifere neuropathie CMT1A gebruikt om het therapeutische potentieel van de PDE4D-subtyperemmer Gebr32a verder te evalueren. In lijn met de waargenomen myelineregeneratieve eigenschappen in het centrale zenuwstelsel verhoogde Gebr32a de zenuwgeleiding significant in een CMT1A-dieren, hetgeen wijst op een functionele en verbeterde myelinisatie. Verdere karakterisering van motorische functie toonde een verbeterde motorische coördinatie, grijpsterkte en sensorimotorische functies aan. De *post mortem* analyse bevestigde het remyelinisatiebevorderend effect van PDE4D-inhibitie in de *nervus ischiadicus*, hetgeen het potentieel van PDE4D-remming aangeeft om functioneel en moleculair herstel te bevorderen in kader van de CMT1A-pathologie.

Samengevat kan de ontwikkeling van nieuwe en verbeterde remyelinisatiebevorderende en immunomodulerende therapieën van groot belang zijn voor de behandeling van een breed scala aan neurodegeneratieve en demyeliniserende aandoeningen, waaronder MS, ruggenmergletsel, beroerte, perifere zenuwbeschadiging en CMT1A. In deze dissertatie tonen we dan ook voor het eerst aan dat PDE4-subtypes nieuwe en klinisch relevante doelwitten kunnen zijn voor de verdere ontwikkeling van nieuwe therapieën bij de behandeling van zowel centrale als perifere zenuwstelselaandoeningen.

Impact

Societal impact

One of the major hurdles regarding the treatment of neurodegenerative and demyelinating disorders, is the impairment of endogenous recovery and repair processes in these diseases. Chronic neuroinflammation, persistent demyelination and nutrient deprivation leaves neurons vulnerable, ultimately leaving to neurodegeneration. Unfortunately, current treatment strategies are insufficient in providing long term neuroprotection and -repair. Hence, there is an urgent medical need for efficient therapeutic strategies capable of supporting glial cell functioning, thereby allowing neuroreparative processes to occur.

Target group - MS patients

MS is the most common neurodegenerative disease in young adolescents and affects 1 in 1000 people in Belgium and over 2.5 million people worldwide (600 000 in Europe). Globally, over 1 million patients suffer in particular from secondary PMS. Currently, the treatment of MS patients comprises the administration of immunomodulatory and immunosuppressive drugs. The disease-modifying therapies either decrease relapse rate or reduced relapse severity by dampening the immune response. Unfortunately, these drugs are only partly effective in RRMS patients as they target the overreactive immune response and are unable to halt or reverse disease progression. Therefore, more efficient anti-inflammatory treatments or remyelinating therapies are highly needed. In Belgium, the first line treatment includes dimethyl fumarate, teriflunomide, glatiramer acetate and interferon-β (47-50). When the first line drugs are ineffective at reducing clinical symptoms, second line treatment like fingolimod, cladribine, ocrelizumab or natalizumab are initiated (51-53). Compared to the first line treatment, second line treatment strategies are often more effective but are accompanied with a higher risk of adverse events. Even though all disease modifying treatments are currently approved for treating RRMS patients, only ocrelizumab has been approved for treating progressive MS patients (53). The average yearly costs for therapeutic management of a MS patient is estimated at €37.948, which increases up to €63.047 with progressive severity of MS. This constitutes 1.8% of the total economic costs for brain disorders. These numbers would translate in a yearly health cost of €350 million for pMS patients in Belgium.

Target group - SCI patients

Yearly, 250.000 to 500.00 people worldwide suffer from **SCI**. A SCI can be either traumatic (e.g. falls, violent crimes or vehicle accidents) or non-traumatic (e.g. infection or tumor) in nature and mainly affect young males although with the increase in activity more and more elderly are also at risk (57). Current treatment strategies nowadays include surgical intervention to stabilize and decompress the spinal cord to limit additional damage, physical rehabilitation and corticosteroid drug administration (e.g. methylprednisolone) to temper secondary injury responses (57, 484-486). However, long term perspective and recovery is limited as no regenerative and therefore curative treatment exists for managing SCI, rendering the yearly cost of SCI care management to be around €35.000 yearly per patient in Belgium.

Target group - stroke patients

Globally, **stroke** is the second highest cause of disability and death. Stroke can be broadly classified into hemorrhagic and ischemic stroke. While hemorrhagic stroke is caused by a bleeding in the brain, ischemic stroke, which account for about 71% of all strokes, is caused by a blockage of blood flow to the brain (75). Approximately 1 out of 4 adults are estimated to experience a stroke throughout their lifespan rendering a total of over 80 million stroke survivors globally. For ischemic stroke specifically, 9.8 million people globally are affected per year leading to over 2.7 million deaths yearly (82, 83). Nowadays, the status of stroke treatment only includes recombinant tissue plasminogen activators (rtPAs) and mechanical thrombectomy surgery to treat the acute phase (78). However, the narrow therapeutic window (within 4.5 hours following stroke onset for rtPAs and 6-24 hours for endovascular thrombectomy) limits the application potential of the current treatment strategies, highlighting the importance of investigating novel therapeutic strategies for ischemic stroke (78, 85-87). The lifetime costs per person are averaged to be over €38.700 for ischemic stroke management in Belgium and account for 45% of acute-care costs, 20% of nursing home costs and aggregated lifetime costs and 35% for long-term ambulatory care (487, 488).

Target group - peripheral nerve injury and CMT patients

In the PNS, **peripheral nerve injuries** caused by trauma are estimated to have a worldwide prevalence of 13 to 23 in 1.000.000 people (489). The core strategy for treating peripheral nerve injuries include surgical coaptation of nerve ends with or without nerve grafts or nerve transfers. However, still 50% of patients do not benefit from surgical nerve reconstruction leaving them with a dysfunctional nerve function (93). Combining socio-economical costs with patient treatment costs renders the lifetime socio-economic burden of peripheral nerve injuries over €45.000 (490). A second peripheral neuropathy is **CMT**. CMT is the most common hereditary motor and sensory neuropathy of the PNS and has an estimated worldwide prevalence of 1 in 2500 (94). Currently, treatment strategy mainly include symptom management by physiotherapy and controlling neuropathic muscle and joint pain using non-steroidal anti-inflammatory drugs or tricyclic antidepressants (101). Rarely, surgery is required to correct CMT induced deformities. However, no effective treatments have been developed for CMT patients. The total annual costs of management CMT are estimated to be around €20.000 yearly per patient (based on results from Germany) (491).

Taken together, even though significant progress has been made in the field of many neurodegenerative disorders, as of to date, no effective treatments have been developed yet. Therefore, developing a **new drug-based therapy** capable of supporting glia functioning, thereby inducing neuroreparative processes would dramatically reduce the emotional and socio-economic burden for patients, caretakers and government.

PDE4 (gene) inhibition to treat neurodegenerative and demyelinating disorders

The full PDE4 inhibitor roflumilast, targeting all PDE4 subtypes and isoforms, is currently FDA-approved and marketed for treating chronic obstructive pulmonary disease (COPD) patients. However, 25% to 30% of the patients treated with roflumilast experience side effects and often need to stop their treatment (492). Roflumilast drug-repurposing for treating neuro-inflammatory and neurodegenerative disorders is therefore not possible due to the high drug concentration required for sufficient CNS penetration, which is accompanied with even more severe dose-limiting toxicities including emesis. Recently, a phase II double-blinded clinical trial with the small molecule ibudilast, which inhibits PDE4

as well as PDE10, toll-like-receptor-4 (TLR4) and the macrophage migration factor (MIF), was conducted to evaluate its activity and safety in PMS (SPRINT-MS) and ALS patients (COMBAT-ALS) (340, 493). The SPRINT-MS study preliminary reported that the rate of brain atrophy was significantly slowed down by 48% in PMS patients treated with ibudilast. Although generally well tolerated, patients treated with ibudilast did report a higher incidence of gastrointestinal disorders (304, 340). Unravelling more specific players within this therapeutic cascade can therefore hold the key for safely modulating CNS-related processes. In line, **within this dissertation**, we demonstrate that PDE4 gene specific inhibition possesses potent therapeutic potential for treating neurodegenerative and demyelinating disorders without having pre-clinical indications of emesis related side effects. By attenuating neuroinflammation, PDE4B specific inhibition diminished neuroinflammatory insults in an animal model for MS. In line, prophylactic PDE4B inhibition reduced neutrophil activation in an animal model for ischemic stroke. Furthermore, PDE4D specific inhibition stimulates myelin and neuronal regeneration in an animal model for MS, demyelinating CNS disorders , spinal cord injury and peripheral neuropathies. These findings paved the way towards multiple patents on both the use of selective PDE4D inhibitors against demyelinating diseases and the composition of matter for the development of such selective PDE4D inhibitors (EP18165843.6 PCT/EP2019/05495 WO 2019/193091 and EP21177320.5). Furthermore, our pending patents are underlying the setup of a drug platform for PDE4D inhibitors as **spin off finality** to translate the preclinical findings into a clinical application for a variety of neurodegenerative diseases. However, due to the preclinical nature of the studies conducted within this dissertation, it remains highly essential to validate and generalize the observed biological effects in other confirmatory studies.

Scientific impact

Over the past years, PDE4 research is often kept fundamental in nature due to the described side effects accompanied by full PDE4 inhibition. However, the new concept introduced here that inhibiting PDE4 subtypes (PDE4B or PDE4D specific inhibition) and even isoforms can outperform the therapeutic properties of pan PDE4 inhibitors while being tolerable, opens new perspectives for past and future research. Diminishing neuroinflammation by inhibiting PDE4B or stimulating neuronal and myelin regeneration are not only crucial for treating MS, SCI, stroke and peripheral neuropathies but can be therapeutically valuable for other neurodegenerative and demyelinating research fields (e.g. leukodystrophies and amyotrophic lateral sclerosis). Therefore, the data obtained within this dissertation can lead to long term novel research projects investigating the therapeutic potential of PDE4 gene specific inhibitors in other disease domains. Furthermore, we are the first to show the PDE4D isoform expression profile in human area postrema derived neurons. This information is highly valuable for designing and the clinical development of next generation PDE4D inhibitors with distinct isoform specificity to circumvent gastro-intestinal side effects. Finally, on a technical level, we successfully demonstrated the myelination potential of human iPSC-derived OPCs, by implementing the microfiber myelination assay, in which remyelinating drugs can be functionally evaluated, which is of added value to both the scientific and industrial community active in the field of remyelination

Taken together, the methodology implemented in this dissertation combined with the scientific findings will ultimately lead to an academic and societal breakthrough.

Reference list

1. Lago-Baldaia I, Fernandes VM, Ackerman SD. More Than Mortar: Glia as Architects of Nervous System Development and Disease. Front Cell Dev Biol. 2020;8:611269.
2. von Bartheld CS, Bahney J, Herculano-Houzel S. The search for true numbers of neurons and glial cells in the human brain: A review of 150 years of cell counting. J Comp Neurol. 2016;524(18):3865-95.
3. Ludwig PE, Reddy V, Varacallo M. Neuroanatomy, Neurons. StatPearls. Treasure Island (FL)2022.
4. Steward MM, Sridhar A, Meyer JS. Neural regeneration. Curr Top Microbiol Immunol. 2013;367:163-91.
5. Akassoglou K, Merlini M, Rafalski VA, Real R, Liang L, Jin Y, et al. In Vivo Imaging of CNS Injury and Disease. J Neurosci. 2017;37(45):10808-16.
6. Canty AJ, Huang L, Jackson JS, Little GE, Knott G, Maco B, et al. In-vivo single neuron axotomy triggers axon regeneration to restore synaptic density in specific cortical circuits. Nat Commun. 2013;4:2038.
7. Huebner EA, Strittmatter SM. Axon regeneration in the peripheral and central nervous systems. Results Probl Cell Differ. 2009;48:339-51.
8. Cooke P, Janowitz H, Dougherty SE. Neuronal Redevelopment and the Regeneration of Neuromodulatory Axons in the Adult Mammalian Central Nervous System. Front Cell Neurosci. 2022;16:872501.
9. Ginhoux F, Prinz M. Origin of microglia: current concepts and past controversies. Cold Spring Harb Perspect Biol. 2015;7(8):a020537.
10. Goldmann T, Prinz M. Role of microglia in CNS autoimmunity. Clin Dev Immunol. 2013;2013:208093.
11. Lehnardt S. Innate immunity and neuroinflammation in the CNS: the role of microglia in Toll-like receptor-mediated neuronal injury. Glia. 2010;58(3):253-63.
12. Nimmerjahn A, Kirchhoff F, Helmchen F. Resting microglial cells are highly dynamic surveillants of brain parenchyma in vivo. Science. 2005;308(5726):1314-8.
13. Tang Y, Le W. Differential Roles of M1 and M2 Microglia in Neurodegenerative Diseases. Mol Neurobiol. 2016;53(2):1181-94.
14. Wendimu MY, Hooks SB. Microglia Phenotypes in Aging and Neurodegenerative Diseases. Cells. 2022;11(13).
15. Hughes V. Microglia: The constant gardeners. Nature. 2012;485(7400):570-2.
16. Blank T, Prinz M. Microglia as modulators of cognition and neuropsychiatric disorders. Glia. 2013;61(1):62-70.
17. Askew K, Li K, Olmos-Alonso A, Garcia-Moreno F, Liang Y, Richardson P, et al. Coupled Proliferation and Apoptosis Maintain the Rapid Turnover of Microglia in the Adult Brain. Cell Rep. 2017;18(2):391-405.
18. Dong Y, Benveniste EN. Immune function of astrocytes. Glia. 2001;36(2):180-90.
19. Gallo V, Deneen B. Glial development: the crossroads of regeneration and repair in the CNS. Neuron. 2014;83(2):283-308.

20. Nave KA. Myelination and the trophic support of long axons. Nat Rev Neurosci. 2010;11(4):275-83.
21. Simons M, Nave KA. Oligodendrocytes: Myelination and Axonal Support. Cold Spring Harb Perspect Biol. 2015;8(1):a020479.
22. Graca DL, Bondan EF, Pereira LA, Fernandes CG, Maiorka PC. Behaviour of oligodendrocytes and Schwann cells in an experimental model of toxic demyelination of the central nervous system. Arq Neuropsiquiatr. 2001;59(2-B):358-61.
23. Menn B, Garcia-Verdugo JM, Yaschine C, Gonzalez-Perez O, Rowitch D, Alvarez-Buylla A. Origin of oligodendrocytes in the subventricular zone of the adult brain. J Neurosci. 2006;26(30):7907-18.
24. Aguirre A, Dupree JL, Mangin JM, Gallo V. A functional role for EGFR signaling in myelination and remyelination. Nat Neurosci. 2007;10(8):990-1002.
25. Franklin RJ. Why does remyelination fail in multiple sclerosis? Nat Rev Neurosci. 2002;3(9):705-14.
26. Chen ZL, Yu WM, Strickland S. Peripheral regeneration. Annu Rev Neurosci. 2007;30:209-33.
27. Jessen KR, Mirsky R, Lloyd AC. Schwann Cells: Development and Role in Nerve Repair. Cold Spring Harb Perspect Biol. 2015;7(7):a020487.
28. Arthur-Farraj PJ, Latouche M, Wilton DK, Quintes S, Chabrol E, Banerjee A, et al. c-Jun reprograms Schwann cells of injured nerves to generate a repair cell essential for regeneration. Neuron. 2012;75(4):633-47.
29. Compston A, Coles A. Multiple sclerosis. Lancet. 2008;372(9648):1502-17.
30. Lucchinetti CF, Bruck W, Rodriguez M, Lassmann H. Distinct patterns of multiple sclerosis pathology indicates heterogeneity on pathogenesis. Brain Pathol. 1996;6(3):259-74.
31. Wucherpfennig KW, Newcombe J, Li H, Keddy C, Cuzner ML, Hafler DA. T cell receptor V alpha-V beta repertoire and cytokine gene expression in active multiple sclerosis lesions. J Exp Med. 1992;175(4):993-1002.
32. Prineas JW, Wright RG. Macrophages, lymphocytes, and plasma cells in the perivascular compartment in chronic multiple sclerosis. Lab Invest. 1978;38(4):409-21.
33. Hedley ML. Gene therapy of chronic inflammatory disease. Adv Drug Deliv Rev. 2000;44(2-3):195-207.
34. Hopkins SJ, Rothwell NJ. Cytokines and the nervous system. I: Expression and recognition. Trends Neurosci. 1995;18(2):83-8.
35. Weiner HL. The challenge of multiple sclerosis: how do we cure a chronic heterogeneous disease? Ann Neurol. 2009;65(3):239-48.
36. Zawadzka M, Rivers LE, Fancy SP, Zhao C, Tripathi R, Jamen F, et al. CNS-resident glial progenitor/stem cells produce Schwann cells as well as oligodendrocytes during repair of CNS demyelination. Cell Stem Cell. 2010;6(6):578-90.
37. Kotter MR, Stadelmann C, Hartung HP. Enhancing remyelination in disease--can we wrap it up? Brain. 2011;134(Pt 7):1882-900.

38. Kuhlmann T, Miron V, Cui Q, Wegner C, Antel J, Bruck W. Differentiation block of oligodendroglial progenitor cells as a cause for remyelination failure in chronic multiple sclerosis. Brain. 2008;131(Pt 7):1749-58.
39. Wolswijk G. Chronic stage multiple sclerosis lesions contain a relatively quiescent population of oligodendrocyte precursor cells. J Neurosci. 1998;18(2):601-9.
40. Nally FK, De Santi C, McCoy CE. Nanomodulation of Macrophages in Multiple Sclerosis. Cells. 2019;8(6).
41. Thompson AJ, Baranzini SE, Geurts J, Hemmer B, Ciccarelli O. Multiple sclerosis. Lancet. 2018;391(10130):1622-36.
42. Adamczyk-Sowa M, Adamczyk B, Kulakowska A, Rejdak K, Nowacki P. Secondary progressive multiple sclerosis - from neuropathology to definition and effective treatment. Neurol Neurochir Pol. 2020;54(5):384-98.
43. Ontaneda D, Thompson AJ, Fox RJ, Cohen JA. Progressive multiple sclerosis: prospects for disease therapy, repair, and restoration of function. Lancet. 2017;389(10076):1357-66.
44. Burke T, Hooper K, Barlow S, Hatter L. Multiple sclerosis. Aust Nurs Midwifery J. 2013;21(5):30-3.
45. Rao SM, Leo GJ, Bernardin L, Unverzagt F. Cognitive dysfunction in multiple sclerosis. I. Frequency, patterns, and prediction. Neurology. 1991;41(5):685-91.
46. Rao SM, Leo GJ, Ellington L, Nauertz T, Bernardin L, Unverzagt F. Cognitive dysfunction in multiple sclerosis. II. Impact on employment and social functioning. Neurology. 1991;41(5):692-6.
47. Mokhber N, Azarpazhooh A, Orouji E, Khorram B, Modares Gharavi M, Kakhi S, et al. Therapeutic effect of Avonex, Rebif and Betaferon on quality of life in multiple sclerosis. Psychiatry Clin Neurosci. 2015;69(10):649-57.
48. Lalive PH, Neuhaus O, Benkhoucha M, Burger D, Hohlfeld R, Zamvil SS, et al. Glatiramer acetate in the treatment of multiple sclerosis: emerging concepts regarding its mechanism of action. CNS Drugs. 2011;25(5):401-14.
49. Papadopoulou A, Kappos L, Sprenger T. Teriflunomide for oral therapy in multiple sclerosis. Expert Rev Clin Pharmacol. 2012;5(6):617-28.
50. Salmen A, Gold R. Mode of action and clinical studies with fumarates in multiple sclerosis. Exp Neurol. 2014;262 Pt A:52-6.
51. Signoriello E, Landi D, Monteleone F, Sacca F, Nicoletti CG, Buttari F, et al. Fingolimod reduces the clinical expression of active demyelinating lesions in MS. Mult Scler Relat Disord. 2018;20:215-9.
52. Derfuss T, Kuhle J, Lindberg R, Kappos L. Natalizumab therapy for multiple sclerosis. Semin Neurol. 2013;33(1):26-36.
53. Montalban X, Hauser SL, Kappos L, Arnold DL, Bar-Or A, Comi G, et al. Ocrelizumab versus Placebo in Primary Progressive Multiple Sclerosis. N Engl J Med. 2017;376(3):209-20.
54. Wolinsky JS, Arnold DL, Brochet B, Hartung HP, Montalban X, Naismith RT, et al. Long-term follow-up from the ORATORIO trial of ocrelizumab for primary progressive multiple sclerosis: a post-hoc analysis from the ongoing

open-label extension of the randomised, placebo-controlled, phase 3 trial. Lancet Neurol. 2020;19(12):998-1009.
55. Kappos L, Bar-Or A, Cree BAC, Fox RJ, Giovannoni G, Gold R, et al. Siponimod versus placebo in secondary progressive multiple sclerosis (EXPAND): a double-blind, randomised, phase 3 study. Lancet. 2018;391(10127):1263-73.
56. M. Bear BC, M. Paradiso. Neuroscience: exploring the brain. Wilkins CLW, editor2007.
57. Ahuja CS, Nori S, Tetreault L, Wilson J, Kwon B, Harrop J, et al. Traumatic Spinal Cord Injury-Repair and Regeneration. Neurosurgery. 2017;80(3S):S9-S22.
58. Alizadeh A, Dyck SM, Karimi-Abdolrezaee S. Traumatic Spinal Cord Injury: An Overview of Pathophysiology, Models and Acute Injury Mechanisms. Front Neurol. 2019;10:282.
59. Ahuja CS, Wilson JR, Nori S, Kotter MRN, Druschel C, Curt A, et al. Traumatic spinal cord injury. Nat Rev Dis Primers. 2017;3:17018.
60. O'Shea TM, Burda JE, Sofroniew MV. Cell biology of spinal cord injury and repair. J Clin Invest. 2017;127(9):3259-70.
61. Anjum A, Yazid MD, Fauzi Daud M, Idris J, Ng AMH, Selvi Naicker A, et al. Spinal Cord Injury: Pathophysiology, Multimolecular Interactions, and Underlying Recovery Mechanisms. Int J Mol Sci. 2020;21(20).
62. Hagg T, Oudega M. Degenerative and spontaneous regenerative processes after spinal cord injury. J Neurotrauma. 2006;23(3-4):264-80.
63. Schwab JM, Brechtel K, Mueller CA, Failli V, Kaps HP, Tuli SK, et al. Experimental strategies to promote spinal cord regeneration--an integrative perspective. Prog Neurobiol. 2006;78(2):91-116.
64. Oyinbo CA. Secondary injury mechanisms in traumatic spinal cord injury: a nugget of this multiply cascade. Acta Neurobiol Exp (Wars). 2011;71(2):281-99.
65. Kim YH, Ha KY, Kim SI. Spinal Cord Injury and Related Clinical Trials. Clin Orthop Surg. 2017;9(1):1-9.
66. Ren Y, Young W. Managing inflammation after spinal cord injury through manipulation of macrophage function. Neural Plast. 2013;2013:945034.
67. Donnelly DJ, Popovich PG. Inflammation and its role in neuroprotection, axonal regeneration and functional recovery after spinal cord injury. Exp Neurol. 2008;209(2):378-88.
68. Silver J, Miller JH. Regeneration beyond the glial scar. Nat Rev Neurosci. 2004;5(2):146-56.
69. Orr MB, Gensel JC. Spinal Cord Injury Scarring and Inflammation: Therapies Targeting Glial and Inflammatory Responses. Neurotherapeutics. 2018;15(3):541-53.
70. Cheriyan T, Ryan DJ, Weinreb JH, Cheriyan J, Paul JC, Lafage V, et al. Spinal cord injury models: a review. Spinal Cord. 2014;52(8):588-95.
71. McDonald JW, Sadowsky C. Spinal-cord injury. Lancet. 2002;359(9304):417-25.

72. Sweis R, Biller J. Systemic Complications of Spinal Cord Injury. Curr Neurol Neurosci Rep. 2017;17(2):8.
73. Tran AP, Warren PM, Silver J. The Biology of Regeneration Failure and Success After Spinal Cord Injury. Physiol Rev. 2018;98(2):881-917.
74. Feigin VL, Forouzanfar MH, Krishnamurthi R, Mensah GA, Connor M, Bennett DA, et al. Global and regional burden of stroke during 1990-2010: findings from the Global Burden of Disease Study 2010. Lancet. 2014;383(9913):245-54.
75. Campbell BCV, De Silva DA, Macleod MR, Coutts SB, Schwamm LH, Davis SM, et al. Ischaemic stroke. Nat Rev Dis Primers. 2019;5(1):70.
76. Barthels D, Das H. Current advances in ischemic stroke research and therapies. Biochim Biophys Acta Mol Basis Dis. 2020;1866(4):165260.
77. Donnan GA, Fisher M, Macleod M, Davis SM. Stroke. Lancet. 2008;371(9624):1612-23.
78. Khandelwal P, Yavagal DR, Sacco RL. Acute Ischemic Stroke Intervention. J Am Coll Cardiol. 2016;67(22):2631-44.
79. Krishnamurthi RV, Feigin VL, Forouzanfar MH, Mensah GA, Connor M, Bennett DA, et al. Global and regional burden of first-ever ischaemic and haemorrhagic stroke during 1990-2010: findings from the Global Burden of Disease Study 2010. Lancet Glob Health. 2013;1(5):e259-81.
80. Jian Z, Liu R, Zhu X, Smerin D, Zhong Y, Gu L, et al. The Involvement and Therapy Target of Immune Cells After Ischemic Stroke. Front Immunol. 2019;10:2167.
81. Krishnamurthi RV, Feigin VL, Forouzanfar MH, Mensah GA, Connor M, Bennett DA, et al. Global and regional burden of first-ever ischaemic and haemorrhagic stroke during 1990-2010: findings from the Global Burden of Disease Study 2010. Lancet Glob Health. 2013;1(5):e259-81.
82. Collaborators GBDLRoS, Feigin VL, Nguyen G, Cercy K, Johnson CO, Alam T, et al. Global, Regional, and Country-Specific Lifetime Risks of Stroke, 1990 and 2016. N Engl J Med. 2018;379(25):2429-37.
83. Feigin VL, Forouzanfar MH, Krishnamurthi R, Mensah GA, Connor M, Bennett DA, et al. Global and regional burden of stroke during 1990-2010: findings from the Global Burden of Disease Study 2010. Lancet. 2014;383(9913):245-54.
84. Bejot Y, Daubail B, Giroud M. Epidemiology of stroke and transient ischemic attacks: Current knowledge and perspectives. Rev Neurol (Paris). 2016;172(1):59-68.
85. Hacke W, Kaste M, Bluhmki E, Brozman M, Davalos A, Guidetti D, et al. Thrombolysis with alteplase 3 to 4.5 hours after acute ischemic stroke. N Engl J Med. 2008;359(13):1317-29.
86. Rabinstein AA. Treatment of Acute Ischemic Stroke. Continuum (Minneap Minn). 2017;23(1, Cerebrovascular Disease):62-81.
87. Nogueira RG, Jadhav AP, Haussen DC, Bonafe A, Budzik RF, Bhuva P, et al. Thrombectomy 6 to 24 Hours after Stroke with a Mismatch between Deficit and Infarct. N Engl J Med. 2018;378(1):11-21.

88. Sunderland S. The anatomy and physiology of nerve injury. Muscle Nerve. 1990;13(9):771-84.
89. Burnett MG, Zager EL. Pathophysiology of peripheral nerve injury: a brief review. Neurosurg Focus. 2004;16(5):E1.
90. Jessen KR, Mirsky R. The repair Schwann cell and its function in regenerating nerves. J Physiol. 2016;594(13):3521-31.
91. Salzer JL. Schwann cell myelination. Cold Spring Harb Perspect Biol. 2015;7(8):a020529.
92. Balakrishnan A, Belfiore L, Chu TH, Fleming T, Midha R, Biernaskie J, et al. Insights Into the Role and Potential of Schwann Cells for Peripheral Nerve Repair From Studies of Development and Injury. Front Mol Neurosci. 2020;13:608442.
93. Bhandari PS. Management of peripheral nerve injury. J Clin Orthop Trauma. 2019;10(5):862-6.
94. Juneja M, Burns J, Saporta MA, Timmerman V. Challenges in modelling the Charcot-Marie-Tooth neuropathies for therapy development. J Neurol Neurosurg Psychiatry. 2019;90(1):58-67.
95. van Paassen BW, van der Kooi AJ, van Spaendonck-Zwarts KY, Verhamme C, Baas F, de Visser M. PMP22 related neuropathies: Charcot-Marie-Tooth disease type 1A and Hereditary Neuropathy with liability to Pressure Palsies. Orphanet J Rare Dis. 2014;9:38.
96. Prior R, Van Helleputte L, Benoy V, Van Den Bosch L. Defective axonal transport: A common pathological mechanism in inherited and acquired peripheral neuropathies. Neurobiol Dis. 2017;105:300-20.
97. Benoy V, Van Helleputte L, Prior R, d'Ydewalle C, Haeck W, Geens N, et al. HDAC6 is a therapeutic target in mutant GARS-induced Charcot-Marie-Tooth disease. Brain. 2018;141(3):673-87.
98. Baets J, De Jonghe P, Timmerman V. Recent advances in Charcot-Marie-Tooth disease. Curr Opin Neurol. 2014;27(5):532-40.
99. Timmerman V, Strickland AV, Zuchner S. Genetics of Charcot-Marie-Tooth (CMT) Disease within the Frame of the Human Genome Project Success. Genes (Basel). 2014;5(1):13-32.
100. Tozza S, Bruzzese D, Severi D, Spina E, Iodice R, Ruggiero L, et al. The impact of symptoms on daily life as perceived by patients with Charcot-Marie-Tooth type 1A disease. Neurol Sci. 2022;43(1):559-63.
101. Young P, De Jonghe P, Stogbauer F, Butterfass-Bahloul T. Treatment for Charcot-Marie-Tooth disease. Cochrane Database Syst Rev. 2008;2008(1):CD006052.
102. Roggeri A, Schepers M, Tiane A, Rombaut B, van Veggel L, Hellings N, et al. Sphingosine-1-Phosphate Receptor Modulators and Oligodendroglial Cells: Beyond Immunomodulation. Int J Mol Sci. 2020;21(20).
103. Knott EP, Assi M, Rao SN, Ghosh M, Pearse DD. Phosphodiesterase Inhibitors as a Therapeutic Approach to Neuroprotection and Repair. Int J Mol Sci. 2017;18(4).

104. Sommer N, Martin R, McFarland HF, Quigley L, Cannella B, Raine CS, et al. Therapeutic potential of phosphodiesterase type 4 inhibition in chronic autoimmune demyelinating disease. J Neuroimmunol. 1997;79(1):54-61.
105. Knott EP, Assi M, Pearse DD. Cyclic AMP signaling: a molecular determinant of peripheral nerve regeneration. Biomed Res Int. 2014;2014:651625.
106. Sassone-Corsi P. The cyclic AMP pathway. Cold Spring Harb Perspect Biol. 2012;4(12).
107. Bender AT, Beavo JA. Cyclic nucleotide phosphodiesterases: molecular regulation to clinical use. Pharmacol Rev. 2006;58(3):488-520.
108. Paes D, Schepers M, Rombaut B, van den Hove D, Vanmierlo T, Prickaerts J. The Molecular Biology of Phosphodiesterase 4 Enzymes as Pharmacological Targets: An Interplay of Isoforms, Conformational States, and Inhibitors. Pharmacol Rev. 2021;73(3):1016-49.
109. Baillie GS, Tejeda GS, Kelly MP. Therapeutic targeting of 3',5'-cyclic nucleotide phosphodiesterases: inhibition and beyond. Nat Rev Drug Discov. 2019;18(10):770-96.
110. Li H, Zuo J, Tang W. Phosphodiesterase-4 Inhibitors for the Treatment of Inflammatory Diseases. Front Pharmacol. 2018;9:1048.
111. Chiricozzi A, Caposiena D, Garofalo V, Cannizzaro MV, Chimenti S, Saraceno R. A new therapeutic for the treatment of moderate-to-severe plaque psoriasis: apremilast. Expert Rev Clin Immunol. 2016;12(3):237-49.
112. Peter D, Jin SL, Conti M, Hatzelmann A, Zitt C. Differential expression and function of phosphodiesterase 4 (PDE4) subtypes in human primary CD4+ T cells: predominant role of PDE4D. J Immunol. 2007;178(8):4820-31.
113. Omori K, Kotera J. Overview of PDEs and their regulation. Circ Res. 2007;100(3):309-27.
114. Spencer T, Filbin MT. A role for cAMP in regeneration of the adult mammalian CNS. J Anat. 2004;204(1):49-55.
115. Lerner A, Kim DH, Lee R. The cAMP signaling pathway as a therapeutic target in lymphoid malignancies. Leuk Lymphoma. 2000;37(1-2):39-51.
116. Raker VK, Becker C, Steinbrink K. The cAMP Pathway as Therapeutic Target in Autoimmune and Inflammatory Diseases. Front Immunol. 2016;7:123.
117. Boczek T, Cameron EG, Yu W, Xia X, Shah SH, Castillo Chabeco B, et al. Regulation of Neuronal Survival and Axon Growth by a Perinuclear cAMP Compartment. J Neurosci. 2019;39(28):5466-80.
118. Syed YA, Baer A, Hofer MP, Gonzalez GA, Rundle J, Myrta S, et al. Inhibition of phosphodiesterase-4 promotes oligodendrocyte precursor cell differentiation and enhances CNS remyelination. EMBO Mol Med. 2013;5(12):1918-34.
119. Vang AG, Housley W, Dong H, Basole C, Ben-Sasson SZ, Kream BE, et al. Regulatory T-cells and cAMP suppress effector T-cells independently of PKA-CREM/ICER: a potential role for Epac. Biochem J. 2013;456(3):463-73.

120. Ponsaerts L, Alders L, Schepers M, de Oliveira RMW, Prickaerts J, Vanmierlo T, et al. Neuroinflammation in Ischemic Stroke: Inhibition of cAMP-Specific Phosphodiesterases (PDEs) to the Rescue. Biomedicines. 2021;9(7).
121. Propper DJ, Saunders MP, Salisbury AJ, Long L, O'Byrne KJ, Braybrooke JP, et al. Phase I study of the novel cyclic AMP (cAMP) analogue 8-chloro-cAMP in patients with cancer: toxicity, hormonal, and immunological effects. Clin Cancer Res. 1999;5(7):1682-9.
122. Spina D. PDE4 inhibitors: current status. Br J Pharmacol. 2008;155(3):308-15.
123. Peng T, Qi B, He J, Ke H, Shi J. Advances in the Development of Phosphodiesterase-4 Inhibitors. J Med Chem. 2020;63(19):10594-617.
124. Schepers M, Tiane A, Paes D, Sanchez S, Rombaut B, Piccart E, et al. Targeting Phosphodiesterases-Towards a Tailor-Made Approach in Multiple Sclerosis Treatment. Front Immunol. 2019;10:1727.
125. Hebenstreit GF, Fellerer K, Fichte K, Fischer G, Geyer N, Meya U, et al. Rolipram in major depressive disorder: results of a double-blind comparative study with imipramine. Pharmacopsychiatry. 1989;22(4):156-60.
126. Lipworth BJ. Phosphodiesterase-4 inhibitors for asthma and chronic obstructive pulmonary disease. Lancet. 2005;365(9454):167-75.
127. Chao AC, de Sauvage FJ, Dong YJ, Wagner JA, Goeddel DV, Gardner P. Activation of intestinal CFTR Cl- channel by heat-stable enterotoxin and guanylin via cAMP-dependent protein kinase. EMBO J. 1994;13(5):1065-72.
128. McDonough W, Aragon IV, Rich J, Murphy JM, Abou Saleh L, Boyd A, et al. PAN-selective inhibition of cAMP-phosphodiesterase 4 (PDE4) induces gastroparesis in mice. FASEB J. 2020;34(9):12533-48.
129. Robichaud A, Stamatiou PB, Jin SL, Lachance N, MacDonald D, Laliberte F, et al. Deletion of phosphodiesterase 4D in mice shortens alpha(2)-adrenoceptor-mediated anesthesia, a behavioral correlate of emesis. J Clin Invest. 2002;110(7):1045-52.
130. Kelly MP, Adamowicz W, Bove S, Hartman AJ, Mariga A, Pathak G, et al. Select 3',5'-cyclic nucleotide phosphodiesterases exhibit altered expression in the aged rodent brain. Cell Signal. 2014;26(2):383-97.
131. Gajofatto A, Benedetti MD. Treatment strategies for multiple sclerosis: When to start, when to change, when to stop? World J Clin Cases. 2015;3(7):545-55.
132. Ponzio M, Brichetto G, Zaratin P, Battaglia MA. Workers with disability: the case of multiple sclerosis. Neurol Sci. 2015;36(10):1835-41.
133. Compston A, Coles A. Multiple sclerosis. Lancet. 2002;359(9313):1221-31.
134. Lublin FD, Reingold SC. Defining the clinical course of multiple sclerosis: results of an international survey. National Multiple Sclerosis Society (USA) Advisory Committee on Clinical Trials of New Agents in Multiple Sclerosis. Neurology. 1996;46(4):907-11.
135. Lopez-Diego RS, Weiner HL. Novel therapeutic strategies for multiple sclerosis--a multifaceted adversary. Nat Rev Drug Discov. 2008;7(11):909-25.

136. Loma I, Heyman R. Multiple sclerosis: pathogenesis and treatment. Curr Neuropharmacol. 2011;9(3):409-16.
137. Zurawski J, Stankiewicz J. Multiple Sclerosis Re-Examined: Essential and Emerging Clinical Concepts. Am J Med. 2018;131(5):464-72.
138. Zeydan B, Lowe VJ, Schwarz CG, Przybelski SA, Tosakulwong N, Zuk SM, et al. Pittsburgh compound-B PET white matter imaging and cognitive function in late multiple sclerosis. Mult Scler. 2018;24(6):739-49.
139. Trojano M, Paolicelli D, Bellacosa A, Cataldo S. The transition from relapsing-remitting MS to irreversible disability: clinical evaluation. Neurol Sci. 2003;24 Suppl 5:S268-70.
140. Ontaneda D, Fox RJ. Progressive multiple sclerosis. Curr Opin Neurol. 2015;28(3):237-43.
141. Lucchinetti C, Bruck W, Parisi J, Scheithauer B, Rodriguez M, Lassmann H. Heterogeneity of multiple sclerosis lesions: implications for the pathogenesis of demyelination. Ann Neurol. 2000;47(6):707-17.
142. Daneman R, Prat A. The blood-brain barrier. Cold Spring Harb Perspect Biol. 2015;7(1):a020412.
143. Larochelle C, Alvarez JI, Prat A. How do immune cells overcome the blood-brain barrier in multiple sclerosis? FEBS Lett. 2011;585(23):3770-80.
144. Bogie JF, Stinissen P, Hendriks JJ. Macrophage subsets and microglia in multiple sclerosis. Acta Neuropathol. 2014;128(2):191-213.
145. Xuan W, Qu Q, Zheng B, Xiong S, Fan GH. The chemotaxis of M1 and M2 macrophages is regulated by different chemokines. J Leukoc Biol. 2015;97(1):61-9.
146. Bruck W, Bitsch A, Kolenda H, Bruck Y, Stiefel M, Lassmann H. Inflammatory central nervous system demyelination: correlation of magnetic resonance imaging findings with lesion pathology. Ann Neurol. 1997;42(5):783-93.
147. Bruck W, Stadelmann C. Inflammation and degeneration in multiple sclerosis. Neurol Sci. 2003;24 Suppl 5:S265-7.
148. Erickson BJ. Imaging of remyelination and neuronal health. Curr Top Microbiol Immunol. 2008;318:73-92.
149. Staugaitis SM, Chang A, Trapp BD. Cortical pathology in multiple sclerosis: experimental approaches to studies on the mechanisms of demyelination and remyelination. Acta Neurol Scand Suppl. 2012(195):97-102.
150. Hagemeier K, Bruck W, Kuhlmann T. Multiple sclerosis - remyelination failure as a cause of disease progression. Histol Histopathol. 2012;27(3):277-87.
151. Hanafy KA, Sloane JA. Regulation of remyelination in multiple sclerosis. FEBS Lett. 2011;585(23):3821-8.
152. Chang A, Nishiyama A, Peterson J, Prineas J, Trapp BD. NG2-positive oligodendrocyte progenitor cells in adult human brain and multiple sclerosis lesions. J Neurosci. 2000;20(17):6404-12.
153. Kipp M, van der Valk P, Amor S. Pathology of multiple sclerosis. CNS Neurol Disord Drug Targets. 2012;11(5):506-17.

154. Wolswijk G. Oligodendrocyte precursor cells in the demyelinated multiple sclerosis spinal cord. Brain. 2002;125(Pt 2):338-49.
155. Dutta R, Trapp BD. Mechanisms of neuronal dysfunction and degeneration in multiple sclerosis. Prog Neurobiol. 2011;93(1):1-12.
156. Trapp BD, Nave KA. Multiple sclerosis: an immune or neurodegenerative disorder? Annu Rev Neurosci. 2008;31:247-69.
157. Schaal SM, Garg MS, Ghosh M, Lovera L, Lopez M, Patel M, et al. The therapeutic profile of rolipram, PDE target and mechanism of action as a neuroprotectant following spinal cord injury. PLoS One. 2012;7(9):e43634.
158. Sanabra C, Johansson EM, Mengod G. Critical role for PDE4 subfamilies in the development of experimental autoimmune encephalomyelitis. J Chem Neuroanat. 2013;47:96-105.
159. Pifarre P, Gutierrez-Mecinas M, Prado J, Usero L, Roura-Mir C, Giralt M, et al. Phosphodiesterase 5 inhibition at disease onset prevents experimental autoimmune encephalomyelitis progression through immunoregulatory and neuroprotective actions. Exp Neurol. 2014;251:58-71.
160. Khezri S, Javan M, Goudarzvand M, Semnanian S, Baharvand H. Dibutyryl cyclic AMP inhibits the progression of experimental autoimmune encephalomyelitis and potentiates recruitment of endogenous neural stem cells. J Mol Neurosci. 2013;51(2):298-306.
161. Bollen E, Prickaerts J. Phosphodiesterases in neurodegenerative disorders. IUBMB Life. 2012;64(12):965-70.
162. Conti M, Beavo J. Biochemistry and physiology of cyclic nucleotide phosphodiesterases: essential components in cyclic nucleotide signaling. Annu Rev Biochem. 2007;76:481-511.
163. Heckman PR, Blokland A, Ramaekers J, Prickaerts J. PDE and cognitive processing: beyond the memory domain. Neurobiol Learn Mem. 2015;119:108-22.
164. Francis SH, Blount MA, Corbin JD. Mammalian cyclic nucleotide phosphodiesterases: molecular mechanisms and physiological functions. Physiol Rev. 2011;91(2):651-90.
165. Rutten K, Basile JL, Prickaerts J, Blokland A, Vivian JA. Selective PDE inhibitors rolipram and sildenafil improve object retrieval performance in adult cynomolgus macaques. Psychopharmacology (Berl). 2008;196(4):643-8.
166. Rutten K, Van Donkelaar EL, Ferrington L, Blokland A, Bollen E, Steinbusch HW, et al. Phosphodiesterase inhibitors enhance object memory independent of cerebral blood flow and glucose utilization in rats. Neuropsychopharmacology. 2009;34(8):1914-25.
167. Bartholomaus I, Kawakami N, Odoardi F, Schlager C, Miljkovic D, Ellwart JW, et al. Effector T cell interactions with meningeal vascular structures in nascent autoimmune CNS lesions. Nature. 2009;462(7269):94-8.
168. Rubin LL, Hall DE, Porter S, Barbu K, Cannon C, Horner HC, et al. A cell culture model of the blood-brain barrier. J Cell Biol. 1991;115(6):1725-35.
169. Rodrigues SF, Granger DN. Blood cells and endothelial barrier function. Tissue Barriers. 2015;3(1-2):e978720.

170. Michinaga S, Koyama Y. Dual Roles of Astrocyte-Derived Factors in Regulation of Blood-Brain Barrier Function after Brain Damage. Int J Mol Sci. 2019;20(3).
171. Mayhan WG. VEGF increases permeability of the blood-brain barrier via a nitric oxide synthase/cGMP-dependent pathway. Am J Physiol. 1999;276(5):C1148-53.
172. Folcik VA, Smith T, O'Bryant S, Kawczak JA, Zhu B, Sakurai H, et al. Treatment with BBB022A or rolipram stabilizes the blood-brain barrier in experimental autoimmune encephalomyelitis: an additional mechanism for the therapeutic effect of type IV phosphodiesterase inhibitors. J Neuroimmunol. 1999;97(1-2):119-28.
173. Kraft P, Schwarz T, Gob E, Heydenreich N, Brede M, Meuth SG, et al. The phosphodiesterase-4 inhibitor rolipram protects from ischemic stroke in mice by reducing blood-brain-barrier damage, inflammation and thrombosis. Exp Neurol. 2013;247:80-90.
174. He Z, He B, Behrle BL, Fejleh MP, Cui L, Paule MG, et al. Ischemia-induced increase in microvascular phosphodiesterase 4D expression in rat hippocampus associated with blood brain barrier permeability: effect of age. ACS Chem Neurosci. 2012;3(6):428-32.
175. Yanai S, Toyohara J, Ishiwata K, Ito H, Endo S. Long-term cilostazol administration ameliorates memory decline in senescence-accelerated mouse prone 8 (SAMP8) through a dual effect on cAMP and blood-brain barrier. Neuropharmacology. 2017;116:247-59.
176. Geng Y, Shao Y, He W, Hu W, Xu Y, Chen J, et al. Prognostic Role of Tumor-Infiltrating Lymphocytes in Lung Cancer: a Meta-Analysis. Cell Physiol Biochem. 2015;37(4):1560-71.
177. Romagnani S. T-cell subsets (Th1 versus Th2). Ann Allergy Asthma Immunol. 2000;85(1):9-18; quiz , 21.
178. Hu D, Notarbartolo S, Croonenborghs T, Patel B, Cialic R, Yang TH, et al. Transcriptional signature of human pro-inflammatory TH17 cells identifies reduced IL10 gene expression in multiple sclerosis. Nat Commun. 2017;8(1):1600.
179. Tesmer LA, Lundy SK, Sarkar S, Fox DA. Th17 cells in human disease. Immunol Rev. 2008;223:87-113.
180. Babaloo Z, Aliparasti MR, Babaiea F, Almasi S, Baradaran B, Farhoudi M. The role of Th17 cells in patients with relapsing-remitting multiple sclerosis: interleukin-17A and interleukin-17F serum levels. Immunol Lett. 2015;164(2):76-80.
181. Venken K, Hellings N, Broekmans T, Hensen K, Rummens JL, Stinissen P. Natural naive CD4+CD25+CD127low regulatory T cell (Treg) development and function are disturbed in multiple sclerosis patients: recovery of memory Treg homeostasis during disease progression. J Immunol. 2008;180(9):6411-20.
182. Sonar SA, Lal G. Differentiation and Transmigration of CD4 T Cells in Neuroinflammation and Autoimmunity. Front Immunol. 2017;8:1695.

183. Neumann H, Medana IM, Bauer J, Lassmann H. Cytotoxic T lymphocytes in autoimmune and degenerative CNS diseases. Trends Neurosci. 2002;25(6):313-9.
184. Serafini B, Rosicarelli B, Magliozzi R, Stigliano E, Capello E, Mancardi GL, et al. Dendritic cells in multiple sclerosis lesions: maturation stage, myelin uptake, and interaction with proliferating T cells. J Neuropathol Exp Neurol. 2006;65(2):124-41.
185. Aronoff DM, Carstens JK, Chen GH, Toews GB, Peters-Golden M. Short communication: differences between macrophages and dendritic cells in the cyclic AMP-dependent regulation of lipopolysaccharide-induced cytokine and chemokine synthesis. J Interferon Cytokine Res. 2006;26(11):827-33.
186. Koga K, Takaesu G, Yoshida R, Nakaya M, Kobayashi T, Kinjyo I, et al. Cyclic adenosine monophosphate suppresses the transcription of proinflammatory cytokines via the phosphorylated c-Fos protein. Immunity. 2009;30(3):372-83.
187. Bopp T, Becker C, Klein M, Klein-Hessling S, Palmetshofer A, Serfling E, et al. Cyclic adenosine monophosphate is a key component of regulatory T cell-mediated suppression. J Exp Med. 2007;204(6):1303-10.
188. Li L, Yee C, Beavo JA. CD3- and CD28-dependent induction of PDE7 required for T cell activation. Science. 1999;283(5403):848-51.
189. Smith SJ, Brookes-Fazakerley S, Donnelly LE, Barnes PJ, Barnette MS, Giembycz MA. Ubiquitous expression of phosphodiesterase 7A in human proinflammatory and immune cells. Am J Physiol Lung Cell Mol Physiol. 2003;284(2):L279-89.
190. Gonzalez-Garcia C, Bravo B, Ballester A, Gomez-Perez R, Eguiluz C, Redondo M, et al. Comparative assessment of PDE 4 and 7 inhibitors as therapeutic agents in experimental autoimmune encephalomyelitis. Br J Pharmacol. 2013;170(3):602-13.
191. Yang G, McIntyre KW, Townsend RM, Shen HH, Pitts WJ, Dodd JH, et al. Phosphodiesterase 7A-deficient mice have functional T cells. J Immunol. 2003;171(12):6414-20.
192. Reyes-Irisarri E, Sanchez AJ, Garcia-Merino JA, Mengod G. Selective induction of cAMP phosphodiesterase PDE4B2 expression in experimental autoimmune encephalomyelitis. J Neuropathol Exp Neurol. 2007;66(10):923-31.
193. Kureshiro J, Miyamoto K, Tanaka N, Kusunoki S. Selective phosphodiesterase-3 inhibitor cilostazol ameliorates experimental autoimmune encephalomyelitis. Neuroreport. 2009;20(7):718-22.
194. Deviller P, Cille Y, Betuel H. Guanyl cyclase activity of human blood lymphocytes. Enzyme. 1975;19(5-6):300-13.
195. Takemoto DJ, Dunford C, Vaughn D, Kramer KJ, Smith A, Powell RG. Guanylate cyclase activity in human leukemic and normal lymphocytes. Enzyme inhibition and cytotoxicity of plant extracts. Enzyme. 1982;27(3):179-88.
196. Cille Y, Deviller P, Betuel H. Guanylate cyclase activity of human lymphocytes from peripheral blood, thymus, and tonsils. A comparative study. Enzyme. 1983;29(2):86-92.

197. Wong D, Prameya R, Wu V, Dorovini-Zis K, Vincent SR. Nitric oxide reduces T lymphocyte adhesion to human brain microvessel endothelial cells via a cGMP-dependent pathway. Eur J Pharmacol. 2005;514(2-3):91-8.
198. Bar-Or A, Grove RA, Austin DJ, Tolson JM, VanMeter SA, Lewis EW, et al. Subcutaneous ofatumumab in patients with relapsing-remitting multiple sclerosis: The MIRROR study. Neurology. 2018;90(20):e1805-e14.
199. Hauser SL, Bar-Or A, Comi G, Giovannoni G, Hartung HP, Hemmer B, et al. Ocrelizumab versus Interferon Beta-1a in Relapsing Multiple Sclerosis. N Engl J Med. 2017;376(3):221-34.
200. Li R, Patterson KR, Bar-Or A. Reassessing B cell contributions in multiple sclerosis. Nat Immunol. 2018;19(7):696-707.
201. Ado AD, Dontsov VI, Gol'dshtein MM. [Regulation of the cell cycle of B-lymphocytes in mice by substances elevating the levels of intracellular cAMP and cGMP]. Biull Eksp Biol Med. 1985;99(4):455-8.
202. de Vente J. cGMP: a second messenger for acetylcholine in the brain? Neurochem Int. 2004;45(6):799-812.
203. Lomo J, Blomhoff HK, Beiske K, Stokke T, Smeland EB. TGF-beta 1 and cyclic AMP promote apoptosis in resting human B lymphocytes. J Immunol. 1995;154(4):1634-43.
204. Le Quement C, Guenon I, Gillon JY, Valenca S, Cayron-Elizondo V, Lagente V, et al. The selective MMP-12 inhibitor, AS111793 reduces airway inflammation in mice exposed to cigarette smoke. Br J Pharmacol. 2008;154(6):1206-15.
205. Schafer PH, Parton A, Capone L, Cedzik D, Brady H, Evans JF, et al. Apremilast is a selective PDE4 inhibitor with regulatory effects on innate immunity. Cell Signal. 2014;26(9):2016-29.
206. Gantner F, Gotz C, Gekeler V, Schudt C, Wendel A, Hatzelmann A. Phosphodiesterase profile of human B lymphocytes from normal and atopic donors and the effects of PDE inhibition on B cell proliferation. Br J Pharmacol. 1998;123(6):1031-8.
207. Szczypka M, Obminska-Mrukowicz B. Modulating effects of nonselective and selective phosphodiesterase inhibitors on lymphocyte subsets and humoral immune response in mice. Pharmacol Rep. 2010;62(6):1148-58.
208. Reu P, Khosravi A, Bernard S, Mold JE, Salehpour M, Alkass K, et al. The Lifespan and Turnover of Microglia in the Human Brain. Cell Rep. 2017;20(4):779-84.
209. Sierra A, Encinas JM, Deudero JJ, Chancey JH, Enikolopov G, Overstreet-Wadiche LS, et al. Microglia shape adult hippocampal neurogenesis through apoptosis-coupled phagocytosis. Cell Stem Cell. 2010;7(4):483-95.
210. Prinz M, Tay TL, Wolf Y, Jung S. Microglia: unique and common features with other tissue macrophages. Acta Neuropathol. 2014;128(3):319-31.
211. Hickman S, Izzy S, Sen P, Morsett L, El Khoury J. Microglia in neurodegeneration. Nat Neurosci. 2018;21(10):1359-69.

212. Diaz-Lucena D, Gutierrez-Mecinas M, Moreno B, Martinez-Sanchez JL, Pifarre P, Garcia A. Mechanisms Involved in the Remyelinating Effect of Sildenafil. J Neuroimmune Pharmacol. 2018;13(1):6-23.
213. Makranz C, Cohen G, Reichert F, Kodama T, Rotshenker S. cAMP cascade (PKA, Epac, adenylyl cyclase, Gi, and phosphodiesterases) regulates myelin phagocytosis mediated by complement receptor-3 and scavenger receptor-AI/II in microglia and macrophages. Glia. 2006;53(4):441-8.
214. Ghosh M, Xu Y, Pearse DD. Cyclic AMP is a key regulator of M1 to M2a phenotypic conversion of microglia in the presence of Th2 cytokines. J Neuroinflammation. 2016;13:9.
215. Ke X, Terashima M, Nariai Y, Nakashima Y, Nabika T, Tanigawa Y. Nitric oxide regulates actin reorganization through cGMP and Ca(2+)/calmodulin in RAW 264.7 cells. Biochim Biophys Acta. 2001;1539(1-2):101-13.
216. Boran MS, Garcia A. The cyclic GMP-protein kinase G pathway regulates cytoskeleton dynamics and motility in astrocytes. J Neurochem. 2007;102(1):216-30.
217. Boran MS, Baltrons MA, Garcia A. The ANP-cGMP-protein kinase G pathway induces a phagocytic phenotype but decreases inflammatory gene expression in microglial cells. Glia. 2008;56(4):394-411.
218. Raposo C, Luna RL, Nunes AK, Thome R, Peixoto CA. Role of iNOS-NO-cGMP signaling in modulation of inflammatory and myelination processes. Brain Res Bull. 2014;104:60-73.
219. Jin SL, Lan L, Zoudilova M, Conti M. Specific role of phosphodiesterase 4B in lipopolysaccharide-induced signaling in mouse macrophages. J Immunol. 2005;175(3):1523-31.
220. Yang JX, Hsieh KC, Chen YL, Lee CK, Conti M, Chuang TH, et al. Phosphodiesterase 4B negatively regulates endotoxin-activated interleukin-1 receptor antagonist responses in macrophages. Sci Rep. 2017;7:46165.
221. Jin SL, Conti M. Induction of the cyclic nucleotide phosphodiesterase PDE4B is essential for LPS-activated TNF-alpha responses. Proc Natl Acad Sci U S A. 2002;99(11):7628-33.
222. Zhang B, Yang L, Konishi Y, Maeda N, Sakanaka M, Tanaka J. Suppressive effects of phosphodiesterase type IV inhibitors on rat cultured microglial cells: comparison with other types of cAMP-elevating agents. Neuropharmacology. 2002;42(2):262-9.
223. Wilson NM, Gurney ME, Dietrich WD, Atkins CM. Therapeutic benefits of phosphodiesterase 4B inhibition after traumatic brain injury. PLoS One. 2017;12(5):e0178013.
224. Gurney ME. Genetic Association of Phosphodiesterases With Human Cognitive Performance. Front Mol Neurosci. 2019;12:22.
225. Pilakka-Kanthikeel S, Huang S, Fenton T, Borkowsky W, Cunningham CK, Pahwa S. Increased gut microbial translocation in HIV-infected children persists in virologic responders and virologic failures after antiretroviral therapy. Pediatr Infect Dis J. 2012;31(6):583-91.

226. Myers SA, Gobejishvili L, Saraswat Ohri S, Garrett Wilson C, Andres KR, Riegler AS, et al. Following spinal cord injury, PDE4B drives an acute, local inflammatory response and a chronic, systemic response exacerbated by gut dysbiosis and endotoxemia. Neurobiol Dis. 2019;124:353-63.
227. Schulz C, Schutte K, Malfertheiner P. Helicobacter pylori and Other Gastric Microbiota in Gastroduodenal Pathologies. Dig Dis. 2016;34(3):210-6.
228. Pan Y, Liu B, Li R, Zhang Z, Lu L. Bowel dysfunction in spinal cord injury: current perspectives. Cell Biochem Biophys. 2014;69(3):385-8.
229. Avila DV, Myers SA, Zhang J, Kharebava G, McClain CJ, Kim HY, et al. Phosphodiesterase 4b expression plays a major role in alcohol-induced neuro-inflammation. Neuropharmacology. 2017;125:376-85.
230. Ahmad F, Chung YW, Tang Y, Hockman SC, Liu S, Khan Y, et al. Phosphodiesterase 3B (PDE3B) regulates NLRP3 inflammasome in adipose tissue. Sci Rep. 2016;6:28056.
231. Baumer W, Hoppmann J, Rundfeldt C, Kietzmann M. Highly selective phosphodiesterase 4 inhibitors for the treatment of allergic skin diseases and psoriasis. Inflamm Allergy Drug Targets. 2007;6(1):17-26.
232. Papp K, Cather JC, Rosoph L, Sofen H, Langley RG, Matheson RT, et al. Efficacy of apremilast in the treatment of moderate to severe psoriasis: a randomised controlled trial. Lancet. 2012;380(9843):738-46.
233. Schett G, Wollenhaupt J, Papp K, Joos R, Rodrigues JF, Vessey AR, et al. Oral apremilast in the treatment of active psoriatic arthritis: results of a multicenter, randomized, double-blind, placebo-controlled study. Arthritis Rheum. 2012;64(10):3156-67.
234. Maier C, Ramming A, Bergmann C, Weinkam R, Kittan N, Schett G, et al. Inhibition of phosphodiesterase 4 (PDE4) reduces dermal fibrosis by interfering with the release of interleukin-6 from M2 macrophages. Ann Rheum Dis. 2017;76(6):1133-41.
235. Pearse DD, Hughes ZA. PDE4B as a microglia target to reduce neuroinflammation. Glia. 2016;64(10):1698-709.
236. Santiago A, Soares LM, Schepers M, Milani H, Vanmierlo T, Prickaerts J, et al. Roflumilast promotes memory recovery and attenuates white matter injury in aged rats subjected to chronic cerebral hypoperfusion. Neuropharmacology. 2018;138:360-70.
237. Zou ZQ, Chen JJ, Feng HF, Cheng YF, Wang HT, Zhou ZZ, et al. Novel Phosphodiesterase 4 Inhibitor FCPR03 Alleviates Lipopolysaccharide-Induced Neuroinflammation by Regulation of the cAMP/PKA/CREB Signaling Pathway and NF-kappaB Inhibition. J Pharmacol Exp Ther. 2017;362(1):67-77.
238. You T, Cheng Y, Zhong J, Bi B, Zeng B, Zheng W, et al. Roflupram, a Phosphodiesterase 4 Inhibitior, Suppresses Inflammasome Activation through Autophagy in Microglial Cells. ACS Chem Neurosci. 2017;8(11):2381-92.
239. Rathinam VA, Vanaja SK, Fitzgerald KA. Regulation of inflammasome signaling. Nat Immunol. 2012;13(4):333-42.
240. Hedde JR, Hanks AN, Schmidt CJ, Hughes ZA. The isozyme selective phosphodiesterase-4 inhibitor, ABI-4, attenuates the effects of

lipopolysaccharide in human cells and rodent models of peripheral and CNS inflammation. Brain Behav Immun. 2017;64:285-95.
241. Mestre L, Redondo M, Carrillo-Salinas FJ, Morales-Garcia JA, Alonso-Gil S, Perez-Castillo A, et al. PDE7 inhibitor TC3.6 ameliorates symptomatology in a model of primary progressive multiple sclerosis. Br J Pharmacol. 2015;172(17):4277-90.
242. Zhao S, Zhang L, Lian G, Wang X, Zhang H, Yao X, et al. Sildenafil attenuates LPS-induced pro-inflammatory responses through down-regulation of intracellular ROS-related MAPK/NF-kappaB signaling pathways in N9 microglia. Int Immunopharmacol. 2011;11(4):468-74.
243. Agusti A, Hernandez-Rabaza V, Balzano T, Taoro-Gonzalez L, Ibanez-Grau A, Cabrera-Pastor A, et al. Sildenafil reduces neuroinflammation in cerebellum, restores GABAergic tone, and improves motor in-coordination in rats with hepatic encephalopathy. CNS Neurosci Ther. 2017;23(5):386-94.
244. Hernandez-Rabaza V, Agusti A, Cabrera-Pastor A, Fustero S, Delgado O, Taoro-Gonzalez L, et al. Sildenafil reduces neuroinflammation and restores spatial learning in rats with hepatic encephalopathy: underlying mechanisms. J Neuroinflammation. 2015;12:195.
245. Zhang J, Guo J, Zhao X, Chen Z, Wang G, Liu A, et al. Phosphodiesterase-5 inhibitor sildenafil prevents neuroinflammation, lowers beta-amyloid levels and improves cognitive performance in APP/PS1 transgenic mice. Behav Brain Res. 2013;250:230-7.
246. Giampa C, Laurenti D, Anzilotti S, Bernardi G, Menniti FS, Fusco FR. Inhibition of the striatal specific phosphodiesterase PDE10A ameliorates striatal and cortical pathology in R6/2 mouse model of Huntington's disease. PLoS One. 2010;5(10):e13417.
247. Suzumura A, Ito A, Yoshikawa M, Sawada M. Ibudilast suppresses TNFalpha production by glial cells functioning mainly as type III phosphodiesterase inhibitor in the CNS. Brain Res. 1999;837(1-2):203-12.
248. Wiese S, Karus M, Faissner A. Astrocytes as a source for extracellular matrix molecules and cytokines. Front Pharmacol. 2012;3:120.
249. Colombo E, Farina C. Astrocytes: Key Regulators of Neuroinflammation. Trends in Immunology. 2016;37(9):608-20.
250. Ludwin SK, Rao V, Moore CS, Antel JP. Astrocytes in multiple sclerosis. Mult Scler. 2016;22(9):1114-24.
251. Pekny M, Pekna M. Astrocyte Reactivity and Reactive Astrogliosis: Costs and Benefits. Physiological Reviews. 2014;94(4):1077-98.
252. Borysiewicz E, Fil D, Dlaboga D, O'Donnell JM, Konat GW. Phosphodiesterase 4B2 gene is an effector of Toll-like receptor signaling in astrocytes. Metab Brain Dis. 2009;24(3):481-91.
253. Schwenkgrub J, Zaremba M, Joniec-Maciejak I, Cudna A, Mirowska-Guzel D, Kurkowska-Jastrzębska I. The phosphodiesterase inhibitor, ibudilast, attenuates neuroinflammation in the MPTP model of Parkinson's disease. PloS one. 2017;12(7):e0182019-e.

254. Cueva Vargas JL, Belforte N, Di Polo A. The glial cell modulator ibudilast attenuates neuroinflammation and enhances retinal ganglion cell viability in glaucoma through protein kinase A signaling. Neurobiol Dis. 2016;93:156-71.
255. Takuma K, Lee E, Enomoto R, Mori K, Baba A, Matsuda T. Ibudilast attenuates astrocyte apoptosis via cyclic GMP signalling pathway in an in vitro reperfusion model. British journal of pharmacology. 2001;133(6):841-8.
256. de Santana Nunes AK, Raposo C, Bjorklund U, da Cruz-Hofling MA, Peixoto CA, Hansson E. Sildenafil (Viagra((R))) prevents and restores LPS-induced inflammation in astrocytes. Neurosci Lett. 2016;630:59-65.
257. Laureys G, Gerlo S, Spooren A, Demol F, De Keyser J, Aerts JL. beta(2)-adrenergic agonists modulate TNF-alpha induced astrocytic inflammatory gene expression and brain inflammatory cell populations. J Neuroinflammation. 2014;11:21.
258. Ballestas ME, Benveniste EN. Elevation of Cyclic AMP Levels in Astrocytes Antagonizes Cytokine-Induced Adhesion Molecule Expression. Journal of Neurochemistry. 1997;69(4):1438-48.
259. Bradl M, Lassmann H. Oligodendrocytes: biology and pathology. Acta neuropathologica. 2010;119(1):37-53.
260. Franklin RJ, Ffrench-Constant C. Remyelination in the CNS: from biology to therapy. Nat Rev Neurosci. 2008;9(11):839-55.
261. Arai K, Lo EH. Experimental models for analysis of oligodendrocyte pathophysiology in stroke. Experimental & translational stroke medicine. 2009;1:6.
262. Peferoen L, Kipp M, van der Valk P, van Noort JM, Amor S. Oligodendrocyte-microglia cross-talk in the central nervous system. Immunology. 2014;141(3):302-13.
263. Raible DW, McMorris FA. Oligodendrocyte differentiation and progenitor cell proliferation are independently regulated by cyclic AMP. J Neurosci Res. 1993;34(3):287-94.
264. Raible DW, McMorris FA. Induction of oligodendrocyte differentiation by activators of adenylate cyclase. Journal of neuroscience research. 1990;27(1):43-6.
265. Medina-Rodriguez EM, Arenzana FJ, Pastor J, Redondo M, Palomo V, Garcia de Sola R, et al. Inhibition of endogenous phosphodiesterase 7 promotes oligodendrocyte precursor differentiation and survival. Cellular and molecular life sciences : CMLS. 2013;70(18):3449-62.
266. Whitaker CM, Beaumont E, Wells MJ, Magnuson DS, Hetman M, Onifer SM. Rolipram attenuates acute oligodendrocyte death in the adult rat ventrolateral funiculus following contusive cervical spinal cord injury. Neurosci Lett. 2008;438(2):200-4.
267. Miyamoto N, Tanaka R, Shimura H, Watanabe T, Mori H, Onodera M, et al. Phosphodiesterase III Inhibition Promotes Differentiation and Survival of Oligodendrocyte Progenitors and Enhances Regeneration of Ischemic White Matter Lesions in the Adult Mammalian Brain. Journal of Cerebral Blood Flow & Metabolism. 2010;30(2):299-310.

268. Garthwaite G, Hampden-Smith K, Wilson GW, Goodwin DA, Garthwaite J. Nitric oxide targets oligodendrocytes and promotes their morphological differentiation. Glia. 2015;63(3):383-99.
269. Nunes AK, Raposo C, Luna RL, Cruz-Hofling MA, Peixoto CA. Sildenafil (Viagra(R)) down regulates cytokines and prevents demyelination in a cuprizone-induced MS mouse model. Cytokine. 2012;60(2):540-51.
270. Munoz-Esquivel J, Gottle P, Aguirre-Cruz L, Flores-Rivera J, Corona T, Reyes-Teran G, et al. Sildenafil Inhibits Myelin Expression and Myelination of Oligodendroglial Precursor Cells. ASN Neuro. 2019;11:1759091419832444.
271. Waxman SG. Axonal conduction and injury in multiple sclerosis: the role of sodium channels. Nat Rev Neurosci. 2006;7(12):932-41.
272. Hauser SL, Oksenberg JR. The neurobiology of multiple sclerosis: genes, inflammation, and neurodegeneration. Neuron. 2006;52(1):61-76.
273. Gupta S, Singh P, Sharma BM, Sharma B. Neuroprotective Effects of Agomelatine and Vinpocetine Against Chronic Cerebral Hypoperfusion Induced Vascular Dementia. Curr Neurovasc Res. 2015;12(3):240-52.
274. Bliss TV, Collingridge GL. A synaptic model of memory: long-term potentiation in the hippocampus. Nature. 1993;361(6407):31-9.
275. Boess FG, Hendrix M, van der Staay FJ, Erb C, Schreiber R, van Staveren W, et al. Inhibition of phosphodiesterase 2 increases neuronal cGMP, synaptic plasticity and memory performance. Neuropharmacology. 2004;47(7):1081-92.
276. Soares LM, Meyer E, Milani H, Steinbusch HW, Prickaerts J, de Oliveira RM. The phosphodiesterase type 2 inhibitor BAY 60-7550 reverses functional impairments induced by brain ischemia by decreasing hippocampal neurodegeneration and enhancing hippocampal neuronal plasticity. Eur J Neurosci. 2017;45(4):510-20.
277. Xu Y, Pan J, Sun J, Ding L, Ruan L, Reed M, et al. Inhibition of phosphodiesterase 2 reverses impaired cognition and neuronal remodeling caused by chronic stress. Neurobiol Aging. 2015;36(2):955-70.
278. Yoneyama M, Tanaka M, Hasebe S, Yamaguchi T, Shiba T, Ogita K. Beneficial effect of cilostazol-mediated neuronal repair following trimethyltin-induced neuronal loss in the dentate gyrus. J Neurosci Res. 2015;93(1):56-66.
279. Prickaerts J, Heckman PRA, Blokland A. Investigational phosphodiesterase inhibitors in phase I and phase II clinical trials for Alzheimer's disease. Expert Opin Investig Drugs. 2017;26(9):1033-48.
280. Blokland A, Menniti FS, Prickaerts J. PDE inhibition and cognition enhancement. Expert Opin Ther Pat. 2012;22(4):349-54.
281. Vanmierlo T, Creemers P, Akkerman S, van Duinen M, Sambeth A, De Vry J, et al. The PDE4 inhibitor roflumilast improves memory in rodents at non-emetic doses. Behav Brain Res. 2016;303:26-33.
282. Zhang C, Xu Y, Chowdhary A, Fox D, 3rd, Gurney ME, Zhang HT, et al. Memory enhancing effects of BPN14770, an allosteric inhibitor of phosphodiesterase-4D, in wild-type and humanized mice. Neuropsychopharmacology. 2018;43(11):2299-309.

283. Li YF, Cheng YF, Huang Y, Conti M, Wilson SP, O'Donnell JM, et al. Phosphodiesterase-4D knock-out and RNA interference-mediated knock-down enhance memory and increase hippocampal neurogenesis via increased cAMP signaling. J Neurosci. 2011;31(1):172-83.
284. Nikulina E, Tidwell JL, Dai HN, Bregman BS, Filbin MT. The phosphodiesterase inhibitor rolipram delivered after a spinal cord lesion promotes axonal regeneration and functional recovery. Proc Natl Acad Sci U S A. 2004;101(23):8786-90.
285. Pearse DD, Pereira FC, Marcillo AE, Bates ML, Berrocal YA, Filbin MT, et al. cAMP and Schwann cells promote axonal growth and functional recovery after spinal cord injury. Nat Med. 2004;10(6):610-6.
286. Hulley P, Hartikka J, Abdel'Al S, Engels P, Buerki HR, Wiederhold KH, et al. Inhibitors of type IV phosphodiesterases reduce the toxicity of MPTP in substantia nigra neurons in vivo. Eur J Neurosci. 1995;7(12):2431-40.
287. Yang L, Calingasan NY, Lorenzo BJ, Beal MF. Attenuation of MPTP neurotoxicity by rolipram, a specific inhibitor of phosphodiesterase IV. Exp Neurol. 2008;211(1):311-4.
288. DeMarch Z, Giampa C, Patassini S, Bernardi G, Fusco FR. Beneficial effects of rolipram in the R6/2 mouse model of Huntington's disease. Neurobiol Dis. 2008;30(3):375-87.
289. Giampa C, Middei S, Patassini S, Borreca A, Marullo F, Laurenti D, et al. Phosphodiesterase type IV inhibition prevents sequestration of CREB binding protein, protects striatal parvalbumin interneurons and rescues motor deficits in the R6/2 mouse model of Huntington's disease. Eur J Neurosci. 2009;29(5):902-10.
290. Prickaerts J, de Vente J, Honig W, Steinbusch HW, Blokland A. cGMP, but not cAMP, in rat hippocampus is involved in early stages of object memory consolidation. Eur J Pharmacol. 2002;436(1-2):83-7.
291. Puzzo D, Sapienza S, Arancio O, Palmeri A. Role of phosphodiesterase 5 in synaptic plasticity and memory. Neuropsychiatr Dis Treat. 2008;4(2):371-87.
292. Puerta E, Hervias I, Barros-Minones L, Jordan J, Ricobaraza A, Cuadrado-Tejedor M, et al. Sildenafil protects against 3-nitropropionic acid neurotoxicity through the modulation of calpain, CREB, and BDNF. Neurobiol Dis. 2010;38(2):237-45.
293. Sikandaner HE, Park SY, Kim MJ, Park SN, Yang DW. Neuroprotective effects of sildenafil against oxidative stress and memory dysfunction in mice exposed to noise stress. Behav Brain Res. 2017;319:37-47.
294. Morales-Garcia JA, Redondo M, Alonso-Gil S, Gil C, Perez C, Martinez A, et al. Phosphodiesterase 7 inhibition preserves dopaminergic neurons in cellular and rodent models of Parkinson disease. PLoS One. 2011;6(2):e17240.
295. Perez-Gonzalez R, Pascual C, Antequera D, Bolos M, Redondo M, Perez DI, et al. Phosphodiesterase 7 inhibitor reduced cognitive impairment and pathological hallmarks in a mouse model of Alzheimer's disease. Neurobiol Aging. 2013;34(9):2133-45.

296. Kroker KS, Mathis C, Marti A, Cassel JC, Rosenbrock H, Dorner-Ciossek C. PDE9A inhibition rescues amyloid beta-induced deficits in synaptic plasticity and cognition. Neurobiol Aging. 2014;35(9):2072-8.
297. Beaumont V, Zhong S, Lin H, Xu W, Bradaia A, Steidl E, et al. Phosphodiesterase 10A Inhibition Improves Cortico-Basal Ganglia Function in Huntington's Disease Models. Neuron. 2016;92(6):1220-37.
298. Hojsgaard Chow H, Schreiber K, Magyari M, Ammitzboll C, Bornsen L, Romme Christensen J, et al. Progressive multiple sclerosis, cognitive function, and quality of life. Brain Behav. 2018;8(2):e00875.
299. Sidiropoulos K, Viteri G, Sevilla C, Jupe S, Webber M, Orlic-Milacic M, et al. Reactome enhanced pathway visualization. Bioinformatics. 2017;33(21):3461-7.
300. Bielekova B, Richert N, Howard T, Packer AN, Blevins G, Ohayon J, et al. Treatment with the phosphodiesterase type-4 inhibitor rolipram fails to inhibit blood--brain barrier disruption in multiple sclerosis. Mult Scler. 2009;15(10):1206-14.
301. Barkhof F, Hulst HE, Drulovic J, Uitdehaag BM, Matsuda K, Landin R, et al. Ibudilast in relapsing-remitting multiple sclerosis: a neuroprotectant? Neurology. 2010;74(13):1033-40.
302. Cho Y, Crichlow GV, Vermeire JJ, Leng L, Du X, Hodsdon ME, et al. Allosteric inhibition of macrophage migration inhibitory factor revealed by ibudilast. Proc Natl Acad Sci U S A. 2010;107(25):11313-8.
303. Ruiz-Perez D, Benito J, Polo G, Largo C, Aguado D, Sanz L, et al. The Effects of the Toll-Like Receptor 4 Antagonist, Ibudilast, on Sevoflurane's Minimum Alveolar Concentration and the Delayed Remifentanil-Induced Increase in the Minimum Alveolar Concentration in Rats. Anesth Analg. 2016;122(5):1370-6.
304. Fox RJ, Coffey CS, Conwit R, Cudkowicz ME, Gleason T, Goodman A, et al. Phase 2 Trial of Ibudilast in Progressive Multiple Sclerosis. N Engl J Med. 2018;379(9):846-55.
305. G. Burke SM, N. Davies, J.A. Palace, P.M. Matthews. Effect of sildenafil citrate (Viagra) on cerebral blood flow in patients with multiple sclerosis. Journal of Neurology Neurosurgery and Psychiatry 2005;77 (1): 023.
306. Huang Z, Liu S, Zhang L, Salem M, Greig GM, Chan CC, et al. Preferential inhibition of human phosphodiesterase 4 by ibudilast. Life Sci. 2006;78(23):2663-8.
307. Bao F, Fleming JC, Golshani R, Pearse DD, Kasabov L, Brown A, et al. A selective phosphodiesterase-4 inhibitor reduces leukocyte infiltration, oxidative processes, and tissue damage after spinal cord injury. J Neurotrauma. 2011;28(6):1035-49.
308. Reyes-Irisarri E, Pérez-Torres S, Mengod G. Neuronal expression of cAMP-specific phosphodiesterase 7B mRNA in the rat brain. Neuroscience. 2005;132(4):1173-85.

309. Paterniti I, Mazzon E, Gil C, Impellizzeri D, Palomo V, Redondo M, et al. PDE 7 inhibitors: new potential drugs for the therapy of spinal cord injury. PLoS One. 2011;6(1):e15937.
310. Titus DJ, Sakurai A, Kang Y, Furones C, Jergova S, Santos R, et al. Phosphodiesterase Inhibition Rescues Chronic Cognitive Deficits Induced by Traumatic Brain Injury. The Journal of Neuroscience. 2013;33(12):5216.
311. Lindsay MP, Norrving B, Sacco RL, Brainin M, Hacke W, Martins S, et al. World Stroke Organization (WSO): Global Stroke Fact Sheet 2019. Int J Stroke. 2019;14(8):806-17.
312. Anrather J, Iadecola C. Inflammation and Stroke: An Overview. Neurotherapeutics. 2016;13(4):661-70.
313. Yang F, Sumbria RK, Xue D, Yu C, He D, Liu S, et al. Effects of PDE4 pathway inhibition in rat experimental stroke. J Pharm Pharm Sci. 2014;17(3):362-70.
314. Xu B, Xu J, Cai N, Li M, Liu L, Qin Y, et al. Roflumilast prevents ischemic stroke-induced neuronal damage by restricting GSK3beta-mediated oxidative stress and IRE1alpha/TRAF2/JNK pathway. Free Radic Biol Med. 2021;163:281-96.
315. Xu B, Wang T, Xiao J, Dong W, Wen HZ, Wang X, et al. FCPR03, a novel phosphodiesterase 4 inhibitor, alleviates cerebral ischemia/reperfusion injury through activation of the AKT/GSK3beta/ beta-catenin signaling pathway. Biochem Pharmacol. 2019;163:234-49.
316. Chen J, Yu H, Zhong J, Feng H, Wang H, Cheng Y, et al. The phosphodiesterase-4 inhibitor, FCPR16, attenuates ischemia-reperfusion injury in rats subjected to middle cerebral artery occlusion and reperfusion. Brain Res Bull. 2018;137:98-106.
317. Bonato JM, Meyer E, de Mendonca PSB, Milani H, Prickaerts J, Weffort de Oliveira RM. Roflumilast protects against spatial memory impairments and exerts anti-inflammatory effects after transient global cerebral ischemia. Eur J Neurosci. 2021;53(4):1171-88.
318. Soares LM, De Vry J, Steinbusch HWM, Milani H, Prickaerts J, Weffort de Oliveira RM. Rolipram improves cognition, reduces anxiety- and despair-like behaviors and impacts hippocampal neuroplasticity after transient global cerebral ischemia. Neuroscience. 2016;326:69-83.
319. Redondo M, Zarruk JG, Ceballos P, Perez DI, Perez C, Perez-Castillo A, et al. Neuroprotective efficacy of quinazoline type phosphodiesterase 7 inhibitors in cellular cultures and experimental stroke model. Eur J Med Chem. 2012;47(1):175-85.
320. Bechay KR, Abduljawad N, Latifi S, Suzuki K, Iwashita H, Carmichael ST. PDE2A Inhibition Enhances Axonal Sprouting, Functional Connectivity, and Recovery after Stroke. J Neurosci. 2022;42(44):8225-36.
321. Beker MC, Pence ME, Yagmur S, Caglayan B, Caglayan A, Kilic U, et al. Phosphodiesterase 10A deactivation induces long-term neurological recovery, Peri-infarct remodeling and pyramidal tract plasticity after transient focal cerebral ischemia in mice. Exp Neurol. 2022;358:114221.

322. You JY, Liu XW, Bao YX, Shen ZN, Wang Q, He GY, et al. A novel phosphodiesterase 9A inhibitor LW33 protects against ischemic stroke through the cGMP/PKG/CREB pathway. Eur J Pharmacol. 2022;925:174987.
323. Jongen PJ, Ter Horst AT, Brands AM. Cognitive impairment in multiple sclerosis. Minerva Med. 2012;103(2):73-96.
324. Walikonis RS, Poduslo JF. Activity of cyclic AMP phosphodiesterases and adenylyl cyclase in peripheral nerve after crush and permanent transection injuries. J Biol Chem. 1998;273(15):9070-7.
325. Udina E, Ladak A, Furey M, Brushart T, Tyreman N, Gordon T. Rolipram-induced elevation of cAMP or chondroitinase ABC breakdown of inhibitory proteoglycans in the extracellular matrix promotes peripheral nerve regeneration. Exp Neurol. 2010;223(1):143-52.
326. Guo L, Moon C, Niehaus K, Zheng Y, Ratner N. Rac1 controls Schwann cell myelination through cAMP and NF2/merlin. J Neurosci. 2012;32(48):17251-61.
327. Ansi Chang MD, Wallace W. Tourtellotte, M.D., Ph.D., Richard Rudick, M.D., and Bruce D. Trapp, Ph.D. Premyelinating Oligodendrocytes in Chronic Lesions of Multiple Sclerosis. The New England Journal of Medicine. 2002;346:165-73.
328. Charles FRJMF-C. Remyelination in the CNS: from biology to therapy. Nature Reviews Neuroscience. 2008;9:839-55.
329. Wingerchuk DM, Carter JL. Multiple sclerosis: current and emerging disease-modifying therapies and treatment strategies. Mayo Clin Proc. 2014;89(2):225-40.
330. Henze T, Rieckmann P, Toyka KV, Multiple Sclerosis Therapy Consensus Group of the German Multiple Sclerosis S. Symptomatic treatment of multiple sclerosis. Multiple Sclerosis Therapy Consensus Group (MSTCG) of the German Multiple Sclerosis Society. Eur Neurol. 2006;56(2):78-105.
331. Raible DW, McMorris FA. Cyclic AMP regulates the rate of differentiation of oligodendrocytes without changing the lineage commitment of their progenitors. Dev Biol. 1989;133(2):437-46.
332. Mosenden R, Tasken K. Cyclic AMP-mediated immune regulation--overview of mechanisms of action in T cells. Cell Signal. 2011;23(6):1009-16.
333. Braun NN, Reutiman TJ, Lee S, Folsom TD, Fatemi SH. Expression of phosphodiesterase 4 is altered in the brains of subjects with autism. Neuroreport. 2007;18(17):1841-4.
334. Ugarte A, Gil-Bea F, Garcia-Barroso C, Cedazo-Minguez A, Ramirez MJ, Franco R, et al. Decreased levels of guanosine 3', 5'-monophosphate (cGMP) in cerebrospinal fluid (CSF) are associated with cognitive decline and amyloid pathology in Alzheimer's disease. Neuropathol Appl Neurobiol. 2015;41(4):471-82.
335. Richter W, Menniti FS, Zhang HT, Conti M. PDE4 as a target for cognition enhancement. Expert Opin Ther Targets. 2013;17(9):1011-27.
336. Houslay MD. Underpinning compartmentalised cAMP signalling through targeted cAMP breakdown. Trends Biochem Sci. 2010;35(2):91-100.

337. Bolger GB. Molecular biology of the cyclic AMP-specific cyclic nucleotide phosphodiesterases: a diverse family of regulatory enzymes. Cell Signal. 1994;6(8):851-9.
338. Johnson KR, Nicodemus-Johnson J, Danziger RS. An evolutionary analysis of cAMP-specific Phosphodiesterase 4 alternative splicing. BMC Evol Biol. 2010;10:247.
339. Bielekova B, Lincoln A, McFarland H, Martin R. Therapeutic potential of phosphodiesterase-4 and -3 inhibitors in Th1-mediated autoimmune diseases. J Immunol. 2000;164(2):1117-24.
340. Fox RJ, Coffey CS, Cudkowicz ME, Gleason T, Goodman A, Klawiter EC, et al. Design, rationale, and baseline characteristics of the randomized double-blind phase II clinical trial of ibudilast in progressive multiple sclerosis. Contemp Clin Trials. 2016;50:166-77.
341. Blokland A, Heckman P, Vanmierlo T, Schreiber R, Paes D, Prickaerts J. Phosphodiesterase Type 4 Inhibition in CNS Diseases. Trends Pharmacol Sci. 2019;40(12):971-85.
342. Mohammadnejad A, Li W, Lund JB, Li S, Larsen MJ, Mengel-From J, et al. Global Gene Expression Profiling and Transcription Factor Network Analysis of Cognitive Aging in Monozygotic Twins. Front Genet. 2021;12:675587.
343. Xiang J, Wang X, Gao Y, Li T, Cao R, Yan T, et al. Phosphodiesterase 4D Gene Modifies the Functional Network of Patients With Mild Cognitive Impairment and Alzheimer's Disease. Front Genet. 2020;11:890.
344. Zhang C, Xu Y, Zhang HT, Gurney ME, O'Donnell JM. Comparison of the Pharmacological Profiles of Selective PDE4B and PDE4D Inhibitors in the Central Nervous System. Sci Rep. 2017;7:40115.
345. Shi Y, Lv J, Chen L, Luo G, Tao M, Pan J, et al. Phosphodiesterase-4D Knockdown in the Prefrontal Cortex Alleviates Memory Deficits and Synaptic Failure in Mouse Model of Alzheimer's Disease. Front Aging Neurosci. 2021;13:722580.
346. Zhang C, Cheng Y, Wang H, Wang C, Wilson SP, Xu J, et al. RNA interference-mediated knockdown of long-form phosphodiesterase-4D (PDE4D) enzyme reverses amyloid-beta42-induced memory deficits in mice. J Alzheimers Dis. 2014;38(2):269-80.
347. Sierksma AS, van den Hove DL, Pfau F, Philippens M, Bruno O, Fedele E, et al. Improvement of spatial memory function in APPswe/PS1dE9 mice after chronic inhibition of phosphodiesterase type 4D. Neuropharmacology. 2014;77:120-30.
348. Cui SY, Yang MX, Zhang YH, Zheng V, Zhang HT, Gurney ME, et al. Protection from Amyloid beta Peptide-Induced Memory, Biochemical, and Morphological Deficits by a Phosphodiesterase-4D Allosteric Inhibitor. J Pharmacol Exp Ther. 2019;371(2):250-9.
349. Mori F, Perez-Torres S, De Caro R, Porzionato A, Macchi V, Beleta J, et al. The human area postrema and other nuclei related to the emetic reflex express cAMP phosphodiesterases 4B and 4D. J Chem Neuroanat. 2010;40(1):36-42.

350. Bruno O, Fedele E, Prickaerts J, Parker LA, Canepa E, Brullo C, et al. GEBR-7b, a novel PDE4D selective inhibitor that improves memory in rodents at non-emetic doses. Br J Pharmacol. 2011;164(8):2054-63.
351. Ricciarelli R, Brullo C, Prickaerts J, Arancio O, Villa C, Rebosio C, et al. Memory-enhancing effects of GEBR-32a, a new PDE4D inhibitor holding promise for the treatment of Alzheimer's disease. Sci Rep. 2017;7:46320.
352. Hatzelmann A, Morcillo EJ, Lungarella G, Adnot S, Sanjar S, Beume R, et al. The preclinical pharmacology of roflumilast--a selective, oral phosphodiesterase 4 inhibitor in development for chronic obstructive pulmonary disease. Pulm Pharmacol Ther. 2010;23(4):235-56.
353. Fox D, 3rd, Burgin AB, Gurney ME. Structural basis for the design of selective phosphodiesterase 4B inhibitors. Cell Signal. 2014;26(3):657-63.
354. Vanmierlo T, Rutten K, Dederen J, Bloks VW, van Vark-van der Zee LC, Kuipers F, et al. Liver X receptor activation restores memory in aged AD mice without reducing amyloid. Neurobiol Aging. 2011;32(7):1262-72.
355. Bailey CH, Bartsch D, Kandel ER. Toward a molecular definition of long-term memory storage. Proc Natl Acad Sci U S A. 1996;93(24):13445-52.
356. Garcia-Leon JA, Garcia-Diaz B, Eggermont K, Caceres-Palomo L, Neyrinck K, Madeiro da Costa R, et al. Generation of oligodendrocytes and establishment of an all-human myelinating platform from human pluripotent stem cells. Nat Protoc. 2020;15(11):3716-44.
357. Neyrinck K, Garcia-Leon JA. Single Transcription Factor-Based Differentiation Allowing Fast and Efficient Oligodendrocyte Generation via SOX10 Overexpression. Methods Mol Biol. 2021;2352:149-70.
358. Tiane A, Schepers M, Riemens R, Rombaut B, Vandormael P, Somers V, et al. DNA methylation regulates the expression of the negative transcriptional regulators ID2 and ID4 during OPC differentiation. Cell Mol Life Sci. 2021;78(19-20):6631-44.
359. Wouters K, Cudejko C, Gijbels MJ, Fuentes L, Bantubungi K, Vanhoutte J, et al. Bone marrow p16INK4a-deficiency does not modulate obesity, glucose homeostasis or atherosclerosis development. PLoS One. 2012;7(3):e32440.
360. Bechler ME. A Neuron-Free Microfiber Assay to Assess Myelin Sheath Formation. Methods Mol Biol. 2019;1936:97-110.
361. Shen MW, Arbab M, Hsu JY, Worstell D, Culbertson SJ, Krabbe O, et al. Predictable and precise template-free CRISPR editing of pathogenic variants. Nature. 2018;563(7733):646-51.
362. Peng H, Bria A, Zhou Z, Iannello G, Long F. Extensible visualization and analysis for multidimensional images using Vaa3D. Nat Protoc. 2014;9(1):193-208.
363. Maheshwari A, Janssens K, Bogie J, Van Den Haute C, Struys T, Lambrichts I, et al. Local overexpression of interleukin-11 in the central nervous system limits demyelination and enhances remyelination. Mediators Inflamm. 2013;2013:685317.

364. Branch SY, Beckstead MJ. Methamphetamine produces bidirectional, concentration-dependent effects on dopamine neuron excitability and dopamine-mediated synaptic currents. J Neurophysiol. 2012;108(3):802-9.
365. Nelissen E, van Goethem NP, Bonassoli VT, Heckman PRA, van Hagen BTJ, Suay D, et al. Validation of the xylazine/ketamine anesthesia test as a predictor of the emetic potential of pharmacological compounds in rats. Neurosci Lett. 2019;699:41-6.
366. Marenna S, Huang SC, Dalla Costa G, d'Isa R, Castoldi V, Rossi E, et al. Visual Evoked Potentials to Monitor Myelin Cuprizone-Induced Functional Changes. Front Neurosci. 2022;16:820155.
367. Sun X, Liu Y, Liu B, Xiao Z, Zhang L. Rolipram promotes remyelination possibly via MEK-ERK signal pathway in cuprizone-induced demyelination mouse. Exp Neurol. 2012;237(2):304-11.
368. Moore CS, Earl N, Frenette R, Styhler A, Mancini JA, Nicholson DW, et al. Peripheral phosphodiesterase 4 inhibition produced by 4-[2-(3,4-Bis-difluoromethoxyphenyl)-2-[4-(1,1,1,3,3,3-hexafluoro-2-hydroxypropan -2-yl)-phenyl]-ethyl]-3-methylpyridine-1-oxide (L-826,141) prevents experimental autoimmune encephalomyelitis. J Pharmacol Exp Ther. 2006;319(1):63-72.
369. Qin J, Sikkema AH, van der Bij K, de Jonge JC, Klappe K, Nies V, et al. GD1a Overcomes Inhibition of Myelination by Fibronectin via Activation of Protein Kinase A: Implications for Multiple Sclerosis. J Neurosci. 2017;37(41):9925-38.
370. Ridder WH, 3rd, Nusinowitz S. The visual evoked potential in the mouse--origins and response characteristics. Vision Res. 2006;46(6-7):902-13.
371. Wang SS, Bi HZ, Chu SF, Dong YX, He WB, Tian YJ, et al. CZ-7, a new derivative of Claulansine F, promotes remyelination induced by cuprizone by enhancing myelin debris clearance. Brain Res Bull. 2020;159:67-78.
372. Ding ZB, Han QX, Wang Q, Song LJ, Chu GG, Guo MF, et al. Fasudil enhances the phagocytosis of myelin debris and the expression of neurotrophic factors in cuprizone-induced demyelinating mice. Neurosci Lett. 2021;753:135880.
373. Thompson KK, Tsirka SE. Guanabenz modulates microglia and macrophages during demyelination. Sci Rep. 2020;10(1):19333.
374. Ran FA, Hsu PD, Wright J, Agarwala V, Scott DA, Zhang F. Genome engineering using the CRISPR-Cas9 system. Nat Protoc. 2013;8(11):2281-308.
375. Talla V, Yu H, Chou TH, Porciatti V, Chiodo V, Boye SL, et al. NADH-dehydrogenase type-2 suppresses irreversible visual loss and neurodegeneration in the EAE animal model of MS. Mol Ther. 2013;21(10):1876-88.
376. Locri F, Cammalleri M, Pini A, Dal Monte M, Rusciano D, Bagnoli P. Further Evidence on Efficacy of Diet Supplementation with Fatty Acids in Ocular Pathologies: Insights from the EAE Model of Optic Neuritis. Nutrients. 2018;10(10).
377. Sekyi MT, Lauderdale K, Atkinson KC, Golestany B, Karim H, Feri M, et al. Alleviation of extensive visual pathway dysfunction by a remyelinating drug in a chronic mouse model of multiple sclerosis. Brain Pathol. 2021;31(2):312-32.

378. Dos Santos N, Novaes LS, Dragunas G, Rodrigues JR, Brandao W, Camarini R, et al. High dose of dexamethasone protects against EAE-induced motor deficits but impairs learning/memory in C57BL/6 mice. Sci Rep. 2019;9(1):6673.
379. Hou B, Zhang Y, Liang P, He Y, Peng B, Liu W, et al. Inhibition of the NLRP3-inflammasome prevents cognitive deficits in experimental autoimmune encephalomyelitis mice via the alteration of astrocyte phenotype. Cell Death Dis. 2020;11(5):377.
380. Dutra RC, Moreira EL, Alberti TB, Marcon R, Prediger RD, Calixto JB. Spatial reference memory deficits precede motor dysfunction in an experimental autoimmune encephalomyelitis model: the role of kallikrein-kinin system. Brain Behav Immun. 2013;33:90-101.
381. Yoshimura T, Takeda A, Hamano S, Miyazaki Y, Kinjyo I, Ishibashi T, et al. Two-sided roles of IL-27: induction of Th1 differentiation on naive CD4+ T cells versus suppression of proinflammatory cytokine production including IL-23-induced IL-17 on activated CD4+ T cells partially through STAT3-dependent mechanism. J Immunol. 2006;177(8):5377-85.
382. Villarino A, Hibbert L, Lieberman L, Wilson E, Mak T, Yoshida H, et al. The IL-27R (WSX-1) is required to suppress T cell hyperactivity during infection. Immunity. 2003;19(5):645-55.
383. Hamano S, Himeno K, Miyazaki Y, Ishii K, Yamanaka A, Takeda A, et al. WSX-1 is required for resistance to Trypanosoma cruzi infection by regulation of proinflammatory cytokine production. Immunity. 2003;19(5):657-67.
384. Ariga M, Neitzert B, Nakae S, Mottin G, Bertrand C, Pruniaux MP, et al. Nonredundant function of phosphodiesterases 4D and 4B in neutrophil recruitment to the site of inflammation. J Immunol. 2004;173(12):7531-8.
385. Sunke R, Bankala R, Thirupataiah B, Ramarao E, Kumar JS, Doss HM, et al. InCl3 mediated heteroarylation of indoles and their derivatization via CH activation strategy: Discovery of 2-(1H-indol-3-yl)-quinoxaline derivatives as a new class of PDE4B selective inhibitors for arthritis and/or multiple sclerosis. Eur J Med Chem. 2019;174:198-215.
386. Batten M, Li J, Yi S, Kljavin NM, Danilenko DM, Lucas S, et al. Interleukin 27 limits autoimmune encephalomyelitis by suppressing the development of interleukin 17-producing T cells. Nat Immunol. 2006;7(9):929-36.
387. Stumhofer JS, Laurence A, Wilson EH, Huang E, Tato CM, Johnson LM, et al. Interleukin 27 negatively regulates the development of interleukin 17-producing T helper cells during chronic inflammation of the central nervous system. Nat Immunol. 2006;7(9):937-45.
388. Basole CP, Nguyen RK, Lamothe K, Billis P, Fujiwara M, Vang AG, et al. Treatment of Experimental Autoimmune Encephalomyelitis with an Inhibitor of Phosphodiesterase-8 (PDE8). Cells. 2022;11(4).
389. Glavas NA, Ostenson C, Schaefer JB, Vasta V, Beavo JA. T cell activation up-regulates cyclic nucleotide phosphodiesterases 8A1 and 7A3. Proc Natl Acad Sci U S A. 2001;98(11):6319-24.

390. Houslay MD, Schafer P, Zhang KY. Keynote review: phosphodiesterase-4 as a therapeutic target. Drug Discov Today. 2005;10(22):1503-19.
391. Vilhena ER, Bonato JM, Schepers M, Kunieda JKC, Milani H, Vanmierlo T, et al. Positive effects of roflumilast on behavior, neuroinflammation, and white matter injury in mice with global cerebral ischemia. Behav Pharmacol. 2021;32(6):459-71.
392. Cavalloro V, Russo K, Vasile F, Pignataro L, Torretta A, Donini S, et al. Insight into GEBR-32a: Chiral Resolution, Absolute Configuration and Enantiopreference in PDE4D Inhibition. Molecules. 2020;25(4).
393. Hannila SS, Filbin MT. The role of cyclic AMP signaling in promoting axonal regeneration after spinal cord injury. Exp Neurol. 2008;209(2):321-32.
394. Zhou G, Wang Z, Han S, Chen X, Li Z, Hu X, et al. Multifaceted Roles of cAMP Signaling in the Repair Process of Spinal Cord Injury and Related Combination Treatments. Front Mol Neurosci. 2022;15:808510.
395. Sciarretta C, Minichiello L. The preparation of primary cortical neuron cultures and a practical application using immunofluorescent cytochemistry. Methods Mol Biol. 2010;633:221-31.
396. Lo Monaco M, Gervois P, Beaumont J, Clegg P, Bronckaers A, Vandeweerd JM, et al. Therapeutic Potential of Dental Pulp Stem Cells and Leukocyte- and Platelet-Rich Fibrin for Osteoarthritis. Cells. 2020;9(4).
397. Evens L, Heeren E, Rummens JL, Bronckaers A, Hendrikx M, Deluyker D, et al. Advanced Glycation End Products Impair Cardiac Atrial Appendage Stem Cells Properties. J Clin Med. 2021;10(13).
398. Van Breedam E, Nijak A, Buyle-Huybrecht T, Di Stefano J, Boeren M, Govaerts J, et al. Luminescent Human iPSC-Derived Neurospheroids Enable Modeling of Neurotoxicity After Oxygen-glucose Deprivation. Neurotherapeutics. 2022;19(2):550-69.
399. Nelissen S, Vangansewinkel T, Geurts N, Geboes L, Lemmens E, Vidal PM, et al. Mast cells protect from post-traumatic spinal cord damage in mice by degrading inflammation-associated cytokines via mouse mast cell protease 4. Neurobiol Dis. 2014;62:260-72.
400. Dooley D, Lemmens E, Vangansewinkel T, Le Blon D, Hoornaert C, Ponsaerts P, et al. Cell-Based Delivery of Interleukin-13 Directs Alternative Activation of Macrophages Resulting in Improved Functional Outcome after Spinal Cord Injury. Stem Cell Reports. 2016;7(6):1099-115.
401. Moradi K, Golbakhsh M, Haghighi F, Afshari K, Nikbakhsh R, Khavandi MM, et al. Inhibition of phosphodiesterase IV enzyme improves locomotor and sensory complications of spinal cord injury via altering microglial activity: Introduction of Roflumilast as an alternative therapy. Int Immunopharmacol. 2020;86:106743.
402. Claveau D, Chen SL, O'Keefe S, Zaller DM, Styhler A, Liu S, et al. Preferential inhibition of T helper 1, but not T helper 2, cytokines in vitro by L-826,141 [4-[2-(3,4-Bisdifluromethoxyphenyl)-2-[4-(1,1,1,3,3,3-hexafluoro-2-hydroxypropan- 2-yl)-phenyl]-ethyl]3-methylpyridine-1-oxide], a potent and

selective phosphodiesterase 4 inhibitor. J Pharmacol Exp Ther. 2004;310(2):752-60.
403. Titus DJ, Wilson NM, Freund JE, Carballosa MM, Sikah KE, Furones C, et al. Chronic Cognitive Dysfunction after Traumatic Brain Injury Is Improved with a Phosphodiesterase 4B Inhibitor. J Neurosci. 2016;36(27):7095-108.
404. Erdely A, Kepka-Lenhart D, Clark M, Zeidler-Erdely P, Poljakovic M, Calhoun WJ, et al. Inhibition of phosphodiesterase 4 amplifies cytokine-dependent induction of arginase in macrophages. Am J Physiol Lung Cell Mol Physiol. 2006;290(3):L534-9.
405. Robel S, Berninger B, Gotz M. The stem cell potential of glia: lessons from reactive gliosis. Nature reviews Neuroscience. 2011;12(2):88-104.
406. Sofroniew MV. Molecular dissection of reactive astrogliosis and glial scar formation. Trends Neurosci. 2009;32(12):638-47.
407. Kanemaru K, Kubota J, Sekiya H, Hirose K, Okubo Y, Iino M. Calcium-dependent N-cadherin up-regulation mediates reactive astrogliosis and neuroprotection after brain injury. Proc Natl Acad Sci U S A. 2013;110(28):11612-7.
408. Fawcett JW, Asher RA. The glial scar and central nervous system repair. Brain research bulletin. 1999;49(6):377-91.
409. Costa LM, Pereira JE, Filipe VM, Magalhaes LG, Couto PA, Gonzalo-Orden JM, et al. Rolipram promotes functional recovery after contusive thoracic spinal cord injury in rats. Behav Brain Res. 2013;243:66-73.
410. Freyermuth-Trujillo X, Segura-Uribe JJ, Salgado-Ceballos H, Orozco-Barrios CE, Coyoy-Salgado A. Inflammation: A Target for Treatment in Spinal Cord Injury. Cells. 2022;11(17).
411. Lin ZH, Wang SY, Chen LL, Zhuang JY, Ke QF, Xiao DR, et al. Methylene Blue Mitigates Acute Neuroinflammation after Spinal Cord Injury through Inhibiting NLRP3 Inflammasome Activation in Microglia. Front Cell Neurosci. 2017;11:391.
412. David S, Greenhalgh AD, Kroner A. Macrophage and microglial plasticity in the injured spinal cord. Neuroscience. 2015;307:311-8.
413. Hartline DK, Colman DR. Rapid conduction and the evolution of giant axons and myelinated fibers. Curr Biol. 2007;17(1):R29-35.
414. Lambertsen KL, Finsen B, Clausen BH. Post-stroke inflammation-target or tool for therapy? Acta Neuropathol. 2019;137(5):693-714.
415. Jayaraj RL, Azimullah S, Beiram R, Jalal FY, Rosenberg GA. Neuroinflammation: friend and foe for ischemic stroke. J Neuroinflammation. 2019;16(1):142.
416. Kim E, Cho S. Microglia and Monocyte-Derived Macrophages in Stroke. Neurotherapeutics. 2016;13(4):702-18.
417. Gill D, Veltkamp R. Dynamics of T cell responses after stroke. Curr Opin Pharmacol. 2016;26:26-32.
418. Mracsko E, Liesz A, Stojanovic A, Lou WP, Osswald M, Zhou W, et al. Antigen dependently activated cluster of differentiation 8-positive T cells cause

perforin-mediated neurotoxicity in experimental stroke. J Neurosci. 2014;34(50):16784-95.
419. Liesz A, Hu X, Kleinschnitz C, Offner H. Functional role of regulatory lymphocytes in stroke: facts and controversies. Stroke. 2015;46(5):1422-30.
420. Arumugham VB, Baldari CT. cAMP: a multifaceted modulator of immune synapse assembly and T cell activation. J Leukoc Biol. 2017;101(6):1301-16.
421. Tibbo AJ, Baillie GS. Phosphodiesterase 4B: Master Regulator of Brain Signaling. Cells. 2020;9(5).
422. Kemps H, Dessy C, Dumas L, Sonveaux P, Alders L, Van Broeckhoven J, et al. Extremely low frequency electromagnetic stimulation reduces ischemic stroke volume by improving cerebral collateral blood flow. J Cereb Blood Flow Metab. 2022;42(6):979-96.
423. Perez-de-Puig I, Miro-Mur F, Ferrer-Ferrer M, Gelpi E, Pedragosa J, Justicia C, et al. Neutrophil recruitment to the brain in mouse and human ischemic stroke. Acta Neuropathol. 2015;129(2):239-57.
424. Wuyts A, Schutyser E, Menten P, Struyf S, D'Haese A, Bult H, et al. Biochemical and biological characterization of neutrophil chemotactic protein, a novel rabbit CXC chemokine from alveolar macrophages. Biochemistry. 2000;39(47):14549-57.
425. Bhaskar S, Stanwell P, Cordato D, Attia J, Levi C. Reperfusion therapy in acute ischemic stroke: dawn of a new era? BMC Neurol. 2018;18(1):8.
426. Lakics V, Karran EH, Boess FG. Quantitative comparison of phosphodiesterase mRNA distribution in human brain and peripheral tissues. Neuropharmacology. 2010;59(6):367-74.
427. Lerner A, Epstein PM. Cyclic nucleotide phosphodiesterases as targets for treatment of haematological malignancies. Biochem J. 2006;393(Pt 1):21-41.
428. Jacob C, Leport M, Szilagyi C, Allen JM, Bertrand C, Lagente V. DMSO-treated HL60 cells: a model of neutrophil-like cells mainly expressing PDE4B subtype. Int Immunopharmacol. 2002;2(12):1647-56.
429. Wang H, Gaur U, Xiao J, Xu B, Xu J, Zheng W. Targeting phosphodiesterase 4 as a potential therapeutic strategy for enhancing neuroplasticity following ischemic stroke. Int J Biol Sci. 2018;14(12):1745-54.
430. Han SH, Yun SH, Shin YK, Park HT, Park JI. Heat Shock Protein 90 is Required for cAMP-Induced Differentiation in Rat Primary Schwann Cells. Neurochem Res. 2019;44(11):2643-57.
431. Bacallao K, Monje PV. Requirement of cAMP signaling for Schwann cell differentiation restricts the onset of myelination. PLoS One. 2015;10(2):e0116948.
432. Jessen KR, Mirsky R, Morgan L. Role of cyclic AMP and proliferation controls in Schwann cell differentiation. Ann N Y Acad Sci. 1991;633:78-89.
433. Monje PV, Soto J, Bacallao K, Wood PM. Schwann cell dedifferentiation is independent of mitogenic signaling and uncoupled to proliferation: role of cAMP and JNK in the maintenance of the differentiated state. J Biol Chem. 2010;285(40):31024-36.

434. Parkinson DB, Bhaskaran A, Arthur-Farraj P, Noon LA, Woodhoo A, Lloyd AC, et al. c-Jun is a negative regulator of myelination. J Cell Biol. 2008;181(4):625-37.
435. Monje PV, Rendon S, Athauda G, Bates M, Wood PM, Bunge MB. Non-antagonistic relationship between mitogenic factors and cAMP in adult Schwann cell re-differentiation. Glia. 2009;57(9):947-61.
436. Morgan L, Jessen KR, Mirsky R. The effects of cAMP on differentiation of cultured Schwann cells: progression from an early phenotype (04+) to a myelin phenotype (P0+, GFAP-, N-CAM-, NGF-receptor-) depends on growth inhibition. J Cell Biol. 1991;112(3):457-67.
437. Han SH, Kim YH, Park SJ, Cho JG, Shin YK, Hong YB, et al. COUP-TFII plays a role in cAMP-induced Schwann cell differentiation and in vitro myelination by up-regulating Krox20. J Neurochem. 2023.
438. Yamada H, Komiyama A, Suzuki K. Schwann cell responses to forskolin and cyclic AMP analogues: comparative study of mouse and rat Schwann cells. Brain Res. 1995;681(1-2):97-104.
439. Glenn TD, Talbot WS. Analysis of Gpr126 function defines distinct mechanisms controlling the initiation and maturation of myelin. Development. 2013;140(15):3167-75.
440. Monje PV. To myelinate or not to myelinate: fine tuning cAMP signaling in Schwann cells to balance cell proliferation and differentiation. Neural Regen Res. 2015;10(12):1936-7.
441. Tibbo AJ, Tejeda GS, Baillie GS. Understanding PDE4's function in Alzheimer's disease; a target for novel therapeutic approaches. Biochem Soc Trans. 2019;47(5):1557-65.
442. Schepers M, Paes D, Tiane A, Rombaut B, Piccart E, van Veggel L, et al. Selective PDE4 subtype inhibition provides new opportunities to intervene in neuroinflammatory versus myelin damaging hallmarks of multiple sclerosis. Brain Behav Immun. 2023;109:1-22.
443. Malheiro A, Morgan F, Baker M, Moroni L, Wieringa P. A three-dimensional biomimetic peripheral nerve model for drug testing and disease modelling. Biomaterials. 2020;257:120230.
444. Malheiro A, Harichandan A, Bernardi J, Seijas-Gamardo A, Konings GF, Volders PGA, et al. 3D culture platform of human iPSCs-derived nociceptors for peripheral nerve modeling and tissue innervation. Biofabrication. 2021;14(1).
445. Kaewkhaw R, Scutt AM, Haycock JW. Integrated culture and purification of rat Schwann cells from freshly isolated adult tissue. Nat Protoc. 2012;7(11):1996-2004.
446. Chambers SM, Qi Y, Mica Y, Lee G, Zhang XJ, Niu L, et al. Combined small-molecule inhibition accelerates developmental timing and converts human pluripotent stem cells into nociceptors. Nat Biotechnol. 2012;30(7):715-20.
447. Bacallao K, Monje PV. Opposing roles of PKA and EPAC in the cAMP-dependent regulation of schwann cell proliferation and differentiation [corrected]. PLoS One. 2013;8(12):e82354.

448. Britsch S, Goerich DE, Riethmacher D, Peirano RI, Rossner M, Nave KA, et al. The transcription factor Sox10 is a key regulator of peripheral glial development. Genes Dev. 2001;15(1):66-78.
449. Sobue G, Pleasure D. Schwann cell galactocerebroside induced by derivatives of adenosine 3',5'-monophosphate. Science. 1984;224(4644):72-4.
450. Raff MC, Hornby-Smith A, Brockes JP. Cyclic AMP as a mitogenic signal for cultured rat Schwann cells. Nature. 1978;273(5664):672-3.
451. Sanders O, Rajagopal L. Phosphodiesterase Inhibitors for Alzheimer's Disease: A Systematic Review of Clinical Trials and Epidemiology with a Mechanistic Rationale. J Alzheimers Dis Rep. 2020;4(1):185-215.
452. Parker BJ, Rhodes DI, O'Brien CM, Rodda AE, Cameron NR. Nerve guidance conduit development for primary treatment of peripheral nerve transection injuries: A commercial perspective. Acta Biomater. 2021;135:64-86.
453. Szigeti K, Lupski JR. Charcot-Marie-Tooth disease. Eur J Hum Genet. 2009;17(6):703-10.
454. Timmerman V, Nelis E, Van Hul W, Nieuwenhuijsen BW, Chen KL, Wang S, et al. The peripheral myelin protein gene PMP-22 is contained within the Charcot-Marie-Tooth disease type 1A duplication. Nat Genet. 1992;1(3):171-5.
455. Li J, Parker B, Martyn C, Natarajan C, Guo J. The PMP22 gene and its related diseases. Mol Neurobiol. 2013;47(2):673-98.
456. Gess B, Baets J, De Jonghe P, Reilly MM, Pareyson D, Young P. Ascorbic acid for the treatment of Charcot-Marie-Tooth disease. Cochrane Database Syst Rev. 2015;2015(12):CD011952.
457. Sereda MW, Meyer zu Horste G, Suter U, Uzma N, Nave KA. Therapeutic administration of progesterone antagonist in a model of Charcot-Marie-Tooth disease (CMT-1A). Nat Med. 2003;9(12):1533-7.
458. Bush M. The role of unconscious guilt in psychopathology and psychotherapy. Bull Menninger Clin. 1989;53(2):97-107.
459. Grandis M, Shy ME. Current Therapy for Charcot-Marie-Tooth Disease. Curr Treat Options Neurol. 2005;7(1):23-31.
460. Fledrich R, Stassart RM, Klink A, Rasch LM, Prukop T, Haag L, et al. Soluble neuregulin-1 modulates disease pathogenesis in rodent models of Charcot-Marie-Tooth disease 1A. Nat Med. 2014;20(9):1055-61.
461. Kiepura AJ, Kochanski A. Charcot-Marie-Tooth type 1A drug therapies: role of adenylyl cyclase activity and G-protein coupled receptors in disease pathomechanism. Acta Neurobiol Exp (Wars). 2018;78(3):198-209.
462. Nobbio L, Visigalli D, Mannino E, Fiorese F, Kassack MU, Sturla L, et al. The diadenosine homodinucleotide P18 improves in vitro myelination in experimental Charcot-Marie-Tooth type 1A. J Cell Biochem. 2014;115(1):161-7.
463. Chen CC, Gilmore A, Zuo Y. Study motor skill learning by single-pellet reaching tasks in mice. J Vis Exp. 2014(85).
464. Pollari E, Prior R, Robberecht W, Van Damme P, Van Den Bosch L. In Vivo Electrophysiological Measurement of Compound Muscle Action Potential from the Forelimbs in Mouse Models of Motor Neuron Degeneration. J Vis Exp. 2018(136).

465. Fledrich R, Abdelaal T, Rasch L, Bansal V, Schutza V, Brugger B, et al. Targeting myelin lipid metabolism as a potential therapeutic strategy in a model of CMT1A neuropathy. Nat Commun. 2018;9(1):3025.
466. Passage E, Norreel JC, Noack-Fraissignes P, Sanguedolce V, Pizant J, Thirion X, et al. Ascorbic acid treatment corrects the phenotype of a mouse model of Charcot-Marie-Tooth disease. Nat Med. 2004;10(4):396-401.
467. Prior R, Verschoren S, Vints K, Jaspers T, Rossaert E, Klingl YE, et al. HDAC3 Inhibition Stimulates Myelination in a CMT1A Mouse Model. Mol Neurobiol. 2022;59(6):3414-30.
468. Flora G, Joseph G, Patel S, Singh A, Bleicher D, Barakat DJ, et al. Combining neurotrophin-transduced schwann cells and rolipram to promote functional recovery from subacute spinal cord injury. Cell Transplant. 2013;22(12):2203-17.
469. Schmidt R. Motor learning principles for physical therapy in MJ Lister (ed.), Contemporary management of motor control problems: proceedings of the II-STEP conference (pp. 49-63). Alexandria, VA: Foundation for Physical Therapy. 1991.
470. Honda M, Deiber MP, Ibanez V, Pascual-Leone A, Zhuang P, Hallett M. Dynamic cortical involvement in implicit and explicit motor sequence learning. A PET study. Brain. 1998;121 (Pt 11):2159-73.
471. Karni A, Meyer G, Jezzard P, Adams MM, Turner R, Ungerleider LG. Functional MRI evidence for adult motor cortex plasticity during motor skill learning. Nature. 1995;377(6545):155-8.
472. Kleim JA, Hogg TM, VandenBerg PM, Cooper NR, Bruneau R, Remple M. Cortical synaptogenesis and motor map reorganization occur during late, but not early, phase of motor skill learning. J Neurosci. 2004;24(3):628-33.
473. Parker V, Warman Chardon J, Mills J, Goldsmith C, Bourque PR. Supramaximal Stimulus Intensity as a Diagnostic Tool in Chronic Demyelinating Neuropathy. Neurosci J. 2016;2016:6796270.
474. Ferreira A, Caceres A. Expression of the class III beta-tubulin isotype in developing neurons in culture. J Neurosci Res. 1992;32(4):516-29.
475. Latremoliere A, Cheng L, DeLisle M, Wu C, Chew S, Hutchinson EB, et al. Neuronal-Specific TUBB3 Is Not Required for Normal Neuronal Function but Is Essential for Timely Axon Regeneration. Cell Rep. 2018;24(7):1865-79 e9.
476. Jiang YQ, Oblinger MM. Differential regulation of beta III and other tubulin genes during peripheral and central neuron development. J Cell Sci. 1992;103 (Pt 3):643-51.
477. Jin SL, Goya S, Nakae S, Wang D, Bruss M, Hou C, et al. Phosphodiesterase 4B is essential for T(H)2-cell function and development of airway hyperresponsiveness in allergic asthma. J Allergy Clin Immunol. 2010;126(6):1252-9 e12.
478. Boato F, Hendrix S, Huelsenbeck SC, Hofmann F, Grosse G, Djalali S, et al. C3 peptide enhances recovery from spinal cord injury by improved regenerative growth of descending fiber tracts. J Cell Sci. 2010;123(Pt 10):1652-62.

479. Jucker M. The benefits and limitations of animal models for translational research in neurodegenerative diseases. Nat Med. 2010;16(11):1210-4.
480. Horn CC, Kimball BA, Wang H, Kaus J, Dienel S, Nagy A, et al. Why can't rodents vomit? A comparative behavioral, anatomical, and physiological study. PLoS One. 2013;8(4):e60537.
481. Robichaud A, Savoie C, Stamatiou PB, Tattersall FD, Chan CC. PDE4 inhibitors induce emesis in ferrets via a noradrenergic pathway. Neuropharmacology. 2001;40(2):262-9.
482. Gurney ME, D'Amato EC, Burgin AB. Phosphodiesterase-4 (PDE4) molecular pharmacology and Alzheimer's disease. Neurotherapeutics. 2015;12(1):49-56.
483. Anton SE, Kayser C, Maiellaro I, Nemec K, Moller J, Koschinski A, et al. Receptor-associated independent cAMP nanodomains mediate spatiotemporal specificity of GPCR signaling. Cell. 2022;185(7):1130-42 e11.
484. Rouanet C, Reges D, Rocha E, Gagliardi V, Silva GS. Traumatic spinal cord injury: current concepts and treatment update. Arq Neuropsiquiatr. 2017;75(6):387-93.
485. Filli L, Schwab ME. The rocky road to translation in spinal cord repair. Ann Neurol. 2012;72(4):491-501.
486. Ropper AE, Ropper AH. Acute Spinal Cord Compression. N Engl J Med. 2017;376(14):1358-69.
487. Luengo-Fernandez R, Violato M, Candio P, Leal J. Economic burden of stroke across Europe: A population-based cost analysis. Eur Stroke J. 2020;5(1):17-25.
488. Taylor TN, Davis PH, Torner JC, Holmes J, Meyer JW, Jacobson MF. Lifetime cost of stroke in the United States. Stroke. 1996;27(9):1459-66.
489. Zhang S, Huang M, Zhi J, Wu S, Wang Y, Pei F. Research Hotspots and Trends of Peripheral Nerve Injuries Based on Web of Science From 2017 to 2021: A Bibliometric Analysis. Front Neurol. 2022;13:872261.
490. Karsy M, Watkins R, Jensen MR, Guan J, Brock AA, Mahan MA. Trends and Cost Analysis of Upper Extremity Nerve Injury Using the National (Nationwide) Inpatient Sample. World Neurosurg. 2019;123:e488-e500.
491. Schorling E, Thiele S, Gumbert L, Krause S, Klug C, Schreiber-Katz O, et al. Cost of illness in Charcot-Marie-Tooth neuropathy: Results from Germany. Neurology. 2019;92(17):e2027-e37.
492. Hwang H, Shin JY, Park KR, Shin JO, Song KH, Park J, et al. Effect of a Dose-Escalation Regimen for Improving Adherence to Roflumilast in Patients with Chronic Obstructive Pulmonary Disease. Tuberc Respir Dis (Seoul). 2015;78(4):321-5.
493. Oskarsson B, Maragakis N, Bedlack RS, Goyal N, Meyer JA, Genge A, et al. MN-166 (ibudilast) in amyotrophic lateral sclerosis in a Phase IIb/III study: COMBAT-ALS study design. Neurodegener Dis Manag. 2021;11(6):431-43.

Curriculum Vitae

Personal details:

Nationality	Belgian
Birth	Tongeren, October 25th, 1994
Position title	PhD student

EDUCATION

2017-present **PhD student**

Targeting phosphodiesterase 4 to treat multiple sclerosis.
Joint PhD: department of Neuro-immunology, Hasselt University, Diepenbeek (Belgium) and Department of mental health and neuroscience, Maastricht University, Maastricht (The Netherlands).
Promotors: Prof. Dr. Tim Vanmierlo and Prof. Dr. Jos Prickaerts.
Co-promotors: Prof. Dr. Niels Hellings and Prof. Dr. Bart Rutten.

2015-2017 **Master in Clinical and Molecular Life Sciences**

Transnational University Limburg campus Universiteit Hasselt (Diepenbeek, België)
Magna Cum Lauda (great distinction)

2012-2015 **Bachelor Biomedical Sciences**

Hasselt University (Campus Diepenbeek, België)

SCIENTIFIC OUTPUT

First author publications:

1. **Schepers M.**, Vanmierlo T.
   Novel insights in phosphodiesterase 4 subtype inhibition to target neuroinflammation and stimulate remyelination
   Accepted for publication in Neural Regeneration Research, 2023 (**IF 6.058**)

2. **Schepers M**.*, Malheiro A.*, Seijas Gamardo A., Hellings N., Prickaerts J., Moroni L., Wieringa P. #, Vanmierlo T. #
   Phosphodiesterase (PDE) 4 inhibition boosts Schwann cell myelination in a 3D regeneration model
   European Journal of Pharmaceutical Science, 2023 (**IF 5.112**)

3. **Schepers M.,** Paes D., Tiane A., Rombaut B., Piccart Elisabeth., van Veggel L., Gervois P., Wolfs E., Lambrichts I., Brullo C., Bruno O., Fedele E., Ricciarelli R., ffrench-Constant C., Bechler M.E., van Schaik P., Baron W., Lefevere E., Wasner K., Grünewald A., Verfaillie C., Baeten P., Broux B., Wieringa P., Hellings N., Prickaerts J.*, Vanmierlo T. *
   Selective PDE4 subtype inhibition provides new opportunities to intervene in neuroinflammatory versus myelin damaging hallmarks of multiple sclerosis
   Brain Behavior and Immunity, 2023 (**IF 19.227**)

4. **Schepers M.***, Martens N.*, Zhan N., Leijten F., Voortman G., Tiane A., Rombaut B., Poisquet J., van de Sande N., Kerksiek A., Kuipers F., Jonker J., Liu H. , Lütjohann D. *, Mulder T. *, Vanmierlo T. *
   24(S)-Saringosterol prevents cognitive decline in a mouse model for Alzheimer's disease Mar Drugs. 2021 Mar 27;19(4):190. **(IF 5.118)**

5. **Schepers M.**, Martens N., Tiane A., Vanbrabant K., Liu H.B., Lütjohann D., Mulder M.* & Vanmierlo T.*
   Edible seaweed-derived constituents, an undisclosed source of neuroprotective compounds Neural Regenerative Research 2020 May;15(5):790-795 **(IF 5.14)**

6. **Schepers M.**, Tiane A., Paes D., Sanchez S., Rombaut B., Piccart E., Rutten B.P.F., Brône B., Hellings N., Prickaerts J., Vanmierlo T.
   Targeting phosphodiesterases – towards a tailor-made approach in multiple sclerosis treatment
   Frontiers Immunology, 2019 24;10:1727 **(IF 5.09)**

Last author publications:

1. Mussen F.*, Van Broeckhoven J.*, Hellings N., Vanmierlo T.#, **Schepers M.#**
   Unleashing Spinal Cord Repair: The Role of cAMP-Specific PDE Inhibition in Attenuating Neuroinflammation and Boosting Regeneration after Traumatic Spinal Cord Injury
   International Journal of Molecular Sciences, 2023 (**IF 6.208**)

First author papers in submission or preperation:

1. **Schepers M**.*, Hendrix S.*, van Breedam E., Ponsaerts P., Lemmens S., Ricciarelli R., Fedele E., Bruno O., Brullo C., Hellings N., Prickaerts J., Van Broeckhoven J. #, Vanmierlo T.#
   Inhibition of phosphodiesterase 4D (PDE4D) improves functional and histopathological outcome after hemisection spinal cord injury
   Manuscript in preperation

2. **Schepers M**.*, Vangansewinkel T.,*, Libberecht K.*, Jacobs D., Piccart E., Jeurissen H., Prior R., Ricciarelli R., Brullo C, Fedele E., Bruno O., Prickaerts J., Van Den Bosch L., Lambrichts I.#, Vanmierlo T.#, Wolfs E.#
   PDE4D inhibition to treat Charcot-Marie-Tooth disease type 1A
   Manuscript in preperation

Co-author publications

1. Paes D., **Schepers M.,** Willems E., Rombaut B., Tiane A., Solomina Y., Tibbo A., Blair C., Kyurkchieva E., Baillie G.S., Ricciarelli R., Brullo C., Fedele E., Bruno O., van den Hove D.*, Vanmierlo T.*, Prickaerts J.*
   Ablation of specific long PDE4D isoforms increases neurite elongation and conveys protection against amyloid-β pathology
   Accepted for publication in Clinical and Molecular Life Sciences (**IF 9.234**)

2. Nelissen E., Possemis N., Van Goethem NP., **Schepers M**., Mulder-Jongen DAJ., Dietz L., Janssen W., Gerisch M., Hüser J., Sandner P., Vanmierlo T., Prickaerts J. The sGC stimulator BAY-747 and activator runcaciguat can enhance memory in vivo via differential hippocampal plasticity mechanisms
   Scientific reports 2022; 12(1):3589 **(IF 4.996)**

3. Tiane A., **Schepers M**., Riemens R., Rombaut B., Vandormael P., Somers V., Prickaerts J., Hellings N., van den Hove D., Vanmierlo T.
   DNA methylation regulates the expression of the negative transcriptional regulators ID2 and ID4 during OPC differentiation
   Cellular and molecular life sciences 2021; 78(19-20):6631-6644 **(IF 9.261)**

4. Vilhena E., Bonato J., **Schepers M**, Kunieda J., Milani H., Vanmierlo T., Prickaerts J., de Oliveira R. Positive effects of roflumilast on behavior, neuroinflammation, and white matter injury in mice with global cerebral ischemia
   Behavioural Pharmacology 2021; 32(6):459-471 (**IF 2.148**)

5. Paes D., **Schepers M.,** Rombaut B., van den Hove D., Vanmierlo T. , Prickaerts J.
   The molecular biology of PDE4 enzymes as pharmacological targets: An interplay of isoforms, conformational states, and inhibitors
   Pharmacological Reviews 2021; 73(3):1016-1049 (**IF 25.468**)

6. Ponsaerts L., Alders L., **Schepers M**., de Oliveira R., Prickaerts J., Vanmierlo T., Bronckaers A.
   Neuroinflammation in Ischemic Stroke: Inhibition of cAMP-Specific Phosphodiesterases (PDEs) to the Rescue
   Biomedicines 2021; 22;9(7):703 (**IF 6.08**)

7. Vanbrabant K., Van Meel D., Kerksiek A., Friedrichs S., Dubbeldam M., **Schepers M**., Zhan N., Gutbrod K., Dörmann P., Liu H., Mulder M., Vanmierlo T., Lütjohann D.
   24 (R, S)-Saringosterol From artefact to a biological medical agent
   The Journal of Steroid Biochemistry and Molecular Biology 212:105942 (**IF 3.785**)

8. Spaas J.*, van Veggel L.*, **Schepers M**., Tiane A., van Horssen J., Wilson D.M.III, Moya P., Piccart E., Hellings N., Eijnde B.O., Derave W., Schreiber R., Vanmierlo T.
   Oxidative stress and impaired oligodendrocyte precursor cell differentiation in neurological disorders
   Cellular and molecular life sciences 2021; 202178(10);4615-4637 (**IF 9.261**)

9. Rombaut B., Kessels S., **Schepers M.,** Tiane A., Paes D., Solomina Y., Piccart E., van den Hove D., Brône B., Prickaerts J. and Vanmierlo T.
   PDE inhibition in distinct cell types to reclaim the balance of synaptic plasticity
   Theranostics 2021; 11(5): 2080-2097. **(IF 11.556)**

10. Roggeri A., **Schepers M**., Tiane A., van Veggel L., Hellings N, Prickaerts J, Pittaluga A, Vanmierlo T.
    Sphingosine-1-phospate receptor modulators and oligodendroglial cells: beyond immunomodulation.
    International Journal of Molecular Sciences. 2020 Oct 13;21(20):E7537. (**IF 5.92**)

11. Paes D., Lardenoije R., Carollo R.M., Roubroeks J.A.Y., **Schepers M.,** Coleman P., Mastroeni D., Delvaux E., Pishva E., Lunnon K., van den Hove D[*]. , Prickaerts J. [*] , Vanmierlo T. [*]
    Increased isoform-specific phosphodiesterase 4D (PDE4D) expression is associated with pathology and cognitive impairment in Alzheimer's disease
    Neurobiology of Aging. 2020 Oct 9;97:56-64. (**IF 4.35**)

12. Houben E., Janssens K., Hermans D., Vandooren J. , Van den Haute C., **Schepers M**., Vanmierlo T., Lambrichts I. , van Horssen J., Baekelandt V., Opdenakker G. , Baron W., Broux B., Slaets H, Hellings N., Oncostatin M-induced astrocytic tissue inhibitor of 2 metalloproteinases-1 drives remyelination
    PNAS, 2020 Mar 3;117(9):5028-5038 **(IF 10.70)**

13. Tiane A., **Schepers M**., Rombaut B., Hupperts R., Prickaerts J., Hellings N., van den Hove D., Vanmierlo T.
    From OPC to oligodendrocyte – an epigenetic journey
    Cells. 2019 Oct 11;8(10). pii: E1236. (**IF 4.37**)

14. Bogie J.*, Hoeks C.*, **Schepers M,** Tiane A., Cuypers A., Leijten F., Chintapakorn Y, Suttiyut T, Pornpakakul S., Struik D., Kerksiek A., Liu H.B., Hellings N., Martinez-Martinez P., Jonker J.W., Dewachter I., Sijbrands E., Walter J., Hendriks J., Groen A.K., Staels B., Lütjohann D., Mulder M.* & Vanmierlo T.*
    Dietary Sargassum fusiforme improves memory and reduces amyloid plaque load in an Alzheimer's disease mouse model.,
    Scientific Reports 2019 Mar 20;9(1):4908. (**IF 4.01**)

15. Santiago A., Soares L., **Schepers M**., Milani H., Vanmierlo T., Prickaerts J., Weffort Oliveira R.
    Roflumilast promotes memory recovery and attenuates white matter injury in aged rats subjected to chronic cerebral hypoperfusion.
    Neuropharmacology. 2018 Aug;138:360-370 (**IF 4.37**)

16. Nelissen E., De Vry J., Antonides A., Paes D., **Schepers M**., van der Staay FJ, Prickaerts J., Vanmierlo T.
    Early-postnatal iron deficiency impacts plasticity in the dorsal and ventral hippocampus in piglets.
    International Journal of Developmental Neuroscience. 2017 Jun;59:47-51 **(IF 2.50)**

Patents:

PCT filing PCT/EP2022/065055, title: "COMPOUNDS AND PHARMACEUTICAL COMPOSITIONS FOR USE IN NEURODEGENERATIVE DISORDERS"

Oral presentations (selected):

Title: Selective PDE4 subtype inhibition provides new opportunities to intervene in neuroinflammatory versus myelin damaging hallmarks of MS

Conferences presented:

MS research days 2022

Title: Phosphodiesterase 4D inhibition to boost remyelination in multiple sclerosis

Conferences presented:

Figon DMD 2022

EURON - Life Science PhD days 2019

Title: Myelin, PDE4B and neuroinflammation; the good, the bad, and the ugly

Conferences presented:

Flemish MS Research Days 2023

F-TALES neuroimmune cross-talk in health and disease 2022

Dutch Neuroscience meeting 2021

Title: The phosphodiesterase 4 inhibitor roflumilast improves remyelination in a mouse model for multiple sclerosis

Conferences presented:

Hot topics in signal transduction & cGMP research 2018

Gordon Research Seminar and Conference - Cyclic nucleotide phosphodiesterases 2018

Poster presentations:

Title: Inhibition of phosphodiesterase 4D but not 4B improves functional and histopathological outcome after hemisection spinal cord injury

Conferences presented:

Gordon Research Conference Cyclic nucleotide phosphodiesterases 2022

Title: Myelin, PDE4B and neuroinflammation; the good, the bad, and the ugly

Conferences presented:

F-TALES neuroimmune cross-talk in health and disease 2022

EURON PhD days 2021

Title: Phosphodiesterase 4D inhibition boosts remyelination in multiple sclerosis

Conferences presented:

Biotrinity 2021

Meeting of the Belgian Society for Neuroscience 2019

Title: The phosphodiesterase 4 inhibitor roflumilast improves remyelination in a mouse model for multiple sclerosis

Conferences presented:

Animal behavior, a 'perfect' read-out of the human functioning brain 2018

Glia 2019

Grants:

2023	Network Glia stipend
2019-2023	FWO-SB fellowship
2018-2020	Charcot foundation/MS Liga belgium grant **(€40k)**
2019	EURON mobility grant **(€1500)**
2019	Hasselt University doctoral school mobility grant (neuro-anatomy course Maastricht University) **(€500)**
2018-2020	MS-foundation pilot grant **(€17k)**
2018	Travel grant from Belgian Society for Cell and Developmental Biology **(€500)**
2018	Travel grant FWO **(€1248,26)**

Distinction, prizes and awards:

2022:	Best poster presentation Gordon Research Conference 2022 (Les Diablerets, Switzerland)
2022:	First price Figon PhD Student Competition (Leiden, the Netherlands)
2020:	Provincial finalist "Wetenschapsbattle"
2019:	Best oral talk EURON PhD days (Esch-sur-Alzette, Luxemburg)
2018:	Elected chair Gordon seminar 2020/2022
2018:	Best oral talk Gordon research seminar (Maine, USA)
2018:	Best poster presentation animal behaviour symposium (Hasselt University, Belgium)
2018:	Best oral talk cGMP conference (Tübingen, Germany)
2017:	Nominated for best student higher education VOKA
2017:	Most honourable student – Hasselt University

Academic activity:

2019-Present: Member of the faculty board (Health and Life Sciences)

2020-2022: PhD representative Hasselt University for EURON

2020-2022: Organizational board EURON PhD days 2022

2019-2023: PhD council Hasselt University

2019-2022: Belgium Society for neuroscience junior board

2018-2022: Elected chair Gordon Research seminar 2022

International research stays:

2019: University of Luxembourg; lab of Anne Grünewald

2018: University of Edinburgh; lab of Charles ffrench Constant

National research visit:

2022: University of Antwerp; lab of Peter Ponsaerts

2021: KU Leuven; lab of Catherine Verfaillie

Scientific dissemination:

MHeNs study promotion
https://www.youtube.com/watch?v=26pWZmikLUI

Active contribution at "kinder Universiteit" 2023

Universiteit van Vlaanderen – helpt sushi tegen Alzheimer?
https://www.universiteitvanvlaanderen.be/college/helpt-sushi-tegen-alzheimer

Opiniestuk knack
https://www.knack.be/nieuws/gezondheid/er-zijn-nog-geen-medicijnen-om-van-dementie-te-herstellen-voorkomen-is-beter-dan-genezen/article-opinion-1692339.html

Science figured out – Scriptie vzw
https://www.wetenschapuitgedokterd.be/cognitieverbeteraars-de-sleutel-voor-herstel-ms-patienten

Provincial finalist "Wetenschapsbattle" 2020

Active contribution at "dag van de wetenschap" activity (2 years)

Acknowledgements

Het moment is daar, het moment waarop ik mijn dankwoord moet schrijven. Iets waar ik naar uitkijk, maar tegelijk ook wat tegenop zie. Want dit is het deel wat iedereen gaat lezen. Dit betekent het einde van mijn PhD avontuur, een reis die bezaaid was met uitdagingen en gevuld met overwinningen. Het is niet alleen mijn proefschrift, nee, dit is een verzameling van inspanningen en bijdragen van zovele anderen. Woorden schieten tekort om mijn dankbaarheid te uiten, hoewel het een cliché is, is het toch waar!

Allereerst gaat er een oprechte dank uit naar mijn promotoren, mijn academische mentoren, voor alle kansen wat ik gekregen heb de voorbije jaren. **Tim**, uiteraard kan ik niet anders dan met jou beginnen! Bedankt om mij de kans te geven om een PhD traject te starten in jouw groep en om dit potentieel in mij te zien. Je hebt een onschatbare rol gespeeld gedurende mijn traject en daar ben ik je enorm dankbaar voor. Je enthousiasme voor wetenschap is aanstekelijk en het was meteen duidelijk dat ik van geluk mocht spreken dat je mijn promotor zou zijn. Naast je onuitputtelijke bron van kennis en ideeën ben je ook gewoonweg een fantastische mentor en leid je je groep op een unieke en inspirerende manier. Je zorgt ervoor dat we zowel als team als individueel de kans krijgen om te groeien en excelleren op onze eigen manier en ik hoop dat ik ooit net zo een voorbeeld mag zijn voor iemand zoals jij voor mij was de voorbije jaren. Niet alleen was je op wetenschappelijk en leidinggevend vlak uitzonderlijk maar ook als persoon wil ik je bedanken. Je mopjes (waarvan we het niet altijd toegeven maar wat we stiekem toch appreciëren. Behalve de groene kikker, die kennen we ondertussen al 😊), de steun die je biedt wanneer nodig (vaak na de vraag of alles goed is) en je team spirit zijn uitzonderlijk. Over team spirit en team uitjes gesproken kan ik natuurlijk ook niet anders dan even een extra woordje dank te richten **aan Evy en je kids**. Jaarlijks zorgt je hele gezin ervoor dat je team zich thuis voelt tijdens de 'bbq' avonden. Met gastvrijheid en open armen werden wij ieder jaar verwelkomt en dat apprecieer en waardeer ik enorm! Tim, zonder je humor, begeleiding, coaching, steun en enthousiasme zouden de voorbije jaren niet zo voorbij gevlogen zijn. Met plezier kwam en kom ik iedere dag werken en daar speelt de groep die jij gecreëerd hebt zeker een rol in. Kortom, bedankt voor ALLES Tim, en op nog vele jaren samenwerkingen!

Vervolgens wil ik ook mijn co-promotoren **Niels en Bart** bedanken om mij mee te ondersteunen tijdens dit avontuur. Ik kon en kan steeds op jullie rekenen. **Niels,** van jou kritische blik kan ik nog veel leren, maar je bracht je feedback altijd op een constructieve manier. Ik heb veel van je geleerd de voorbije jaren. Bedankt om zo betrokken te blijven bij mijn onderzoek. Bedankt voor de tijd die je vrij maakte om (bijvoorbeeld wanneer Tim 'even' moest herstellen in het ziekenhuis) mijn thesis hoofdstukken na te lezen want zonder jou zou ik dit gedeelte vandaag nog niet schrijven. Maar vooral bedankt Niels, voor je humor, nostalgische verhalen en de leuke team buildings. **Bart**, jouw klinische en terechte kritische blik hebben me veel nieuwe inzichten verworven. De moleculaire achtergrond wat ik heb is toch (al is het een beetje) gegroeid tot een wat klinisch relevantere blik dankzij jou. Van gaande tot het evalueren wanneer een statistisch significant effect ook biologisch relevant is tot de nodige nuance omtrent mijn data in het algemeen, het zijn maar enkele voorbeelden van wat je me gedurende dit traject hebt bijgeleerd. Het is de laatste maanden nog maar eens extra duidelijk geworden dat ik bij je terecht kan en ik ben je dan ook oprecht dankbaar voor je input en feedback de voorbije jaren.

I would like to thank the pro rector **Prof. Dr. Harry Steinbusch**, as well as the chairman of my reading committee **Prof. Dr. Daniel van den Hove** and all the member of my jury, **Prof. Dr. Andreas Bock**, **Prof. Dr. Inge Huitinga**, **Prof. Dr. Veerle Somers, Prof. Dr. Ir. Guy Nagels, Prof. Dr. Bert Brone** and **Dr**. **Sébastien Foulquier** for reading my thesis and helpful discussions. Echter moet er een extra bedankje uitgaan naar **Daniel** en **Bert**. Jullie hebben zeer actief ideeën en data met me besproken, die hebben geleid tot zinvolle discussies en waardevolle nieuwe experimenten. Jullie extra kennis en bijdrage wil ik daarom even bijkomend aanhalen en jullie expliciet voor bedanken.

Dan nu, mijn paranimfen, **Assia** en **Ben**. Ik was nog even aan het twijfelen om jullie pas op het einde te noemen om jullie even te laten sudderen en te zoeken naar je naam in dit dankwoord maar dat zou serieus teniet doen aan hoeveel ik aan jullie gehad heb de voorbije jaren 😊. Ik wil jullie bedanken voor alle onschatbare steun (zowel mentaal als fysiek zoals wanneer ik bijvoorbeeld mijn enkel breek…) maar vooral voor jullie vriendschap. Samen hebben we gelachen en gediscussieerd, elkaar gemotiveerd en geïnspireerd. Ik denk dat er naar ons

kantoor verwezen wordt op veel verschillende manieren zoals het luidste of het meest ordelijke wanordelijke bureau maar voor mij is het all of the above met aanvulling van gewoon ronduit het beste bureau wat ik ondertussen mijn tweede thuis noem (of eerste aangezien ik daar meer ben dan thuis 😊). Jullie zijn van onschatbare waarde, en ik ben zo dankbaar dat ik jullie mijn paranimfen mag noemen.

Assia, je hebt zo een enorme bijdrage geleverd aan mijn PhD-traject, ik denk dat je dit nog niet half beseft. Ik heb je mogen leren kennen als de gemotiveerde en getalenteerde student maar je bent al snel (nog voor je stage effectief begonnen was) uitgegroeid tot een briljante, slimme, creatieve en vooral onafhankelijke wetenschapper van wie ik letterlijk iedere dag nog dagelijks bijleer. Ik denk in de voorbije jaren dat je vaker mijn mentor en steun was dan ik ooit je begeleider ben geweest. Ondanks we niet meer dagelijks samen in het lab staan hebben we nog steeds amper woorden nodig om elkaar te begrijpen wanneer het moment toch nog eens daar is dat we samen een experiment uitvoeren. Ik hoop oprecht dat we nog lang kunnen blijven samenwerken, en ik kijk uit naar nog veel meer momenten van brain stormen, plezier en fojito's. Bien sûr, votre moitié ne peut pas être oubliée. **Abdel**, merci d'avoir rendu Assia si heureuse, chérissez-la. Merci de m'avoir permis d'être présent lors de votre journée spéciale, vous êtes un couple formidable. À de nombreuses fêtes et soirées conviviales à venir!

Ben, waar moet ik beginnen. Ook jou heb ik leren kennen als student en ik ben zo blij dat je de sprong hebt gewaagd om een PhD bij Tim te doen (misschien onder lichte aanmoediging van Assia en mij 😊). Je hebt je mannetje maar gestaan in zo'n vrouwen bureau, en hoe! Hoe anders zou mijn PhD traject eruit gezien hebben zonder jou tegenover me aan bureau. Jouw humor, creativiteit en scherpe geest hebben ons allemaal keer op keer aan het lachen gebracht en ons opgevrolijkt, zelfs tijdens de meest stressvolle momenten. Niets ontgaat je; van hevig getyp tot intens scrollen, je hebt een talent om alles luchtig en grappig te maken. Maar over talenten gesproken… Dan kan ik niet anders dan uitkomen op de legendarische meme-wall 😊 De muur zullen we moeten vereeuwigen op welke manier dan ook! Kapot gelachen met elke meme op zich, hetgeen de collectie aan de muur alleen nog maar beter maakt! Maar naast je humor ben je ook gewoonweg een geweldige collega en vriend. Je hebt een unieke manier om de

stress te verlichten en ons te herinneren dat het leven niet altijd serieus hoeft te zijn. Vergeet vooral niet hoe getalenteerd je bent. Je skills zijn iets om naar op te kijken, je praktische kennis en inzichten gaan je nog ver brengen! Ook je levenseigen Disney-prinses **Laura** verdient hier een bedankje! Ik herinner me nog je bezoekje aan het bureau na de FWO-uitslag, het werd toen direct duidelijk hoeveel Ben aan je ging hebben tijdens zijn eigen PhD traject. Jullie huwelijk was de kers op de taart en bedankt dat ik erbij mocht zijn! Op een mooie toekomst voor jullie samen!

Dan de vierde musketier, **Lieve.** Je kwam er 3 jaar geleden als laatste bij op onze bureau maar zo voelt het helemaal niet. Altijd even spannend als er iemand nieuw bij komt maar jij was zo iemand waarvan we niet besefte dat we je nodig hadden. Je begon als de enthousiasme zelf. Niet veel mensen doen je na, de flexibiliteit die jij toont en de snelheid waarmee je nieuwe dingen, experimenten en ideeën je eigen maken zijn bewonderingswaardig! En ondanks enkele (lees meer dan goed is voor de gemiddelde mens) tegenslagen blijf jij relativeren zoals alleen jij dat kan. Een skill waar ik nog veel van kan leren! Je nuchterheid is iets wat ik bewonder. Voor mij straal jij gewoon plezier en ontspanning uit. Je staat altijd klaar voor een babbeltje, al dan niet met een wijntje en wat kaas 😊 Het is ook duidelijk dat die warme uitstraling iets is wat je hele gezin deelt als ik kijk naar de gastvrijheid, betrokkenheid en enthousiasme van je ouders. Lieve, ik wens je het allerbeste toe in je toekomst met Omar, en ik kan niet wachten tot we het glas mogen heffen op jullie trouw! Op nog vele jaren vriendschap (en vele wijntjes).

Zoals Lieve als laatste bijkwam op ons bureau ben jij **Emily** de meest recente aanwinst in het PDE-team. En wat voor één! De kennis die jij je ondertussen al eigen hebt gemaakt is zeer knap. Je oog voor detail, skills en perfectionisme gaan je enkel nog een betere wetenschapper maken dan je al bent. Met jou op congres gaan naar Zwitserland zal ik niet snel vergeten. De perfecte balans tussen hardcore wetenschap en ontspanning met een glaasje wijn of cava (alleen gaan we volgende keer misschien sneller een flessenopener halen.. een schoen is toch dat niet 😊). Je enthousiasme voor wetenschap reflecteert duidelijk in hoe je studenten begeleid en hoe je onderwijs geeft. Ik kijk er oprecht naar uit om de

komende jaren met je te werken en je te zien groeien. Op nog vele congressen, discussie, kennis vergaren, samenwerking en vele gezellige avonden!

Ik kan wel letterlijk zeggen dat ik niet zou zijn waar ik nu ben zonder jou **Sam**, aangezien jij er letterlijk verantwoordelijk voor bent dat ik nu een trotse Bilzenaar ben! Sam, je work attitude is noemenswaardig en het motiveerde me wel echt om terug aan de slag te gaan toen je bij ons op bureau zat. Ondertussen zit je jammer genoeg niet meer bij ons op bureau maar je hartelijke lach doorheen de gang horen voor 8h 's morgens doet vermoeden dat het een goede dag gaat worden 😊 Onze gezamenlijke koffiepauzes doorheen de dag of de biertjes op het einde van de dag (met de voeten op bureau) zorgen voor de nodige ontspanning. Eender welk moment van de dag, zijnde het in de ochtend, laat in de avond of in het weekend, biomed voelt vertrouwd omdat ik weet dat jij daar dan ook rond loopt. Sam, je bent een wetenschapper in hart en nieren en ik hoop oprecht dat we nog vele jaren ideeën kunnen sparren. Bedankt voor alles de voorbije jaren!

Uiteraard ver**Dean** jij ook nog een extra vermelding 😊! Dean, we zijn ongeveer samen begonnen aan onze PhD reis en PDE projecten en geloof me als ik zeg dat ik enorm veel van u geleerd heb! Uw kennis is niet te evenaren en ik was, ben en blijf daar steeds enorm van onder de indruk. Je bent een wandelende PDE-encyclopedie. Ik heb vaak naar u opgekeken en ik wist dat als er iets was dat ik bij u terecht kon. Je kwam met waardevolle nieuwe inzichten en je hebt het PDE veld (of zeker mijn kijk ernaar) in de positieve zin verandert. Ik mis het brainstormen over de verzamelde data en nieuwe literatuur met je. Als ik ooit de helft van jou kennis bezit ben ik tevreden 😊 Ik heb er geen twijfels over dat je in wat je ook doet je zult excelleren, zowel op professioneel wetenschappelijk vlak als persoonlijk, onder meer als een papa. Ik wens jou en Stéphanie al het geluk toe.

Next, I would like to thank all the other members of our joint PhD-group RICE. WHAT A UNIQUE TEAM! **Philippos, Sarah, Nikita, and David** thanks for all the dinners, team buildings, brainstorms, but especially all the laughter! I truly mean it when I say that you guys are unique and great scientist. I cannot wait to follow your journey and I will be on the first row to cheer you on in every accomplishment. **Lize**, hoewel je, jammer genoeg, niet heel erg lang bij ons in de groep hebt gewerkt heb ik snel veel van je geleerd. Ik wens je ook het allerbeste

toe in je toekomstige carrière maar ik ben er zeker van dat wat je ook gaat doen je zal knallen!

Ellis, mijn eerste publicatie zal voor altijd Nelissen et al., zijn 😊 Ik wil je bedanken voor alle discussies en brainstorms over westernblot en gedragsdata. Ondanks dat ik nooit met ratten wou werken heb jij het moment kunnen vereeuwigen dat ik toch eens eentje heb vastgehad (niet dat ik er erg comfortabel uitzag maar dat terzijde..). Ik wens je nog veel succes met alles wat je doet, maar ik twijfel er niet over dat jij er komt!

Bijkomend wil ik ook graag **Prof. Dr. Monique Mulder** bedanken. Jouw creativiteit heeft niet alleen mij geïnspireerd maar ook onder andere Tim en Nikita. Bedankt dat ik zowel tijdens mijn master stage als tijdens mijn PhD welkom was bij jou op het lab! Het bezoek aan uw lab was mijn eerste internationale ervaring ooit, en zeker niet het laatste. Monique, bedankt voor je jarenlange gastvrijheid en je inzichten in het zeewier – Alzheimer project!

Of course a joint PhD student means being connected to multiple research groups, which means meeting too many to count amazing scientist but more importantly amazing people. Therefore, I really would like to thank all the current and past members of the NIC&R team at Hasselt University (**Paulien, Jana, Doryssa, Gayel, Lena, Naomi, Lisa, Manon, Cindy, Evelien, Mirre, Annet, Jan**, **Leen**) and the Neuroepigenetics team at Maastricht University (**Renzo, Katherine, Rick, Chris, Ehsan, Laurence, Lars, Nicole, Valentin**) for their valuable feedback on my project and fun team buildings.

Ook wil ik **Jana, Paulien** en **Hannelore** bedanken. Van samen in het studentenkot te zitten op biomed tijdens onze senior stages, naar allemaal het behalen van een PhD. Ik ben trots dat jullie expertises ook duidelijk gereflecteerd worden in deze thesis. Merci voor het geduld als ik weer eens langs kwam met veel FACS vragen en het delen van het enthousiasme als ik weer eens PDEs wou testen in een ander dier model. Jullie hebben mee deze thesis gemaakt en ik ben jullie dankbaar de voorbije en alvast voor de komende jaren.

Uiteraard kan ik het biomed TTO team niet vergeten met voor mij een speciale grote dank gericht aan **An**. Van het idee om voor een FWO-SB project te gaan zijn we vertrokken en ben ik voor het eerst met jou aan tafel gaan zitten. Het

drillen van mogelijke valorisatie vragen vond ik dan initieel wat schrikwekkend omdat het wel snel duidelijk was hoeveel ik niet wist. Maar jou geduld en interesse voor valorisatie hebben ook wel wat getriggerd bij mij. Ik ben enorm dankbaar dat ik tijdens mijn PhD avontuur de kans heb gekregen om de resultaten om te zetten tot een valorisatie project, want alleen zo kan je een impact op langer termijn teweegbrengen. Ik zie jou als mijn valorisatie-mentor en ik kan nog zoveel van je leren. Ik wil je dan niet alleen bedanken voor de voorbije jaren maar ook alvast voor de komende jaren (en sorry alvast als ik weer eens daar ben met mijn naïeve vragen 😊).

Verder ook een grote bedankt aan mijn BIOMED collega's! **Sofie, Dr. Kessels**, ik weet nog dat jij senior student was toen ik mijn eerste stappen op biomed zette als naïeve master student, en geloof me, ik was direct onder de indruk van je spirit, skills maar zeker ook van jou als persoon. Je bent gewoon een heel aangenaam persoon, altijd klaar om te helpen en voor een babbeltje. Ik wens je nog veel geluk in je toekomst. Een extra bedankje mag gaan naar **Kim** (Pannemans). Kim, je bent een duizendpoot met alle taken en organisatie die je op je neemt. Je creativiteit kan hier volledig in uitblinken, denk maar aan de dag van de wetenschap, kinder-universiteit or REVA-run. Maar ik wil je vooral bedanken Kim voor, ondanks hoe hectisch alles kan zijn, je er altijd staat met een lach. Voor mij ben jij de brug waardoor ik mijn enthousiasme voor wetenschap kan overbrengen naar een breder publiek gaande van kinderen, tot het in contact komen met MS patiënten zelf. Ik kijk er naar uit om de komende jaren nog verder met je samen te werken en om deel te blijven uitmaken van het UMSC. Uiteraard ook een grote dank aan de technicians van BIOMED, **Katrien, Leen, Igna, Kim, Laura, Christel, Ellen, Josianne** en **Marie-Paule** voor jullie paraatheid wanneer ik weer eens vragen had, of jullie helpende hand zodat niet alles verloren was wanneer er eens iets in het honderd liep. **Katrien**, wij hebben dankzij meerdere projecten wat intensiever kunnen samenwerken en ik wil je dan ook bedanken voor de kennis en skills wat je aan me geleerd hebt, voor de babbels met betrekking tot onze honden, en vooral voor je betrokkenheid. Het deed me enorm veel deugd als ik je tegenkwam op de gang of aan kantoor en je eens vroeg hoe het met me ging en met mijn onderzoek. Hoe enthousiast je mee werd wanneer ik dit ook was waardeer ik enorm en ik ben je er dan ook zo dankbaar voor! Ook een dikke merci aan het vorige en nieuwere animalium team: **Johan, Jeroen,**

Virginie, Yennick en **Melissa**. Mijn 1000den *in vivo* experimenten waren nooit mogelijk geweest zonder jullie. En uiteraard, last but not least**, Kristina** en **Véronique**. Wat zijn jullie voor een top team. Jullie staan steeds klaar voor een babbel of een helpende hand gerelateerd aan papierwerk of bestellingen/verzendingen. Véronique, dit zal niet de eerste keer en zeker niet de laatste keer zijn dat iemand je prijst voor alle hulp tijdens het afronden van een doctoraat. Maar ook van mij, een welgemeende bedankt uit het diepste van mijn hart. Hoe kalm jij altijd gebleven bent terwijl ik met mijn handen door het haar liep is noemenswaardig. Jouw instructies en action plan is wat iedereen er door helpt!

Ook het UM team verdient een expliciet bedankje**; Sandra, Wouter, Denise, Hellen** en **Barbie**. Hoewel ik niet met iedereen even intens heb samengewerkt wist ik al snel dat ik met mijn vragen bij jullie terecht kon. Dankzij jullie zijn experimenten kunnen blijven doorgaan wanneer er wat onverwachte praktische tegenslag was vanuit UH. Zonder deze hulp stond ik niet waar ik nu sta dus enorm bedankt. Een extra bedankje gaat bij deze dan ook uit naar **Sandra**. Hoe meer we babbelen, hoe meer we beseffen dat we met elkaar gemeen hebben. Maar onze grootste overeenkomst is toch de liefde voor onze viervoeters. Wanneer ik in Maastricht aankom voel ik me direct welkom wanneer jij me welkom heet als eerste op de gang 's morgens. Ik hoop dat we nog lang mogen samenwerken en vooral dat ik nog veel van je mag leren. Want ik ben er van overtuigd dat ik nog niet de helft van je skills heb mogen zien (en op nog vele honden-gerelateerde babbeltjes uiteraard 😊)! Tot slot, ook nog bedankt aan **Rachelle** om me te helpen vanuit de UM zijde met het afronden van mijn PhD traject. Ik zou niet weten met welke voorbeeldbrief ik nog bezig zou zijn moest jij me niet geholpen hebben.

Uiteraard mag ik het EURON team zeker niet vergeten, **Dr. Gunther Kenis**, **Damaris** en **Nicole**. **Nicole**, ik weet nog in Barcelona hoe betrokken je was tijdens het diner met iedere persoon daar aanwezig. Je hebt een warme innemende persoonlijkheid en ik bedank je dan ook voor je motiverende woorden en betrokkenheid tijdens bijvoorbeeld de PhD dagen in Luxemburg. **Damaris**, wij hebben wat nauwer kunnen samenwerking tijdens de organisatie van de EURON PhD dagen in Hasselt en je organisatorische skills kwamen duidelijk naar boven.

Je hebt ons in het gareel gehouden en zonder jou zouden de PhD dagen (en vele andere events) nooit zo een succes geweest zijn zoals ze nu waren. Tot slot **Gunther**, het was me een groot plezier om betrokken te zijn geweest binnen het EURON netwerk. Voor mij heb je EURON doen uitgroeien tot één grote opportuniteit. Dankzij jou en EURON heb ik veel mensen mogen ontmoeten op mijn pad de voorbije jaren en heb ik mijn neuro-kennis kunnen bijschaven. Het is een uniek netwerk waar je trots op mag zijn en waarvoor ik dankbaar ben deel te mogen uitmaken tijdens mijn PhD traject.

What additionally became clear from my PhD trajectory and hopefully my dissertation as a whole, is the need of excelling collaborators, who contribute to bringing research to a higher level. Over the past years, I was blessed to had the opportunity to work with such people. First of all, I had the opportunity to perform a short research visit at Edinburgh University and Luxembourgh University. I'm thankful for everyone who made this possible and guided me during my research visit including **Prof. Dr. Charles ffrench-Constant, Prof. Dr. Marie Bechler, Prof. Dr. Anne Grünewald** and **Dr. Kobi Wasner**. Furthermore, additionally, **Prof. Dr. Catherine Verfaillie** and her talented PhD student **Dr**. **Katrien Neyrinck**, made a research visit at Leuven University possible. A period where I really learned a lot and for which I'm utterly thankful for. A big thanks to the Rewind team with a special acknowledgement to **Evy Lefevre** for expanding my toolbox with the highly innovative VEP measurements and for helping me when I (again) broke the electrode. Next **Prof. Dr. Peter Ponsaerts** and **Dr. Elise van Breedam** lifted the SCI project to the next level thanks to the neuronal spheroid experiments which I could conduct and learn. Furthermore, the contribution of **Prof. Dr. Ernesto Fedele, Prof. Dr. Olga Bruno, Prof. Dr. Chiara Brullo,** and **Prof. Dr. Roberta Ricciarelli** are tremendously appreciated as without them, the potential of the investigated compound would not be unraveled. Thanks to the contagious enthusiasm science can bring, a new PhD project was initiated thanks to **Laura Ponsaerts** in collaboration with **Prof. Dr. Annelies Bronckaers**. I'm convinced there lies a great potential in PDE inhibition in stroke pathology and who else to better explore this than you as a power team. Thank you for all your help and expertise, together with Hannelore, and I'm looking forward to what the future will hold. Next, **Dr. Afonso Malheiro** and **Prof. Dr. Paul Wieringa**, I thank you for your expertise in 3D models and Schwann cell biology and I'm

grateful for the past fruitful collaboration. I hope to continue this in the future. Last but not least, the power team **Dr. Tim Vangansewinkel** and **Karen Libberecht**. I'm truly thankful that I had the opportunity to collaborate with you guys! Your knowledge and work attitude is something that needs to be explicitly mentioned. I'm excited for what the future results will bring and I wish you all the best in your future career. Of course, **Prof. Dr. Esther Wolfs**, I would like to thank you for the valuable discussions and insights on CMT pathology. Taken together, you all have truly changed my scientific point of view and contributed more than you will ever realize to my scientific and personal development. Thank you all.

I would like to thank all the students (master and external PhD student) who have helped, contributed to my research and came into my life. A special shoutout goes to **Carola**, who introduced Tim Team and who brought Italian joy into our lives. Furthermore, the beautiful brazilian **Emanuella** who bridged the group of Prof. Dr. Rubia with the group of Tim (which led to nice caipirinha's and Brazilian barbecues). Thank you all, **Kenneth, Janne, Laura Ponsaert, Laura van der Taelen, Darren, Mariana, Laura Pintado Almeida, Lucrezia, Marieke, Alana, Emina, Alessandra, Georgia, Kasper, Lotte, Ilse, Liam,** and **Zhenya** and I wish you all the best.

Uiteraard dienen niet alleen collega's maar ook familie en vrienden bedankt worden voor de onvoorwaardelijke steun wat ik de voorbije jaren heb gekregen. **Kelly, Esmee en Paulien**, van samen onze biomedische studie te starten tot het uitgroeien van de getalenteerde artsen en onderzoeker die jullie nu zijn, zijn er mooie jaren aan voorbij gegaan. Hoewel we elkaar niet zo heel vaak zien weet ik dat ik op jullie kan rekenen. Maar wanneer we dan eindelijk nog eens een moment hebben gevonden waarop we samen kunnen zijn, verstrijken de uren alsof het niets is. We kunnen dan gemakkelijk uren bijbabbelen en het voelt alsof er geen tijd is verstreken. Bedankt voor de gezellige etentjes, de urenlange babbels en de motivatie wat jullie me dan (onverwachts) hebben gegeven!

Een grote dank ook aan mijn **nonk, oma** en **Pierre** voor de etentjes die van tijd tot tijd mijn gedachtes konden verzetten wanneer het nodig was. Bedankt aan **Bram** om steeds weer voor een luchtige ludieke namiddag te zorgen wanneer je langs kwam. Bedankt aan de hele **familie van Kevin** om me zo te includeren. De

familie feestjes en neven-en-nicht feestjes zorgde voor de nodige ontspanning net zoals de vraag "hoe is het met de muizen" zorgde voor de nodige lach op mijn gezicht en enthousiasme om een update te geven. Oprecht bedankt allemaal!

In een apart stukje wil ik graag jou bedanken **mama**! Ik wil je graag bedanken voor alles wat je voor mij hebt gedaan en nog steeds doet. We hebben samen ups en downs gekend, en hoewel het niet altijd makkelijk is geweest, zijn we er altijd samen doorheen gekomen. Ik ben zo dankbaar voor jouw onvoorwaardelijke liefde, steun en doorzettingsvermogen. Jij bent een voorbeeld voor mij, mama. Ondanks de uitdagingen waarmee we zijn geconfronteerd, ben je altijd sterk gebleven. Je hebt nooit opgegeven, en je vastberadenheid om te blijven vechten heeft me geïnspireerd en gemotiveerd om hetzelfde te doen. Je hebt me geleerd om door te zetten, zelfs als het leven moeilijk is, en om altijd te geloven in mezelf en mijn dromen. Ik ben zo dankbaar dat ik jou als mijn moeder heb!

Last but not least, wil ik graag mijn diepste dankbaarheid uitspreken aan jou **Kevin**, voor de onschatbare steun die je mij hebt gegeven tijdens mijn PhD-traject. Vanaf het allereerste begin heb je naast me gestaan en me aangemoedigd, en ik ben ontzettend dankbaar dat ik jou aan mijn zijde heb gehad tijdens deze uitdagende reis. Je hebt me altijd aangemoedigd om mijn dromen na te jagen en mijn doelen te bereiken. Je hebt me geholpen bij het balanceren van mijn werk (hoewel dit nog steeds soms wat moeilijk voor me blijft 😊) en hebt me altijd aangemoedigd om door te zetten, zelfs als het moeilijk werd. Bedankt om het te begrijpen als ik weer eens wat langer bleef door werken of weer eens moe thuis kwam na het vroege opstaan. Niet alleen ben ik je dankbaar maar ben ik ook zeker trots op de man die je geworden bent en ik kijk uit naar de toekomst die we samen zullen delen, vol avonturen, uitdagingen en groei.

Melissa

"Alone we can do so little; together we can do so much."
- Helen Keller